

CHARLES UNIVERSITY

HABILITATION THESIS

Effective field theories of
meson interactions at low energies

Karol Kampf



Institute of Particle and Nuclear Physics
Faculty of Mathematics and Physics

Prague
May 2015

The text of this thesis in Chapter 2 is a reprint of the materials:

Section 2.1 © 2009 The American Physical Society

Section 2.2 © 2010 Elsevier B.V.

Section 2.3 © 2011 American Physical Society

Section 2.4 © 2012 Elsevier B.V.

Section 2.5 © SISSA 2013

Acknowledgements

I would like to thank people I have had the pleasure and honour to work with on different projects connected with the subject of this thesis, namely: Hans Bijnens, Cliff Cheung, Jiří Hořejší, Tomáš Husek, Marc Knecht, Bachir Moussallam, Jiří Novotný, Stefan Lanz, Jaroslav Trnka and Martin Zdráhal. My special thanks go to Prof. J. Hořejší for his support during my whole scientific life and especially for his help during thesis writing process.

Contents

Acknowledgements	3
Contents	5
1 Introduction	7
1.1 Chiral perturbation theory	8
1.2 Resonance theory	18
1.3 New methods	23
1.3.1 Renormalization in effective field theory: leading logarithms	23
1.3.2 Analytic properties: tree-level diagrams	28
1.4 Summary	33
References	35
2 Original works	38
2.1 Chiral expansions of the pi0 lifetime	38
2.2 Neutral pseudoscalar meson decays: $\pi^0 \rightarrow \gamma\gamma$ and $\eta \rightarrow \gamma\gamma$ in SU(3) limit	50
2.3 Resonance saturation in the odd-intrinsic parity sector of low-energy QCD	55
2.4 Leading logarithms in the anomalous sector of two-flavour QCD	82
2.5 Tree-level Amplitudes in the Nonlinear Sigma Model	105

To my girls, Hanka, Jolana and Jana. . .

Chapter 1

Introduction

The presented habilitation thesis includes in Chapter 2 five original author's papers:

- K. Kampf, B. Moussallam, *Chiral expansions of the π^0 lifetime*, Phys. Rev. D **79**, 076005 (2009). [arXiv:0901.4688 [hep-ph]]
- J. Bijnens and K. Kampf, *Neutral pseudoscalar meson decays: $\pi^0 \rightarrow \gamma\gamma$ and $\eta \rightarrow \gamma\gamma$ in $SU(3)$ limit*, Nucl. Phys. Proc. Suppl. **207-208** (2010) 220 [arXiv:1009.5493 [hep-ph]]
- K. Kampf and J. Novotny, *Resonance saturation in the odd-intrinsic parity sector of low-energy QCD*, Phys. Rev. D **84** (2011) 014036 [arXiv:1104.3137 [hep-ph]].
- J. Bijnens, K. Kampf and S. Lanz, *Leading logarithms in the anomalous sector of two-flavour QCD*, Nucl. Phys. B **860** (2012) 245 [arXiv:1201.2608 [hep-ph]].
- K. Kampf, J. Novotny and J. Trnka, *Tree-level Amplitudes in the Nonlinear Sigma Model*, JHEP **1305** (2013) 032 [arXiv:1304.3048 [hep-th]].

Included papers were selected mainly due to their closeness and relative mutual connection in the field of the low energy effective theories (EFT). On the other hand, in spite of their interrelation, they demonstrate the necessity of different approaches in studying this area. The aim of the first introductory chapter will be thus to briefly introduce and clarify some basic terminology and background of these papers.

1.1 Chiral perturbation theory

Quantum chromodynamics (QCD) describes the dynamics of three degrees of freedom (called colours) of six quarks (u, d, s, c, b, t). It is based on the local gauge group $SU(3)$. The quarks transform in the fundamental representation and gauge bosons (called gluons) in the adjoint representation (their number is thus fixed to eight). The gauge symmetry fixes the Lagrangian to (we will not consider the CP violating ‘ θ -term’ here)

$$\mathcal{L}_{\text{QCD}} = -\frac{1}{4}\vec{G}_{\mu\nu} \cdot \vec{G}^{\mu\nu} + \bar{\mathbf{q}}(i\not{D} - m_f)\mathbf{q} + \mathcal{L}_{\text{GF}} + \mathcal{L}_{\text{FP}}, \quad (1.1)$$

where the gluon field strength tensor is given by (vectors being in the adjoint representation, the colour index is $i = 1, \dots, 8$)

$$G_{\mu\nu}^i = \partial_\mu G_\nu^i - \partial_\nu G_\mu^i + gf^{ijk}G_\mu^j G_\nu^k$$

and the covariant derivative

$$D_\mu = \partial_\mu - igG_\mu^a \frac{\lambda^a}{2},$$

where λ^a are Gell-Mann matrices. \mathcal{L}_{GF} represents the gauge-fixing terms and \mathcal{L}_{FP} the associated Faddeev-Popov ghosts. The quark field \mathbf{q} includes all types or, in other words, flavours. The second term in (1.1) can be rewritten as

$$\mathcal{L}_{\mathbf{q}} = i \sum_{q=u,d,s} \bar{q}\not{D}q - \sum_{q=u,d,s} m_q \bar{q}q + \sum_{Q=c,b,t} \bar{Q}(i\not{D} - M_Q)Q. \quad (1.2)$$

At small distances one can use QCD in a standard way perturbatively. However, due to quark confinement this is no longer true for the low and intermediate energy regions. The running of the coupling constant is responsible for its value becoming large and the perturbative series is thus meaningless. The only existing direct method is the calculations on a finite lattice, and these have the huge demands on computer resources (to say nothing about human resources).¹ At very low energies we can use a method of the chiral perturbation theory, which we will briefly explain in the following.

¹For a recent review of lattice results concerning the low energy particle physics see the report [1] of the lattice community FLAG (Flavour Lattice Averaging Group).

In order to make the text as simple as possible we will focus on the so-called three-flavour ChPT. It is easy to generalize the discussion to the general N_f -flavour ChPT or the other possible real situation: two-flavour ChPT (where light quarks are only u and d). We will briefly comment on both cases when necessary.

The starting point is the study of the global symmetry in the system of light quarks

$$\begin{pmatrix} u \\ d \\ s \end{pmatrix}_{L,R} \rightarrow V_{L,R} \begin{pmatrix} u \\ d \\ s \end{pmatrix}_{L,R}, \quad (1.3)$$

where V_L a V_R represent independent unitary transformation ($V_{L,R} \cdot V_{L,R}^\dagger = \mathbf{1}$). The projector on the right and left quark fields is given by $\frac{1 \pm \gamma_5}{2}$. It is easy to verify that the QCD Lagrangian is invariant under (1.3) if we ignore masses of light quarks (i.e. ignoring the second term in (1.2)). In such a case, we work in the so-called chiral limit. The transformation $U(3)$ is described by nine independent parameters. Thanks to Noether's theorem one can thus expect 18 conserved currents. However, due to the anomaly (see the original works [2]) there are only 17 currents that are conserved also at the quantum level. Using Gell-Mann matrices λ^a (we define $\lambda^0 = \sqrt{2/3}\mathbf{1}$). We express the vector and axial-vector combinations of currents as (here $a = 0 \dots 8$)

$$V_\mu^a = R_\mu^a + L_\mu^a = \bar{q} \gamma_\mu \frac{\lambda^a}{2} q, \quad (1.4)$$

$$A_\mu^a = R_\mu^a - L_\mu^a = \bar{q} \gamma_\mu \gamma_5 \frac{\lambda^a}{2} q, \quad (1.5)$$

it is possible to write

$$\begin{aligned} \partial^\mu V_\mu^a &= 0, & \text{for } a = 0 \dots 8, \\ \partial^\mu A_\mu^a &= 0, & \text{for } a = 1 \dots 8. \end{aligned} \quad (1.6)$$

As mentioned above one of the eighteen currents is anomalous:

$$\partial_\mu A^{0\mu} = \sqrt{\frac{3}{2}} \frac{g^2}{32\pi^2} \varepsilon_{\mu\nu\alpha\beta} \vec{G}^{\mu\nu} \cdot \vec{G}^{\alpha\beta}. \quad (1.7)$$

Using a conserved current we can define a time independent charge, i.e.

$$Q_V^i = \int d^3x V_0^i(\vec{x}, t), \quad (1.8)$$

$$Q_A^i = \int d^3x A_0^i(\vec{x}, t), \quad \text{for } i = 1, \dots, 8 \quad (1.9)$$

In the case of the vector current with $i = 0$ we get conserved charge which represents the baryon number. The defined charges represent generators of the group and one can verify the following relations

$$\begin{aligned} [Q_V^i, Q_V^j] &= i f^{ijk} Q_V^k, \\ [Q_A^i, Q_A^j] &= i f^{ijk} Q_V^k, \\ [Q_V^i, Q_A^j] &= i f^{ijk} Q_A^k. \end{aligned} \quad (1.10)$$

The previous relations are valid also for the vector charges with $i = 0$ if we add to the definition of the structure constant $f^{0ij} = 0$.

The time independence of the charges implies the following commutation relations for Hamiltonian of QCD in the chiral limit (denoted as \mathbb{H}_0)

$$[Q_V^i, \mathbb{H}_0] = 0, \quad [Q_A^i, \mathbb{H}_0] = 0. \quad (1.11)$$

In models of quantum field theories there are two possible consequences of these relations. If the charge annihilates the vacuum we have the so called Wigner-Weyl realization of symmetry which includes the degenerate multiplets of states. If this is not the case, and some charge does not annihilate the vacuum, we say that symmetry is spontaneously broken. The consequence of this second possibility, connected with the Goldstone theorem [3], is the massless particle in the spectrum, called Goldstone boson. In our case we will assume (for more details see e.g. [4], [5])

$$Q_V^a |0\rangle = 0, \quad a = 0, \dots, 8, \quad Q_A^a |0\rangle \neq 0, \quad a = 1, \dots, 8. \quad (1.12)$$

So far we were ignoring the fact that the chiral symmetry is weakly broken. Indeed the relations (1.6) are valid only approximately and in reality we should modify

them according to

$$\begin{aligned}\partial^\mu V_\mu^a &= i\bar{q}\left[\mathbb{M}, \frac{\lambda^a}{2}\right]q, & \text{for } a = 0 \dots 8, \\ \partial^\mu A_\mu^a &= i\bar{q}\left\{\mathbb{M}, \frac{\lambda^a}{2}\right\}\gamma_5 q, & \text{for } a = 1 \dots 8,\end{aligned}\tag{1.13}$$

where we have introduced the diagonal matrix of the light quark masses: $\mathbb{M} = \text{diag}(m_u, m_d, m_s)$. If we want to describe the dynamics of the Goldstone bosons in the framework of quantum field theory using effective Lagrangian, we have to divide this Lagrangian into two pieces: $\mathcal{L}_0 + \mathcal{L}_{\text{cor}}$. The first part \mathcal{L}_0 will be invariant under the group $SU(3) \times SU(3)$ spontaneously broken to $SU(3)_V$, while \mathcal{L}_{cor} will break the symmetry explicitly. The definition of the effective Lagrangian can be done formally using the path integral. First we will define the generating functional over the gluon and fermion configurations in QCD.

$$e^{\mathcal{G}_c[v, a, s p]} = \int [d\mu] e^{i \int d^4x \mathcal{L}_{\text{QCD}}[v, a, s p]},\tag{1.14}$$

where we have included the vector, axial, scalar and pseudoscalar sources:

$$\mathcal{L}_{\text{QCD}}[v, a, s p] = \mathcal{L}_{\text{QCD}} + \bar{q}(\gamma_\mu(v^\mu + \gamma_5 a^\mu) - s + \gamma_5 p)q.\tag{1.15}$$

It is useful to notice that scalar source can formally play also the role of the light quark masses (by a redefinition $s \rightarrow s + \mathbb{M}$ they can be absorbed in the source). This can also elegantly solve the problem how to incorporate systematically the mass corrections. Including the masses in the definition of scalar source s , it is possible to calculate any Green function using

$$\langle 0|T(W^a(x_1) \dots W^z(x_n)|0\rangle_c = \left(\frac{1}{i}\right)^n \frac{\delta^n \mathcal{G}_c}{\delta w^a(x_1) \dots \delta w^z(x_n)} \Big|_{v=a=p=0, s=\mathbb{M}},\tag{1.16}$$

where W represents any current V, A, S, P and similarly w the corresponding source with

$$w = w^i \frac{\lambda^i}{2}.\tag{1.17}$$

In the following step it is necessary to reformulate the investigated symmetries in terms of transformation properties of currents. This is connected with the study of the so-called Ward identities, which represent non-trivial relations among Green functions of currents. We can obtain them by moving from global to local transformations $V_L \rightarrow V_L(x)$ and $V_R \rightarrow V_R(x)$. Considering now the infinitesimal

transformation $V_{L,R} = 1 + i\alpha_{L,R}$ we will readily get

$$\begin{aligned} v'_\mu &= v_\mu + \partial_\mu \alpha_V + i[\alpha_V, v_\mu] + i[\alpha_A, a_\mu], \\ a'_\mu &= a_\mu + \partial_\mu \alpha_A + i[\alpha_V, a_\mu] + i[\alpha_A, v_\mu], \\ s' &= i[\alpha_V, s] - \{\alpha_A, p\}, \\ p' &= i[\alpha_V, p] - \{\alpha_A, s\}, \end{aligned} \quad (1.18)$$

where we have defined $\alpha_V = \alpha_R + \alpha_L$ and $\alpha_A = \alpha_R - \alpha_L$. Putting the transforming quantities to (1.14) one can get the prescription for the transformations of Green functions, generally in the form

$$\mathcal{G}_c[v', a', s', p'] = \mathcal{G}_c[v, a, s, p] + \Delta[v, a, s, p, V_L V_R^\dagger], \quad (1.19)$$

where the existence of the last term Δ is tied to the fact that the Jacobian of the transformation (1.18) is not one. The exact form was calculated by W. Bardeen [6]:

$$\Delta = -\frac{N_C}{16\pi^2} \int d^4x \text{Tr} \left(\alpha_A(x) \Omega(x) \right), \quad (1.20)$$

where

$$\Omega = \varepsilon^{\alpha\beta\mu\nu} \left(v_{\alpha\beta} v_{\mu\nu} + \frac{4}{3} D_\alpha a_\beta D_\mu a_\nu + \frac{2i}{3} \{v_{\alpha\beta}, a_\mu a_\nu\} + \frac{8i}{3} a_\mu v_{\alpha\beta} a_\nu + \frac{4}{3} a_\alpha a_\beta a_\mu a_\nu \right)$$

and

$$v_{\alpha\beta} = \partial_\alpha v_\beta - \partial_\beta v_\alpha - i[v_\alpha, v_\beta], \quad D_\alpha a_\beta = \partial_\alpha a_\beta - i[v_\alpha, a_\beta].$$

The relation (1.19) represents in a compact form all the Ward identities.

The basis of ChPT is an effective Lagrangian, which can be formally connected with QCD via the relation

$$e^{\mathcal{G}_c[v, a, s, p]} = \int [dU] e^{i \int d^4x \mathcal{L}_{\text{eff}}[U; v, a, s, p]}. \quad (1.21)$$

The matrix U incorporates the octet of Goldstone particles

$$\phi(x) = \frac{1}{\sqrt{2}} \pi^i(x) \lambda^i, \quad \phi(x) = \begin{pmatrix} \frac{1}{\sqrt{2}} \pi^0(x) + \frac{1}{\sqrt{6}} \eta(x) & \pi^+(x) & K^+(x) \\ \pi^-(x) & -\frac{1}{\sqrt{2}} \pi^0 + \frac{1}{\sqrt{6}} \eta(x) & K^0(x) \\ K^-(x) & \bar{K}^0(x) & -\frac{2}{\sqrt{6}} \eta(x) \end{pmatrix}. \quad (1.22)$$

In order to use the Ward identities also in the framework of the chiral Lagrangian we have to specify first the transformation properties of the matrix field U .

The standard procedure how to implement the symmetry transformation of the Goldstone fields is due to two works of Callan, Coleman, Wess and Zumino [7], [8]. Let us denote the space of Goldstone particles as Π and the particles themselves $\vec{\pi}$. We want to study a system, which is invariant under the group \mathcal{G} spontaneously broken to the subgroup $\mathcal{H} \subset \mathcal{G}$. The state with the lowest energy, vacuum, is invariant under the action of \mathcal{H} . It is convenient to denote the vacuum by $\vec{\pi} = 0$. We want to find out how the group \mathcal{G} acts on the field Π . We will define the homomorphic mapping φ :

$$\varphi : \quad \mathcal{G} \times \Pi \rightarrow \Pi \quad (1.23)$$

It is possible to establish an isomorphism between the quotient \mathcal{G}/\mathcal{H} and Goldstone bosons $\vec{\pi}$. The transformation will have the form

$$\vec{\pi}' = \varphi(g, \vec{\pi}) = \varphi(g, \varphi(g_\pi h, 0)) = \varphi(gg_\pi h, 0).$$

For h , the element of the conserved subgroup, the name ‘‘compensator’’ is sometimes used.

In our case of the chiral symmetry the transformation is given by

$$g = (V_L, V_R)$$

and the Goldstone representatives can be expressed as $(1, U)h$, for $U = V_R V_L^\dagger$. The wanted transformation thus gets the following form

$$gg_\pi h = (V_L, V_R)(1, U)h = (V_L, V_R U)h = (1, V_R U V_L^\dagger)(V_L, V_L)h = (1, V_R U V_L^\dagger)h, \quad (1.24)$$

or alternatively

$$U'(x) = V_R(x)U(x)V_L^\dagger(x). \quad (1.25)$$

The suitable parametrization of $SU(3)$ is the exponential. We will set the following form

$$U = e^{i\sqrt{2}\frac{\phi}{F_0}}. \quad (1.26)$$

Trivially it is consistent with

$$U^\dagger U = U U^\dagger = 1, \quad \det U = 1. \quad (1.27)$$

Let us mention here that in the case of the two-flavour ChPT there are more suitable parametrizations which can be employed. For their explicit definitions and advantages (i.e. the reason for their different forms) see articles in Chapter 2, e.g. in Sections 2.1 and 2.4 (see also discussion connected with $SU(N_f)$ case in 2.5 (part 2.3)).

Now we can carry on our construction of \mathcal{L}_{eff} in (1.21). We will demand that Green functions calculated using the effective Lagrangian fulfil the same Ward identities as those obtained from QCD, i.e. (1.19). The solution will be given by means of the general solution of the homogeneous equation (i.e. without anomaly) plus one particular solution for the complete equation. As we assume that the measure of the functional integration is invariant under the transformation of the field U (1.25), the homogeneous Ward equations are fulfilled by a requirement

$$\mathcal{L}_{\text{eff}}[U'; v', a', s', p'] = \mathcal{L}_{\text{eff}}[U; v, a, s, p], \quad (1.28)$$

which gives us a strong restriction on the form of the Lagrangian. If we introduce the covariant derivative

$$D_\mu U = \partial_\mu U - i(v_\mu + a_\mu)U + iU(v_\mu - a_\mu), \quad (1.29)$$

we obtain the basic building block for the construction of the chiral Lagrangian including the clear power counting (connected with the derivative or equivalently momentum). In the case of the power counting w.r.t. mass the situation is not that clear. We know that the mass is given by the explicit symmetry breaking and can be connected with the scalar source. If we form the building block by

$$\chi = 2B_0(s + ip), \quad (1.30)$$

the chiral symmetry fixes

$$\chi \rightarrow V_R \chi V_L^\dagger. \quad (1.31)$$

It is natural to take a mass of the Goldstone bosons of the same order of magnitude as the momentum, i.e. $m_q \sim O(p^2)$. Let us stress at this point, that this choice, however natural, is not the only one. From the last definition it follows that the mass is connected with the parameter B_0 . From the general Nambu-Goldstone theorem we can conclude that a nonzero value of B_0 is a sufficient, but not necessary condition for spontaneous breakdown of chiral symmetry. The unnatural

smallness of B_0 would lead to the necessity to reorder the perturbative expansion. This possibility led to the formulation of the so-called generalized chiral perturbation theory (see e.g. [9]). Recently also a hypothesis of different behaviour of the parameter B_0 for two-flavour and three-flavour ChPT was opened (see e.g. [10], [11], [12]). For another possibility how to “undemocratically” count differently masses of u and d quarks on one hand and s quark on the other hand, directly within the framework of $SU(3)$, see the so-called modified chiral counting scheme defined and used in Chapter 2, Section 2.1.

In the standard approach the lowest order (called $O(p^2)$) is given by Lagrangian [13]

$$\mathcal{L}_2 = \frac{F_0}{4} \langle D_\mu U^\dagger D^\mu U + \chi U^\dagger + U \chi^\dagger \rangle, \quad (1.32)$$

where we have introduced $\langle A \rangle = \text{Tr}_F(A)$, that represents trace over the quark flavours. The next-to-leading order (NLO) or equivalently $O(p^4)$ is given by [14] [15]

$$\begin{aligned} \mathcal{L}_4 = & L_1 \langle D_\mu U (D^\mu U)^\dagger \rangle^2 + L_2 \langle D_\mu U (D_\nu U)^\dagger \rangle \langle D^\mu U (D^\nu U)^\dagger \rangle \\ & + L_3 \langle D_\mu U (D^\mu U)^\dagger D_\nu U (D^\nu U)^\dagger \rangle + L_4 \langle D_\mu U (D^\mu U)^\dagger \rangle \langle \chi U^\dagger + U \chi^\dagger \rangle \\ & + L_5 \langle D_\mu U (D^\mu U)^\dagger (\chi U^\dagger + U \chi^\dagger) \rangle + L_6 \langle \chi U^\dagger + U \chi^\dagger \rangle^2 \\ & + L_7 \langle \chi U^\dagger - U \chi^\dagger \rangle^2 + L_8 \langle U \chi^\dagger U \chi^\dagger + \chi U^\dagger \chi U^\dagger \rangle \\ & - i L_9 \langle f_{\mu\nu}^R D^\mu U (D^\nu U)^\dagger + f_{\mu\nu}^L (D^\mu U)^\dagger D^\nu U \rangle + L_{10} \langle U f_{\mu\nu}^L U^\dagger f_R^{\mu\nu} \rangle \\ & + H_1 \langle f_{\mu\nu}^R f_R^{\mu\nu} + f_{\mu\nu}^L f_L^{\mu\nu} \rangle + H_2 \langle \chi \chi^\dagger \rangle. \end{aligned} \quad (1.33)$$

where we have used the standard notation for the field strengths of the external gauge fields

$$f_{\mu\nu}^I = \partial_\mu I_\nu - \partial_\nu I_\mu - i[I_\mu, I_\nu], \quad I_\alpha = r_\alpha, l_\alpha. \quad (1.34)$$

We can continue to the next-to-next-to-leading order (NNLO, or $O(p^6)$). Its form and details of the construction can be found in [16]. In this context, let us mention here the standard nomenclature and notation. The parameters used in these pieces of Lagrangian are called low energy constants (LECs). For the $SU(3)$ NLO there are 10 L_i (note that H_i s have no direct phenomenological application and are induced by the renormalization procedure). In the two-flavour ChPT usually small letters are introduced in connection to the capital letters of $SU(3)$, i.e. l_i at NLO. The exact number and notations of LECs up to NNLO is summarized in Tab. 1.1. It will be useful for further discussion to introduce an equivalent for-

order	notation and number for $SU(2)$	notation and number for $SU(3)$
LO	F, B 2	F_0, B_0 2
NLO	l_i 7	L_i 10
NNLO	c_i 52	C_i 90

TABLE 1.1: Notation and number of LECs up to $O(p^6)$ for the chiral Lagrangian of the even sector.

malism, which follows directly from the original construction of Callan, Coleman, Wess and Zumino, when the coset space G/H is parametrized directly by $u(\phi)$, i.e. $u(\phi) \in G/H$. The transformation is given by

$$u(\phi') = g_R u(\phi) h^{-1} = h u(\phi) g_L^\dagger \quad (1.35)$$

and our familiar U is obtained by $U = u^2$. In order to be consistent with our previous notation we have the following exponential parametrization for u

$$u = e^{i \frac{\phi}{\sqrt{2}F_0}}. \quad (1.36)$$

The covariant tensors needed for the lowest order are given by

$$u_\mu = i(u^\dagger(\partial_\mu - ir_\mu)u - u(\partial_\mu - il_\mu)u^\dagger) \quad (1.37)$$

$$\chi_\pm = u^\dagger \chi u^\dagger \pm u \chi^\dagger u. \quad (1.38)$$

The leading order Lagrangian is then

$$\mathcal{L}_2 = \frac{F_0^2}{4} \langle u_\mu u^\mu + \chi_+ \rangle, \quad (1.39)$$

which is equivalent to (1.32). Similarly we can rewrite the higher orders. This new formalism is more appropriate for the construction of resonances as we will see in the next Section and Chapter 2.

It is important to notice that our Lagrangian is still not complete. The presented forms (either LO, or NLO or of higher orders) solve only the homogeneous Ward identities. That something is missing can be shown also phenomenologically. All these Lagrangians are symmetric under the change $\phi \rightarrow -\phi$, which means that processes they can describe will cover only even number of Goldstone particles. However, this is an unphysical requirement: we know for example that there must exist a process $KK \rightarrow \pi\pi\pi$ (the resonance $\phi(1020)$ can decay both to two kaons

and three pions). After all, also the decay $\pi^0 \rightarrow \gamma\gamma$ (important for us in Chapter 2), when photon is represented by the external vector field v^μ , could not be described solely using the Lagrangian of the so-called even sector.

The details of construction can be found in the works of Wess and Zumino [17] and Witten [18]. As we need only one particular solution of the full Ward identity (1.19), it is sufficient to verify that the eventual solution leads indeed to the Bardeen's function Δ . For the $SU(3)$ the exact form can be found in this thesis in Sect. 2.3. In the case of the $SU(2)$ ChPT the situation is slightly different. Naively we would expect no anomalies (the $SU(2)$ case is anomaly free). However, due to the fact that the electromagnetic charge is not a generator of $SU(2)$ (the diagonal matrix $Q = \text{diag}(2/3, -1/3)$ is not traceless) the initial symmetry must be extended by a singlet vector part (if we want to describe the electromagnetic processes). The construction of the two-flavour anomalous Lagrangian was done in [19] and is again reproduced in Sect. 2.4.

As we are working in the framework of quantum field theory, it is inevitable to consider the quantum corrections as well. The loops coming from the LO vertices are of course divergent and have to be renormalized. Provided we have constructed the most general Lagrangian consistent with all assumed symmetry principles (cf. also Weinberg's conjecture in [13]) we will use naturally a regularization prescription which conserves the symmetries. In our case it will be the dimensional regularization. All divergences we will obtain in the calculation must be local. As we have all terms in our Lagrangian consistent with the symmetry we must also find the corresponding counterterms which can absorb the eventual divergences. The number of such terms will be finite, once we cut the expansion series according to some power counting. For NLO it is given by

$$L_i = L_i^r(\mu) + \Gamma_i \lambda(\mu), \quad \lambda = \frac{\mu^{d-4}}{(4\pi)^2} \left(\frac{1}{d-4} - \frac{1}{2} (\log 4\pi - \gamma_E + 1) \right). \quad (1.40)$$

with [15]

$$\begin{aligned} \Gamma_1 &= \frac{3}{32}, & \Gamma_2 &= \frac{3}{16}, & \Gamma_3 &= 0, & \Gamma_4 &= \frac{1}{8}, & \Gamma_5 &= \frac{3}{8}, \\ \Gamma_6 &= \frac{11}{144}, & \Gamma_7 &= 0, & \Gamma_8 &= \frac{5}{48}, & \Gamma_9 &= \frac{1}{4}, & \Gamma_{10} &= -\frac{1}{4}. \end{aligned} \quad (1.41)$$

1.2 Resonance theory

ChPT as an effective field theory of QCD must be the *correct* theory for a description of the low energy phenomenology of pseudoscalar hadron states, that represent Goldstone bosons (see previous section). The strong statement about the ‘correctness’ desires an explanation, which will relativize the possibility of the eventual application of such a theory. The necessity to cut the perturbative series to the finite number of terms, at the same time the necessity to choose the correct scheme for the expansion in masses as well as the possibility of a choice of two N_f cases (two-flavour and three-flavour ChPT) lead in real calculation to different predictions. From the theory point of view all such predictions are correct and the different results can be used as an estimate of the error for the effective calculations. Too big error, however, can be a sign of bad convergence properties of perturbative series. In such a case we are naturally forced to go to higher orders, which inevitably increases number of new, a priori unknown parameters (LECs). If we want to have phenomenologically useful theory it is essential, in some cases, to model some of the unknown parameters. We are thus leaving solid ground of our theory and the prediction becomes model dependent. In this section we will briefly describe how it is possible to estimate some of LECs by means of resonances.

We know that the mass of the lightest resonance M_ρ is a natural scale up to which the study of the dynamics of the pseudoscalar meson multiplet within ChPT is meaningful. However, starting around this energy and above, the resonances should be taken as dynamical degrees of freedom, whereas below this energy their effect is hidden in the low energy constants. Resonance chiral theory (R χ T) will represent a model which describes the intermediate energy region, where in addition to pseudoscalar mesons the resonances will act as dynamical degrees of freedom. For simplicity we restrict ourselves only to the lowest multiplet of vector, axial, scalar and pseudoscalar resonances. At this point it is also important to emphasize that vector particles in our description have not a special position and their properties are dictated only by nonlinear realization of the chiral group. There are of course other alternatives to interpolate between ChPT and QCD. These models are different both in the technical structure and physical motivation and interpretation. For example, we can mention the Nambu-Jona-Lasinio models [20], where the hadron field is generated dynamically and one obtains automatically the spontaneous symmetry breaking. As we have emphasized, the ρ meson

does not play a special role, but this is not the case for the models with the so-called hidden local symmetry (or hidden gauge symmetry), see for example [21] [22]. A nice feature of these models is usually a small number of parameters and therefore their easier testing. On the other hand, it is important to stress that the base for these models is not the direct consequence of QCD and their results may therefore be misleading.

The limit of large number of colours (will be denoted by N here) plays an important role in applications for low energy QCD (and not only there, but it represents an important concept for the theory of gauge fields itself). Let us thus summarize the most important points of this limit (for further details see e.g. [18]). The crucial step in the generalization of $SU(3)$ gauge group to $SU(N)$ is finding of 't Hooft [23] about the scaling of the strong coupling constant g

$$g \sim \frac{1}{\sqrt{N}} \quad (1.42)$$

(this can be obtained for example from an assumption of the existence of large N limit for the β -function of the QCD coupling constant g). By systematic studies of Feynman diagrams one can show that dominant contributions are due to the so-called planar diagrams (diagrams that can be drawn on a plane). Another important assumption will be that the confinement valid for $N = 3$ stays valid also for large N . If we limit ourselves only to study of mesons, we can focus on properties of quark bilinears $J(x) = \bar{q}\Gamma q$. In the simplest case we have a correlator $\langle J(x)J(y) \rangle$. By cutting any planar diagram for such an object one can be easily convinced that the intermediate state will be always the one-meson state. We can write

$$\langle J(k)J(-k) \rangle = \sum_n^{\infty} \frac{f_n^2}{k^2 - m_n^2}, \quad (1.43)$$

where the sum has to go to infinity in order to obtain the logarithmic behaviour for large k . The constant f_n represents the matrix element for creation of the corresponding meson by the current J . It thus follows that $f_n \sim \sqrt{N}$. If we continued in studying the correlators for higher number of meson states we would find out that effective interaction of n mesons behaves as $\sim N^{1-n/2}$.

From the above general statements we can use directly for ChPT that F_π behaves as \sqrt{N} . What is also important for the following discussion is the fact that every trace represents a sum over the quark flavours which originated from the quark loops. As every such loop is suppressed by factor $1/N$, it is also the case for every

trace. Another important consequence of the large- N limit is the so-called singlet-octet degeneration, which means that mesons come in nonets. The explanation using the large N is based on the fact that the diagrams which would separate singlet from octet would include $q\bar{q}$ annihilation, which is suppressed as $1/N$. As an immediate consequence of this finding we should return back to our previous section and add to the pseudoscalar octet also the singlet η' meson. It is nevertheless possible to keep the octet structure and integrate out the ninth particle. The effect of this particle will be visible in the existence of multiple-trace operators (for detailed discussion see Appendix A in Section 2.3).

Besides the octet of Goldstone bosons we will deal with nonets of resonances, schematically $R(J^{PC})$, more precisely $V(1^{--})$, $A(1^{++})$, $S(0^{++})$ a $P(0^{-+})$. These fields can be divided to the singlet R_0 and octet R_8

$$R = \frac{1}{\sqrt{3}}R_0 + \sum_i \frac{\lambda_i}{\sqrt{2}}R_i. \quad (1.44)$$

The explicit form for the vector multiplet reads

$$V_{\mu\nu} = \begin{pmatrix} \frac{1}{\sqrt{2}}\rho^0 + \frac{1}{\sqrt{6}}\omega_8 + \frac{1}{\sqrt{3}}\omega_1 & \rho^+ & K^{*+} \\ \rho^- & -\frac{1}{\sqrt{2}}\rho^0 + \frac{1}{\sqrt{6}}\omega_8 + \frac{1}{\sqrt{3}}\omega_1 & K^{*0} \\ K^{*-} & \frac{K^{*0}}{\sqrt{2}} & -\frac{2}{\sqrt{6}}\omega_8 + \frac{1}{\sqrt{3}}\omega_1 \end{pmatrix}_{\mu\nu}, \quad (1.45)$$

and similarly for other multiplets. Before discussing the transformation properties for the resonance multiplets it is important to discuss shortly the possible formalisms which can be employed for describing the vector fields. There are two main possibilities how to describe the spin-one field: using the Proca field V_μ or an antisymmetric tensor field $R_{\mu\nu}$ (see Appendix in [24]). It is very well known fact that these formalisms are not trivially equivalent as we are in the effective field theory and some of the terms in one formalism can be of different order in other formalism. The most important fact is that without additional contact terms the effective Lagrangian starts at the order $O(p^6)$ for the Proca formalism whereas for $R_{\mu\nu}$ it starts at $O(p^4)$. We will be working here with the antisymmetric-tensor formalism. For another (third) possibility, the so-called first order formalism, see [25]. More detailed discussion on the equivalence of different formalisms, consistency and technical details see [26], [27].

	C	P
$V_{\mu\nu}$	$-V_{\mu\nu}^T$	$V_{\tilde{\mu}\tilde{\nu}}$
$A_{\mu\nu}$	$A_{\mu\nu}^T$	$-A_{\tilde{\mu}\tilde{\nu}}$
S	S^T	S
P	P^T	$-P$

TABLE 1.2: Charge and parity conjugation for nonets of vector, axial, scalar and pseudoscalar fields. The symbol tilde represents the change of sign for space indices (e.g. $V_{\tilde{0}\tilde{0}} = V_{00}$, $V_{\tilde{0}\tilde{1}} = -V_{01}$, $V_{\tilde{1}\tilde{2}} = V_{12}$).

We will demand that R transforms as nonet under $U(3)_V$. Nonlinear realization of group G is given by the prescription

$$R \rightarrow hRh^\dagger. \quad (1.46)$$

The transformation h plays a role of compensator in transformation of Goldstone bosons in the coset space. $R\chi T$ will be constructed as EFT which describes interactions of pseudoscalar mesons and resonances. Without having a natural mass gap it is not enough to use as an expansion parameter only the momenta, but we have to include also the expansion in the large number of colours. We want to build the most general Lagrangian, compatible with the symmetries of QCD. Besides the mentioned chiral transformation we have to consider also a charge and a parity conjugation (see Table 1.2).

Kinetic terms for vector and axial-vector resonances are fixed by the choice of the formalism. In our case we can write in the compact form

$$\mathcal{L}_{RR,\text{kin}} = -\frac{1}{2}\langle \nabla^\mu R_{\mu\nu} \nabla_\alpha R^{\alpha\nu} \rangle + \frac{1}{4}M_R^2 \langle R_{\mu\nu} R^{\mu\nu} \rangle + \frac{1}{2}\langle \nabla^\alpha \mathcal{R} \nabla_\alpha \mathcal{R} \rangle - \frac{1}{2}M_{\mathcal{R}}^2 \langle \mathcal{R} \mathcal{R} \rangle, \quad (1.47)$$

where R represents $V^{\mu\nu}$ or $A^{\mu\nu}$ while calligraphic \mathcal{R} stands for S or P .

The large N_c limit is important for the systematic ordering of further terms of resonance Lagrangian. According to the number of resonance fields we will talk about linear, quadratic, quartic, ... interaction terms. The study of linear $R\chi T$

was pursued in the seminal work of G. Ecker et al. [24]. It concerns these monomials:

$$\mathcal{L}_V = \frac{F_V}{2\sqrt{2}} \langle V_{\mu\nu} f_+^{\mu\nu} \rangle + \frac{iG_V}{2\sqrt{2}} \langle V_{\mu\nu} [u^\mu, u^\nu] \rangle \quad (1.48)$$

$$\mathcal{L}_A = \frac{F_A}{2\sqrt{2}} \langle A_{\mu\nu} f_-^{\mu\nu} \rangle \quad (1.49)$$

$$\mathcal{L}_S = c_d \langle S u^\mu u_\mu \rangle + c_m \langle S \chi_+ \rangle \quad (1.50)$$

$$\mathcal{L}_P = id_m \langle P \chi_- \rangle + i \frac{d_{m0}}{N_F} \langle P \rangle \langle \chi_- \rangle \quad (1.51)$$

The importance of these terms for ChPT lies in the fact that after integrating out the resonances we end up in saturation of LECs of $O(p^4)$, i.e. L_i (or l_i for $SU(2)$). What does it mean can be seen using the path integral, formally employing

$$\exp \left(i \int d^4x \mathcal{L}_{\chi PT} \right) = \int \mathcal{D}R \exp \left(i \int d^4x \mathcal{L}_{R\chi T} \right) \quad (1.52)$$

we have to obtain the same monomials as those that can be found in ChPT. The only difference is in constants which stand in front of these objects. For terms originating from $R\chi T$ these are combinations of resonance masses and parameters (coupling constants) of resonance Lagrangian, on the other hand, for ChPT these are LECs (e.g. L_i). By matching of both theories one gets relations for LECs by means of resonances. If we assume that nothing else contributes to LECs, we talk about the (full) saturation of constants by resonances. In the case of vector resonances we will get the following relations:

$$L_1 = \frac{G_V^2}{8M_V^2}, \quad L_2 = \frac{G_V^2}{4M_V^2}, \quad L_3 = -\frac{3G_V^2}{4M_V^2}, \quad L_9 = \frac{F_V G_V}{2M_V^2}, \quad L_{10} = -\frac{F_V^2}{4M_V^2}. \quad (1.53)$$

We can also continue to higher orders. The $O(p^6)$ saturation of the even sector was studied in [28]. In Section 2.3 we extend this procedure also to the odd sector.

The last possible and important step which we have not discussed yet is the connection with QCD at small distances. This is a region where QCD works in its standard perturbative expansion. As already stated, the fundamental objects of quantum field theory are Green functions of (for QCD, colourless) currents. On one hand we have the calculation within the perturbative QCD, on the other hand the calculation using the resonance Lagrangian. Comparing these two results we get in principle other nontrivial conditions for $R\chi T$ parameters. However, we

must be very careful to take the possible outcome without reservation. $R\chi T$ has its fundamental limitation (e.g. in finite number of resonances) which forbids to use it over the intermediate region. However, it seems that this formal matching with perturbative QCD can give us very interesting phenomenological results (see for example [29]).

It is natural to focus first on the simplest Green functions in the studied anomalous sector. These are the three-point Green functions, and one can show that there exist only five nontrivial combinations, namely: $\langle VVP \rangle$, $\langle VAS \rangle$, $\langle AAP \rangle$, $\langle VVA \rangle$ and $\langle AAA \rangle$. The first two are subject of Sec. 2.3, and the others are planned to be part of the diploma thesis of an author's student [30].

1.3 New methods

In the following two Subsections we want to present an introduction to Sections 2.4 and 2.5, respectively. The title 'New methods' was used to stress a different character in comparison with methods of the previous text. It is not so much the fact that the original works are the most recent in publications, but that these works are of different concept. While chiral perturbation theory and also resonance models can be viewed as standard tools for studying physics at low energies, here we want to outline methods whose phenomenological applications are not that clear. However, we believe that they are important from the theoretical point of view and can contribute to new discoveries about studied theories.

1.3.1 Renormalization in effective field theory: leading logarithms

At the end of Section 1.1 we have briefly sketched the problem of quantum corrections for ChPT. Here we would like to pursue this problem further, i.e. the problem of renormalization in EFT and study it from a different angle. The paradigm for the renormalization is the following procedure. The aim is to rewrite measured quantities by means of other physical observables rather than by direct use of parameters of Lagrangians. Let us imagine that we measure three quantities, X, Y, Z . In our effective theory we will have for simplicity just two parameters, f and l (for example from LO and NLO Lagrangian). The measured quantities X

and Y can be calculated in the theory with *given precision* (e.g. given by order NLO), we get $X = X(f, l)$, $Y = Y(f, l)$. Now we can make a prediction for Z , inverting the relations for X and Y , and thus obtaining the prescription for f, l by means of physical quantities. At the end of the day the parameter Z will be a function only of these physical and finite quantities. The crucial problem of EFTs is the expression “given precision”. It is both strong and weak point of any EFT. The reason is simple: either the theory is not accurate, has insufficient number of parameters, or the precision is satisfactory at the cost of introducing a huge number of parameters. Of course both cases are inconvenient and one can ask if it is possible to find an optimum. The situation is very complicated already at NNLO. In fact there are three possible contributions: 1) at LO: tree-level contributions; 2) at NLO: tree-level contributions from NLO Lagrangian and one-loop diagrams from LO Lagrangian 3) at NNLO: tree-level contributions from NNLO Lagrangian, one-loop diagrams from NLO Lagrangian and two loops from LO. It is difficult because of different nature of every contribution and different source of errors for every parameters, to estimate the speed of convergence of perturbative series. Some indicator can be found in the calculation of leading logarithms. Here we will briefly introduce this method, which will be further developed in the next chapter.

The leading logarithms (or LL for short) are logarithms with the highest power for the given order. In ChPT one can show this is \log^1 for one-loop level, \log^2 for two loops, etc. What is interesting about the leading logs is the fact that for their calculation we need to know only the form of LO Lagrangian. In fact it is a generalization of the Weinberg consistency relations for two-loop diagrams [13]. The full proof using the beta-function can be found in [31], alternative way of proof was used in [32]. Here we will show it only schematically.

For simplicity we will study a quantity, which depends only on one scale, let us denote it for example $F(M)$ (in the case of ChPT one can have in mind e.g. the pion decay constant, and the parameter is the mass of $O(p^2)$ Lagrangian). The calculation within the quantum field theory for $F(M)$ will be typically performed in the dimensional regularization (which brings up the subtraction scale μ). In the renormalizable theory we have a finite number of coupling constants and parameters, that after renormalization procedure lead to finite results. For simplicity, let us assume that there is only one such parameter, coupling constant α ; we can

anticipate the result in the following general form of expansion in α :

$$F = \alpha + \alpha^2 f_1^1 L + \alpha^2 f_0^1 + \alpha^3 f_2^2 L^2 + \alpha^3 f_1^2 L + \alpha^3 f_0^2 + O(\alpha^4). \quad (1.54)$$

The shorthand notation L represents a logarithm

$$L = \log(\mu/M). \quad (1.55)$$

(warning for the careful reader: unfortunately in the original papers in Chapter 2 we are not systematic in notation, L can stand for $\log(m^2/\mu^2)$ (Sec. 2.1), or $\frac{1}{(4\pi)^2} \log(m^2/\mu^2)$ (Sec. 2.2) or even $\frac{m^2}{16\pi^2 F^2} \log(\mu^2/m^2)$ (Sec. 2.4).)

A physical observable should be independent on the renormalization scale μ

$$\mu \frac{dF}{d\mu} = 0. \quad (1.56)$$

If we define the so-called beta function for parameter α , i.e we prescribe

$$\mu \frac{d\alpha}{d\mu} = \beta_0 \alpha^2 + \beta_1 \alpha^3 + \dots \quad (1.57)$$

the renormalization condition is fulfilled if

$$f_1^1 = -\beta_0, \quad f_2^2 = (\beta_0)^2, \quad f_3^3 = -(\beta_0)^3, \quad \dots \quad (1.58)$$

where we have also used the fact that divergences in quantum field theory should be local. These are the coefficients in front of the leading logs. This means that LL can be calculated from the one-loop beta function (β_0), in summary written as

$$f_i^i = (-1)^i (\beta_0)^i. \quad (1.59)$$

It is interesting to notice that such contributions can be summed over:

$$F \Big|_{\text{LL}} = \alpha + \sum_{i=1}^{\infty} \alpha^{i+1} f_i^i L^i = \alpha \sum_{i=0}^{\infty} \alpha^i (-1)^i (\beta_0)^i L^i = \frac{\alpha}{1 + \alpha \beta_0 L}, \quad (1.60)$$

which is well-known result for the running coupling constant. Let us recall that this result was obtained for a renormalizable theory. However, our subject of interest here are effective, non-renormalizable theories, in which case we cannot use the simple recursive formulae. For an effective field theory we have to write

generally:

$$F = F_0 + F_1^1 L + F_0^1 + F_2^2 L^2 + F_1^2 L + F_0^2 + \dots \quad (1.61)$$

The leading logarithms are terms with F_1^1, F_2^2, \dots i.e. F_i^i . Even though we cannot use the consequences of renormalization group, we can still show that LLs have special status, which relies on the fact that they can be calculated to all orders only by using the one-loop graphs. Schematically, this procedure can be described as follows.

We will focus on probably the simplest physical object which is naturally the physical mass. Again we can be more specific, and work for example in $SU(2)$ ChPT, however, we will describe only the general recipe without going into technical details. Our starting Lagrangian is the lowest order of effective theory, which we can denote as nonlinear sigma model ($n\sigma$). This is $O(p^2)$ in ChPT, here denoted as ‘zeroth’ order (zero number of loops). The given Lagrangian can generate any even number of legs, schematically

$$\mathcal{L}_{n\sigma} \Rightarrow \boxed{0}$$

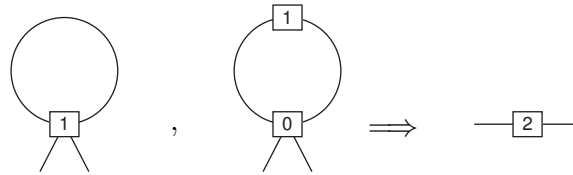
The mass can be represented by the two-point Green function, at lowest-order:

$$\text{---}\boxed{0}\text{---} \Leftrightarrow M_\pi = M$$

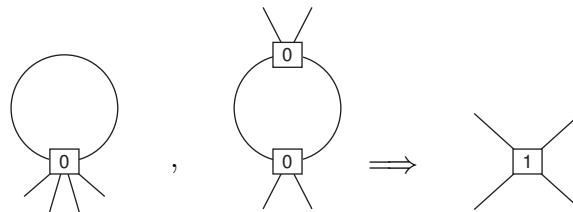
(it is natural to set the convention of LO Lagrangian so that the parameter M corresponds directly to physical mass). At the next order, i.e. at one loop, there is only one possible way how to draw the contribution to the two-point function (see below). Such tadpole graph is singular and must be renormalized. As already stated in Sec. 1.1 the necessary constant (counter-term) is hidden in the next-order Lagrangian. However, we do not know the explicit form of it (we assume that the only thing we have in hands is $\mathcal{L}_{n\sigma}$). We have to construct such Lagrangian, or equivalently just the Feynman rule for the corresponding vertex. Schematically up to NLO:

The diagram shows a tadpole graph on the left, consisting of a circle (loop) attached to a vertex labeled '0' in a box. Two lines extend downwards from this vertex. This is followed by a double-lined arrow pointing to the right, where a vertex labeled '1' in a box is shown with two lines extending horizontally from it.

At the next order, NNLO, the situation is naturally more complex. We can draw two diagrams, and again we can fix the form of the counterterm, schematically:

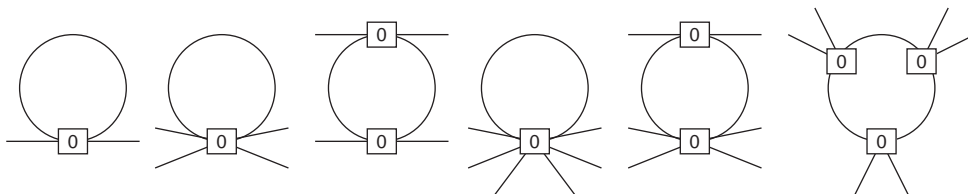

(1.62)

This is not the whole story for this order. The second diagram can be calculated without problem. Indeed, we know the vertex with ‘0’ with any number of legs and the vertex ‘1’ with two particles was obtained and defined in the previous step. What we are missing, however, is the vertex for the first diagram, i.e. ‘1’ with four particles. At this moment it only remains to calculate it and define:


(1.63)

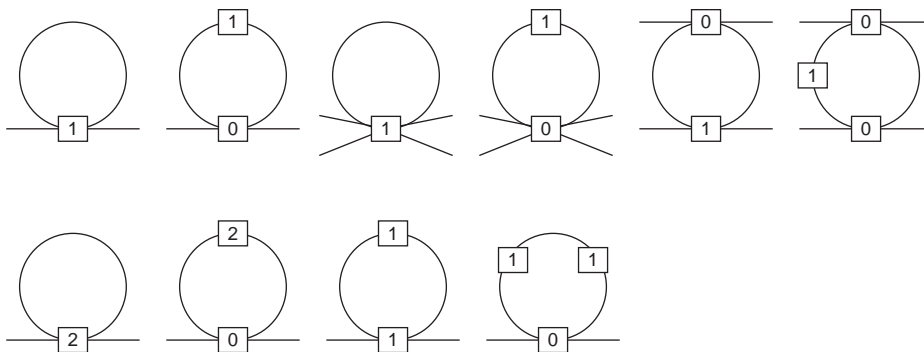
Now everything is known in order to obtain LL^2 (cf. diagrammatic relation (1.62)).

The nonexistence of the nonlocal divergences ensures that the mentioned procedure can be used to calculate the leading logs (but, of course, not the complete result). The following steps for higher orders are now clear: for the given Green function (here two-point) up to a given order it is necessary to calculate all one-loop diagrams with all possible insertions of interacting vertices. This also means that we have to calculate new Green function with higher number of legs (but of lower order). Let us mention here the next step, i.e. all diagrams needed to calculate LLs for the mass corrections up to NNNLO



i	number of graphs	result c_i
1	1	$-1 c$
2	5	$17/2 c^2$
3	16	$-103/3 c^3$
4	45	$24367/72 c^4$
5	116	$-17642/9 c^5$
6	303	$1922964667/97200 c^6$
7	790	$-1804453729667/13395375 c^7$

TABLE 1.3: Calculation of LL to the correction of pion mass. We have introduced a constant $c = \frac{M^2}{16\pi^2 F^2}$.



Let us remind that in a full calculation this is equivalent to the tree-loop order.

The process of this calculation up to LL^3 was shown here mainly for illustration purposes. Nevertheless, on a point of order, we will also show the result. Let us remind that this result represents leading-log contributions to the physical mass of pion in two-flavour ChPT, i.e.

$$M_\pi^2 = M^2(1 + c_1 L + c_2 L^2 + \dots). \quad (1.64)$$

The individual coefficients up to the seven-loop order are summarized in Tab. 1.3.

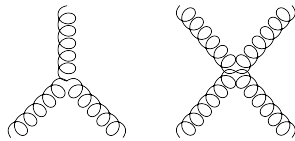
1.3.2 Analytic properties: tree-level diagrams

The non-linear $SU(N)$ sigma model, which is the principal model for all works presented here, plays important role also in other areas of theoretical particle physics. Probably the most important phenomenological application is the low energy QCD, i.e. the area of the previous subsections. We have shown how to systematize this effective theory in the framework of ChPT and order by order

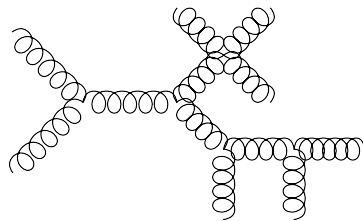
improve the eventual calculations and predictions. In the recent 20 years² there was a huge activity in calculating different processes up to NNLO order (i.e. including two-loop graphs) and one calculation will be also presented in the next Chapter. It is interesting to notice that one direction – technically similarly complicated – was left out from the mainstream. This direction is connected with studies of tree-level diagrams with higher number of particles. As a detailed and dedicated introduction to this problem in the framework of the non-linear sigma model can be found in Section 2.5, we will focus here merely on the motivation which stood behind the idea of calculating tree-level diagrams using new methods.

The studied area will be again QCD, more precisely the gluonic sector of high-energy amplitude. We will focus on calculation of tree level n -point gluon amplitudes (without fermions). Using the standard methods we can divide the calculations into the following steps:

- We will consider all possible elementary interaction vertices, in this case: three- and four-point:



- construct all allowed Feynman diagrams; for example one of such contributions for eight-point diagram:



We can see that even though we are calculating ‘only’ tree-level diagrams, the problem is complicated already for relatively small number of external legs. For our example of eight-gluon scattering, the above explicitly mentioned example is only one of 34300 diagrams needed for the complete amplitude. What is interesting is the fact that after long and tedious calculations with long algebraic expressions we end up with a relatively simple and in some special cases even trivial answer. Indeed, in the so-called helicity formalism we can express all (!) tree level graphs

²The first full two-loop calculation was done for the process $\gamma\gamma \rightarrow \pi^0\pi^0$ published in [33] in 1994.

for the maximally helicity violating amplitudes in one closed formula [34]

$$A_n(- - + \dots +) = \frac{\langle 12 \rangle^4}{\langle 12 \rangle \langle 23 \rangle \dots \langle n1 \rangle}, \quad (1.65)$$

where

$$\langle ij \rangle = \sqrt{|2p_i \cdot p_j|} e^{i\phi_{ij}}. \quad (1.66)$$

This unexpected simplicity was one of the main motivation of the current studies of scattering amplitudes. In the following we will briefly summarize a method BCFW (named after Britto, Cachazo, Feng and Witten [35], [36]) recurrence relations for physical (on-shell) tree-level amplitudes. These relations reconstruct the result by means of basic analytic properties.

In the first step we will define the colour ordered stripped amplitude

$$M^{a_1 \dots a_n}(p_1, \dots, p_n) = \sum_{\sigma \in Z_n} \text{Tr}(t^{a_{\sigma(1)}} \dots t^{a_{\sigma(n)}}) M_\sigma(p_1, \dots, p_n) \quad (1.67)$$

The number of stripped diagrams is naturally smaller than the original number of all colour combinations. (For eight-point amplitude this number is 654.) It is probably of some interest to stress one possible geometrical interpretation of these diagrams and their number. This is due to Susskind and Frye [37]: for the n -point scattering amplitude it is possible to connect the number of diagrams with the number of ways how to divide the polygon (more precisely n -gon) with the non-crossing diagonals so that the resulting objects have the number of sides equal to the allowed number of vertices (3 or 4 for gluons). For the sake of clarity let us show one example that concerns gluons, for simplicity the scattering of six gluons – see the Fig. 1.1

The possibility to order the amplitudes is important for the following discussion. We will be interested in the pole structure of amplitudes. The only possible poles of the ordered tree-level diagrams are:

$$P_{ij}^2 = (p_i + p_{i+1} + \dots + p_{j-1} + p_j)^2. \quad (1.68)$$

Using the one-particle unitarity (so-called Weinberg theorem [13]) we can separate left and right amplitude. In fact, if we sit at the factorization channel we get

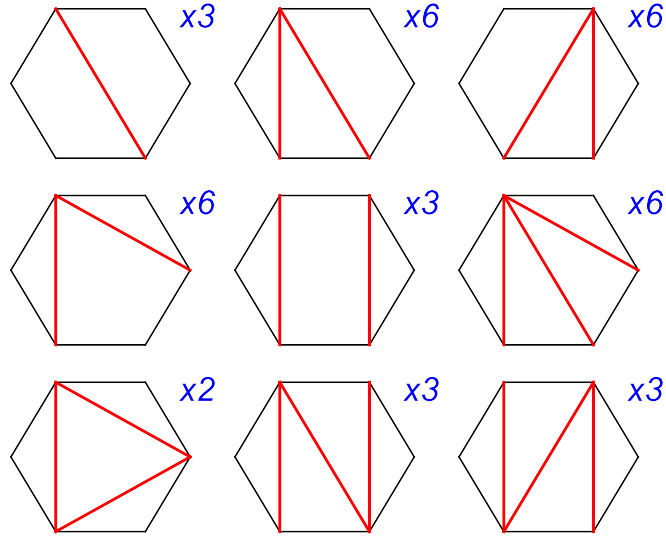


FIGURE 1.1: Representation of tree-level diagrams for six gluons (for example $ggg \rightarrow ggg$) by means of hexagon. Altogether we have 38 diagrams (cf. also Tab. 1.4 below).

schematically

$$\lim_{P_{1j}^2 \rightarrow 0} M(1, 2, \dots, n) = \sum_{h_l} M_L(1, 2, \dots, j, l) \cdot \frac{i}{P_{1j}^2} \cdot M_R(l, j+1, \dots, n). \quad (1.69)$$

The last expression is self-evidently a trivial consequence of Feynman diagrammatic representation, see Fig. 1.2).

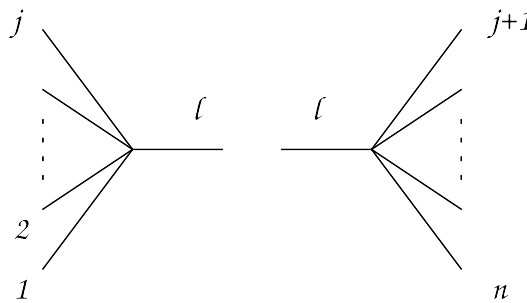


FIGURE 1.2: A representation of the factorization for $P_{1j}^2 \rightarrow 0$.

Our objective is to reconstruct the amplitude using its poles in the complex plane. In order to get complex parameters into the game we will use the following trick. We will shift *two* external momenta p_i a p_j

$$p_i \rightarrow p_i + zq, \quad p_j \rightarrow p_j - zq, \quad (1.70)$$

so that both p_i and p_j stay on-shell (n.b. gluons are massless particles), i.e.

$$q^2 = q \cdot p_i = q \cdot p_j = 0. \quad (1.71)$$

The amplitude will thus become a meromorphic function $A(z)$ of complex parameter z . Taking $z = 0$ one can obtain the original function and the wanted amplitude. It is important to realize that we can have only simple poles that correspond to $P_{ab}(z)$. Employing the Cauchy's theorem one can get

$$\frac{1}{2\pi i} \int \frac{dz}{z} A(z) = A(0) + \sum_k \frac{\text{Res}(A, z_k)}{z_k}. \quad (1.72)$$

Provided that $A(z)$ vanishes for $z \rightarrow \infty$ we will obtain the original amplitude as a trivial consequence of this theorem:

$$A = A(0) = - \sum_k \frac{\text{Res}(A, z_k)}{z_k}. \quad (1.73)$$

The complex propagator can be equal to zero, $P_{ab}^2(z) = 0$, only under the condition that one and only one of the shifted momenta is in $(a, a + 1, \dots, b)$. The solution is given by

$$z_{ab} = - \frac{P_{ab}^2}{2(q \cdot P_{ab})} \quad (1.74)$$

and assuming only allowed combinations of helicities, the amplitude will factorize to two sub-amplitudes:

$$\text{Res}(A, z_{ab}) = \sum_s A_L^{-s}(z_{ab}) \frac{i}{2(q \cdot P_{ab})} A_R^s(z_{ab}). \quad (1.75)$$

Using the Cauchy's theorem we have finally:

$$A = \sum_{k,s} A_L^{-s_k}(z_k) \frac{i}{P_k^2} A_R^{s_k}(z_k). \quad (1.76)$$

To summarize the result: using the two-line shift we have obtained simple recurrence relations where the base is a three-point amplitude. The number of relevant terms is small and is equal to number of factorization channels. What is also important, that all inputs are on-shell (though complex). The efficiency of this method is obvious from the following table (Tab. 1.4) which summarizes the number of relevant diagrams in the given scheme.

n	3	4	5	6	7	8
# diagrams (inc. crossing)	1	4	25	220	2485	34300
# diagrams (col.ordered)	1	3	10	38	154	654
# BCFW terms	–	1	2	3	6	20

TABLE 1.4: Number of diagrams for n -point gluon amplitude at the tree-level

1.4 Summary

This thesis presents in the subsequent pages five original papers of the author created between years 2009 and 2013. They are theoretical works dealing with both phenomenological and theoretical questions connected with effective field theories at low energies. First work focuses on the decay process $\pi^0 \rightarrow \gamma\gamma$, which is a very important process for the history of particle theory itself. New experimental activity in PrimEx experiment at JLab (Newport News, USA) was the main motivation why the calculation at the two-loop order for this process was started. However, also some theoretical questions were also asked in connection with it and were successfully worked out within this project. Second article is natural continuation in this direction and enlarges the possible application also for the process $\eta \rightarrow \gamma\gamma$, though for the moment only in the simplified $SU(3)$ limit. The calculation in the full three-flavour ChPT which is also needed by experimentalists is in preparation [38]. Both processes $\pi^0 \rightarrow \gamma\gamma$ and $\eta \rightarrow \gamma\gamma$ represent processes from the so-called odd-intrinsic sector. This sector within ChPT, being shifted by one order (it starts at $O(p^4)$), is naturally not that known and examined as the even sector. The possible contribution in this respect is the third and fourth article. The former deals with the resonance saturations for low-energy constants in the odd sector. The latter studies the so-called leading logarithms not only for already mentioned process $\pi \rightarrow \gamma\gamma$ but also for another important process of the two-flavour anomalous sector $\pi\gamma \rightarrow \pi\pi$. The last article contributes to another important subject, which are tree-level diagrams for pseudoscalar bosons. This is studied from a completely different perspective and shown that it is possible to reconstruct here all tree-level diagrams with modified BCFW-like reconstruction. This demonstrates possibility to use new modern on-shell methods also in the case of effective field theories.

The non-linear sigma model is thus the starting point for many different approaches which can help us to understand the current experimental activities in the low

energy hadron sector. It can also have an impact on completely different areas of theoretical physics (e.g. for new theories beyond the standard model, cosmology etc.). This can be also demonstrated by the author's latest projects (cf. e.g. [39], [40]).

References

- [1] S. Aoki, Y. Aoki, C. Bernard, T. Blum, G. Colangelo, M. Della Morte, S. Dürer and A. X. El Khadra *et al.*, Eur. Phys. J. C **74** (2014) 2890 [arXiv:1310.8555 [hep-lat]].
- [2] S. L. Adler, Phys. Rev. **177** (1969) 2426; J. S. Bell and R. Jackiw, Nuovo Cim. A **60** (1969) 47.
- [3] J. Goldstone, Nuovo Cim. **19** (1961) 154.
- [4] C. Vafa and E. Witten, Nucl. Phys. B **234** (1984) 173.
- [5] G. 't Hooft, C. Itzykson, A. Jaffe, H. Lehmann, P. K. Mitter, I. M. Singer and R. Stora, NATO Sci. Ser. B **59** (1980) pp.1.
- [6] W. A. Bardeen, Phys. Rev. **184** (1969) 1848.
- [7] S. R. Coleman, J. Wess and B. Zumino, Phys. Rev. **177** (1969) 2239.
- [8] C. G. Callan, Jr., S. R. Coleman, J. Wess and B. Zumino, Phys. Rev. **177** (1969) 2247.
- [9] M. Knecht and J. Stern, 2nd DAPHNE Physics Handbook:169-190 [hep-ph/9411253].
- [10] S. Descotes-Genon, N. H. Fuchs, L. Girlanda and J. Stern, Eur. Phys. J. C **24** (2002) 469 [hep-ph/0112088].
- [11] S. Descotes-Genon, N. H. Fuchs, L. Girlanda and J. Stern, Eur. Phys. J. C **34** (2004) 201 [hep-ph/0311120].
- [12] M. Kolesar and J. Novotny, arXiv:1409.3380 [hep-ph].
- [13] S. Weinberg, Physica A **96** (1979) 327.

-
- [14] J. Gasser and H. Leutwyler, *Annals Phys.* **158** (1984) 142.
- [15] J. Gasser and H. Leutwyler, *Nucl. Phys. B* **250** (1985) 465.
- [16] J. Bijnens, G. Colangelo and G. Ecker, *JHEP* **9902** (1999) 020 [hep-ph/9902437].
- [17] J. Wess and B. Zumino, *Phys. Lett. B* **37** (1971) 95.
- [18] E. Witten, *Nucl. Phys. B* **160** (1979) 57.
- [19] R. Kaiser, *Phys. Rev. D* **63** (2001) 076010 [hep-ph/0011377].
- [20] Y. Nambu and G. Jona-Lasinio, *Phys. Rev.* **122** (1961) 345.
- [21] M. Bando, T. Kugo, S. Uehara, K. Yamawaki and T. Yanagida, *Phys. Rev. Lett.* **54** (1985) 1215.
- [22] M. Bando, T. Kugo and K. Yamawaki, *Phys. Rept.* **164** (1988) 217.
- [23] G. 't Hooft, *Nucl. Phys. B* **72** (1974) 461.
- [24] G. Ecker, J. Gasser, A. Pich and E. de Rafael, *Nucl. Phys. B* **321** (1989) 311.
- [25] K. Kampf, J. Novotny and J. Trnka, *Eur. Phys. J. C* **50** (2007) 385 [hep-ph/0608051].
- [26] G. Ecker, J. Gasser, H. Leutwyler, A. Pich and E. de Rafael, *Phys. Lett. B* **223** (1989) 425.
- [27] K. Kampf, J. Novotny and J. Trnka, *Phys. Rev. D* **81** (2010) 116004 [arXiv:0912.5289 [hep-ph]].
- [28] V. Cirigliano, G. Ecker, M. Eidemuller, R. Kaiser, A. Pich and J. Portoles, *Nucl. Phys. B* **753** (2006) 139 [hep-ph/0603205].
- [29] M. Knecht and A. Nyffeler, *Eur. Phys. J. C* **21** (2001) 659 [hep-ph/0106034].
- [30] T. Kadavý, “*Green functions of currents in the odd-intrinsic parity sector of QCD*,” diploma thesis, in preparation
- [31] M. Buchler and G. Colangelo, *Eur. Phys. J. C* **32** (2003) 427 [hep-ph/0309049].

-
- [32] J. Bijnens and L. Carloni, Nucl. Phys. B **827** (2010) 237 [arXiv:0909.5086 [hep-ph]].
- [33] S. Bellucci, J. Gasser and M. E. Sainio, Nucl. Phys. B **423** (1994) 80 [Nucl. Phys. B **431** (1994) 413] [hep-ph/9401206].
- [34] S. J. Parke and T. R. Taylor, Phys. Rev. Lett. **56** (1986) 2459.
- [35] R. Britto, F. Cachazo and B. Feng, Nucl. Phys. B **715** (2005) 499 [hep-th/0412308].
- [36] R. Britto, F. Cachazo, B. Feng and E. Witten, Phys. Rev. Lett. **94** (2005) 181602 [hep-th/0501052].
- [37] L. Susskind and G. Frye, Phys. Rev. D **1** (1970) 1682.
- [38] J. Bijnens and K. Kampf, *in preparation*
- [39] K. Kampf and J. Novotny, JHEP **1410** (2014) 006 [arXiv:1403.6813 [hep-th]].
- [40] C. Cheung, K. Kampf, J. Novotny and J. Trnka, arXiv:1412.4095 [hep-th].

Chapter 2

Original works

2.1 Chiral expansions of the π^0 lifetime

K. Kampf, B. Moussallam, *Chiral expansions of the π^0 lifetime*, Phys. Rev. D **79**, 076005 (2009). [arXiv:0901.4688 [hep-ph]]

PHYSICAL REVIEW D **79**, 076005 (2009)**Chiral expansions of the π^0 lifetime**Karol Kampf^{*}*Paul Scherrer Institut, CH-5232 Villigen PSI, Switzerland and IPNP, Faculty of Mathematics and Physics, Charles University, V Holešovičkách 2, CZ-180 00 Prague 8, Czech Republic*Bachir Moussallam[†]*Groupe de Physique Théorique, Institut de Physique Nucléaire, Université Paris-Sud 11, F-91406 Orsay, France*
(Received 13 March 2009; published 14 April 2009)

The corrections induced by light quark masses to the current algebra result for the π^0 lifetime are reexamined. We consider next-to-next-to-leading order corrections and we compute all the one-loop and the two-loop diagrams which contribute to the decay amplitude at this order in the two-flavor chiral expansion. We show that the result is renormalizable, as Weinberg consistency conditions are satisfied. We find that chiral logarithms are present at this order unlike the case at next-to-leading order. The result could be used in conjunction with lattice QCD simulations, the feasibility of which was recently demonstrated. We discuss the matching between the two-flavor and the three-flavor chiral expansions in the anomalous sector at order one-loop and derive the relations between the coupling constants. A modified chiral counting is proposed, in which m_s counts as $O(p)$. We have updated the various inputs needed and used this to make a phenomenological prediction.

DOI: [10.1103/PhysRevD.79.076005](https://doi.org/10.1103/PhysRevD.79.076005)

PACS numbers: 11.30.Rd, 12.39.Fe, 13.40.Hq, 12.15.Ff

I. INTRODUCTION

The close agreement between the current algebra prediction for the lifetime of the neutral pion and experiment is one of the two compelling experimental signatures, together with the Nambu-Goldberger-Treiman relation, for the spontaneous breaking of chiral symmetry in QCD. There is an ongoing effort by the PrimEx collaboration [1] to improve significantly the accuracy of the lifetime measurement, which is now around 8%, down to the 1%–2% level. This motivates us to study the corrections to the current algebra prediction.

Starting with the detailed study by Kitazawa [2], this problem has been addressed several times in the literature [3–11]. The approach used in Ref. [2] was to extrapolate from the soft pion limit to the physical pion mass result using the Pagels-Zepeda [12] sum rule method. This was reconsidered in Ref. [10], who implemented a more elaborate treatment of $\pi^0 - \eta - \eta'$ mixing and also recently in Ref. [11]. The latter work shows some disagreement concerning the size of the η' meson contribution in the sum rule as compared to earlier results.

In this paper, we reconsider the issue of the corrections to the current algebra result to the $\pi^0 \rightarrow 2\gamma$ amplitude from the point of view of a strict expansion as a function of the light quark masses. This is most easily implemented by using chiral Lagrangian methods (see e.g. [13] for a review). The same framework also allows one to compute radiative corrections [14]. We believe that it is somewhat easier to control the size of the errors in this kind of

approach, which is important for exploiting the forthcoming high experimental accuracy. Another interest in deriving a quark mass expansion is the ability to perform comparisons with lattice QCD results where quark masses can be varied. The feasibility of computing the π^0 to two photon amplitude in lattice QCD has been studied very recently [15].

A priori, it is expected that one can make use of $SU(2)$ ChPT, i.e. expand as a function of m_u, m_d without making any assumption concerning m_s (except that it is heavier than m_u, m_d). In $SU(2)$ ChPT it is often the case that chiral logarithms provide a reasonable order of magnitude for the size of the chiral corrections. This is the case, for instance, for the $\pi\pi$ scattering amplitude [16,17]. It was observed in Refs. [3,4] that there was no chiral logarithm in the next-to-leading order (NLO) correction to the π^0 lifetime once the amplitude is expressed in terms of the physical value of F_π . We have asked ourselves whether chiral logarithms are present in the NNLO corrections. At this order, the coefficient of the double chiral logarithm depends only on F_π . Depending on its numerical coefficient, such a term could modify the NLO results. In order to obtain this coefficient it is, in principle, sufficient to compute a set of one-loop graphs containing one divergent NLO vertex [18]. For completeness, we will perform a complete calculation of the two-loop graphs as well. This is described in Sec. III.

In the framework of two-flavor ChPT, however, one faces the practical problem that the polynomial terms in m_u, m_d at NLO involve a number of low-energy couplings (LEC's) which are not known. We will show that it is possible to make estimates for the relevant combinations, and then make quantitative predictions for the π^0 decay, under the minimal additional assumption that the mass of

^{*}karol.kampf@psi.ch[†]moussall@ipno.in2p3.fr

KAROL KAMPF AND BACHIR MOUSSALLAM

the strange quark is sufficiently small, justifying a chiral expansion in m_s . We will obtain the first two terms in the m_s expansion of the NLO $SU(2)$ LEC's. The result can be implemented in association with a modified chiral counting scheme, in which m_s is counted as $O(p)$, which respects the hierarchy $m_u, m_d \ll m_s$. This leads to simpler formulas than previously obtained. Finally, we will update all the inputs needed to compute the lifetime.

II. LEADING AND NEXT-TO-LEADING ORDERS IN THE $SU(2)$ EXPANSION

In the odd-intrinsic-parity sector, the Lagrangian of lowest chiral order has order p^4 , it is the Wess-Zumino [19] Lagrangian, \mathcal{L}^{WZ} , which form is dictated by the ABJ anomaly [20]. Writing the $\pi^0 \rightarrow \gamma(k_1)\gamma(k_2)$ decay amplitude in the form

$$\mathcal{T} = e^2 \epsilon(e_1^*, k_1, e_2^*, k_2) T, \quad (1)$$

a tree level computation of the pion decay amplitude gives the well known result

$$\begin{aligned} \mathcal{L}_{6,N_f=2}^W = & \epsilon^{\alpha\beta\mu\nu} \{ c_1^W \langle \chi_+ [f_{-\mu\nu}, u_\alpha u_\beta] \rangle + c_2^W \langle \chi_- [f_{+\mu\nu}, u_\alpha u_\beta] \rangle + c_3^W i \langle \chi_- f_{+\mu\nu} f_{+\alpha\beta} \rangle + c_4^W i \langle \chi_- f_{-\mu\nu} f_{-\alpha\beta} \rangle \\ & + c_5^W i \langle \chi_+ [f_{+\mu\nu}, f_{-\alpha\beta}] \rangle + c_6^W \langle f_{+\mu\nu} \rangle \langle \chi_- u_\alpha u_\beta \rangle + c_7^W i \langle f_{+\mu\nu} \rangle \langle f_{+\alpha\beta} \chi_- \rangle + c_8^W i \langle f_{+\mu\nu} \rangle \langle f_{+\alpha\beta} \rangle \langle \chi_- \rangle \\ & + c_9^W i \langle f_{+\gamma\mu} \rangle \langle h^\nu_{\nu} u_\alpha u_\beta \rangle + c_{10}^W i \langle f_{+\mu}^\gamma \rangle \langle f_{-\gamma\nu} u_\alpha u_\beta \rangle + c_{11}^W \langle f_{+\mu\nu} \rangle \langle f_{+\gamma\alpha} h^\gamma_{\beta} \rangle + c_{12}^W \langle f_{+\mu\nu} \rangle \langle f_{+\alpha}^\gamma f_{-\gamma\beta} \rangle \\ & + c_{13}^W \langle \nabla^\gamma f_{+\gamma\mu} \rangle \langle f_{+\nu\alpha} u_\beta \rangle \}. \end{aligned} \quad (3)$$

The relations between the bare and the renormalized couplings may be written as [23]

$$c_i^W = c_i^{Wr}(\mu) + \eta_i^W \frac{(c\mu)^{d-4}}{16\pi^2(d-4)} \quad (4)$$

with $\log(c) = -(\log(4\pi) - \gamma + 1)/2$ as usual in ChPT (note that the couplings c_i^{Wr} have dimension $(\text{mass})^{-2}$). The coefficients η_i^W vanish for $i = 1 \dots 5$ and the remaining ones read [23]

$$\begin{aligned} \eta_6^W = 3\alpha, & \quad \eta_7^W = 3\alpha, & \quad \eta_8^W = -\frac{3}{2}\alpha, \\ \eta_9^W = 6\alpha & \quad \eta_{10}^W = -18\alpha, & \quad \eta_{11}^W = 12\alpha, \\ \eta_{12}^W = 0, & \quad \eta_{13}^W = -12\alpha, \end{aligned} \quad (5)$$

with

$$\alpha = 1/(384\pi^2 F^2). \quad (6)$$

The above results for η_i^W were obtained by using, in the ordinary sector at p^4 , the chiral Lagrangian term proportional to l_4 which differs from the form originally used in Ref. [25]

$$\mathcal{L}_{l_4}^{(\text{orig})} = \frac{i l_4}{4} \langle u^\mu \chi_{\mu-} \rangle \quad (7)$$

PHYSICAL REVIEW D **79**, 076005 (2009)

$$T_{\text{LO}} = \frac{1}{4\pi^2 F}, \quad (2)$$

where F is the pion decay constant in the two-flavor chiral limit $m_u = m_d = 0$. At leading order one can set $F = F_\pi$ in Eq. (2). According to the Weinberg rules [18] for ChPT, the NLO corrections are generated from:

- One-loop diagrams with one vertex taken from \mathcal{L}^{WZ} and other vertices from the $O(p^2)$ chiral Lagrangian. These diagrams were first computed in Refs. [3,4].
- Tree diagrams having one vertex from \mathcal{L}^{WZ} and one vertex from the $O(p^4)$ chiral Lagrangian.
- Tree diagrams from the $O(p^6)$ Lagrangian in the anomalous-parity sector, $\mathcal{L}_{(6)}^W$.

The classification of a minimal set of independent terms in this Lagrangian was initiated in Refs. [21,22]. We will use here the result of Ref. [23] who further reduced the set to 23 terms in the case of three flavors and to 13 independent terms in the case of two flavors (this result was also obtained in Ref. [24]). The list, in the case of two flavors, is recalled below:

by a term proportional to the equation of motion

$$\mathcal{L}_{l_4} = \mathcal{L}_{l_4}^{(\text{orig})} + \frac{i l_4}{4} \left\langle \hat{\chi}_- \left(\nabla_\mu u^\mu - \frac{i}{2} \hat{\chi}_- \right) \right\rangle. \quad (8)$$

If one uses $\mathcal{L}_{l_4}^{(\text{orig})}$ then, in the odd-intrinsic-parity sector, the coefficients with labels 6, 7, and 8 are modified to \tilde{c}_i^W [7,26]. The relations between \tilde{c}_i^W and c_i^W are easily worked out by performing a field redefinition,

$$\begin{aligned} \tilde{c}_6^W = c_6^W - \frac{N_c}{128\pi^2} \frac{l_4}{F^2} & \quad \tilde{c}_7^W = c_7^W + \frac{N_c}{256\pi^2} \frac{l_4}{F^2} \\ \tilde{c}_8^W = c_8^W - \frac{N_c}{512\pi^2} \frac{l_4}{F^2}. \end{aligned} \quad (9)$$

In the present work, we use the original $\mathcal{L}_{l_4}^{(\text{orig})}$ in our calculations but we will express the final result in terms of c_i^{Wr} rather than \tilde{c}_i^{Wr} , making use of the relations (9) [which will prove slightly more convenient below when we perform a matching with the $SU(3)$ expansion].

Returning to the π^0 decay amplitude, the contributions from the one-loop Feynman diagrams can be shown to be absorbed into the reexpression of F into F_π [3,4], the physical pion decay constant at order p^4 , such that the decay amplitude including the NLO corrections reads

CHIRAL EXPANSIONS OF THE π^0 LIFETIME

$$T_{\text{LO+NLO}} = \frac{1}{F\pi} \left\{ \frac{1}{4\pi^2} + \frac{16}{3} m_\pi^2 (-4c_3^{Wr} - 4c_7^{Wr} + c_{11}^{Wr}) + \frac{64}{9} B(m_d - m_u)(5c_3^{Wr} + c_7^{Wr} + 2c_8^{Wr}) \right\}, \quad (10)$$

where $B = -\lim_{m_u=m_d=0} \langle \bar{u}u \rangle / F^2$ and m_π^2 denotes the mass squared of the neutral pion which, at this order, is equal to $M^2 = B(m_d + m_u)$. Equation (10) shows that the decay amplitude at NLO receives a contribution proportional to the isospin breaking mass difference $m_d - m_u$. As can be seen from Eqs. (5) the two combinations of chiral couplings which enter into the expression of T_{NLO} are finite. The expression of $T_{\text{LO+NLO}}$ therefore involves no chiral logarithm. The chiral corrections to the current algebra result are purely polynomial in m_u , m_d and are controlled by four coupling constants from Eq. (3). In order to estimate quantitatively the effects of the NLO corrections, we will show below that it is useful to express these couplings as an expansion in powers of the strange quark mass. Before doing so, let us now investigate the presence of chiral logarithms, which could possibly be numerically important, in the NNLO corrections.

III. π^0 DECAY TO NNLO IN THE TWO-FLAVOR EXPANSION

We must calculate now a) the one-loop Feynman diagrams with one vertex involving an NLO chiral coupling, either l_i or c_i^W and b) the two-loop Feynman diagrams with one vertex taken from the LO Wess-Zumino Lagrangian and the other one taken from the $O(p^2)$ chiral Lagrangian. It is convenient to use the following representation for the chiral field

$$U = \sigma + i \frac{\vec{\tau} \cdot \vec{\pi}}{F}, \quad \sigma = \sqrt{1 - \frac{\vec{\pi}^2}{F^2}} \quad (11)$$

(since, in this representation, there is no $\gamma 4\pi$ vertex at LO). At the order considered, all the reducible diagrams are generated from wave function renormalization. The expression for the WF renormalization constant Z [corresponding to (11)] was first given by Burgi [27],

$$Z^{1/2} = 1 - \frac{T_M}{2F^2} + \frac{1}{F^4} \left[-\frac{1}{8} T_M^2 + \frac{M^4}{2} \times \left(r_Z + \dot{T}_M^2 Q^Z - \dot{T}_M \sum_{i=1}^3 l_i Q_i^Z \right) + B^2(m_d - m_u)^2 \times (-8F^2(c_7 + c_9) + \dot{T}_M l_7) \right] \quad (12)$$

with

$$T_M = \frac{(M^2)^{(d/2)-1} \Gamma(1 - \frac{d}{2})}{(4\pi)^{d/2}}, \quad \dot{T}_M = \frac{dT_M}{dM^2}, \quad (13)$$

PHYSICAL REVIEW D **79**, 076005 (2009)

($d = 4 + 2w$). We have indicated explicitly here the contributions proportional to $(m_d - m_u)^2$ for completeness because isospin breaking contributions play an important role for the π^0 decay amplitude. We will also need the expression for the chiral expansion of F_π at order p^6 (from [28])

$$\frac{F_\pi}{F} = 1 + \frac{1}{F^2} [M^2 l_4 - T_M] + \frac{M^4}{F^4} \left[r_F + \dot{T}_M^2 Q^F - \dot{T}_M \sum_{i=1}^4 l_i Q_i^F \right] + \frac{8B^2(m_d - m_u)^2}{F^2} (c_7 + c_9). \quad (14)$$

The numerical parameters Q^Z and Q^F which appear above read

$$Q^Z = \frac{1}{96}(96 - 464w + 1185w^2), \quad (15)$$

$$Q^F = -\frac{1}{192}(240 - 656w + 1125w^2)$$

and will need the following relations obeyed by the numerical parameters Q_i^Z and Q_i^F

$$Q_1^F = \frac{-1}{2} Q_1^Z, \quad Q_2^F = \frac{-1}{2} Q_2^Z, \quad (16)$$

$$Q_3^F = Q_3^Z = 2, \quad Q_4^F = \frac{1}{2(1+w)}.$$

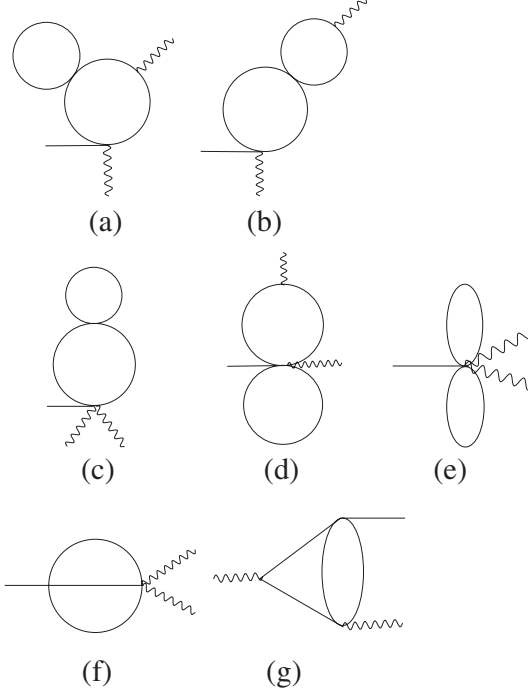
Finally, the entries r_Z and r_F in Eqs. (12) and (14) represent combinations of coupling constants from the $O(p^6)$ chiral Lagrangian. The π^0 amplitude involves the combination $r_Z + 2r_F$ which is expressed in terms of a single p^6 coupling, called c_6 in the classification of Ref. [29]

$$r_Z + 2r_F = -64F^2 c_6. \quad (17)$$

The two-loop one-particle irreducible diagrams which one must compute [using the representation (11)] are shown in Fig. 1. It turns out to be possible to express all of them analytically in terms of known special functions by combining the methods exposed in Ref. [30] with integration by parts methods. We give the results corresponding to the two diagrams (f) and (g), which are the most difficult ones, in Appendix A.

Collecting all the pieces together, we find that the expression for the NNLO contribution to the π^0 decay amplitude into two photons has the following expression,

KAROL KAMPF AND BACHIR MOUSSALLAM

PHYSICAL REVIEW D **79**, 076005 (2009)FIG. 1. Two-loop Feynman graphs (one-particle irreducible) contributions to the $\pi^0 \rightarrow 2\gamma$ amplitude.

$$\begin{aligned}
F_\pi T_{\text{NNLO}} = & -\frac{M^4}{24\pi^2 F^4} \left(\frac{1}{16\pi^2} L_\pi \right)^2 + \frac{M^4}{16\pi^2 F^4} L_\pi \left[\frac{3}{256\pi^4} \right. \\
& + \frac{32F^2}{3} (2c_2^{Wr} + 4c_3^{Wr} + 2c_6^{Wr} + 4c_7^{Wr} - c_{11}^{Wr}) \left. \right] \\
& + \frac{32M^2 B(m_d - m_u)}{48\pi^2 F^4} L_\pi [-6c_2^{Wr} - 11c_3^{Wr} \\
& + 6c_4^{Wr} - 12c_5^{Wr} - c_7^{Wr} - 2c_8^{Wr}] + \frac{M^4}{F^4} \lambda_+ \\
& + \frac{M^2 B(m_d - m_u)}{F^4} \lambda_- + \frac{B^2(m_d - m_u)^2}{F^4} \lambda_{--},
\end{aligned} \tag{18}$$

where L_π represents the chiral logarithm

$$L_\pi = \log \frac{m_\pi^2}{\mu^2} \tag{19}$$

and λ_+ , λ_- , λ_{--} can be expressed as follows in terms of renormalized chiral coupling constants,

$$\begin{aligned}
\lambda_+ = & \frac{1}{\pi^2} \left[-\frac{2}{3} d_+^{Wr}(\mu) - 8c_6^r - \frac{1}{4} (l_4^r)^2 + \frac{1}{512\pi^4} \right. \\
& \times \left(-\frac{983}{288} - \frac{4}{3} \zeta(3) + 3\sqrt{3} \text{Cl}_2(\pi/3) \right) \left. \right] \\
& + \frac{16}{3} F^2 [8l_3^r (c_3^{Wr} + c_7^{Wr}) + l_4^r (-4c_3^{Wr} - 4c_7^{Wr} + c_{11}^{Wr})] \\
\lambda_- = & \frac{64}{9} [d_-^{Wr}(\mu) + F^2 l_4^r (5c_3^{Wr} + c_7^{Wr} + 2c_8^{Wr})] \\
\lambda_{--} = & d_{--}^{Wr}(\mu) - 128F^2 l_7^r (c_3^{Wr} + c_7^{Wr}).
\end{aligned} \tag{20}$$

Here, the notation d^{Wr} refer to combinations of couplings from the NNLO Lagrangian (i.e. of order p^8) in the anomalous sector.

A few remarks are in order concerning this calculation. First, concerning nonlocal divergences, i.e. terms of the form $M^4 \log(M^2)/(d-4)$, we have verified that those which are generated from the two-loop diagrams are canceled exactly by those generated from the one-loop diagrams proportional to l_i , c_i^W as expected from the Weinberg consistency conditions. The divergences that are left are proportional to M^4 , $M^2(m_d - m_u)$ and $(m_d - m_u)^2$. They are canceled by the contributions, at tree level, from the chiral Lagrangian of order p^8 in the anomalous sector. We have denoted the three independent combinations of $O(p^8)$ chiral couplings by d_+^W , d_-^W , and d_{--}^W . Our calculation shows that the relation between these and the corresponding renormalized combinations must be as follows,

$$\begin{aligned}
d_+^W = & \frac{(c\mu)^{2(d-4)}}{F^2} \left[d_+^{Wr}(\mu) - \Lambda^2 \left(-\frac{17}{3} \right) - \Lambda \left(-11l_1^r \right. \right. \\
& - 7l_2^r - \frac{1}{2} l_3^r - \frac{3}{2} l_4^r - \frac{53}{4608\pi^2} + 16\pi^2 F^2 (-4c_2^{Wr} \\
& - 2c_3^{Wr} - 4c_6^{Wr} - 2c_7^{Wr} + c_{11}^{Wr}) \left. \left. \right) \right] \\
d_-^W = & \frac{(c\mu)^{2(d-4)}}{F^2} [d_-^{Wr}(\mu) - \Lambda F^2 (-18c_2^{Wr} - 23c_3^{Wr} \\
& + 18c_4^{Wr} - 36c_5^{Wr} - c_7^{Wr} - 2c_8^{Wr})] \\
d_{--}^W = & \frac{(c\mu)^{2(d-4)}}{F^2} \left(d_{--}^{Wr}(\mu) + \frac{\Lambda l_7^r}{\pi^2} \right).
\end{aligned} \tag{21}$$

Equation (18) shows that chiral logarithms are indeed present at NNLO. The coefficient of the dominant one, as can be shown quite generally, depends only on F . The coefficient of the subdominant chiral logarithm has one part depending only on F and another one depending on the NLO chiral couplings c_i^{Wr} . From a numerical point of view, the contribution from the dominant chiral logarithm turns out to be very small, of the order of a few per mille. This lack of enhancement could indicate a fast convergence of the chiral perturbation series. In this respect, the detailed formula (18) could be used in association with results from lattice QCD simulations, in which the quark masses m_u , m_d are larger than the physical ones and can be

CHIRAL EXPANSIONS OF THE π^0 LIFETIME

varied. This would allow one to determine the relevant combinations of chiral couplings. In the following section we discuss an alternative, more approximate method, to estimate these combinations.

IV. CHIRAL EXPANSION IN m_s

From now on, we assume that the mass of the strange quark is sufficiently small, such that the chiral expansion in m_s is meaningful. One can then calculate the π^0 lifetime using the three-flavor chiral expansion. Instead of doing so directly, as it remains true that $m_u, m_d \ll m_s$, it is instructive to start from the $SU(2)$ expression, Eq. (18) and perform a chiral expansion of the couplings c_i^W as a function of m_s . A priori, one expects expressions of the following form to arise

$$c_i^{Wr} = \frac{\alpha_i}{m_s} + \left(\beta_i + \sum_a \gamma_{ia} C_a^{Wr} + \delta_i \log \frac{B_0 m_s}{\mu^2} \right) + O(m_s), \quad (22)$$

where C_a^{Wr} , $a = 1 \dots 24$ are the coupling constants of the NLO Lagrangian in the anomalous sector in the $SU(3)$ expansion [23] and $B_0 = \lim_{m_s \rightarrow 0} B$. Analogous expansions were established in Ref. [31] for the $SU(2)$ couplings B , F and I_i^r . This problem was reconsidered recently in Ref. [32] in which the NNLO terms in that expansion have been derived. Also in Ref. [33] the m_s expansions of the $SU(2)$ LEC's in the electromagnetic sector were studied. In order to generate such expansions one can work in the $SU(2)$ chiral limit $m_u = m_d = 0$, compute sets of correlations functions having $SU(2)$ flavor structure in both the $SU(2)$ and the $SU(3)$ chiral expansions and equate the expressions. The authors of Ref. [32] have shown how to perform this matching at the level of the generating functionals. In the $SU(3)$ generating functional, one must use external sources s , p , v_μ , a_μ which correspond to those used in the $SU(2)$ functional embedded into 3×3 matrices. Since there is no source for strangeness, the classical $SU(3)$ chiral field involves the three pions π_a and the η field but no kaons

$$U_{cl} = \exp \frac{i\lambda_a \pi_a}{F_0} \exp \frac{i\eta \lambda_8}{F_0} \quad (23)$$

(F_0 being the pion decay constant in the three-flavor chiral limit). Using the equation of motion one can express the field η_{cl} in terms of an $SU(2)$ chiral building-block [32,33]

$$\frac{\eta_{cl}}{\sqrt{3}F_0} = i\langle \chi_- \rangle \left(-\frac{1}{16m_s B} \right) + O(p^4). \quad (24)$$

The terms proportional to η_{cl} thus generate contributions proportional to $1/(m_s B)$. These can be also seen as resulting from η meson propagators in tree diagrams. Besides, Eq. (24) shows that η_{cl} counts as $O(p^2)$ in the $SU(2)$ counting. Inserting U_{cl} from Eq. (23) in the $SU(3)$ Wess-Zumino action and expanding to first order in η_{cl} we

PHYSICAL REVIEW D **79**, 076005 (2009)

obtain,

$$\begin{aligned} \mathcal{L}_\eta = & -\frac{iN_c}{48\pi^2} \frac{\eta_{cl}}{\sqrt{3}F_0} \epsilon^{\mu\nu\alpha\beta} \left\{ \frac{1}{2} \langle f_{+\alpha\beta} u_\mu u_\nu \rangle \right. \\ & - \frac{3}{8} i \langle f_{+\alpha\beta} f_{+\mu\nu} \rangle + \frac{3}{4} i \langle f_{+\alpha\beta} \rangle \langle f_{+\mu\nu} \rangle \\ & \left. - \frac{1}{8} i \langle f_{-\alpha\beta} f_{-\mu\nu} \rangle \right\}. \quad (25) \end{aligned}$$

This allows one to deduce the leading terms, which behave as $1/m_s$, in the expansion of the couplings c_i^{Wr} . Next, the terms proportional to $(m_s)^0$ are generated from three sources.

- (1) From the $SU(3)$ Lagrangian \mathcal{L}_6^W , by inserting U_{cl} (with η_{cl} set to zero), which gives contributions proportional to LEC's C_i^{Wr} .
- (2) From one-loop irreducible graphs with one vertex taken from the Wess-Zumino action and having one kaon or one eta running in the loop.
- (3) From corrections to the η pole contributions stemming from tadpoles or from vertices proportional to the $O(p^4)$ couplings L_i .

The results are presented in Eqs. (26) below and (B1) in Appendix B.

Let us now examine the applications of this exercise to the problem of the π^0 lifetime. As seen in sec. II the NLO corrections involve two independent pieces, one proportional to m_π^2 and one to $B(m_d - m_u)$, and they are controlled by two combinations of the four couplings c_3^{Wr} , c_7^{Wr} , c_8^{Wr} and c_{11}^{Wr} . For these, we take into account the first two terms in the m_s expansion which read

$$\begin{aligned} c_3^{Wr} &= -\frac{3}{2}c_0 + C_7^{Wr} + 3C_8^{Wr} + O(m_s) \\ c_7^{Wr} &= \frac{3}{2}c_0 - 3C_8^{Wr} + \frac{1}{4}C_{22}^{Wr} + O(m_s) \\ c_8^{Wr} &= \frac{3}{4}c_0 + \frac{1}{2}C_7^{Wr} + 3C_8^{Wr} - \frac{1}{8}C_{22}^{Wr} + O(m_s) \\ c_{11}^{Wr} &= C_{22}^{Wr} + O(m_s), \end{aligned} \quad (26)$$

where

$$\begin{aligned} c_0 = & \frac{1}{32\pi^2} \left[-\frac{1}{16Bm_s} + \frac{2}{F_0^2} \left(3L_7^r + L_8^r \right. \right. \\ & \left. \left. - \frac{1}{512\pi^2} \left(L_K + \frac{2}{3}L_\eta \right) \right) \right] \end{aligned} \quad (27)$$

and

$$L_K = \log \frac{m_s B_0}{\mu^2}, \quad L_\eta = L_K + \log \frac{4}{3}. \quad (28)$$

At this point, one observes that by using the m_s expansion, we have expressed four $SU(2)$ couplings in terms of three $SU(3)$ ones. This might look as a modest improvement. Fortunately, the combinations relevant for the π^0 lifetime at NLO actually involve only two couplings C_7^{Wr} , C_8^{Wr} while C_{22}^{Wr} drops out.

KAROL KAMPF AND BACHIR MOUSSALLAM

Let us now consider the terms proportional to m_π^4 and $m_\pi^2(m_d - m_u)$. One can see from Eq. (18) that they involve four more LEC's, c_2^{Wr} , c_4^{Wr} , c_5^{Wr} , c_6^{Wr} . It makes sense here to retain only the part of these LEC's which are dominant in the m_s expansion, i.e. the $1/m_s$ part,

$$\begin{aligned} c_2^{Wr} &\simeq \tilde{c}_0, & c_4^{Wr} &\simeq -\frac{1}{2}\tilde{c}_0, & c_5^{Wr} &\simeq 0, \\ c_6^{Wr} &\simeq -\tilde{c}_0, & \tilde{c}_0 &= -\frac{1}{512\pi^2 B m_s} \end{aligned} \quad (29)$$

and we perform a similar approximation in Eq. (26). We will also retain the part involving the LEC C_8^W as it will appear that the size of this coupling is comparable to that of the $1/m_s$ terms. Inserting the m_s expansions (26) and (29), in the $SU(2)$ chiral expansion of the π^0 decay amplitude (18) we obtain the following expression

$$\begin{aligned} T_{(\text{LO+NLO})_+} &= \frac{1}{F_\pi} \left\{ \frac{1}{4\pi^2} - \frac{64}{3} m_\pi^2 C_7^{Wr} + \frac{1}{16\pi^2} \frac{m_d - m_u}{m_s} \right. \\ &\times \left[1 - \frac{3}{2} \frac{m_\pi^2}{16\pi^2 F_\pi^2} L_\pi \right] + 32B(m_d - m_u) \\ &\times \left[\frac{4}{3} C_7^{Wr} + 4C_8^{Wr} \left(1 - 3 \frac{m_\pi^2}{16\pi^2 F_\pi^2} L_\pi \right) \right. \\ &- \frac{1}{16\pi^2 F_\pi^2} \left(3L_7^r + L_8^r - \frac{1}{512\pi^2} \right. \\ &\left. \left. \times \left(L_K + \frac{2}{3} L_\eta \right) \right) \right] - \frac{1}{24\pi^2} \left(\frac{m_\pi^2}{16\pi^2 F_\pi^2} L_\pi \right)^2 \left. \right\}. \end{aligned} \quad (30)$$

A modified $SU(3)$ chiral counting

Some comments are in order concerning Eq. (30). In particular, one expects it to be related to the formula that one can compute starting from $SU(3)$ ChPT. Such a computation was performed, e.g. in Ref. [7]. In $SU(3)$ ChPT m_u , m_d and m_s are counted on the same footing,

$$m_u, \quad m_d \sim m_s \sim O(p^2) \quad [\text{standard } SU(3)]. \quad (31)$$

In the physical situation, however, $m_u, m_d \ll m_s$. For processes which involve only pions this can be accounted for by adopting the following modified counting,

$$m_u, \quad m_d \sim O(p^2), \quad m_s \sim O(p) \quad (32)$$

[modified $SU(3)$].

The formula (30) for the π^0 lifetime can be argued to be a consistent expansion in this modified counting. One notes first that all the corrections must be proportional to m_u, m_d since the starting point is exact in the $SU(2)$ chiral limit. The formula (30) includes the leading corrections of order p (which must be proportional to $m_u/m_s, m_d/m_s$) as well as the subleading corrections of order p^2 (which must be proportional to m_u, m_d). It also includes the corrections of

PHYSICAL REVIEW D **79**, 076005 (2009)

order p^3 which are logarithmically enhanced (which must be proportional to $m_u m_s, m_d m_s$ multiplied by $\log(m_u + m_d)$) as well as the corrections of order p^4 which are double logarithmically enhanced. Obviously, by retaining logarithmically enhanced terms at a given order instead of the full set of terms, one introduces a chiral scale dependence into the amplitude. Clearly, one should use a value of the scale of the order of the kaon or the eta mass for this approximation to make sense. Finally, we have verified that, starting from the expression for the amplitude in standard $SU(3)$ at NLO obtained in Ref. [7], and expanding in powers of $m_u/m_s, m_d/m_s$ one recovers exactly the terms of order p, p^2 and $p^3 \log(p^2)$ in the modified $SU(3)$ expansion (32). In practice, the expression (30) is somewhat simpler than the standard $SU(3)$ NLO expression and contains the double logarithm term. The latter turns out to be numerically small so that the two expressions are essentially equivalent in practice. In order to derive a numerical prediction from Eq. (30) one needs inputs for: $F_\pi, (m_d - m_u)/m_s, B(m_d - m_u)$ and C_7^W, C_8^W . We will give an update on the determination of these quantities in Sec. V

In addition to the chiral corrections induced by the quark masses, one should also take electromagnetic corrections into account. These have been considered in Ref. [7], where the correction terms of order e^2 and of order $e^2(m_u + m_d)/m_s$ have been computed. Here, it is consistent to retain only the term of order e^2 , its expression in terms of Urech's chiral couplings [14] is recalled,

$$\begin{aligned} T_{e^2} &= \frac{e^2}{4\pi^2 F_\pi} \left\{ -\frac{4}{3} (K_1^r + K_2^r) + 2K_3^r - K_4^r \right. \\ &\left. - \frac{10}{9} (K_5^r + K_6^r) + \frac{C}{32\pi^2 F_\pi^4} (5 + 4L_\pi + L_K) \right\}. \end{aligned} \quad (33)$$

This term is defined such that the $\pi^0 \rightarrow 2\gamma$ amplitude is expressed in terms of F_{π^0} which is the neutral pion decay constant in *pure QCD* and m_π^2 which is the *physical* neutral pion mass (i.e. including EM corrections).

V. PHENOMENOLOGICAL UPDATES

Let us now update the various inputs needed to calculate the numerical prediction for the π^0 lifetime in ChPT.

A. The pion decay constant

An obviously essential input here is F_π , the value of the pion decay constant. Marciano and Sirlin [34] have evaluated the radiative corrections in the process $\pi^+ \rightarrow \mu^+ \nu(\gamma)$ decay rate such that it is expressed in terms of F_{π^+} the charged pion decay constant in pure QCD. In pure QCD the difference between F_{π^0} and F_{π^+} is quadratic in the quark mass difference $m_d - m_u$ and can be expressed as follows in ChPT,

CHIRAL EXPANSIONS OF THE π^0 LIFETIME

$$\frac{F_{\pi^+}}{F_{\pi^0}} \Big|_{\text{QCD}} - 1 = \frac{B^2(m_d - m_u)^2}{F_\pi^4} \left[-16c_9^r(\mu) - \frac{l_7}{16\pi^2} \left(1 + \log \frac{m_\pi^2}{\mu^2} \right) \right] \approx 0.710^{-4}. \quad (34)$$

A rough numerical evaluation has been made by using leading order $1/m_s$ estimates

$$l_7 \approx \frac{F_\pi^2}{8Bm_s}, \quad c_9^r \approx -\frac{3}{2} \left(\frac{F_\pi^2}{Bm_s} \right)^2. \quad (35)$$

Equation (34) shows that the difference between F_{π^+} and F_{π^0} is negligibly small for our purposes, and we will ignore it. In the expression of Ref. [34] for the radiative corrections, one constant term, called C_1 , was left undetermined. Matching with the ChPT expansion of the π^+ decay rate at $O(p^4)$ one can express C_1 in terms of chiral logarithms and a set of chiral couplings [35]. The latter can then be estimated using chiral sum rules and resonance saturation [36]. Using these results and the updated value of V_{ud} from Ref. [37]

$$V_{ud} = 0.97418(26), \quad (36)$$

we find

$$F_\pi = 92.22 \pm 0.07 \text{ MeV}. \quad (37)$$

B. $B(m_d - m_u)$, $(m_d - m_u)/m_s$, $3L_7 + L_8^r$

Because of the Kaplan-Manohar invariance [38] it is not possible to determine independently the quark mass ratios and the couplings L_7 , L_8 in ChPT using low-energy data. One may use an input from lattice QCD, e.g. on the quark mass ratio $r = 2m_s/(m_u + m_d)$. Using the results obtained in Ref. [39] as well as those from other recent QCD simulations which are collected in table XVI of that reference and averaging, one can deduce

$$r \equiv \frac{2m_s}{m_u + m_d} = 28.0 \pm 1.5. \quad (38)$$

Using this input for r , we may treat terms linear in the quark masses in NLO ChPT expressions as follows,

$$(m_u + m_d)B_0 \approx m_\pi^2, \quad m_s B_0 = \frac{r}{2} m_\pi^2. \quad (39)$$

The value of the LEC combination $3L_7 + L_8^r$ can be deduced using r and standard $O(p^4)$ ChPT formulas for the pseudoscalar meson masses [31]

$$3L_7 + L_8^r(\mu) = (0.10 \pm 0.06)10^{-3} \quad (\mu = M_\eta). \quad (40)$$

Concerning the quark mass difference $m_d - m_u$, we will use the recent determination made in Ref. [40]. It is based on the $\eta \rightarrow 3\pi$ decay amplitude which is an isospin break-

PHYSICAL REVIEW D **79**, 076005 (2009)

ing observable with very small sensitivity to electromagnetic effects [41,42]. The amplitude has been computed at order p^6 in ChPT by the authors of Ref. [40] and they deduce the following result,¹

$$R \equiv \frac{m_s - \hat{m}}{m_d - m_u} = 42.2 \quad (41)$$

(with $\hat{m} = (m_u + m_d)/2$). No figure for the uncertainty is given. We have estimated it by noting that the main source of uncertainty in this result comes from the unknown values of the coupling constants C_i^r from the $O(p^6)$ Lagrangian. For these couplings, it was shown that simple resonance models are sometimes misleading [44] because of their strong scale dependence. We have estimated the order of magnitude of the uncertainty by taking the difference between the value of R obtained from a p^6 calculation and the value obtained from a p^4 calculation and dividing by two, which gives

$$\Delta R \approx 5. \quad (42)$$

Using (38), (41), and (42), we obtain²

$$\frac{m_d - m_u}{m_s} = (2.29 \pm 0.23)10^{-2}, \quad (43)$$

$$B(m_d - m_u) = (0.32 \pm 0.03)M_{\pi^0}^2.$$

C. C_7^W

This constant obeys a sum rule in terms of the form factor associated with the photon-photon matrix element of the pseudoscalar current [2]. A simple resonance saturation approximation in this sum rule gives a relation between C_7^W and the $\pi(1300)$ mass and its couplings to the pseudoscalar current (d_m) and to two photons ($g_{\pi\gamma}$) [7]

$$C_7^W \approx \frac{g_{\pi\gamma} d_m}{M_\pi^2}. \quad (44)$$

Recent experimental data by the Belle collaboration has confirmed the extreme smallness of the coupling of the

¹An alternative evaluation of R can be made based on the $K^+ - K^0$ mass difference. As one can see from Table 6 of Ref. [40] this method tends to give values of R smaller than Eq. (41). The calculation of the $K^+ - K^0$ mass difference in ChPT, however, has uncertainties related to the couplings C_i and also from estimates of the electromagnetic contributions, beyond the Dashen low-energy theorem, which have some model dependence. One could also use isospin violation in K_{I3} form factors. For an updated discussion of these effects, see [43].

²In Ref. [45] a determination of the quantity $B_0(m_d - m_u)$ from $\eta \rightarrow 3\pi^0$ was proposed, based on using both the decay rate and the slope parameter α , obtaining $B_0(m_d - m_u) = (0.25 \pm 0.02)M_{\pi^0}^2$. This appears somewhat smaller than the result in Eq. (43) but one should keep in mind that the ratio B_0/B , while expected to be close to 1, is not accurately known.

KAROL KAMPF AND BACHIR MOUSSALLAM

 $\pi(1300)$ meson to two photons [46]

$$\Gamma_{\pi \rightarrow 2\gamma} < 72 \text{ eV}. \quad (45)$$

The validity of the resonance saturation approximation in this case might be questioned since, in the sum rule, C_7^W , could pick up more important contributions from energies higher than the mass of the $\pi(1300)$ resonance. There has been several attempts at estimating this high-energy contribution to C_7^W in the literature: Using a quark-hadron duality picture, Kitazawa [2] argue that this contribution arises from a triangle diagram and should thus be proportional to the constituent quark mass (this result was applied to η decay in Ref. [47]). In QCD, one expects the constituent quark mass to be momentum dependent (see e.g. [48]) and to decrease at high momenta, which is not taken into account in this evaluation. A calculation of the triangle diagram in the NJL model was performed in Ref. [49]. As this model implements a momentum cutoff, however, it rather concerns the low-energy rather than the high-energy contribution to C_7^W . An alternative idea was proposed in Ref. [50] based on a minimal resonance saturation modeling of the three-point function VVP and enforcing a correct asymptotic matching to the OPE expansion of this three-point function. The result, unfortunately, cannot be shown to remain stable under inclusion of more resonances. None of the estimates, finally, appear to be quantitatively very compelling. It seems however quite safe to assume that the coupling C_7^W should be suppressed, say by 1 order of magnitude, as compared to the coupling C_8^W . Indeed, in an analogous sum rule representation, C_8^W picks up a strong contribution from the η' resonance. We will therefore take

$$|C_7^W| < 0.1 |C_8^W|. \quad (46)$$

D. C_8^W

Having assumed the validity of $SU(3)$ ChPT, together with the result (46) of the above discussion on C_7^W , one can determine C_8^W from the experimental information on the $\eta \rightarrow 2\gamma$ decay width. According to the PDG³ [53]

$$\Gamma_{\eta \rightarrow 2\gamma} = 0.510 \pm 0.026 \text{ keV}, \quad (47)$$

while the corresponding amplitude computed in ChPT, including LO and NLO contributions, reads

$$T_\eta = \frac{e^2}{\sqrt{3}F_\pi} \left[\frac{F_\pi}{4\pi^2 F_\eta} (1 + x_\eta) - \frac{64}{3} m_\pi^2 C_7^W + \frac{256}{3} (r-1) m_\pi^2 \left(\frac{1}{6} C_7^W + C_8^W \right) \right] + O(m_s^2), \quad (48)$$

³The PDG now rejects the Primakoff experiment [51] which gave a smaller result. A rediscussion of that experiment has recently appeared [52].

PHYSICAL REVIEW D **79**, 076005 (2009)where x_η encodes isospin breaking effects

$$x_\eta = \sqrt{3}(-\epsilon_1 + e^2(\delta_\eta - \delta_1)) \simeq -0.023, \quad (49)$$

using notations and results from Refs. [7,31]. We need an input for F_η in Eq. (48). Up to corrections quadratic in m_s , F_η is linearly related to F_π and F_K [31],

$$F_\eta = \frac{4F_K - F_\pi}{3} + \frac{m_\pi^2}{96\pi^2 F_\pi} \left[2(r+1) \log \frac{2(2r+1)}{3(r+1)} - \log \frac{2r+1}{3} \right] + O(m_s^2). \quad (50)$$

The review in Ref. [54] quotes the following result for F_K from averaging over recent experiments on π_{12} and K_{12} decays

$$\frac{F_K V_{us}}{F_\pi V_{ud}} = 0.27599(59). \quad (51)$$

Assuming exact Cabibbo-Kobayashi-Maskawa quark-mixing matrix (CKM) unitarity we can deduce F_K and then F_η

$$F_K = 109.84 \pm 0.63, \quad F_\eta = 118.4 \pm 8.0 \text{ (MeV)}. \quad (52)$$

The error on F_η is dominated by the $O(m_s^2)$ contributions in Eq. (50). We have estimated that it should be smaller than the $O(m_s)$ contribution by a factor of 3. Finally, using these results in conjunction with Eqs. (47) and (48) we determine the coupling C_8^W

$$C_8^W = (0.58 \pm 0.20) 10^{-3} \text{ (GeV}^{-2}\text{)}. \quad (53)$$

We have estimated that the uncertainty stemming from unknown $O(m_s^2)$ chiral corrections in the η decay amplitude to be of order 30% compared to the $O(m_s)$ corrections.

E. Numerical result

The numerical results for the current algebra amplitude and the corrections according to the modified chiral $SU(3)$ counting, using the updated inputs presented above, are collected in Table I. One remarks that the $O(p^2)$ contribution is larger than the $O(p)$ one. This is induced by the size

TABLE I. Current algebra contribution to the $\pi^0 \rightarrow 2\gamma$ decay width (in eV) and corrections of various chiral orders using the modified $SU(3)$ counting.

CA	$O(p)$	$O(p^2)$	$O(e^2)$	$O(p^3 \log p)$	$O(p^4 \log^2 p)$
7.76	0.09	0.29	-0.05	0.005	-0.004

CHIRAL EXPANSIONS OF THE π^0 LIFETIME

of the LEC C_8^W . Expressed as a sum rule, C_8^W is dominated by the η' contribution, which can be written [7]

$$C_8^W \simeq \frac{g_{\eta'} \tilde{d}_m}{M_{\eta'}^2}, \quad (54)$$

where $M_{\eta'}$ is the mass of the η' in the chiral limit. In the large N_c limit one has,

$$g_{\eta'} = \frac{\sqrt{6}}{128\pi^2 F_0}, \quad \tilde{d}_m = \frac{F_0}{2\sqrt{6}}, \quad C_8^W \simeq \frac{1}{256\pi^2 M_{\eta'}^2}. \quad (55)$$

The enhancement of C_8^W can then be understood, qualitatively, as a large N_c effect. In practice, the value of C_8^W that one can estimate using the resonance saturation formula (54) agrees reasonably well with the one deduced from a ChPT expansion of the $\eta \rightarrow 2\gamma$ amplitude⁴ [Eq. (53)]. The enhancement of the $O(p^2)$ contribution is therefore a well understood effect and does not signal a breakdown of the expansion. Table I shows that the logarithmically enhanced contributions of order $p^3 \log(p)$ and $p^4 \log^2(p)$ are quite small in practice and tend to cancel each other. Finally, the prediction for the π^0 decay width reads,

$$\Gamma_{\pi^0 \rightarrow 2\gamma} = (8.09 \pm 0.11) \text{ eV}. \quad (56)$$

The two main sources for the uncertainty are: $m_d - m_u$ (± 0.05) and C_8^W (± 0.098). We have added the errors in quadrature. Compared to Ref. [7] the main modification in the input is the value of the $\eta \rightarrow 2\gamma$ width in the PDG. The branching fraction for the 2γ decay mode is $(98.798 \pm 0.032)\%$ [53] (the most sizable other decay being the Dalitz mode $\pi^0 \rightarrow \gamma e^+ e^-$, for review see e.g. [55]). Our result, Eq. (56), then corresponds to the following value for the π^0 lifetime

$$\tau_{\pi^0} = (8.04 \pm 0.11) 10^{-17} \text{ s}. \quad (57)$$

VI. SUMMARY

In this paper, we have reconsidered the chiral expansion of the $\pi^0 \rightarrow 2\gamma$ amplitude. At first, we have focused on the two-flavor expansion. We have considered the expansion beyond the known NLO (which we have expressed in terms of the coupling constants introduced in Ref. [23]). We have computed all the loop graphs which contribute at NNLO. As expected, we found that the divergences are renormalizable by Lagrangian terms of chiral order p^8 in the anomalous sector. We found that chiral logarithms are present at this order. For physical values of the quark

⁴Our result disagrees with Ref. [11] in which the corresponding contribution is smaller by 1 order of magnitude.

PHYSICAL REVIEW D **79**, 076005 (2009)

masses m_u, m_d these NNLO corrections turn out to be negligible. Even the terms enhanced by logarithms are numerically very small in practice. Our final expression [Eq. (18)] could be useful in association with lattice QCD simulations in which unphysical quark masses can be used. This would provide a direct evaluation of the $SU(2)$ couplings. As an interesting application, one could deduce (using also experimental data such as from PrimEx) a precision determination of F_π uncorrelated with the value of V_{ud} . Such simulations have not yet been performed for correlation functions in the anomalous sector, but this would be of obvious interest.

In order to perform a more detailed phenomenological analysis at present, it is possible to enlarge the chiral expansion from $SU(2)$ to $SU(3)$. This allows one to derive some information on the $SU(2)$ coupling constants. We have derived the expansion of the $SU(2)$ couplings c_i^{Wr} as a function of m_s up to $O(m_s)$ and inserted this result into the $SU(2)$ expansion formula. The leading, $1/m_s$ terms in this expansion, reflect the influence of $\pi^0 - \eta$ mixing. We then implemented a modified chiral counting in which m_s is counted as $O(p)$ rather than $O(p^2)$. This counting accommodates the fact that m_u, m_d are significantly smaller than m_s . The formulas obtained in this way are somewhat simpler and easier to interpret than those obtained in the usual chiral counting but the numerical results are essentially identical.

We have updated the inputs to be used in the chiral formula. A key input is the value of F_π , the pion decay constant in pure QCD. Another important input is the value of the $\eta \rightarrow 2\gamma$ decay width, which we use to determine the value of the $SU(3)$ LEC C_8^W . In the chiral approach, this LEC encodes the effect of $\eta - \eta'$ mixing. Our result agrees well with that of approaches which account for $\eta - \eta'$ mixing explicitly, using large N_c arguments in addition to chiral counting [2,9,10]. The overall uncertainty is dominated by the unknown terms of order p^3 , i.e. proportional to $m_u m_s, m_d m_s$ in the chiral expansion. As a final remark, we note that F_π is determined from the weak decay of the π^+ assuming the validity of the standard model. Some recently proposed Higgsless variants can accommodate deviations from the standard $V - A$ coupling of quarks to the W as large as a few percent [56]. Precision measurements of the π^0 lifetime can provide constraints on such models.

ACKNOWLEDGMENTS

We want to acknowledge useful comments and discussions with J. Bijnens, G. Ecker, B. Jantzen, H. Neufeld, R. Rosenfelder and P. Talavera. This work is supported in part by the European commission MRTN FLAVIANet [MRTN-CT-2006035482], Center for Particle Physics [LC 527] and GACR [202/07/P249]. K. K. gratefully acknowledges the hospitality of the Institut de Physique Nucléaire at Orsay during his visits.

KAROL KAMPF AND BACHIR MOUSSALLAM

PHYSICAL REVIEW D **79**, 076005 (2009)**APPENDIX A**

We give here the result of our computation of diagrams 1(f) and 1(g) in Fig. 1:

$$F_{\pi T(f)} = \frac{M^4}{\pi^2 F^4} \left\{ -\frac{11}{4} \left[\Lambda^2 + \Lambda \left(L_\pi - \frac{31}{1056\pi^2} \right) + \frac{1}{2} L_\pi^2 - \frac{31}{1056\pi^2} L_\pi + \frac{1}{6144\pi^2} \right] - \frac{467}{98304\pi^4} \right\}, \quad (\text{A1})$$

$$F_{\pi T(g)} = \frac{M^4}{\pi^2 F^4} \left\{ \frac{7}{3} \left[\Lambda^2 + \Lambda \left(L_\pi - \frac{59}{1792\pi^2} \right) + \frac{1}{2} L_\pi^2 - \frac{59}{1792\pi^2} L_\pi + \frac{1}{6144\pi^2} \right] + \frac{1}{512\pi^4} \times \left[3\sqrt{3}\text{Cl}_2\left(\frac{\pi}{3}\right) - \frac{4}{3}\zeta(3) - \frac{1135}{576} \right] \right\}, \quad (\text{A2})$$

with

$$\Lambda = \frac{1}{16\pi^2(d-4)}. \quad (\text{A3})$$

APPENDIX B

We collect below the expansions of the $SU(2)$ couplings c_i^{Wr} as a function of m_s up to $O(m_s)$. The notations L_K, L_η and c_0 having been introduced in Eqs. (27) and (28) these expansions read

$$c_1^{Wr} = C_2^{Wr} - \frac{1}{2} C_3^{Wr} + \frac{1}{4} \frac{1}{(32\pi^2)^2 F_0^2} \left(L_K + 1 + \frac{1}{3} L_\eta \right)$$

$$c_2^{Wr} = c_0 + C_4^{Wr} - \frac{1}{2} C_5^{Wr} + \frac{3}{2} C_6^{Wr}$$

$$c_3^{Wr} = -\frac{3}{2} c_0 + C_7^{Wr} + 3C_8^{Wr}$$

$$c_4^{Wr} = -\frac{1}{2} c_0 + C_9^{Wr} + 3C_{10}^{Wr}$$

$$c_5^{Wr} = C_{11}^{Wr} + \frac{1}{8} \frac{1}{(32\pi^2)^2 F_0^2} \left(L_K + 1 + \frac{2}{3} L_\eta \right)$$

$$c_6^{Wr} = -c_0 + C_5^{Wr} - \frac{3}{2} C_6^{Wr} - \frac{1}{2} C_{14}^{Wr} - \frac{1}{2} C_{15}^{Wr}$$

$$c_7^{Wr} = \frac{3}{2} c_0 - 3C_8^{Wr} + \frac{1}{4} C_{22}^{Wr}$$

$$c_8^{Wr} = \frac{3}{4} c_0 + \frac{1}{2} C_7^{Wr} + 3C_8^{Wr} - \frac{1}{8} C_{22}^{Wr}$$

$$c_9^{Wr} = -C_{13}^{Wr} + C_{14}^{Wr} + C_{15}^{Wr} - \frac{3}{2} \frac{1}{(32\pi^2)^2 F_0^2} (L_K + 1)$$

$$c_{10}^{Wr} = C_{19}^{Wr} - C_{20}^{Wr} - C_{21}^{Wr} - C_{22}^{Wr} + \frac{3}{2} \frac{1}{(32\pi^2)^2 F_0^2} (L_K + 1)$$

$$c_{11}^{Wr} = C_{22}^{Wr} \quad c_{12}^{Wr} = 0$$

$$c_{13}^{Wr} = -2C_{22}^{Wr} + \frac{1}{(32\pi^2)^2 F_0^2} (L_K + 1). \quad (\text{B1})$$

-
- [1] M. Kubantsev, I. Larin, and A. Gasparyan (PrimEx Collaboration), in *Calorimetry in High Energy Physics*, edited by S. R. Magill and R. Yoshida, AIP Conf. Proc. 867 (AIP, New York, 2006), p. 51.
- [2] Y. Kitazawa, Phys. Lett. **151B**, 165 (1985).
- [3] J. F. Donoghue, B. R. Holstein, and Y. C. R. Lin, Phys. Rev. Lett. **55**, 2766 (1985).
- [4] J. Bijnens, A. Bramon, and F. Cornet, Phys. Rev. Lett. **61**, 1453 (1988).
- [5] Riazuddin and Fayyazuddin, Phys. Rev. D **37**, 149 (1988).
- [6] B. Moussallam, Phys. Rev. D **51**, 4939 (1995).
- [7] B. Ananthanarayan and B. Moussallam, J. High Energy Phys. 05 (2002) 052.
- [8] N. F. Nasrallah, Phys. Rev. D **66**, 076012 (2002).
- [9] R. Kaiser, *Proceedings of the Institute for Nuclear Theory, Phenomenology of Large N_c QCD*, , edited by R. F. Lebed (World Scientific, Singapore 2002), Vol. 12.
- [10] J. L. Goity, A. M. Bernstein, and B. R. Holstein, Phys. Rev. D **66**, 076014 (2002).
- [11] B. L. Ioffe and A. G. Oganesian, Phys. Lett. B **647**, 389 (2007).
- [12] H. Pagels and A. Zepeda, Phys. Rev. D **5**, 3262 (1972).
- [13] S. Scherer, Adv. Nucl. Phys. **27**, 277 (2003).
- [14] R. Urech, Nucl. Phys. **B433**, 234 (1995).
- [15] S. D. Cohen, H. W. Lin, J. Dudek, and R. G. Edwards, arXiv:0810.5550.
- [16] G. Colangelo, Phys. Lett. B **350**, 85 (1995); **361**, 234(E) (1995).
- [17] J. Bijnens, G. Colangelo, and G. Ecker, Phys. Lett. B **441**, 437 (1998).
- [18] S. Weinberg, Physica A (Amsterdam) **96**, 327 (1979).
- [19] J. Wess and B. Zumino, Phys. Lett. **37B**, 95 (1971); E. Witten, Nucl. Phys. **B223**, 422 (1983); R. Kaiser, Phys. Rev. D **63**, 076010 (2001).
- [20] S. L. Adler, Phys. Rev. **177**, 2426 (1969); J. S. Bell and R. Jackiw, Nuovo Cimento A **60**, 47 (1969); W. A. Bardeen, Phys. Rev. **184**, 1848 (1969).
- [21] H. W. Fearing and S. Scherer, Phys. Rev. D **53**, 315 (1996).
- [22] R. Akhoury and A. Alfakih, Ann. Phys. (N.Y.) **210**, 81 (1991).
- [23] J. Bijnens, L. Girlanda, and P. Talavera, Eur. Phys. J. C **23**, 539 (2002).
- [24] T. Ebertshauser, H. W. Fearing, and S. Scherer, Phys. Rev. D **65**, 054033 (2002).
- [25] J. Gasser and H. Leutwyler, Ann. Phys. (N.Y.) **158**, 142 (1984).
- [26] K. Kampf and J. Novotny, Acta Phys. Slovaca **52**, 265 (2002).
- [27] U. Bürgi, Nucl. Phys. **B479**, 392 (1996).
- [28] J. Bijnens, G. Colangelo, G. Ecker, J. Gasser, and M. E.

CHIRAL EXPANSIONS OF THE π^0 LIFETIME

- Sainio, Nucl. Phys. **B508**, 263 (1997), **B517**, 639(E) (1998).
- [29] J. Bijnens, G. Colangelo, and G. Ecker, J. High Energy Phys. 02 (1999) 020.
- [30] J. Gasser and M. E. Sainio, Eur. Phys. J. C **6**, 297 (1999).
- [31] J. Gasser and H. Leutwyler, Nucl. Phys. **B250**, 465 (1985).
- [32] J. Gasser, C. Haefeli, M. A. Ivanov, and M. Schmid, Phys. Lett. B **652**, 21 (2007).
- [33] C. Haefeli, M. A. Ivanov, and M. Schmid, Eur. Phys. J. C **53**, 549 (2008).
- [34] W. J. Marciano and A. Sirlin, Phys. Rev. Lett. **71**, 3629 (1993).
- [35] M. Knecht, H. Neufeld, H. Rupertsberger, and P. Talavera, Eur. Phys. J. C **12**, 469 (2000).
- [36] S. Descotes-Genon and B. Moussallam, Eur. Phys. J. C **42**, 403 (2005).
- [37] I. S. Towner and J. C. Hardy, Phys. Rev. C **77**, 025501 (2008).
- [38] D. B. Kaplan and A. V. Manohar, Phys. Rev. Lett. **56**, 2004 (1986).
- [39] C. Allton *et al.* (RBC-UKQCD Collaboration), Phys. Rev. D **78**, 114509 (2008).
- [40] J. Bijnens and K. Ghorbani, J. High Energy Phys. 11 (2007) 030.
- [41] R. Baur, J. Kambor, and D. Wyler, Nucl. Phys. **B460**, 127 (1996).
- PHYSICAL REVIEW D **79**, 076005 (2009)
- [42] C. Ditsche, B. Kubis, and U. G. Meissner, Eur. Phys. J. C **60**, 83 (2009).
- [43] A. Kastner and H. Neufeld, Eur. Phys. J. C **57**, 541 (2008).
- [44] K. Kampf and B. Moussallam, Eur. Phys. J. C **47**, 723 (2006).
- [45] A. Deandrea, A. Nehme, and P. Talavera, Phys. Rev. D **78**, 034032 (2008).
- [46] K. Abe *et al.* (Belle Collaboration), arXiv:hep-ex/0610022.
- [47] T. N. Pham, Phys. Lett. B **246**, 175 (1990).
- [48] B. Holdom, J. Terning, and K. Verbeek, Phys. Lett. B **245**, 612 (1990).
- [49] J. Bijnens and J. Prades, Z. Phys. C **64**, 475 (1994).
- [50] B. Moussallam, Phys. Rev. D **51**, 4939 (1995).
- [51] A. Browman, J. DeWire, B. Gittelman, K. M. Hanson, E. Loh, and R. Lewis, Phys. Rev. Lett. **32**, 1067 (1974).
- [52] T. E. Rodrigues *et al.*, Phys. Rev. Lett. **101**, 012301 (2008).
- [53] C. Amsler *et al.* (Particle Data Group), Phys. Lett. B **667**, 1 (2008).
- [54] M. Antonelli, arXiv:0712.0734.
- [55] K. Kampf, M. Knecht, and J. Novotny, Eur. Phys. J. C **46**, 191 (2006).
- [56] V. Bernard, M. Oertel, E. Passemar, and J. Stern, J. High Energy Phys. 01 (2008) 015.

2.2 Neutral pseudoscalar meson decays: $\pi^0 \rightarrow \gamma\gamma$ and $\eta \rightarrow \gamma\gamma$ in SU(3) limit

J. Bijnens and K. Kampf, *Neutral pseudoscalar meson decays: $\pi^0 \rightarrow \gamma\gamma$ and $\eta \rightarrow \gamma\gamma$ in SU(3) limit*, Nucl. Phys. Proc. Suppl. **207-208** (2010) 220 [arXiv:1009.5493 [hep-ph]]

Available online at www.sciencedirect.com

Nuclear Physics B (Proc. Suppl.) 207–208 (2010) 220–223

NUCLEAR PHYSICS B
PROCEEDINGS
SUPPLEMENTS
www.elsevier.com/locate/nphys

Neutral pseudoscalar meson decays: $\pi^0 \rightarrow \gamma\gamma$ and $\eta \rightarrow \gamma\gamma$ in $SU(3)$ limit**

Johan Bijnens^a, Karol Kampf^{a,b,*}
^aDepartment of Astronomy and Theoretical Physics, Lund University,
 Sölvegatan 14A, SE 223-62 Lund, Sweden.

^bCharles University, Faculty of Mathematics and Physics,
 V Holešovičkách 2, Prague, Czech Republic

Abstract

Present and planned experiments motivate new theoretical study of properties of light unflavoured pseudoscalar meson decays. An overview including details on two-loop calculation in $SU(3)$ limit is given.

Keywords: chiral perturbation theory, radiative decay of π^0 , higher-order correction

1. Introduction

We would like to study unflavoured decays of light neutral pseudoscalar mesons. This reduces the particle content to π^0 , η and eventually η' , ruling out K^0 decays that violate hypercharge conservation and are suppressed by G_F^2 (two-photon decays are further suppressed by α^2 compared to hadronic ones). Standard model is thus reduced to QCD (extended eventually only by QED corrections) which is successfully described by an effective theory known as chiral perturbation theory (ChPT).

The π^0 meson being the lightest meson cannot decay to other hadronic states. Its dominant decay mode (with more than 98% probability) is $\pi^0 \rightarrow \gamma\gamma$ and is connected with the Adler-Bell-Jackiw triangle anomaly [1]. The $\pi^0\gamma\gamma$ vertex is closely connected with other allowed π^0 decay modes: $e^+e^-\gamma$, $e^+e^-e^+e^-$, e^+e^- (with branching ratios [2]: $0.01174(35)$, $3.34(16)\times 10^{-5}$, $6.46(33)\times 10^{-8}$, respectively). In order to describe these processes with sufficient precision one can employ two-flavour ChPT at appropriate order. This can simply incorporate corrections to the current algebra result attributed either to $m_{u,d}$ masses or electromagnetic corrections with other effects hidden in the low energy constants (LECs). Naively,

two-flavour ChPT should converge very fast and next-to-leading order (NLO) should be sufficient from the point of view of today's experiments. However, as we are exploring the anomalous sector which is poorly known, phenomenologically richer $SU(3)$ ChPT must be also used in order to obtain numerical prediction for low energy constants. This on the other hand enables to describe $\eta \rightarrow \gamma\gamma$ in the same framework.

The motivation for our study is both theoretical and experimental. As mentioned, $\pi^0 \rightarrow \gamma\gamma$ represents (probably) the most important example of the triangle anomaly in quantum field theory. It is interesting that at NLO the amplitude gets no chiral corrections from the so-called chiral logarithms [3] and this motivate the calculation at NNLO even for $SU(2)$ ChPT as was done in [4]. It was found that there are indeed chiral logarithms generated by two-loop diagrams, but they are relatively small. It turns one's attention back to NLO order and contributions proportional to LECs. To this end the phenomenology of $\eta \rightarrow \gamma\gamma$ and inevitably $\eta-\eta'$ mixing must be employed. We intend to do the full two-loop calculation of both $\pi^0 \rightarrow \gamma\gamma$ and $\eta \rightarrow \gamma\gamma$ in three-flavour ChPT. As a first step we will present here the calculation and result in the $SU(3)$ limit, i.e. for $m_u = m_d = m_s$.

From the experimental side let us mention the PrimEx experiment at JLab. It is designed to perform the most precise measurement of the neutral pion lifetime using the Primakoff effect (for first run results see [5]). After JLab's 12 GeV upgrade the extension of the experiment for η and η' radiative width measurements is planned. Neutral pion decay modes were studied with interesting

*Speaker

**Supported by European Commission RTN network, Contract MRTN-CT-2006-035482 (FLAVIANet), European Community-Research Infrastructure Integrating Activity (HadronPhysics2, Grant Agreement n. 227431) and the Swedish Research Council.

Email addresses: bijnens@thep.lu.se (Johan Bijnens),
karol.kampf@thep.lu.se (Karol Kampf)

results at KTeV and it is promising to measure them in forthcoming NA62 at CERN.

2. Chiral expansion

Let us briefly summarize main points of ChPT, for details see [6]. Starting point is the chiral symmetry of QCD, called chiral because it acts differently on left and right-handed quarks, which is exact for $m_u = m_d = m_s = 0$:

$$G = SU(3)_L \times SU(3)_R,$$

where we dropped $U(1)_A$ which is not a good symmetry due the anomaly. However, this anomaly is proportional to a divergence which must thus vanish in any order of perturbation theory. We are touching the problem referred as $U(1)$ problem and we will avoid further discussion assuming that the ninth axial current is really not conserved and a possible divergence term is not present in QCD Lagrangian (referred itself as strong CP problem). Assuming further confinement it can be proven that the axial subgroup of G is spontaneously broken and the associated 8 Goldstone bosons can be identified with pions, kaons and eta. The real non-zero masses of u, d, s quarks, explicit symmetry breaking, are added as a perturbation and this expansion around the chiral limit together with the momentum expansion is referred to as ChPT. Standard power counting assumes that $m_{u,d,s} = O(p^2)$, and Lorentz invariance implies that only even powers of derivatives (p) can occur. The leading order (LO) thus starts at $O(p^2)$ and one can have only tree diagrams. The next-to-leading order (NLO) is $O(p^4)$ and can include one-loop contribution and similarly next-to-next-to-leading order (NNLO) is $O(p^6)$ and can have up to two-loop diagrams. The last important point to be discussed here is the so-called chiral or external anomaly which would correctly incorporate the full symmetry pattern of QCD. It is connected with the fact that quarks carry also electromagnetic charge. In fact some Green functions of QCD (e.g. VVA) are not invariant under chiral symmetry, the difference was calculated first by Bardeen [1] and incorporated to the action by Wess, Zumino and Witten (WZW) [7]. This action starts at $O(p^4)$ and thus the anomalous vertex shifts our counting by one order (i.e. NNLO here is $O(p^8)$).

3. Decay modes

We are primarily interested now in two-photon decays of π^0 and η . Nevertheless let us summarize shortly their “spin-off” products, namely

- $\pi^0 \rightarrow e^+e^-\gamma$ so called Dalitz decay is important in normalization of rare pion and kaon decays. This was supported by its precise and stable prediction: for 30 years its official PDG value was same (based on LAMPF experiment). However the last edition changed this number, based on ALEPH results and so it will have impact in other measurements via the normalization. The differential decay rate is discussed in [8].
- $\pi^0 \rightarrow e^+e^-e^+e^-$ or double Dalitz decay enables experimental verification of π^0 parity. KTeV set recently new limits on parity and CPT violation [9]
- $\pi^0 \rightarrow e^+e^-$ depends directly only on fully off-shell $\pi^0\gamma^*\gamma^*$ vertex. KTeV measurement [10] is off by 3.5σ from the existing models. It can set valuable limits on models beyond SM
- $\pi^0 \rightarrow \text{invisible}(\gamma)$, exotics and violation processes were also studied in π^0 decays. It includes mainly decay to neutrinos but is also interesting in beyond SM scenarios (neutralinos, extra-light neutral vector particle, etc.)

(for more references cf. [2]). The same modes are also possible in η decays, see e.g. [11].

4. LO and NLO calculation

In the chiral limit the decay width is fixed by axial anomaly with the result

$$\Gamma(\pi^0 \rightarrow \gamma\gamma)^{CA} = \frac{m_{\pi^0}^3}{64\pi} \left(\frac{\alpha N_C}{3\pi F_\pi} \right)^2 \approx 7.76 \text{ eV}. \quad (1)$$

It is in excellent agreement with experiment, which is the opposite situation to two-photon η decay. In $SU(3)$ limit (and also in chiral limit) the two studied amplitudes are connected by Wigner-Eckart theorem $\sqrt{3}T_\eta = T_{\pi^0}$, i.e.

$$\Gamma(\eta \rightarrow \gamma\gamma)^{CA} = \frac{m_\eta^3}{64\pi} \left(\frac{\alpha N_C}{3\sqrt{3}\pi F_\pi} \right)^2 \approx 173 \text{ eV}, \quad (2)$$

which is far from experiment $0.510 \pm 0.026 \text{ keV}$ [2]. (Note that using F_η instead of F_π makes this difference even larger.) The difference is attributed to η - η' mixing. At NLO order, apart from tree diagrams coming from WZW and $O(p^6)$ odd-parity Lagrangian, we should include two one-loop topologies (depicted in Fig.1).

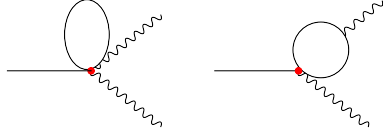


Figure 1: One-loop corrections to two photon pseudoscalar decays. A (red) dot represents the odd-parity coupling.

The full one-loop calculation based on wave function renormalization and chiral expansion of masses and decay constants leads to:

$$\begin{aligned}\Gamma(\pi^0 \rightarrow \gamma\gamma)^{NLO} &= \Gamma(\pi^0 \rightarrow \gamma\gamma)^{CA} \times \left[1 - \frac{256\pi^2}{3} m_\pi^2 C_7^{Wr} \right]^2, \\ \Gamma(\eta \rightarrow \gamma\gamma)^{NLO} &= \Gamma(\eta \rightarrow \gamma\gamma)^{CA} \times \left[\frac{F_\pi^2}{F_\eta^2} + \frac{256\pi^2}{9} \right. \\ &\quad \left. \times \left((4m_K^2 - 7m_\pi^2) C_7^{Wr} + 24(m_K^2 - m_\pi^2) C_8^{Wr} \right) \right]^2.\end{aligned}\quad (3)$$

Note, as anticipated, the very simple, polynomial form of the results without logarithms. This is especially accomplished by correct replacement of F_0 , i.e. $F_0 \rightarrow F_\pi$ and F_η in π^0 and η decay respectively.

It is clear from (3) that η - η' mixing must be hidden in C_8^{Wr} LEC. A rough estimate using resonance saturation suggests that C_8^{Wr} must be much bigger than C_7^{Wr} . For further discussion see [12] and [4].

5. Two-loop calculation in $SU(3)$ limit

The $O(p^8)$, (or equivalently NNLO, or two-loop) calculation was already performed for $\pi^0 \rightarrow \gamma\gamma$ in two-flavour ChPT. Natural extension for $SU(3)$ will supply us with both π^0 and also $\eta \rightarrow \gamma\gamma$ and enable to test and verify chiral expansion in odd intrinsic sector (cf. study for even sector [13]). It is, however, clear that this calculation will be difficult: we are facing instead of one, three different scales in overlapping two-loop diagrams (sunset and vertex). Big effort was already given in the simpler two-point (sunset) case, and we still lack general analytic form. We plan to calculate it using method described in [14] but we need to go beyond the loop integrals computed there. There exists, however, apart from chiral limit, one non-trivial limit which can be used to obtain analytical result as it depends again only on one scale. It is an $SU(3)$ limit, where we set $m_u = m_d = m_s = m \neq 0$. This we can simply connect with $O(p^2)$ mass: $M_\pi^{(0)2} = 2Bm$.

The current algebra prediction, fixed by the anomaly, is free from any mass contribution. The mass enters explicitly at NLO order only, and therefore to obtain

NNLO order we need to connect $O(p^2)$ parameter with physical $SU(3)$ mass.

$$\frac{M_\pi^2}{M^2} = 1 + \frac{M_\pi^2}{F_\pi^2} \left[\frac{L}{3} - 8(3L_4^r + L_5^r - 6L_6^r - 2L_8^r) \right] + O(M_\pi^4)$$

with chiral logarithm defined as $(4\pi)^2 L = \ln M_\pi^2/\mu^2$. On the other hand connection of F_0 with physical $SU(3)$ decay constants is needed up to NNLO order

$$\frac{F_\pi}{F_0} = 1 + \frac{M_\pi^2}{F_\pi^2} (12L_4^r + 4L_5^r - \frac{3}{2}L) + \frac{M_\pi^4}{F_\pi^4} f_{NNLO} + O(M_\pi^6).$$

The NNLO part was already calculated in general $SU(N_F)$ in [15] and for our $N_F = 3$ is given by

$$f_{NNLO} = \frac{\lambda_F}{(4\pi)^2} + \bar{\lambda}_F + \mathcal{K}_F + r_F + \frac{1561L}{288(4\pi)^2} - \frac{421}{2304(4\pi)^4}$$

with

$$\begin{aligned}\lambda_F &= -2L_1^r - 9L_2^r - 7/3L_3^r \\ \bar{\lambda}_F &= 8(3L_4^r + L_5^r)(21L_4^r + 7L_5^r - 24L_6^r - 8L_8^r) \\ \mathcal{K}_F &= 1/2(34\mathcal{K}_1 + 13\mathcal{K}_2 + 13\mathcal{K}_3 - 45\mathcal{K}_4 - 15\mathcal{K}_5) \\ r_F &= 8(C_{14}^r + 3C_{15}^r + 3C_{16}^r + C_{17}^r)\end{aligned}$$

and $\mathcal{K}_i = (4L_i^r - \Gamma_i L)L$ using renormalization coefficients taken from [6].

As already mentioned, for $SU(3)$ limit π^0 and η decays are related by Wigner-Eckart theorem and we thus need to calculate only one of these processes. Following Weinberg power-counting at NNLO we need to consider $a)$ tree graphs with either $a_1)$ one vertex from odd $O(p^8)$ sector or $a_2)$ one from odd (even) $O(p^6)$ and second from even (odd) $O(p^4)$; $b)$ one-loop diagrams with one vertex with NLO coupling (even or odd) and $c)$ the two-loop graphs with one vertex taken from the WZW Lagrangian. All other vertices should be generated by the $O(p^2)$ chiral Lagrangian.

Case $a_2)$ is treated via wave function renormalization. However, the odd-sector Lagrangian at $O(p^8)$ for three flavours has not yet been studied. The connected LEC will be denoted as D_i^{Wr} and set only a posteriori to cancel all local divergences. Concerning one-loop Feynman diagrams, we have already summarized them in Fig.1, for NNLO the topology stays the same, we need just to insert higher-order vertices. Non-trivial part of calculation is hidden in two loops. The Feynman diagrams to deal with are summarized in Fig.2. Corrections (tadpoles) to propagators are not depicted. Note that the most of diagrams are the same as in the two-flavour case. As anticipated by the nature of the anomaly there is one new topology (the last one diagram in Fig.2) with

anomalous vertex without direct photon insertion (so-called Chesire-cat smile). Of course, into these graphs one should insert all possible combinations of pions, kaons and eta (fortunately in $SU(3)$ limit with identical masses).

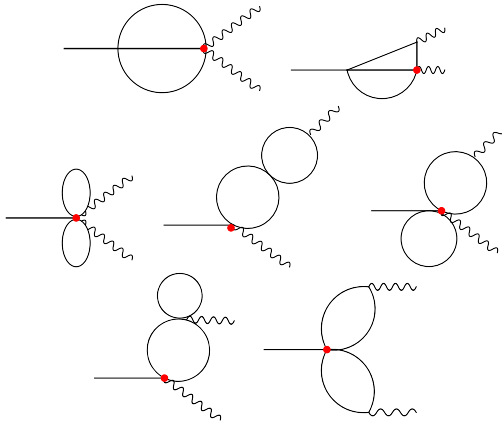


Figure 2: Two-loop corrections to two photon pseudoscalar decays.

We summarize the preliminary result in the following form (T is normalized as $T^{CA} = 1$ at LO, cf. eqs (3)).

$$\frac{F_\pi^4}{m_\pi^4} T^{NNLO} = \frac{\lambda}{(4\pi)^2} + (4\pi)^2 \bar{\lambda} + (4\pi)^2 \mathcal{K} + r + \frac{329L}{96(4\pi)^2} + \frac{9\sqrt{3}\text{Cl}_2(\pi/3) - 4\zeta(3) - \frac{7093}{1152}}{(4\pi)^4} \quad (4)$$

with

$$\lambda = 0$$

$$\bar{\lambda} = -\frac{256}{3} F_0^2 C_7^{Wr} (3L_4^r + L_5^r - 3L_6^r - L_8^r)$$

$$\mathcal{K} = 4\mathcal{K}_4^w + 10\mathcal{K}_7^w - 2\mathcal{K}_9^w + 4\mathcal{K}_{11}^w - \frac{1}{2}\mathcal{K}_{13}^w - 2\mathcal{K}_{14}^w - \mathcal{K}_{15}^w$$

$$r = -32C_{12}^r - 96C_{13}^r - 4D_{lim}^{Wr}$$

and $\mathcal{K}_i^w = (4F_0^2 C_i^{Wr} - \eta_i^{(3)} L) L$ using renormalization coefficients taken from [16]. The $O(p^8)$ chiral coupling which would cancel local divergences in $SU(3)$ limit is denoted by D_{lim}^W and our exact calculation fixes its decomposition

$$D_{lim}^W = \frac{(c\mu)^{2(d-4)}}{F_0^2} \left[D_{lim}^{Wr}(\mu) + \Lambda^2 \frac{127}{12} + \Lambda \left(\frac{208}{3} L_1^r + 32L_2^r + \frac{248}{9} L_3^r + 36L_4^r + 12L_5^r + \frac{91}{128(4\pi)^2} + (4\pi F_0)^2 (8C_4^{Wr} + \frac{100}{9} C_7^{Wr} - 4C_9^{Wr} + 8C_{11}^{Wr} - C_{13}^{Wr} - 4C_{14}^{Wr} - 2C_{15}^{Wr}) \right) \right].$$

6. Conclusion

We have summarized here our preliminary results concerning a two-loop calculation of $\pi^0(\eta) \rightarrow \gamma\gamma$ in $SU(3)$ limit (where $m_{u,d} = m_s = m$). The word preliminary refers also to the fact that independent calculation with physical masses is in progress [17] and it should allow us to crosscheck here presented result in this limit. The possibility of studying two-photon decays of light-meson on lattice was very recently demonstrated in [18]. The simple analytical result can be very useful in this direction as one can vary masses without changing LECs.

Acknowledgements

K.K. would like to thank the organizers for a very enjoyable conference.

References

- [1] S. L. Adler, Phys. Rev. **177** (1969) 2426, J. S. Bell and R. Jackiw, Nuovo Cim. A **60** (1969) 47, W. A. Bardeen, Phys. Rev. **184** (1969) 1848.
- [2] K. Nakamura *et al.* [Particle Data Group], J. Phys. G **37** (2010) 075021.
- [3] J. F. Donoghue, B. R. Holstein and Y. C. R. Lin, Phys. Rev. Lett. **55** (1985) 2766 [Erratum-ibid. **61** (1988) 1527]; J. Bijnens, A. Bramon and F. Cornet, Phys. Rev. Lett. **61** (1988) 1453.
- [4] K. Kampf and B. Moussallam, Phys. Rev. D **79** (2009) 076005 [arXiv:0901.4688 [hep-ph]].
- [5] A. M. Bernstein, PoS C **D09** (2009) 035.
- [6] J. Gasser and H. Leutwyler, Annals Phys. **158** (1984) 142; Nucl. Phys. B **250** (1985) 465.
- [7] J. Wess and B. Zumino, Phys. Lett. B **37** (1971) 95; E. Witten, Nucl. Phys. B **223** (1983) 422.
- [8] K. Kampf, M. Knecht and J. Novotný, Eur. Phys. J. C **46** (2006) 191 [arXiv:hep-ph/0510021].
- [9] E. Abouzaid *et al.* [KTeV Collaboration], Phys. Rev. Lett. **100** (2008) 182001 [arXiv:0802.2064 [hep-ex]].
- [10] E. Abouzaid *et al.* [KTeV Collaboration], Phys. Rev. D **75** (2007) 012004 [arXiv:hep-ex/0610072].
- [11] J. Bijnens and F. Persson, arXiv:hep-ph/0106130.
- [12] B. Ananthanarayan and B. Moussallam, JHEP **0205** (2002) 052 [arXiv:hep-ph/0205232].
- [13] J. Bijnens and I. Jemos, Eur. Phys. J. C **64** (2009) 273 [arXiv:0906.3118 [hep-ph]].
- [14] G. Amorós, J. Bijnens and P. Talavera, Nucl. Phys. B **585** (2000) 293 [Erratum-ibid. B **598** (2001) 665] [arXiv:hep-ph/0003258].
- [15] J. Bijnens and J. Lu, JHEP **0911** (2009) 116 [arXiv:0910.5424 [hep-ph]].
- [16] J. Bijnens, L. Girlanda and P. Talavera, Eur. Phys. J. C **23** (2002) 539 [arXiv:hep-ph/0110400].
- [17] J. Bijnens and K. Kampf, *in preparation*
- [18] S. D. Cohen, H. W. Lin, J. Dudek and R. G. Edwards, PoS LATTICE2008 (2008) 159 [arXiv:0810.5550 [hep-lat]]; E. Shintani, S. Aoki, S. Hashimoto, T. Onogi and N. Yamada [JLQCD Collaboration], arXiv:0912.0253 [hep-lat].

2.3 Resonance saturation in the odd-intrinsic parity sector of low-energy QCD

K. Kampf and J. Novotny, *Resonance saturation in the odd-intrinsic parity sector of low-energy QCD*, Phys. Rev. D **84** (2011) 014036 [arXiv:1104.3137 [hep-ph]].

PHYSICAL REVIEW D **84**, 014036 (2011)**Resonance saturation in the odd-intrinsic parity sector of low-energy QCD**Karol Kampf^{1,2} and Jiří Novotný²¹*Department of Astronomy and Theoretical Physics, Lund University, Sölvegatan 14A, SE 223-62 Lund, Sweden*²*Institute of Particle and Nuclear Physics, Faculty of Mathematics and Physics,**Charles University in Prague, 18000 Prague, Czech Republic*

(Received 10 June 2011; published 29 July 2011)

Using the large N_C approximation we have constructed the most general chiral resonance Lagrangian in the odd-intrinsic parity sector that can generate low-energy chiral constants up to $\mathcal{O}(p^6)$. Integrating out the resonance fields these $\mathcal{O}(p^6)$ constants are expressed in terms of resonance couplings and masses. The role of η' is discussed and its contribution is explicitly factorized. Using the resonance basis we have also calculated two QCD Green functions of currents, $\langle VVP \rangle$ and $\langle VAS \rangle$, and found, imposing high-energy constraints, additional relations for resonance couplings. We have studied several phenomenological implications based on these correlators which provided, for example, a prediction for the π^0 -pole contribution to the muon $g - 2$ factor: $a_\mu^{\pi^0} = 65.8(1.2) \times 10^{-11}$.

DOI: [10.1103/PhysRevD.84.014036](https://doi.org/10.1103/PhysRevD.84.014036)

PACS numbers: 12.39.Fe, 11.15.Pg, 11.30.Rd, 14.40.Be

I. INTRODUCTION

As is well known, there are two regimes where the QCD dynamics of the current correlators is well understood. The first one corresponds to the high energies where the asymptotic freedom allows us to use the perturbative approach in terms of the strong coupling constant α_s and where the asymptotics of the correlators for large Euclidean momenta is governed by operator product expansion (OPE). The second well-understood region is that of low external momenta where the dynamics is constrained by the spontaneously broken chiral symmetry. As a consequence, the dominant contributions to the correlators and related amplitudes of the processes of interest come from the octet of the lightest pseudoscalar mesons (π , K , η) which are the corresponding (pseudo)Goldstone bosons (GBs). The correlators can be studied here by means of chiral perturbation theory (ChPT) [1–3], which is the effective Lagrangian field theory for this region, in terms of systematic simultaneous expansion in powers (and logs) of the momenta and quark masses. The applicability of ChPT extends up to the hadronic scale $\Lambda_H \sim 1$ GeV, which corresponds to the onset of non-Goldstone resonances and where the ChPT expansion fails to converge.

OPE and ChPT provide us with an asymptotic behavior of the correlators in different regimes; however, both these approaches need further nonperturbative information which is not known from the first principles, namely, the values of the vacuum condensates for OPE and the values of the effective low-energy constants (LECs) for ChPT. In the latter case the LECs parametrize our lack of detailed information on the nonperturbative dynamics of the degrees of freedom above the hadronic scale Λ_H and are connected with the order parameters of the spontaneously broken chiral symmetry. The predictivity of ChPT heavily relies on their determination. At the order $\mathcal{O}(p^6)$, which corresponds to the recent accuracy of the next-to-next-to-

leading order (NNLO) ChPT calculation (for a comprehensive review and further references see [4]), 90 + 4 LECs in the even-intrinsic parity sector [5,6] and 23 LECs in the odd sector¹ [7,8] appear in the effective Lagrangian. Though only special linear combinations of them are relevant for particular physical amplitudes, the uncertainty in their estimation is usually the weakest point of the interconnection between the theory and experiment.

A dispersion representation of those correlators which are order parameters of the chiral symmetry breaking (and therefore do not get any genuine perturbative contribution) enables us to make use of information on the asymptotics, both in the low- and high-energy regions, and to relate the unknown LECs to the properties of the corresponding spectral functions in terms of the chiral sum rules [2,9–12]. These are usually assumed to be saturated by the low-lying resonant states; such an assumption (known as the resonance saturation hypothesis) connects the LECs to the phenomenology of resonances in the intermediate-energy region $1 \text{ GeV} \leq E < 2 \text{ GeV}$. Though the inclusion of only a finite number of resonances has been questioned in the literature [13,14], it proved to be consistent in the $\mathcal{O}(p^4)$ case with other phenomenological determinations of LECs.

The necessary ingredient of the resonance saturation approach to the determination/estimation of LECs is the phenomenological information on the physics of the lowest resonances. It can be conveniently parametrized by means of a suitable phenomenological Lagrangian. Along with the chiral symmetry, the guiding theoretical principles for its construction are those based on the large N_C expansion of QCD [15]. Within the leading order in $1/N_C$, the correlators of the quark bilinears are given by an infinite sum of contributions of narrow meson resonance states, the mass

¹These numbers of LECs are relevant for an $SU(3)$ variant of ChPT. In the $SU(2)$ case we get 53 + 4 LECs in the even-intrinsic parity sector and 5(13) LECs in the odd sector.

KAROL KAMPF AND JIŘÍ NOVOTNÝ

PHYSICAL REVIEW D **84**, 014036 (2011)

of which scales as $O(N_C^0)$ and the interaction of which is suppressed by an appropriate power of $1/\sqrt{N_C}$. Such a large N_C representation of the correlators can be reconstructed using the effective Lagrangian \mathcal{L}_∞ , including the GB and an infinite tower of resonance fields with couplings of the order $O(N_C^{1-n/2})$, according to the number n of meson fields in the interaction vertices. The $1/N_C$ expansion is equivalent to the quasiclassical expansion; thus at the leading order only the tree graphs contribute and each additional loop is suppressed by one power of $1/N_C$.

Though \mathcal{L}_∞ is not known from first principles, the information on the large N_C hierarchy of the individual operators together with general symmetry assumptions allows one to construct all the relevant terms necessary to determine the LECs in the leading order of the large N_C expansion up to a given chiral order. The large N_C approximation of LECs can then be formally achieved by means of integrating out the resonance fields from the Lagrangian \mathcal{L}_∞ . One gets LECs expressed in terms of the (unknown from the first principles) masses and couplings of the infinite tower of resonances.

The large N_C inspired phenomenological Lagrangian suitable for the resonance saturation program for LECs can then be obtained as an approximation to \mathcal{L}_∞ , where only a finite number of resonances are kept. Such a truncation of \mathcal{L}_∞ seems to be legitimate at low energies, where the contribution of the higher resonances is expected to be suppressed. However, the lack of an effective cutoff scale which could play a role here analogous to Λ_H for ChPT prevents us from interpreting the resonance phenomenological Lagrangian as a well-defined effective theory in the usual sense. It is rather a QCD inspired phenomenological model which should share as many common features with QCD as possible. The latter principle generally puts various constraints on its effective couplings. For instance, the finite number of resonances involved generally corrupts the asymptotic behavior of the correlators required by perturbative QCD and OPE. However, it is natural to expect that, for the correlators which are order parameters of the spontaneous chiral symmetry breaking, the latter behavior extends down to the region of applicability of the phenomenological Lagrangian; thus, it is desirable to ensure the correct asymptotics by means of adjusting its couplings. This is, however, not enough to fix all of them (often it is not even possible to satisfy all the OPE requirements at once by a finite set of resonances); therefore, further phenomenological input is needed.

At the leading order in $1/N_C$, the above strategy for the determination of LECs is essentially equivalent to a similar approach known as the minimal hadronic ansatz (MHA) [16]. Within this approach the correlators are approximated by a meromorphic function with a correct pole structure corresponding to the resonance poles, and the free parameters are fixed, both by OPE constraints and by experimental inputs. Only a minimal number of resonances are taken

into account, just those necessary to satisfy all the relevant OPE (when only the lowest resonances in each channel are included, the method is called the lowest meson dominance (LMD) ansatz [12,16], but in this case not all OPE constraints are guaranteed to be met [12,17]). Matching this ansatz to the low-energy ChPT expansion enables us to determine relevant linear combinations of LECs.

The method based on the resonance Lagrangian is, however, a little bit more general than the MHA or LMD. On one hand, it enables us to determine (at least in principle) the individual LECs, not only their linear combinations connected with particular correlators; on the other hand, it provides a natural framework for going beyond the leading order in $1/N_C$ by means of integrating out the resonances at one-loop level [18–22], which also correctly takes into account the renormalization scale dependence of the LECs.

The above principles of construction of the phenomenological Lagrangian with resonances have been known since 1989 when the seminal paper [23] on what is now known as resonance chiral theory (R χ T) was published. In this paper the resonance saturation of the $O(p^4)$ LECs was studied systematically, while the $O(p^6)$ LECs of the even-intrinsic parity sector of ChPT was systematically analyzed 17 years later in [24]. For a recent review and further references see [25].

The study of the odd-intrinsic parity sector of R χ T with vector resonances and corresponding saturation of the LECs for the $O(p^6)$ anomaly sector of ChPT started in [12,26–28], where axial-vector resonances were also included and where the particular operator basis of the R χ T Lagrangian contributing to the correlators of interest was constructed. The influence of pseudoscalar resonances on the odd-intrinsic parity LECs has been studied in [11,12] and the corresponding part of the R χ T Lagrangian has been constructed in [29] (see also [30]). In this paper we resume this effort and construct the most general odd-intrinsic parity sector of the R χ T Lagrangian, including the lowest multiplets of the vector $V(1^{--})$, axial-vector $A(1^{++})$, scalar $S(0^{++})$, and pseudoscalar $P(0^{-+})$ resonances. In the 0^{-+} channel we thus introduce, besides the GB, the lowest non-GB resonance multiplet; therefore, we go beyond the LMD approximation (our correlators then correspond to what is called in [12] the LMD + P ansatz). The resulting Lagrangian is then used for the lowest-resonance saturation of the $O(p^6)$ anomaly sector of ChPT. We also illustrate the general strategy of matching the correlators with OPE on the concrete example of $\langle VVP \rangle$ and $\langle VAS \rangle$ three-point functions and discuss related phenomenological applications.

The paper is organized as follows. In Sec. II we fix our notation and briefly mention the principles of the construction of the Lagrangian of the R χ T. Section III is devoted to the presentation of the complete basis of the odd-intrinsic parity sector of R χ T. In Sec. IV we discuss related

RESONANCE SATURATION IN THE ODD-INTRINSIC ...

phenomenological applications, and in Sec. V we give the results of the resonance saturation of the odd-intrinsic parity $O(p^6)$ LECs. A brief summary is provided at the end. The large N_C counting of the relevant operators is discussed in Appendix A, and the operator redefinitions and reduction of the Lagrangian is studied in Appendix B.

II. THE RESONANCE CHIRAL THEORY

The LECs represent nonperturbative characteristics of the low-energy QCD correlators in the chiral limit and, as a consequence, their values do not depend on the quark masses. In what follows we will therefore work in the limit $m_q \rightarrow 0$ without loss of generality. This simplifies the calculations of the LEC saturation considerably.

The standard basic building block which includes the octet of the GB (here we assume that η' has already been integrated out of our effective Lagrangian; for details see Appendix A) is

$$u(\phi) = \exp\left(i\frac{\phi}{\sqrt{2}F}\right), \quad (1)$$

where $\phi = \frac{1}{\sqrt{2}}\lambda^a\phi^a$, λ^i being a standard Gell-Mann matrix and

$$\phi(x) = \begin{pmatrix} \frac{1}{\sqrt{2}}\pi^0 + \frac{1}{\sqrt{6}}\eta_8 & \pi^+ & K^+ \\ \pi^- & -\frac{1}{\sqrt{2}}\pi^0 + \frac{1}{\sqrt{6}}\eta_8 & K^0 \\ K^- & \bar{K}^0 & -\frac{2}{\sqrt{6}}\eta_8 \end{pmatrix}. \quad (2)$$

One can form the basic covariant tensors [5,31,32]

$$V_{\mu\nu} = \begin{pmatrix} \frac{1}{\sqrt{2}}\rho^0 + \frac{1}{\sqrt{6}}\omega_8 + \frac{1}{\sqrt{3}}\omega_1 & \rho^+ & K^{*+} \\ \rho^- & -\frac{1}{\sqrt{2}}\rho^0 + \frac{1}{\sqrt{6}}\omega_8 + \frac{1}{\sqrt{3}}\omega_1 & K^{*0} \\ K^{*-} & \bar{K}^{*0} & -\frac{2}{\sqrt{6}}\omega_8 + \frac{1}{\sqrt{3}}\omega_1 \end{pmatrix}_{\mu\nu} \quad (8)$$

(and similarly for other types). Here we use the antisymmetric tensor field for the description of the spin-1 resonances. The reason is that, though it is, in principle, equivalent to the Proca field formalism [see [33,34] for the general discussion of the equivalence at the orders $O(p^4)$ and $O(p^6)$, respectively, and [35] for a particular discussion of the one-loop equivalence], the antisymmetric tensor has several advantages. This tensor field naturally couples to the lowest order $O(p^2)$ chiral building blocks without derivatives, and therefore it does not require additional contact terms necessary to compensate the wrong high-energy behavior of the amplitudes and form factors of

²In fact, for some correlators calculated within the Proca field formalism, the OPE constraints cannot be satisfied unless operators of the higher chiral order [i.e. those which contribute only to $O(p^8)$ and higher LECs] are taken into account.

PHYSICAL REVIEW D **84**, 014036 (2011)

$$\begin{aligned} u_\mu &= u_\mu^\dagger = i\{u^\dagger(\partial_\mu - ir_\mu)u - u(\partial_\mu - i\ell_\mu)u^\dagger\}, \\ \chi_\pm &= u^\dagger\chi u^\dagger \pm u\chi^\dagger u, \quad f_\pm^{\mu\nu} = uF_L^{\mu\nu}u^\dagger \pm u^\dagger F_R^{\mu\nu}u, \\ h_{\mu\nu} &= \nabla_\mu u_\nu + \nabla_\nu u_\mu, \end{aligned} \quad (3)$$

with $\chi = 2B_0(s + ip)$, where s and p stand for the scalar and pseudoscalar external sources. The vector source v^μ and the axial-vector source a^μ are then related to the right and left sources r^μ and ℓ^μ by the relations $v^\mu = \frac{1}{2}(r^\mu + \ell^\mu)$ and $a^\mu = \frac{1}{2}(r^\mu - \ell^\mu)$, respectively, and $F_{L,R}^{\mu\nu}$ are the corresponding left and right field-strength tensors:

$$\begin{aligned} F_R^{\mu\nu} &= \partial^\mu r^\nu - \partial^\nu r^\mu - i[r^\mu, r^\nu], \\ F_L^{\mu\nu} &= \partial^\mu \ell^\nu - \partial^\nu \ell^\mu - i[\ell^\mu, \ell^\nu]. \end{aligned} \quad (4)$$

The covariant derivative is defined by

$$\nabla_\mu X = \partial_\mu X + [\Gamma_\mu, X], \quad (5)$$

where the chiral connection is

$$\Gamma_\mu = \frac{1}{2}\{u^\dagger(\partial_\mu - ir_\mu)u + u(\partial_\mu - i\ell_\mu)u^\dagger\}. \quad (6)$$

Inspired by the large N_C limit the GBs couple to massive $U(3)$ multiplets of the types $V(1^{--})$, $A(1^{++})$, $S(0^{++})$, and $P(0^{-+})$, denoted generically as a nonet field R . This field can be decomposed into the octet R_8 and singlet R_0 via

$$R = \frac{1}{\sqrt{3}}R_0 + \sum_i \frac{\lambda_i}{\sqrt{2}}R_i. \quad (7)$$

The explicit form of the vector multiplet $V(1^{--})$ is

interest.² Moreover, when using the Proca field without such contact terms, it is not possible to saturate the $O(p^4)$ LECs in the even-intrinsic parity sector. On the other hand, there is a contribution generated by the Proca fields for the $O(p^6)$ LECs of the odd-intrinsic parity sector (see [24,34]). However, integrating out the resonances from the antisymmetric tensor field Lagrangian generates a much richer structure of the resulting effective chiral Lagrangian which covers almost all the structures resulting from the Proca field formalism. A consistent way to incorporate the advantages (if any) of both approaches at the same time is the first-order formalism introduced in [34]. The price to pay

KAROL KAMPF AND JIŘÍ NOVOTNÝ

here is its relative complexity. The discussion of such a general case is beyond the scope of this paper, and we leave this subject open for future studies.

According to the large N_C counting of interaction vertices with resonances, we can organize the Lagrangian $\mathcal{L}_{R\chi T}$ of $R\chi T$ as an expansion in the number of resonance fields,

$$\mathcal{L}_{R\chi T} = \mathcal{L}_{\text{GB}} + \mathcal{L}_{RR,\text{kin}} + \mathcal{L}_R + \mathcal{L}_{RR'} + \mathcal{L}_{RR'R''} + \dots \quad (9)$$

Here \mathcal{L}_{GB} contains only Goldstone bosons and external sources and includes terms with the same structure as the usual $SU(3)_L \times SU(3)_R$ ChPT Lagrangian, but the coupling constants are generally different. The resonance kinetic terms $\mathcal{L}_{RR,\text{kin}}$, which are of the order $O(N_C^0)$, have the form

$$\begin{aligned} \mathcal{L}_{RR,\text{kin}} = & -\frac{1}{2}\langle \nabla^\mu R_{\mu\nu} \nabla_\alpha R^{\alpha\nu} \rangle + \frac{1}{4}M_R^2 \langle R_{\mu\nu} R^{\mu\nu} \rangle \\ & + \frac{1}{2}\langle \nabla^\alpha R' \nabla_\alpha R' \rangle - \frac{1}{2}M_{R'}^2 \langle R'R' \rangle, \end{aligned} \quad (10)$$

where R stands for $V^{\mu\nu}$ and $A^{\mu\nu}$ while R' stands for S and P . The terms \mathcal{L}_R , $\mathcal{L}_{RR'}$, and $\mathcal{L}_{RR'R''}$ collect the interaction vertices linear, quadratic, and cubic in the resonance fields, respectively.

There is also another type of expansion for $\mathcal{L}_{R\chi T}$. It is based on the ordering according to the contribution to chiral coupling constants. Within this counting, the resonance fields are effectively of the order

$$R = O(p^2), \quad (11)$$

while the chiral building blocks with GBs are only counted in the usual way. For \mathcal{L}_{GB} it is therefore just the usual chiral power counting. Combining this with the large N_C expansion (9) we can write

$$\begin{aligned} \mathcal{L}_{R\chi T} = & \mathcal{L}_{\text{GB}}^{(2)} + \mathcal{L}_{\text{GB}}^{(4)} + \mathcal{L}_{RR,\text{kin}}^{(4)} + \mathcal{L}_{RR,\text{kin}}^{(6)} + \mathcal{L}_R^{(4)} \\ & + \mathcal{L}_{\text{GB}}^{(6)} + \mathcal{L}_R^{(6)} + \mathcal{L}_{RR'}^{(6)} + \mathcal{L}_{RR'R''}^{(6)} \dots, \end{aligned} \quad (12)$$

where the subscript (n) stands for the contribution to the $O(p^n)$ chiral constant. For our further discussion we will explicitly need

$$\mathcal{L}_{\text{GB}}^{(2)} = \frac{F^2}{4} \langle u_\mu u^\mu + \chi_+ \rangle. \quad (13)$$

The leading order of the odd-intrinsic parity sector of $\mathcal{L}_{\text{GB}}^{(4)}$ coincides with the Wess-Zumino-Witten (WZW) Lagrangian [36] $\mathcal{L}_{\text{WZW}}^{(4)}$. For the explicit form of the even parity part $\mathcal{L}_{\text{GB}}^{(4)}$ and the complete $\mathcal{L}_{\text{GB}}^{(6)}$, see [3,5,8] (see also [7]).

The most general interaction Lagrangian $\mathcal{L}_R^{(4)}$ which is relevant for the saturation of the $O(p^4)$ LECs [23] is linear in resonance fields, namely,

PHYSICAL REVIEW D **84**, 014036 (2011)

$$\begin{aligned} \mathcal{L}_R^{(4)} = & c_d \langle Su^\mu u_\mu \rangle + c_m \langle S\chi_+ \rangle + i d_m \langle P\chi_- \rangle \\ & + i \frac{d_{m0}}{N_F} \langle P \rangle \langle \chi_- \rangle + \frac{F_V}{2\sqrt{2}} \langle V_{\mu\nu} f_+^{\mu\nu} \rangle \\ & + \frac{iG_V}{2\sqrt{2}} \langle V_{\mu\nu} [u^\mu, u^\nu] \rangle + \frac{F_A}{2\sqrt{2}} \langle A_{\mu\nu} f^{\mu\nu} \rangle, \end{aligned} \quad (14)$$

and all the couplings are of the order $O(N_C^{1/2})$. This is true also for the first term of the second line with two traces which is enhanced due to the η' exchange [see Appendix A, especially (A20)]. This term with d_{m0} (depending solely on the singlet component of P) has not yet been studied in the phenomenology, as it always contributes to the saturation of LECs together with the large N_C enhanced η' exchange. The complete operator basis of the $O(p^6)$ even-intrinsic parity of $R\chi T$ has been constructed in [24].

Integrating out the resonance fields at the tree level we reconstruct the Lagrangian $\mathcal{L}_{\chi\text{PT}}$ of ChPT, schematically

$$\exp\left(i \int d^4x \mathcal{L}_{\chi\text{PT}}\right) = \int \mathcal{D}R \exp\left(i \int d^4x \mathcal{L}_{R\chi T}\right). \quad (15)$$

The integration over R can be effectively done by insertion of the solution R_{EOM} of the classical equations of motion into the Lagrangian $\mathcal{L}_{R\chi T}$ and keeping only the terms up to (and including) the order $O(p^6)$. Let us expand R_{EOM} as

$$R_{\text{EOM}} = R^{(2)} + \Delta^{(4)}R, \quad (16)$$

where $R^{(2)} = O(p^2)$ and $\Delta^{(4)}R$ starts at $O(p^4)$. Then $R^{(2)}$ is, at the same time, the solution of the leading order equations of motion (i.e. those derived from $\mathcal{L}_{R\chi T}^{(4)} \equiv \mathcal{L}_{RR,\text{kin}}^{(4)} + \mathcal{L}_R^{(4)}$). Inserting now the expansion (16) into $\mathcal{L}_{R\chi T}$, the $\Delta^{(4)}R$ can contribute to the order $O(p^6)$ only when R_{EOM} is inserted into the leading order Lagrangian $\mathcal{L}_{R\chi T}^{(4)}$ and then expanded at $R^{(2)}$ up to the terms linear in $\Delta^{(4)}R$. However, the coefficients of these linear terms are just equal to the leading order equations of motion calculated at $R^{(2)}$ and therefore they vanish. As a consequence, effectively up to the order $O(p^6)$ the integration over R is equivalent to the insertion only of the solution $R^{(2)}$ of the lowest order equation of motion into the Lagrangian $\mathcal{L}_{R\chi T}$. Because the resonance field R couples to the $O(p^2)$ building blocks in $\mathcal{L}_R^{(4)}$ and the resonance masses are counted as $O(p^0)$, we are consistent with the chiral counting (11). Finally, we get

$$\mathcal{L}_{\chi\text{PT}} = \mathcal{L}_\chi^{(2)} + \mathcal{L}_\chi^{(4)} + \mathcal{L}_\chi^{(6)} + \dots$$

with an explicit separate contribution from the Goldstone boson part of the $R\chi T$ Lagrangian \mathcal{L}_{GB} and the leading N_C contribution of the resonances

$$\mathcal{L}_\chi^{(2)} = \mathcal{L}_{\text{GB}}^{(2)}, \quad (17)$$

$$\mathcal{L}_\chi^{(n>2)} = \mathcal{L}_{\text{GB}}^{(n)} + \mathcal{L}_{\chi,R}^{(n)}, \quad (18)$$

where, particularly,

RESONANCE SATURATION IN THE ODD-INTRINSIC ...

$$\begin{aligned}\mathcal{L}_{\chi,R}^{(4)} &= (\mathcal{L}_{RR,\text{kin}}^{(4)} + \mathcal{L}_R^{(4)})|_{R \rightarrow R^{(2)}}, \\ \mathcal{L}_{\chi,R}^{(6)} &= (\mathcal{L}_{RR,\text{kin}}^{(6)} + \mathcal{L}_R^{(6)} + \mathcal{L}_{RR'}^{(6)} + \mathcal{L}_{RR'R''}^{(6)})|_{R \rightarrow R^{(2)}}.\end{aligned}$$

The structures of the Lagrangians $\mathcal{L}_{\text{GB}}^{(n)}$ and $\mathcal{L}_{\chi,R}^{(n)}$ are identical to $\mathcal{L}_{\chi}^{(n)}$; just the couplings are different. Then for generic chiral coupling constants k_χ of $\mathcal{L}_{\chi\text{PT}}$, we may write

$$k_\chi = k_{\text{GB}} + k_{\chi,R}, \quad (19)$$

where $k_{\chi,R}$ corresponds to the resonance contribution. The usual hypothesis of resonance saturation assumes the existence of the saturation scale μ at which the renormalized k_{GB} is very small and where the resonance contribution $k_{\chi,R}$ is expected to be dominant.

The above resonance saturation strategy and the construction of all relevant operators have already been studied. The basis for all relevant resonance operators contributing to $\mathcal{O}(p^4)$ and their contribution to LECs were established in [23], while in [24] the authors presented the extension to $\mathcal{O}(p^6)$ in the even-intrinsic parity sector.

In this paper, we complete this effort by presenting the construction of the basis and resonance saturation at $\mathcal{O}(p^6)$ in the odd-intrinsic parity sector.

III. LAGRANGIAN OF $R\chi T$ IN THE ODD-INTRINSIC PARITY SECTOR

Before starting the construction of resonance monomials, let us summarize the structure of the pure Goldstone boson part of the odd-intrinsic sector. The leading order starts at $\mathcal{O}(p^4)$ and the parameters are set entirely by the chiral anomaly. The Lagrangian is given by [36] (see also [8]; note we have the same convention for the Levi-Civita symbol, i.e. $\epsilon_{0123} = 1$):

$$\begin{aligned}\mathcal{L}_{\text{WZW}} &= \frac{N_C}{48\pi^2} \epsilon^{\mu\nu\alpha\beta} \left\{ \int_0^1 d\xi \langle \sigma_\mu^\xi \sigma_\nu^\xi \sigma_\alpha^\xi \sigma_\beta^\xi \frac{\phi}{F} \rangle \right. \\ &\quad \left. - i \langle W_{\mu\nu\alpha\beta}(U, l, r) - W_{\mu\nu\alpha\beta}(1, l, r) \rangle \right\}, \quad (20)\end{aligned}$$

with

$$\begin{aligned}W_{\mu\nu\alpha\beta} &= L_\mu L_\nu L_\alpha R_\beta + \frac{1}{4} L_\mu R_\nu L_\alpha R_\beta + i L_{\mu\nu} L_\alpha R_\beta \\ &\quad + i R_{\mu\nu} L_\alpha R_\beta - i \sigma_\mu L_\nu R_\alpha L_\beta + \sigma_\mu R_\nu \alpha L_\beta \\ &\quad - \sigma_\mu \sigma_\nu R_\alpha L_\beta + \sigma_\mu L_\nu L_\alpha \beta + \sigma_\mu L_\nu \alpha L_\beta - i \sigma_\mu L_\nu L_\alpha L_\beta \\ &\quad + \frac{1}{2} \sigma_\mu L_\nu \sigma_\alpha L_\beta - i \sigma_\mu \sigma_\nu \sigma_\alpha L_\beta - (L \leftrightarrow R),\end{aligned}$$

where we have defined

$$\begin{aligned}L_\mu &= u l_\mu u^\dagger, & L_{\mu\nu} &= u \partial_\mu l_\nu u^\dagger, & R_\mu &= u^\dagger r_\mu u, \\ R_{\mu\nu} &= u \partial_\mu r_\nu u^\dagger, & \sigma_\mu &= \{u^\dagger, \partial_\mu u\}\end{aligned}$$

and $(L \leftrightarrow R)$ also stands for the $\sigma \leftrightarrow \sigma^\dagger$ interchange. The power ξ indicates a change of u to $u^\xi = \exp(i\xi\phi/(F\sqrt{2}))$. Concerning the $\mathcal{O}(p^6)$ part, we will stick to the form introduced in [8]. Let us only note that we will drop the

PHYSICAL REVIEW D **84**, 014036 (2011)

index r and the explicit dependence on the renormalization scale μ from the corresponding LECs C_i^W , but one should have in mind that any C_i^W studied in this text is a renormalized LEC with a scale set to some reasonable value ($\sim M_\rho, M_{\eta'}$) to make good sense of the following study.

For the construction of the operator basis in the odd-intrinsic parity sector of $R\chi T$, we use the same tools as employed in [24], where the reader can find further details. First we construct all possible Hermitian operators built from chiral building blocks and resonance fields that are invariant under C, P , and chiral transformations. Then, in order to find the independent basis, we use the following.

- (1) Partial integration.
- (2) Equation of motion,

$$\nabla^\mu u_\mu = \frac{i}{2} \left(\chi_- - \frac{1}{N_F} \langle \chi_- \rangle \right). \quad (21)$$

- (3) Bianchi identities,

$$\begin{aligned}\nabla_\mu \Gamma_{\nu\rho} + \nabla_\nu \Gamma_{\rho\mu} + \nabla_\rho \Gamma_{\mu\nu} &= 0 \\ \text{for } \Gamma_{\mu\nu} &= \frac{1}{4} [u_\mu, u_\nu] - \frac{i}{2} f_{+\mu\nu}.\end{aligned} \quad (22)$$

- (4) Shouten identity [37],

$$\begin{aligned}g_{\sigma\rho} \epsilon_{\alpha\beta\mu\nu} + g_{\sigma\alpha} \epsilon_{\beta\mu\nu\rho} + g_{\sigma\beta} \epsilon_{\mu\nu\rho\alpha} \\ + g_{\sigma\mu} \epsilon_{\nu\rho\alpha\beta} + g_{\sigma\nu} \epsilon_{\rho\alpha\beta\mu} &= 0.\end{aligned} \quad (23)$$

- (5) Identity,

$$\nabla^\mu h_{\mu\nu} = \nabla_\nu h_\mu^\mu - 2[u^\mu, i\Gamma_{\mu\nu}] - \nabla^\mu f_{-\mu\nu}. \quad (24)$$

All relevant operators in the odd parity sector can be written in the form

$$\mathcal{O}_i^X = \epsilon^{\mu\nu\alpha\beta} \hat{\mathcal{O}}_{i\mu\nu\alpha\beta}^X, \quad (25)$$

with the basis for individual monomials $\hat{\mathcal{O}}_{i\mu\nu\alpha\beta}^X$, where $X = V, A, P, S, VV, AA, SA, SV, VA, PA, PV, VVP, VAS, AAP$; so the Lagrangian becomes

$$\mathcal{L}_{R\chi T}^{(6,\text{odd})} = \sum_X \sum_i \kappa_i^X \mathcal{O}_i^X. \quad (26)$$

The basis of the operators $\hat{\mathcal{O}}_{i\mu\nu\alpha\beta}^X$ is summarized in Tables I, II, III, IV, V, VI, and VII. We have included there only the operators relevant in the leading order in the $1/N_C$ expansion, i.e. operators with one flavor trace and those with two traces that are enhanced by η' exchange (see Appendix A for details). This represents the main result of our work.

As is shown in [24,34], we can further modify the resonance Lagrangian (26). The reason is that the resonance fields play merely the role of the integration

KAROL KAMPF AND JIŘÍ NOVOTNÝ

TABLE I. Monomials with one vector resonance field.

i	$\hat{\mathcal{O}}_{i\mu\nu\alpha\beta}^V$	i	$\hat{\mathcal{O}}_{i\mu\nu\alpha\beta}^V$
1	$i\langle V^{\mu\nu}(h^{\alpha\sigma}u_\sigma u^\beta - u^\beta u_\sigma h^{\alpha\sigma}) \rangle$	11	$\langle V^{\mu\nu}\{f_+^{\alpha\rho}, f_-^{\beta\sigma}\}g_{\rho\sigma}$
2	$i\langle V^{\mu\nu}(u_\sigma h^{\alpha\sigma}u^\beta - u^\beta h^{\alpha\sigma}u_\sigma) \rangle$	12	$\langle V^{\mu\nu}\{f_+^{\alpha\rho}, h^{\beta\sigma}\}g_{\rho\sigma}$
3	$i\langle V^{\mu\nu}(u_\sigma u^\beta h^{\alpha\sigma} - h^{\alpha\sigma}u^\beta u_\sigma) \rangle$	13	$i\langle V^{\mu\nu}f_+^{\alpha\beta}\rangle\chi_-$
4	$i\langle [V^{\mu\nu}, \nabla^\alpha \chi_+]u^\beta \rangle$	14	$i\langle V^{\mu\nu}f_+^{\alpha\beta}\rangle\chi_-$
5	$i\langle V^{\mu\nu}[f_+^{\alpha\beta}, u_\sigma u^\sigma] \rangle$	15	$i\langle V^{\mu\nu}[f_+^{\alpha\beta}, \chi_+] \rangle$
6	$i\langle V^{\mu\nu}(f_-^{\alpha\sigma}u_\sigma u^\beta - u_\sigma u^\beta f_-^{\alpha\sigma}) \rangle$	16	$\langle V^{\mu\nu}\{\nabla^\alpha f_+^{\beta\sigma}, u_\sigma\} \rangle$
7	$i\langle V^{\mu\nu}(u_\sigma f_-^{\alpha\sigma}u^\beta - u^\beta f_-^{\alpha\sigma}u_\sigma) \rangle$	17	$\langle V^{\mu\nu}\{\nabla_\sigma f_+^{\alpha\sigma}, u^\beta\} \rangle$
8	$i\langle V^{\mu\nu}(f_-^{\alpha\sigma}u_\sigma u^\beta - u^\beta u_\sigma f_-^{\alpha\sigma}) \rangle$	18	$\langle V^{\mu\nu}u^\alpha u^\beta\rangle\chi_-$
9	$\langle V^{\mu\nu}\{\chi_-, u^\alpha u^\beta\} \rangle$		
10	$\langle V^{\mu\nu}u^\alpha \chi_- u^\beta \rangle$		

TABLE II. Monomials with one axial-vector resonance field.

i	$\hat{\mathcal{O}}_{i\mu\nu\alpha\beta}^A$	i	$\hat{\mathcal{O}}_{i\mu\nu\alpha\beta}^A$
1	$\langle A^{\mu\nu}[u^\alpha u^\beta, u_\sigma u^\sigma] \rangle$	10	$i\langle A^{\mu\nu}u^\alpha\rangle\langle\nabla^\beta\chi_- \rangle$
2	$\langle A^{\mu\nu}[u^\alpha u^\sigma u^\beta, u^\sigma] \rangle$	11	$i\langle A^{\mu\nu}\{f_-^{\alpha\beta}, \chi_- \} \rangle$
3	$\langle A^{\mu\nu}\{\nabla^\alpha h^{\beta\sigma}, u_\sigma\} \rangle$	12	$i\langle A^{\mu\nu}\{\nabla^\alpha \chi_-, u^\beta\} \rangle$
4	$i\langle A^{\mu\nu}[f_+^{\alpha\beta}, u^\sigma u_\sigma] \rangle$	13	$\langle A^{\mu\nu}\{\chi_+, u^\alpha u^\beta\} \rangle$
5	$i\langle A^{\mu\nu}(f_+^{\alpha\sigma}u_\sigma u^\beta - u^\beta u_\sigma f_+^{\alpha\sigma}) \rangle$	14	$i\langle A^{\mu\nu}[f_+^{\alpha\beta}, \chi_+] \rangle$
6	$i\langle A^{\mu\nu}(f_+^{\alpha\sigma}u^\beta u_\sigma - u_\sigma u^\beta f_+^{\alpha\sigma}) \rangle$	15	$\langle A^{\mu\nu}\{\nabla^\alpha f_+^{\beta\sigma}, u_\sigma\} \rangle$
7	$i\langle A^{\mu\nu}(u_\sigma f_+^{\alpha\sigma}u^\beta - u^\beta f_+^{\alpha\sigma}u_\sigma) \rangle$	16	$\langle A^{\mu\nu}\{\nabla_\sigma f_+^{\alpha\sigma}, u^\beta\} \rangle$
8	$\langle A^{\mu\nu}\{f_-^{\alpha\sigma}, h^{\beta\sigma}\} \rangle$		
9	$i\langle A^{\mu\nu}f_+^{\alpha\beta}\rangle\chi_-$		

TABLE III. Monomials with one scalar or pseudoscalar resonance field.

i	$\hat{\mathcal{O}}_{i\mu\nu\alpha\beta}^P$	i	$\hat{\mathcal{O}}_{i\mu\nu\alpha\beta}^P$	i	$\hat{\mathcal{O}}_{i\mu\nu\alpha\beta}^S$
1	$\langle P\{f_-^{\mu\nu}, f_+^{\alpha\beta}\} \rangle$	4	$\langle P u^\mu u^\nu u^\alpha u^\beta \rangle$	1	$\langle S[f_+^{\alpha\beta}, u^\mu u^\nu] \rangle$
2	$i\langle P u^\alpha f_+^{\mu\nu} u^\beta \rangle$	5	$\langle P\{f_+^{\mu\nu}, f_+^{\alpha\beta}\} \rangle$	2	$i\langle S[f_+^{\mu\nu}, f_+^{\alpha\beta}] \rangle$
3	$i\langle P\{f_+^{\mu\nu}, u^\alpha u^\beta\} \rangle$	6			

TABLE IV. Monomials with two resonance fields of the same kind.

i	Operator $\hat{\mathcal{O}}_{i\mu\nu\alpha\beta}^{RR}$, $R = V, A$	Operator $\hat{\mathcal{O}}_{i\mu\nu\alpha\beta}^{RR}$, $R = P, S$
1*	$i\langle R^{\mu\nu}R^{\alpha\beta}\rangle\chi_-$	
2*	$i\langle\{R^{\mu\nu}, R^{\alpha\beta}\}\chi_- \rangle$	
3*	$\langle\{\nabla_\sigma R^{\mu\nu}, R^{\alpha\sigma}\}u^\beta \rangle$	
4*	$\langle\{\nabla^\beta R^{\mu\nu}, R^{\alpha\sigma}\}u_\sigma \rangle$	

TABLE V. Monomials with two resonance fields of different kinds.

i	Operator $\hat{\mathcal{O}}_{i\mu\nu\alpha\beta}^{SA}$	i	Operator $\hat{\mathcal{O}}_{i\mu\nu\alpha\beta}^{SV}$	Operator $\hat{\mathcal{O}}_{i\mu\nu\alpha\beta}^{SP}$
1*	$i\langle[A^{\mu\nu}, S]f_+^{\alpha\beta}\rangle$	1*	$i\langle[V^{\mu\nu}, S]f_+^{\alpha\beta}\rangle$	
2*	$\langle A^{\mu\nu}[S, u^\alpha u^\beta] \rangle$	2*	$i\langle[V^{\mu\nu}, \nabla^\alpha S]u^\beta \rangle$	

PHYSICAL REVIEW D **84**, 014036 (2011)

variables in the path integral (15) and can therefore be freely redefined without changing the physical content of the theory. As a consequence, we can choose an appropriate field redefinition in order to eliminate some subset $\{\mathcal{O}_i^X\}_{(X,i)\in M}$ of $O(p^6)$ operators from $\mathcal{L}_{\text{R}\chi\text{T}}^{(6,\text{odd})}$ and shift their influence effectively to the $O(p^6)$ terms, including the remaining operators $\{\mathcal{O}_i^X\}_{(X,i)\notin M}$, and also to the higher chiral order terms $\mathcal{L}_{\text{R}\chi\text{T}}^{(>6,\text{odd})}$, symbolically

$$\mathcal{L}_{\text{R}\chi\text{T}}^{(6,\text{odd})} = \sum_{(X,i)} \kappa_i^X \mathcal{O}_i^X \rightarrow \sum_{(X,i)\notin M} \overline{\kappa}_i^X \mathcal{O}_i^X + \mathcal{L}_{\text{R}\chi\text{T}}^{(>6,\text{odd})}. \quad (27)$$

The possible new terms $\mathcal{L}_{\text{R}\chi\text{T}}^{(>6,\text{odd})}$ of the order $O(p^8)$ and higher generated by such a redefinition can be neglected because they do not contribute to the $O(p^6)$ LECs when the resonance fields are integrated out. Note, however, that after such a truncation we get a new Lagrangian,

$$\overline{\mathcal{L}}_{\text{R}\chi\text{T}}^{(6,\text{odd})} = \sum_{(X,i)\notin M} \overline{\kappa}_i^X \mathcal{O}_i^X, \quad (28)$$

which is not equivalent to the previous one on the resonance level. On the other hand, the LECs obtained from $\overline{\mathcal{L}}_{\text{R}\chi\text{T}}^{(6,\text{odd})}$ coincide with those derived from $\mathcal{L}_{\text{R}\chi\text{T}}^{(6,\text{odd})}$.

The stars in Tables I, II, III, IV, V, VI, and VII indicate those operators which can be eliminated by the resonance field redefinitions discussed above and mean, therefore, a redundancy of a given monomial as far as its contribution to the resonance saturation is concerned. The details are shown in Appendix B. Note, however, that this redundancy concerns only the saturation and not the direct calculation of the correlators and amplitudes with resonances in the initial and final states. We will return to this point later on.

In the following section we will demonstrate the use of the resonance basis for two classes of examples. The resonance saturation will be studied in Sec. V.

IV. APPLICATIONS

In this section we illustrate applications of the Lagrangian $\mathcal{L}_{\text{R}\chi\text{T}}^{(6,\text{odd})}$ using two examples. We study two three-point correlators, namely, $\langle VVP \rangle$ and $\langle VAS \rangle$, and use both OPE constraints and phenomenological inputs to fix the relevant coupling constants. In the first case we also discuss some phenomenological applications in more detail.

A. VVP Green function revisited

The standard definition of this correlator is

$$\Pi_{\mu\nu}^{abc}(p, q) = \int d^4x d^4y e^{ip\cdot x + iq\cdot y} \langle 0|T[V_\mu^a(x)V_\nu^b(y)P^c(0)]|0 \rangle \quad (29)$$

with the vector current and the pseudoscalar density defined by

TABLE VI. Monomials with two resonance fields of different kinds.

i	Operator $\hat{\mathcal{O}}_{i\mu\nu\alpha\beta}^{VA}$	i	Operator $\hat{\mathcal{O}}_{i\mu\nu\alpha\beta}^{PA}$	i	Operator $\hat{\mathcal{O}}_{i\mu\nu\alpha\beta}^{PV}$
1*	$i\langle V^{\mu\nu}[A^{\alpha\beta}, u^\sigma u_\sigma] \rangle$	1*	$\langle \{A^{\mu\nu}, P\} f^{\alpha\beta} \rangle$	1*	$i\langle \{V^{\mu\nu}, P\} u^\alpha u^\beta \rangle$
2*	$i\langle V^{\mu\nu}(A^{\alpha\sigma} u_\sigma u^\beta - u^\beta u_\sigma A^{\alpha\sigma}) \rangle$	2*	$\langle \{A^{\mu\nu}, \nabla^\alpha P\} u^\beta \rangle$	2*	$i\langle V^{\mu\nu} u^\alpha P u^\beta \rangle$
3*	$i\langle V^{\mu\nu}(A^{\alpha\sigma} u^\beta u_\sigma - u_\sigma u^\beta A^{\alpha\sigma}) \rangle$			3*	$\langle \{V^{\mu\nu}, P\} f_+^{\alpha\beta} \rangle$
4*	$i\langle V^{\mu\nu}(u_\sigma A^{\alpha\sigma} u^\beta - u^\beta A^{\alpha\sigma} u_\sigma) \rangle$				
5*	$\langle \{V^{\mu\nu}, A^{\alpha\beta}\} f_+^{\beta\sigma} \rangle g_{\rho\sigma}$				
6*	$i\langle [V^{\mu\nu}, A^{\alpha\beta}] \chi_+ \rangle$				

TABLE VII. Monomials with three resonance fields.

i	Operator $\hat{\mathcal{O}}_{i\mu\nu\alpha\beta}^{RRR}$
1*	$\langle V^{\mu\nu} V^{\alpha\beta} P \rangle$
2*	$i\langle [V^{\mu\nu}, A^{\alpha\beta}] S \rangle$
3*	$\langle A^{\mu\nu} A^{\alpha\beta} P \rangle$

$$V_\mu^a(x) = \bar{q}(x) \gamma_\mu \frac{\lambda^a}{2} q(x), \quad P^a(x) = \bar{q}(x) i \gamma_5 \frac{\lambda^a}{2} q(x) \quad (30)$$

(our convention is $\gamma_5 = i\gamma^0\gamma^1\gamma^2\gamma^3$). This correlator was already studied in the past; see e.g. [11,12,28,38]. Here we provide a complete result based on our $\mathcal{L}_{R\chi T}$, i.e. also with two- and three-resonance vertices that were not considered in [28]. Using Ward identities and Lorentz and parity invariance, one can define

$$\Pi(p)_{\mu\nu}^{abc} = d^{abc} \epsilon_{\mu\nu\alpha\beta} p^\alpha q^\beta \Pi(p^2, q^2; r^2). \quad (31)$$

The OPE constraints dictate, for high values of all independent momenta [up to possible $\mathcal{O}(\alpha_s)$ corrections; see [39]],

$$\begin{aligned} \frac{1}{B_0} \Pi^{R\chi T}(p^2, q^2, r^2) = & -\frac{N_C}{16\pi^2 r^2} + \frac{4F_V^2 \kappa_3^{VV} p^2}{r^2(p^2 - M_V^2)(q^2 - M_V^2)} - \frac{16\sqrt{2}d_m F_V \kappa_3^{PV}}{(p^2 - M_V^2)(r^2 - M_P^2)} - \frac{32d_m \kappa_5^P}{r^2 - M_P^2} \\ & - \frac{8d_m F_V^2 \kappa^{VVP}}{(p^2 - M_V^2)(q^2 - M_V^2)(r^2 - M_P^2)} + \frac{2F_V^2}{(p^2 - M_V^2)(q^2 - M_V^2)} [8\kappa_2^{VV} - \kappa_3^{VV}] \\ & - \frac{2\sqrt{2}F_V}{r^2(p^2 - M_V^2)} [p^2(\kappa_{16}^V + 2\kappa_{12}^V) - q^2(\kappa_{16}^V - 2\kappa_{17}^V + 2\kappa_{12}^V) - r^2(8\kappa_{14}^V + \kappa_{16}^V + 2\kappa_{12}^V)] + (p \leftrightarrow q). \end{aligned} \quad (35)$$

From OPE (32) we then get the following constraints for the couplings:

$$\begin{aligned} \kappa_{14}^V &= \frac{N_C}{256\sqrt{2}\pi^2 F_V}, & \kappa_{16}^V + 2\kappa_{12}^V &= -\frac{N_C}{32\sqrt{2}\pi^2 F_V}, & \kappa_{17}^V &= -\frac{N_C}{64\sqrt{2}\pi^2 F_V}, & \kappa_5^P &= 0, \\ \kappa_2^{VV} &= \frac{F^2 + 16\sqrt{2}d_m F_V \kappa_3^{PV}}{32F_V^2} - \frac{N_C M_V^2}{512\pi^2 F_V^2}, & 8\kappa_2^{VV} - \kappa_3^{VV} &= \frac{F^2}{8F_V^2}. \end{aligned} \quad (36)$$

By employing these constraints one gets³

³Note that these constraints also automatically imply the fulfillment of (34). However, the requirement (33) cannot be satisfied until $\kappa_3^{PV} = 0$, which is in contradiction with another high-energy constraint for a related pion transition form factor; see the next subsection (cf. also [12]).

$$\Pi((\lambda p)^2, (\lambda q)^2; (\lambda r)^2) = \frac{B_0 F^2}{2\lambda^4} \frac{p^2 + q^2 + r^2}{p^2 q^2 r^2} + \mathcal{O}\left(\frac{1}{\lambda^6}\right), \quad (32)$$

whereas in the case where only two operators are close to each other, one gets

$$\Pi((\lambda p)^2, (q - \lambda p)^2; q^2) = \frac{B_0 F^2}{\lambda^2} \frac{1}{p^2 q^2} + \mathcal{O}\left(\frac{1}{\lambda^3}\right), \quad (33)$$

$$\Pi((\lambda p)^2, q^2; (q + \lambda p)^2) = \frac{1}{\lambda^2} \frac{1}{p^2} \Pi_{VT}(q^2) + \mathcal{O}\left(\frac{1}{\lambda^3}\right). \quad (34)$$

In the following we will use only all-large-momentum OPE (32). The reason is that, for a general correlator, not all the high-energy constraints can be simultaneously satisfied using only a finite number of resonances in the effective Lagrangian. This statement has been proved in [17] for the case of the $\langle PPS \rangle$ three-point function. For the $\langle VVP \rangle$ this problem has been partially studied in [12] (see also [38,40,41]).

By means of an explicit calculation based on $\mathcal{L}_{R\chi T}^{(6,\text{odd})}$ (the relevant Feynman graphs are depicted in Fig. 1) we get

KAROL KAMPF AND JIŘÍ NOVOTNÝ

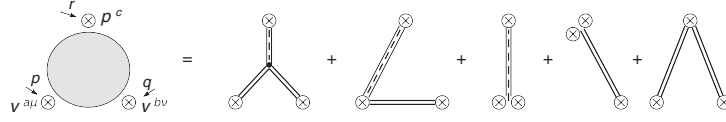
PHYSICAL REVIEW D **84**, 014036 (2011)

FIG. 1. Feynman graphs contributing to the VVP Green function. Double lines stand for resonances and dashed lines for GBs (double lines together with dashed lines show the sum of both possible contributions). The crossing is implicitly assumed.

$$\frac{1}{B_0} \Pi^{\text{R}\chi\text{T}}(p^2, q^2; r^2) = \frac{F^2}{2} \frac{(p^2 + q^2 + r^2) - \frac{N_C M_V^4}{4\pi^2 F^2}}{(p^2 - M_V^2)(q^2 - M_V^2)r^2} - \frac{16d_m F_V^2 \kappa^{VVP}}{(r^2 - M_P^2)(p^2 - M_V^2)(q^2 - M_V^2)} - \frac{16\sqrt{2}d_m F_V \kappa_3^{PV} [(p^2 + q^2)M_P^2 - 2r^2 M_V^2]}{r^2 (r^2 - M_P^2)(q^2 - M_V^2)(p^2 - M_V^2)}. \quad (37)$$

This should be equivalent to the LMD + P ansatz introduced in [11] so that the two independent constants b and c introduced there are directly connected with the phenomenological couplings κ_3^{PV} and κ^{VVP} . Considering just vector resonance interactions, $\kappa^{VVP} = \kappa_3^{PV} = 0$ [or equivalently taking the limit $M_P \rightarrow \infty$ in (35)], we can reconstruct the LMD ansatz [12]

$$\frac{1}{B_0} \Pi^{\text{LMD}}(p^2, q^2; r^2) = \frac{F^2}{2} \cdot \frac{(p^2 + q^2 + r^2) - \frac{N_C M_V^4}{4\pi^2 F^2}}{(p^2 - M_V^2)(q^2 - M_V^2)r^2}. \quad (38)$$

The result in ChPT up to $\mathcal{O}(p^6)$ at the leading order in $1/N_C$ expansion includes two LECs from the $\mathcal{O}(p^6)$ anomalous sector,

$$\frac{1}{B_0} \Pi^{\text{ChPT}}(p^2, q^2; r^2) = -\frac{N_C}{8\pi^2 r^2} + 32C_7^W - \frac{8C_{22}^W(p^2 + q^2)}{r^2}. \quad (39)$$

Comparing this with a low-energy expansion of the $R\chi T$ result (35), we give the following lowest-resonance contribution to C_7^W and C_{22}^W (cf. also Sec. V):

$$C_7^W = \frac{F_V^2(8\kappa_2^{VV} - \kappa_3^{VV})}{8M_V^4} + \frac{d_m F_V^2 \kappa^{VVP}}{2M_P^2 M_V^4} - \frac{\sqrt{2}d_m F_V \kappa_3^{PV}}{M_P^2 M_V^2} - \frac{F_V(2\kappa_{12}^V + 8\kappa_{14}^V + \kappa_{16}^V) + 2d_m \kappa_5^P}{4\sqrt{2}M_V^2 M_P^2},$$

$$C_{22}^W = -\frac{F_V \kappa_{17}^V}{\sqrt{2}M_V^2} - \frac{F_V^2 \kappa_3^{VV}}{2M_V^4}. \quad (40)$$

Using the OPE constraints (36) we obtain

$$C_7^W = \frac{F^2}{64M_V^4} + \frac{d_m F_V (-2\sqrt{2}\kappa_3^{PV} M_V^2 + F_V \kappa^{VVP})}{2M_P^2 M_V^4},$$

$$C_{22}^W = -\frac{F^2}{16M_V^4} + \frac{N_C}{64\pi^2 M_V^2} - \frac{2\sqrt{2}d_m F_V \kappa_3^{PV}}{M_V^4}. \quad (41)$$

1. Form factors

Let us define fully off-shell form factors for the $\mathcal{P}^* \gamma^* \gamma^*$ vertex, where \mathcal{P} can represent either the pion (or any other Goldstone boson) or pseudoscalar resonance via

$$\mathcal{F}_{\mathcal{P}\gamma\gamma}(p^2, q^2; r^2) = \frac{1}{Z_{\mathcal{P}}} (r^2 - m_{\mathcal{P}}^2) \Pi(p^2, q^2; r^2), \quad (42)$$

where the Z factor interpolates between the pseudoscalar source and \mathcal{P} . Let us discuss in detail the $\pi^0 \gamma \gamma$ form factor. We have $Z_{\pi^0} = 3/2BF$, and using the OPE constraints (36), we can define (note we are working in the chiral limit)

$$\mathcal{F}_{\pi^0\gamma\gamma}^{\text{R}\chi\text{T}}(p^2, q^2; r^2) = \frac{2}{3} \frac{1}{BF} r^2 \Pi^{\text{R}\chi\text{T}}(p^2, q^2; r^2), \quad (43)$$

where $\Pi^{\text{R}\chi\text{T}}(p^2, q^2; r^2)$ was introduced in (37). For an on-shell pion the κ^{VVP} drops out (note that this is not connected with the chiral limit simplification) and we get a simple result,

$$\mathcal{F}_{\pi^0\gamma\gamma}^{\text{R}\chi\text{T}}(p^2, q^2; 0) = \frac{F}{3} \frac{(p^2 + q^2)(1 + 32\sqrt{2} \frac{d_m F_V}{F^2} \kappa_3^{PV}) - \frac{N_C M_V^4}{4\pi^2 F^2}}{(p^2 - M_V^2)(q^2 - M_V^2)}. \quad (44)$$

Dropping κ_3^{PV} we can again reconstruct the LMD ansatz,⁴

$$\mathcal{F}_{\pi^0\gamma\gamma}^{\text{R}\chi\text{T}}(p^2, q^2; 0)|_{\kappa_3^{PV}=0} = \mathcal{F}_{\pi^0\gamma\gamma}^{\text{LMD}}(p^2, q^2; 0) = \frac{F}{3} \frac{\pi}{(p^2 - M_V^2)(q^2 - M_V^2)} \frac{p^2 + q^2 - \frac{N_C M_V^4}{4\pi^2 F^2}}{r^2}. \quad (45)$$

Using the Brodsky-Lepage (B-L) behavior for a large momentum [43,44],

$$\text{B-L cond.: } \lim_{Q^2 \rightarrow \infty} \mathcal{F}_{\pi^0\gamma\gamma}(0, -Q^2; m_\pi^2) \sim -\frac{1}{Q^2}, \quad (46)$$

⁴For $p^2 = 0$ we reproduce the incomplete vector meson dominance (VMD) ansatz for the semi-off-shell form factor studied in [42] with the free parameter c expressed in terms of the coupling κ_3^{PV} .

RESONANCE SATURATION IN THE ODD-INTRINSIC ...

one can arrive at the following constraint

$$\text{B-L cond.: } \kappa_3^{PV} = -\frac{F^2}{32\sqrt{2}d_m F_V}. \quad (47)$$

Before discussing a possible violation of the Brodsky-Lepage condition, let us study the influence of the constraint (47) on the original VVP Green function. The $\Pi^{\text{R}\chi\text{T}}$ correlator in (37) will now depend only on one constant, κ^{VVP} , and we get

$$\begin{aligned} & \frac{1}{B_0} \Pi^{\text{R}\chi\text{T}}(p^2, q^2; r^2) \\ &= \frac{F^2}{2} \frac{(p^2 + q^2 + r^2) - \frac{N_C M_V^4}{4\pi^2 F^2}}{(p^2 - M_V^2)(q^2 - M_V^2)r^2} \\ &+ \frac{F^2}{2} \frac{[(p^2 + q^2)M_P^2 - 2r^2 M_V^2]}{r^2(r^2 - M_P^2)(q^2 - M_V^2)(p^2 - M_V^2)} \\ &- \frac{16d_m F_V^2 \kappa^{VVP}}{(r^2 - M_P^2)(p^2 - M_V^2)(q^2 - M_V^2)}. \quad (48) \end{aligned}$$

The violation of the OPE (33) is manifest here. The remaining constant κ^{VVP} will drop out for an on-shell pion in the form factor, and one gets

PHYSICAL REVIEW D **84**, 014036 (2011)

$$\begin{aligned} \text{B-L cond.: } & \mathcal{F}_{\pi^0\gamma\gamma}^{\text{R}\chi\text{T}}(p^2, q^2; 0) \\ &= -\frac{N_C}{12\pi^2 F} \frac{M_V^4}{(p^2 - M_V^2)(q^2 - M_V^2)}. \quad (49) \end{aligned}$$

For completeness, let us also provide the ChPT result. From (39) using (41) we have

$$\begin{aligned} \mathcal{F}_{\pi^0\gamma\gamma}^{\text{ChPT}}(p^2, q^2; 0) &= -\frac{N_C}{12\pi^2 F} \left[1 + \frac{p^2 + q^2}{M_V^2} \left(1 - \frac{4\pi^2 F^2}{N_C M_V^2} \right. \right. \\ &\quad \left. \left. \times \left(1 + 32\sqrt{2} \frac{d_m F_V}{F^2} \kappa_3^{PV} \right) \right) \right] \quad (50) \end{aligned}$$

and

$$\text{B-L cond.: } \mathcal{F}_{\pi^0\gamma\gamma}^{\text{ChPT}}(p^2, q^2; 0) = -\frac{N_C}{12\pi^2 F} \left(1 + \frac{p^2 + q^2}{M_V^2} \right). \quad (51)$$

For the reader's convenience let us also summarize previous results based on the VMD and LMD + V ansätze⁵ [12] (see also [38] for corresponding terms in Lagrangian formalism):

$$\mathcal{F}_{\pi^0\gamma\gamma}^{\text{VMD}}(p^2, q^2; 0) = -\frac{N_C}{12\pi^2 F_\pi} \frac{M_V^2}{(p^2 - M_V^2)} \frac{M_V^2}{(q^2 - M_V^2)}, \quad (52)$$

$$\mathcal{F}_{\pi^0\gamma\gamma}^{\text{LMD+V}}(p^2, q^2; 0) = \frac{F_\pi}{3} \frac{p^2 q^2 (p^2 + q^2) + h_1 (p^2 + q^2)^2 + h_2 p^2 q^2 + h_3 (p^2 + q^2) + h_7}{(p^2 - M_{V_1}^2)(p^2 - M_{V_2}^2)(q^2 - M_{V_1}^2)(q^2 - M_{V_2}^2)}, \quad (53)$$

with (valid in the chiral limit)

$$h_7 = -\frac{N_C}{4\pi^2} \frac{M_{V_1}^4 M_{V_2}^4}{F_\pi^2}.$$

We therefore have the following relation [compare with (45)],

$$\mathcal{F}_{\pi^0\gamma\gamma}^{\text{R}\chi\text{T}}(p^2, q^2; 0)|_{\text{B-L}} = \mathcal{F}_{\pi^0\gamma\gamma}^{\text{VMD}}(p^2, q^2; 0). \quad (54)$$

Now let us turn back to the Brodsky-Lepage condition. We have seen that it has important consequences on the actual form of the $\pi^0 - \gamma - \gamma$ form factor within $R\chi T$. However, recent the *BABAR* measurement [45] showed phenomenological disagreement with this condition. There are also theoretical arguments [17] which showed that high-energy constraints cannot all be satisfied for a given form factor within the ansatz with only a finite number of resonance poles. (For a recent study on the Brodsky-Lepage revision, see [46]; see also [47] and references therein.) We will thus relax the Brodsky-Lepage condition by allowing a small deviation from (47) parametrized with $\delta_{\text{B-L}}$,

$$\kappa_3^{PV} = -\frac{F^2}{32\sqrt{2}d_m F_V} (1 + \delta_{\text{B-L}}). \quad (55)$$

Its actual value can be set by fitting the *BABAR* and *CLEO* data. In this fit, and also in the following phenomenological applications, we set

$$\begin{aligned} M_V &= m_\rho \approx 0.775 \text{ GeV}, & M_P &= m_{\pi'} \approx 1.3 \text{ GeV}, \\ F &= F_\pi \approx 92.22 \text{ MeV} \end{aligned} \quad (56)$$

and also (for details see [48])

$$F_V = F_\rho = 146.3 \pm 1.2 \text{ MeV}, \quad d_m \approx 26 \text{ MeV}. \quad (57)$$

The new *BABAR* data indicate an important negative shift in $\delta_{\text{B-L}}$, with the result

$$\delta_{\text{B-L}} = -0.055 \pm 0.025. \quad (58)$$

⁵The LMD + V ansatz adds one extra vector multiplet in comparison with the LMD one (45). This corresponds to MHA for which all the OPE and B-L constraints can be satisfied simultaneously.

KAROL KAMPF AND JIŘÍ NOVOTNÝ

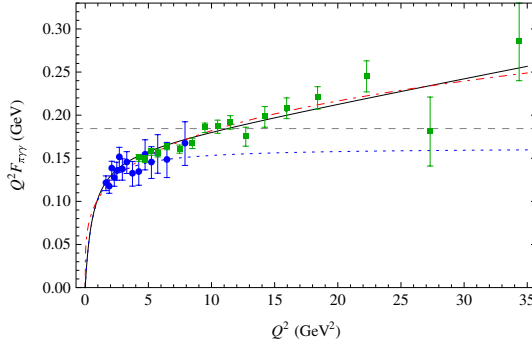


FIG. 2 (color online). The CLEO (blue points) and *BABAR* (green squares) data with the fitted function $\mathcal{F}_{\pi^0\gamma\gamma}^{\text{R}\chi\text{T}}(0, -Q^2; 0)$ defined in (44) using the modified Brodsky-Lepage condition in (55). The solid line is for $\delta_{\text{B-L}} = -0.055$, and the (blue) dotted line stands for the standard B-L condition (i.e. $\delta_{\text{B-L}} = 0$). The dot-dashed (red) line shows the fitted function $A(Q^2/(10 \text{ GeV}^2))^\beta$ with $A = 0.182 \text{ GeV}$ and $\beta = 0.25$ as obtained by the *BABAR* Collaboration [45]. The asymptotic $2F$ is represented by the horizontal dashed line.

Our fit, together with CLEO and *BABAR* data, is depicted in Fig. 2.

2. Decay $\rho \rightarrow \pi\gamma$

In this subsection we illustrate a particular phenomenological application of the above results, namely, a prediction for $\rho \rightarrow \pi\gamma$ decay. For this process we can use a connection with the off-shell $\pi\gamma\gamma$ form factor introduced in the previous subsection. First, let us define the amplitude \mathcal{A} for the process $\rho^+(p) \rightarrow \pi^+(p)\gamma(k)$ (we will use only the charged decay process to avoid the discussion on ω - ρ mixing for the neutral one):

$$\Gamma_{\rho \rightarrow \pi\gamma} = \frac{1}{8\pi} \frac{1}{3} \sum_{\text{pol}} |\mathcal{A}_{\rho \rightarrow \pi\gamma} \varepsilon^{\mu\nu\alpha\beta} p_\alpha q_\beta \epsilon_\mu(p) \epsilon_\nu^*(k)|^2 \times \frac{m_\rho^2 - m_\pi^2}{2m_\rho^3}, \quad (59)$$

from which we have already factorized out the Levi-Civita and momentum dependence. Similarly, one can define the amplitude for $\pi^0(p) \rightarrow \gamma(k)\gamma(l)$,

$$\Gamma_{\pi^0 \rightarrow \gamma\gamma} = \frac{1}{32\pi} \sum_{\text{pol}} |\mathcal{A}_{\pi^0 \rightarrow \gamma\gamma} \varepsilon^{\mu\nu\alpha\beta} k_\alpha l_\beta \epsilon_\mu^*(k) \epsilon_\nu^*(l)|^2 \frac{1}{m_{\pi^0}}. \quad (60)$$

The connection with the $\pi\gamma\gamma$ form factor is obtained via

$$\mathcal{A}_{\rho \rightarrow \pi\gamma} = \frac{e}{2} \frac{1}{F_V M_V} \lim_{q^2 \rightarrow M_V^2} (q^2 - M_V^2) \mathcal{F}_{\pi\gamma\gamma}(0, q^2; 0) \quad (61)$$

and quite simply,

PHYSICAL REVIEW D **84**, 014036 (2011)

$$\mathcal{A}_{\pi \rightarrow \gamma\gamma} = e^2 \mathcal{F}_{\pi\gamma\gamma}(0, 0; 0). \quad (62)$$

Putting these two definitions together, we can extract the ratio and the corresponding parameter x [11]:

$$\frac{2eF_V}{M_V} \left| \frac{\mathcal{A}_{\rho \rightarrow \pi\gamma}}{\mathcal{A}_{\pi \rightarrow \gamma\gamma}} \right| \equiv 1 + x. \quad (63)$$

Using the experimental value $\Gamma_{\rho \rightarrow \pi\gamma} = 68 \pm 7 \text{ keV}$, this parameter was obtained to be equal to $x = 0.022 \pm 0.051$ in [11] based on the 1992 edition of the particle data book (the same number was also used later e.g. in [12]). Updating this prediction with a new experimental input we can get a flip in the sign,

$$\text{exp: } x = -0.003 \pm 0.054. \quad (64)$$

The change is mainly due to a new value of F_V (studied e.g. in [48]) and a new precise measurement of the π^0 lifetime by the PrimEx group [49] (see also [30]).

Within our formalism, the parameter x defined above is proportional to the deviation from the simple VMD ansatz (52), or in other words, from the exact Brodsky-Lepage condition [cf. (54)]. Using (44) and (55) we get, in terms of $\delta_{\text{B-L}}$,

$$x = \frac{4\pi^2 F^2}{M_V^2 N_C} \delta_{\text{B-L}}. \quad (65)$$

The results of the previous subsection allow us to make a rather precise determination of this value (cf. also a similar fit in [42] which yields a compatible value of x),

$$\text{R}\chi\text{T: } x = -0.010 \pm 0.005, \quad (66)$$

which, using (63) and experimental input for $\Gamma_{\pi^0 \rightarrow \gamma\gamma}$, leads to the following prediction:

$$\text{R}\chi\text{T: } \Gamma_{\rho \rightarrow \pi\gamma} = 67.0 \pm 2.3 \text{ keV}. \quad (67)$$

3. Decays of $\pi(1300)$

In the previous section we have obtained a prediction for the $\rho \rightarrow \pi\gamma$ decay width. However, it was based on the ratio of two decay widths [cf. (63)] and the experimental input from one of them. We could also predict the absolute value for $\rho \rightarrow \pi\gamma$ directly from (59) and (61) without the necessity to use the experimental value of $\pi^0 \rightarrow \gamma\gamma$ (in fact, we will discuss briefly the latter process in the very next subsection), but one should remember that we have been making several simplifications; namely, we are working in the large N_C limit, using only lowest-lying resonances, and we are in the chiral limit. All together, within this approximation we cannot expect the accuracy of the result to be better than 30%–40%. On the other hand, one can expect that some of the systematic uncertainties will cancel out in ratios similar to the ones studied in the previous subsection.

RESONANCE SATURATION IN THE ODD-INTRINSIC ...

The same strategy can be repeated for $\pi(1300)$ decays. In fact, we can work in exact correspondence; the two decays would now be $\pi(1300) \rightarrow \rho\gamma$ and $\pi(1300) \rightarrow \gamma\gamma$. The only problem now is that neither of these two processes have been seen so far. The most recent limit on $\pi(1300) \rightarrow \gamma\gamma$ by the Belle Collaboration [50],

$$\Gamma_{\pi' \rightarrow \gamma\gamma} < 72 \text{ eV}, \quad (68)$$

sets at least a rough limit in our studies. Using the definition (42) the main object needed here is

$$\begin{aligned} & \mathcal{F}_{P\gamma\gamma}^{\text{R}\chi\text{T}}(p^2, q^2; m_p^2) \\ &= \frac{8\sqrt{2}}{3} F_V \frac{\sqrt{2}\kappa_3^{PV}(2M_V^2 - p^2 - q^2) - F_V\kappa^{VVP}}{(p^2 - M_V^2)(q^2 - M_V^2)}. \end{aligned} \quad (69)$$

The amplitude for $\pi(1300) \rightarrow \gamma\gamma$ is given by

$$\mathcal{A}_{\pi' \rightarrow \gamma\gamma} = e^2 \mathcal{F}_{P\gamma\gamma}(0, 0; m_\pi^2) \quad (70)$$

and similarly for $\pi(1300) \rightarrow \rho\gamma$ [see also (61)]. Then

$$\mathcal{A}_{\pi' \rightarrow \rho\gamma}^{\text{R}\chi\text{T}} = e^2 \frac{8\sqrt{2}}{3} F_V \frac{2\sqrt{2}\kappa_3^{PV}M_V^2 - F_V\kappa^{VVP}}{M_V^4}, \quad (71)$$

$$\mathcal{A}_{\pi' \rightarrow \rho\gamma}^{\text{R}\chi\text{T}} = -e \frac{4\sqrt{2}}{3M_V} \frac{\sqrt{2}\kappa_3^{PV}M_V^2 - F_V\kappa^{VVP}}{M_V^2}. \quad (72)$$

Both of these amplitudes depend on one so far undetermined constant κ^{VVP} . Provided we have experimental values of both the branching ratios, we could verify the consistency of our model. In the present situation we can visualize how one decay mode depends on the second one, and this was done in Fig. 3. One can see that we have two solutions for κ^{VVP} , as we have a quadratic equation for the decay width as a function of κ^{VVP} , and neither of these two solutions can be ruled out. Note that the full width for

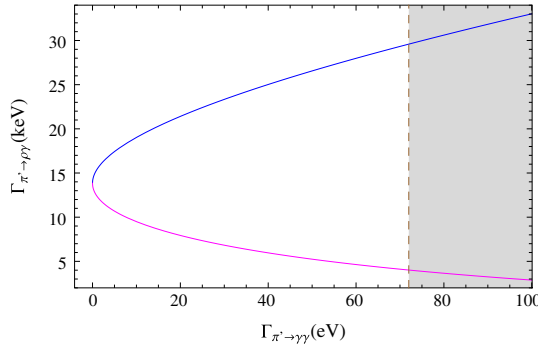


FIG. 3 (color online). The connection of the decay width for $\pi(1300) \rightarrow \gamma\gamma$ and $\pi(1300) \rightarrow \rho\gamma$ (note that we have two possible solutions). The dashed line represents Belle's limit (68) on $\Gamma_{\pi' \rightarrow \rho\pi}$ (the grey area is thus excluded by this experiment).

PHYSICAL REVIEW D **84**, 014036 (2011)

$\pi(1300)$ is assumed to be between 200 and 600 MeV (see [51]), so both processes are extremely suppressed for either of these two solutions.

The experimental bound on $\Gamma_{\pi' \rightarrow \gamma\gamma}$ can be used to get the estimate of κ^{VVP} . In order to fulfill the limit (68), we expect the numerator in (69) to be suppressed. This expected suppression leads, in analogy with (55), to the following ansatz:

$$\kappa_{VVP} = -\frac{F^2 M_V^2}{16d_m F_V^2} (1 + \delta_A), \quad (73)$$

with the parameter δ_A , which should be reasonably small. In terms of this parameter we get the decay width in a compact form,

$$\begin{aligned} \Gamma_{\pi' \rightarrow \gamma\gamma} &= \left(\frac{\alpha F^2}{6\sqrt{2}d_m M_V^2} \right)^2 \pi m_\pi^3 (\delta_{\text{B-L}} - \delta_A)^2 \\ &\approx (1514.0 \text{ eV}) \times (\delta_{\text{B-L}} - \delta_A)^2, \end{aligned} \quad (74)$$

and thus the extreme phenomenological suppression of $\pi(1300) \rightarrow \gamma\gamma$ can be understood within our formalism to be due to the small factor $(\delta_{\text{B-L}} - \delta_A)^2$. The experimental limit, together with (58), sets the allowed range for the parameter δ_A ,

$$-0.27 \lesssim \delta_A \lesssim 0.16, \quad (75)$$

which is good enough to set the value of κ_{VVP} to

$$\kappa_{VVP} \approx (-0.57 \pm 0.13) \text{ GeV}. \quad (76)$$

4. Decays $\pi^0 \rightarrow \gamma\gamma$ and $\eta \rightarrow \gamma\gamma$

As we have stated, the absolute decay widths are accessible via our approach only with limited precision. For instance, for the $\pi^0 \rightarrow \gamma\gamma$ amplitude we have obtained only a very simple prediction (62). It turns out, however, that it agrees very well with the experimental determination. On the other hand, a similar determination for $\eta \rightarrow \gamma\gamma$ would be a phenomenological disaster.

In order to go beyond the leading order, we can use the chiral corrections calculated with ChPT. The most recent study of the $\pi^0 \rightarrow \gamma\gamma$ amplitude went up to NNLO [30]. The motivation for going beyond next-to-leading order (NLO) lies in the fact that there are no chiral logarithms at NLO [52,53]. At NNLO these logarithms, though nonzero, are relatively small, so the C_i^W play a very important role. We can therefore use existing calculations within ChPT with our estimate (41) of C_i^W . Here our approximation, namely, the chiral limit, does not make any difference, as by construction, LECs (C_i^W in our case) do not depend on light quark masses. With the previous phenomenological determination of the couplings κ_3^{PV} and κ_{VVP} , we obtain

$$\begin{aligned} C_7^W &= \frac{F^2}{64M_V^4} \left(1 + 2 \frac{M_V^2}{M_\rho^2} (\delta_{\text{B-L}} - \delta_A) \right) \\ &\approx (0.35 \pm 0.07) \times 10^{-3} \text{ GeV}^{-2}. \end{aligned} \quad (77)$$

KAROL KAMPF AND JIŘÍ NOVOTNÝ

The second and last unknown LEC at NLO for $\pi^0 \rightarrow \gamma\gamma$ and $\eta \rightarrow \gamma\gamma$ is C_8^W . Anticipating the result of the next section and using the OPE constraints (36), we get

$$C_8^W = \frac{N_C}{768M_0^2\pi^2} - \frac{N_C}{512\pi^2M_V^2} - \frac{F_V\kappa_{13}^V}{\sqrt{2}M_V^2} + \frac{F_V^2\kappa_1^{VV}}{2M_V^4} + \frac{d_{m0}F^2}{96d_mM_p^2M_V^2} + \frac{d_{m0}F_V^2\kappa_{VVP}}{6M_p^2M_V^4}, \quad (78)$$

where we have also dropped the term proportional to δ_{B-L} because it is not numerically relevant. Unfortunately, at this moment, similarly as for the already-mentioned d_{m0} , we cannot make an estimate for κ_{13}^V and κ_1^{VV} (all these couplings are dominated by the η' exchange, cf. Appendix A). We may, however, again connect the two-gamma decay widths of π^0 and η . For example, we can set the unknown C_8^W from the experimental value of $\Gamma(\eta \rightarrow \gamma\gamma)$. This was done for the NLO $\eta \rightarrow \gamma\gamma$ expression in [30]. There is an ongoing project which should enlarge this calculation to the NNLO within ChPT (for the preliminary results in the $SU(3)$ limit, see [54]). We thus postpone, as a future project, the final determination of $\pi^0 \rightarrow \gamma\gamma$ based on the experimental value $\Gamma_{\eta \rightarrow \gamma\gamma}$. Let us only mention that, if we assume that the NNLO corrections for η are indeed small as for $\pi^0 \rightarrow \gamma\gamma$, the value in (77) has roughly the influence at the 0.5% level for $\Gamma_{\pi^0 \rightarrow \gamma\gamma}$ (with the opposite sign). A new study of isospin breaking effects in [55] indicates another shift of similar size (however, now with a positive sign), and thus at this moment we do not expect a quantitative change of the prediction made in [30].

5. $g - 2$

The main motivation for studying the VVP correlator is probably hidden in the determination of the muon $g - 2$ factor. It is beyond the scope of this paper to discuss this problem in great detail (for details see e.g. [56]). Let us only mention that the main source of theoretical error for its standard model prediction comes from hadronic contributions, more precisely, from the hadronic light-by-light scattering which cannot be related to any available data. The hadronic four-point correlator $VVVV$ is further simplified into three classes of contributions: (a) π^\pm and K^\pm loops, (b) π^0 , η , η' exchanges, and finally, (c) the rest, usually modeled via constituent quark loops. It is clear that this separation is not without ambiguity, and different approaches can calculate the contribution differently, especially between (a) and (c) or (b) and (c). Our contribution based on the VVP correlator study belongs to group (b). To avoid inconsistency we will work in close relation to similar work done for LMD or VMD ansätze [57–59]. Using the fully off-shell (i.e. including also the π^0 off-shellness) $\pi^0 - \gamma - \gamma$ form factor (43), we arrive at

$$a_\mu^{\text{LbyL};\pi^0} = (65.8 \pm 1.2) \times 10^{-11}. \quad (79)$$

PHYSICAL REVIEW D **84**, 014036 (2011)

TABLE VIII. Contribution of the π^0 exchange to the muon $g - 2$ factor for different models.

Model	$a_\mu^{\text{LbyL};\pi^0} \times 10^{11}$
VMD	57.2
LMD	73.7
LMD + V “on-shell”	58.2
LMD + V “off-shell”	72 ± 12
This work	65.8 ± 1.2

In the error only the uncertainties of our model (i.e. its parameters) were included. The systematic is mainly influenced by the above-mentioned ambiguity of how one defines and splits the pion-pole and regular parts from the $\langle VVVV \rangle$. We have put the cutoff energy at 10 GeV. For a better comparison let us present in Table VIII predictions for the studied contribution to the muon $g - 2$ for the different models summarized in (53). We have recalculated there the light-by-light contributions based on VMD and LMD ansätze. We have also reevaluated the case of LMD + V ansatz or, more precisely, its on-shell simplification as defined in (53). Three unknown constants are set similarly to what was done in [12]; i.e. $h_{1,2} = 0$ and h_5 is based on the $\rho \rightarrow \pi\gamma$ phenomenology $h_5 = 6.99$ [obtained for the updated value in (64)]. The full LMD + V “off-shell” ansatz has seven parameters (for details see [40,41]). One relation can be obtained from the chiral anomaly, and others can be from Brodsky-Lepage behavior, higher-twist corrections in the OPE and one-large momentum OPE, together with data (CLEO for this turn) we are still left with two undetermined parameters. Their variations in a reasonable range set the final error for the corresponding LMD + V value in Table VIII. Let us note that the possibility of B-L violation, together with the new fit of two parameters (h_1 and h_5), was also studied in [40,41] with no influence on the central value of the $g - 2$ contribution. Having too many parameters is not the only problem connected with the LMD + V ansatz. The status of $\rho(1450)$ as a first radial excitation of $\rho(770)$ is doubted by the possible existence of lighter $\rho(1250)$ [60]. Its presence is also supported by the study within AdS/QCD approaches [61]. On top of that, the inclusion of the complete set of all excitations in all channels (i.e. inclusion of π'') can again change the studied ansatz, similar to what we have encountered for the first excitation [see (45) and (54)].

Let us also note the quite astonishing coincidence of our result with the most recent study based on the AdS/QCD conjecture [62] $a_\mu^{\pi^0} = 65.4(2.5) \times 10^{-11}$.

B. VAS Green function

The $\langle VVP \rangle$ Green function studied in the previous section represents, without any doubts, the most important example of the odd-intrinsic sector of QCD. However, it is not the only quantity one can analyze using our complete

RESONANCE SATURATION IN THE ODD-INTRINSIC ...

lowest-lying resonance model. As the second example, we have chosen $\langle VAS \rangle$, which has not yet been studied (to our knowledge) in the literature. It also enables us to demonstrate the use of the ‘‘second half’’ of our resonance Lagrangian, i.e. those terms with 1^{++} and 0^{++} states.

We define (beware of the same symbol as for $\langle VVP \rangle$)

$$\Pi_{\mu\nu}^{abc}(p, q) = \int d^4x d^4y e^{ip \cdot x + iq \cdot y} \langle 0 | T [V_\mu^a(x) A_\nu^b(y) S^c(0)] | 0 \rangle, \quad (80)$$

with [cf. also (30)]

$$A_\mu^a(x) = \bar{q}(x) \gamma_\mu \gamma_5 \frac{\lambda^a}{2} q(x), \quad S_\mu^a(x) = \bar{q}(x) \frac{\lambda^a}{2} q(x).$$

Similarly as for VVP , one can write

$$\Pi(p, q)_{\mu\nu}^{abc} = f^{abc} \epsilon_{\mu\nu\alpha\beta} P^\alpha q^\beta \Pi(p^2, q^2; r^2), \quad (81)$$

where $r = -(p + q)$. In the resonance region, we have

$$\begin{aligned} \frac{1}{B_0} \Pi(p^2, q^2; r^2) &= \frac{8\sqrt{2}F_V(\kappa_4^V - 2\kappa_{15}^V) + 16\sqrt{2}F_A\kappa_{14}^A}{p^2 - M_V^2} + \frac{16\sqrt{2}F_A\kappa_{14}^A}{q^2 - M_A^2} \\ &+ \frac{32c_m\kappa_2^S}{r^2 - M_S^2} + \frac{16\sqrt{2}F_A c_m \kappa_1^{SA}}{(q^2 - M_A^2)(r^2 - M_S^2)} \\ &- \frac{8\sqrt{2}F_V c_m (2\kappa_1^{SV} + \kappa_2^{SV})}{(p^2 - M_V^2)(r^2 - M_S^2)} \\ &- \frac{16F_A F_V \kappa_6^{VA}}{(q^2 - M_A^2)(p^2 - M_V^2)} \\ &+ \frac{16F_A F_V c_m \kappa^{VAS}}{(q^2 - M_A^2)(p^2 - M_V^2)(r^2 - M_S^2)}. \end{aligned} \quad (82)$$

At high energies one can obtain the following OPE relation (cf. [39]):

$$\begin{aligned} &\Pi((\lambda p)^2, (\lambda q)^2; (\lambda r)^2) \\ &= \frac{B_0 F^2}{2\lambda^4} \frac{p^2 - q^2 - r^2}{p^2 q^2 r^2} + \mathcal{O}\left(\alpha_s, \frac{1}{\lambda^6}\right) \end{aligned} \quad (83)$$

and again we will not consider here one-momentum OPE limits. The high-energy constraint leads to

$$\begin{aligned} \kappa_2^S = \kappa_{14}^A = 0, \quad \kappa_4^V = 2\kappa_{15}^V, \quad \kappa_6^{VA} = \frac{F^2}{32F_A F_V}, \\ F_V(2\kappa_1^{SV} + \kappa_2^{SV}) = 2F_A \kappa_1^{SA} = \frac{F^2}{16\sqrt{2}c_m}. \end{aligned} \quad (84)$$

Finally, if we use these relations, we have only one free parameter: κ^{VAS} ; the result is

$$\begin{aligned} &\frac{1}{B_0} \Pi^{R\chi T}(p^2, q^2; r^2) \\ &= \frac{F^2(p^2 - q^2 - r^2 - M_V^2 + M_A^2 + M_S^2) + 32F_A F_V c_m \kappa^{VAS}}{2(q^2 - M_A^2)(p^2 - M_V^2)(r^2 - M_S^2)}. \end{aligned} \quad (85)$$

PHYSICAL REVIEW D **84**, 014036 (2011)

From the theoretical point of view, we are thus in a better position than we were for $\langle VVP \rangle$. After imposing OPE we are left with one free parameter, whereas in the case of $\langle VVP \rangle$ we had two [cf. (37)]. We can thus simply connect all processes schematically, represented as

$$\begin{aligned} (V: \rho, \omega, K^*, \gamma, \dots) &\sim (A: a_1, f_1, K_1, GB, W \dots) \\ &\sim (S: \sigma, \kappa, a_0, f_0, H \dots) \end{aligned} \quad (86)$$

via a single parameter. The problem is that they are very rare and have not yet been measured; on top of that, the status of some of the particle content is controversial by itself (especially if talking about a scalar sector). The parameter κ^{VAS} can be, however, set using other (not that rare) processes it enters. One way is to check, in the next section, to which of the 23 parameters it contributes, and directly use the system of LECs. This can be done here already within the calculation of $\langle VAS \rangle$. At low energies, up to $\mathcal{O}(p^6)$ one has

$$\frac{1}{B_0} \Pi(p^2, q^2, r^2) = -32C_{11}^W. \quad (87)$$

Comparing with the low-energy expansion of the full $R\chi T$ result (82), we get

$$\begin{aligned} C_{11}^W &= \frac{F_A \kappa_{14}^A}{\sqrt{2}M_A^2} + \frac{F_V(\kappa_4^V - 2\kappa_{15}^V)}{2\sqrt{2}M_V^2} + \frac{c_m \kappa_2^S}{M_S^2} + \frac{F_A F_V \kappa_6^{VA}}{2M_A^2 M_V^2} \\ &+ \frac{c_m F_V (2\kappa_1^{SV} + \kappa_2^{SV})}{2\sqrt{2}M_S^2 M_V^2} - \frac{F_A c_m \kappa_1^{SA}}{\sqrt{2}M_A^2 M_S^2} + \frac{F_A F_V c_m \kappa^{VAS}}{2M_A^2 M_S^2 M_V^2}. \end{aligned} \quad (88)$$

Using the OPE (84) we obtain

$$C_{11}^W = \frac{F^2}{64} \left[\frac{1}{M_S^2 M_V^2} + \frac{1}{M_A^2 M_V^2} - \frac{1}{M_A^2 M_S^2} \right] + \frac{F_A F_V c_m \kappa^{VAS}}{2M_A^2 M_S^2 M_V^2}.$$

The knowledge of C_{11}^W leads directly to the value of κ^{VAS} and thus to the rare processes schematically specified above. The current attempts for a C_{11}^W estimation were summarized in Table I of [63] with rather inconsistent values obtained both from the phenomenology [64,65] and from a model-dependent determination [63]. The most precise value seems to be obtained from $K^+ \rightarrow l^+ \nu \gamma$ data [66]: $C_{11}^W = (0.68 \pm 0.21) \times 10^{-3} \text{ GeV}^{-2}$ [64]. Using the values set in (56) and (57), together with

$$M_S = m_{a_0} \approx 984.7 \text{ MeV}, \quad c_m \approx 42 \text{ MeV} \quad (89)$$

and the Weinberg sum rules (to get values of M_A and F_A), we arrive at

$$\kappa^{VAS} = 0.61 \pm 0.40 \text{ GeV}. \quad (90)$$

C. Short note on the field redefinition

The previous two examples were calculated using the full resonance Lagrangian $\mathcal{L}_{R\chi T}^{(6,\text{odd})}$. Here we would like to

KAROL KAMPF AND JIŘÍ NOVOTNÝ

address the question of what would happen if one repeated the same calculation but instead used the reduced resonance Lagrangian $\overline{\mathcal{L}}_{R\chi T}^{(6,\text{odd})}$. This Lagrangian is established in Appendix B and can be obtained from the full Lagrangian (26) by dropping the operators marked by the star symbol in Tables I, II, III, IV, V, VI, and VII, i.e. by means of omitting 26 two- and three-resonance parameters: κ_i^{RR} , κ_i^{SA} , κ_i^{SV} , κ_i^{VA} , κ_i^{PA} , κ_i^{PV} , κ_i^{RRR} , and using the bar over the rest of κ_i^X (see Appendix B 5). This can be motivated by its equivalent contribution to the saturation of LECs. This exercise was already performed in [24] for $\langle VAP \rangle$ with an interesting finding, that after imposing the OPE condition both results are the same. In our case the conclusion is, however, different. Using the reduced resonance Lagrangian we would not be able to simply fulfill the OPE constraints by imposing some conditions on $\overline{\kappa_i^X}$. In addition, the precise definition of the reduced Lagrangian is up to one's taste. One can keep some of the two- or three-resonance monomials and, in exchange, drop some of the one-resonance terms (for example, dropping κ_1^V and keeping κ_3^{VV}). One can also decide not to drop all possible 26 terms, but a smaller number. In all cases we have, in principle, a big set of nonequivalent Lagrangians that can produce different predictions, but still the same contributions to the resonance saturation. One can then obtain curious conditions in order to fulfill the OPE (the relation $M_V = \frac{4\pi F}{\sqrt{N_C}}$ is a typical outcome of such a study: it can be obtained, for example, for the above-mentioned exchange $\kappa_1^V \leftrightarrow \kappa_3^{VV}$).

Thus we have to conclude that the equivalence of both calculations in the even sector for $\langle VAP \rangle$ was just a coincidence and it is not a general feature.

V. RESONANCE CONTRIBUTIONS TO THE LECs OF THE ANOMALOUS SECTOR

We have seen in the previous two applications the explicit examples of the calculation with the resonance

$$\begin{aligned}
C_1^W &= \frac{d_m \kappa_3^P}{M_p^2} + \frac{2\sqrt{2}d_m G_V \kappa_1^{PV}}{M_p^2 M_V^2} - \frac{\sqrt{2}d_m G_V \kappa_2^{PV}}{M_p^2 M_V^2} + \frac{\sqrt{2}G_V \kappa_3^V}{M_V^2} - \frac{2\sqrt{2}G_V \kappa_9^V}{M_V^2} + \frac{\sqrt{2}G_V \kappa_{10}^V}{M_V^2} \\
&\quad - \frac{4G_V^2 \kappa_2^{VV}}{M_V^4} - \frac{3G_V^2 \kappa_3^{VV}}{2M_V^4} - \frac{2\kappa^{VVP} d_m G_V^2}{M_p^2 M_V^4}, \\
C_2^W &= \frac{F_A \kappa_{13}^A}{\sqrt{2}M_A^2} + \frac{c_m \kappa_1^S}{M_3^2} + \frac{c_m F_A \kappa_2^{SA}}{\sqrt{2}M_A^2 M_3^2} + \frac{\sqrt{2}c_m G_V \kappa_3^{SV}}{M_3^2 M_V^2} + \frac{c_m F_V \kappa_2^{SV}}{2\sqrt{2}M_3^2 M_V^2} + \frac{F_V \kappa_4^V}{2\sqrt{2}M_V^2} - \frac{\sqrt{2}G_V \kappa_{15}^V}{M_V^2} + \frac{F_A G_V \kappa_6^{VA}}{M_A^2 M_V^2} + \frac{\kappa^{VAS} c_m F_A G_V}{M_A^2 M_3^2 M_V^2}, \\
C_3^W &= 0, \\
C_4^W &= -\frac{F_A \kappa_3^A}{2\sqrt{2}M_A^2} - \frac{d_m \kappa_3^P}{M_p^2} + \frac{\sqrt{2}d_m G_V \kappa_3^{PV}}{M_p^2 M_V^2} + \frac{F_A F_V \kappa_3^{VA}}{2M_A^2 M_V^2} + \frac{\sqrt{2}F_A \kappa_4^A}{M_A^2} - \frac{F_A \kappa_{12}^A}{2\sqrt{2}M_A^2} + \frac{F_A \kappa_{15}^A}{2\sqrt{2}M_A^2} - \frac{F_A^2 \kappa_4^{AA}}{4M_A^4} \\
&\quad - \frac{d_m F_A \kappa_2^{PA}}{2\sqrt{2}M_A^2 M_p^2} + \frac{d_m F_V \kappa_1^{PV}}{\sqrt{2}M_p^2 M_V^2} + \frac{2c_d \kappa_2^S}{M_3^2} - \frac{\sqrt{2}c_d F_A \kappa_1^{SA}}{M_A^2 M_3^2} + \frac{\sqrt{2}c_d F_V \kappa_1^{SV}}{M_3^2 M_V^2}
\end{aligned}$$

PHYSICAL REVIEW D **84**, 014036 (2011)

fields. A match between this result in a region of small momenta (i.e. $p \ll M_R$) on one side and the ChPT result on the other side enables us to extract the dependence of LECs on resonances. In this way, we have obtained within the VVP calculation C_7^W and C_{22}^W [see (40)], and from VAS it was possible to extract C_{11}^W (88). The dependence of all other C_i^W on the parameters of the resonance model can be obtained by systematically integrating out all resonances. A Lagrangian obtained in this way can be expanded over the canonical basis of the NLO odd-intrinsic Lagrangian established, for example, in [8]. In this way, we have saturated 21 of the 23 constants, and only C_3^W and C_{18}^W stayed intact, as they are subleading in the large N_C limit. The η' was considered (see Appendix A), and its contribution generated by WZW is explicit in C_6^W , C_8^W , and C_{10}^W (see also [67]). It is always the first term in these LECs (see below) to stress its large N_C dominance over the rest. Generally, we have the following expansion in the large N_C limit for all C_i^W , schematically,

$$C_i^W = a_i N_C^2 + b_i N_C + O(N_C^0), \quad (91)$$

where $a_i \neq 0$ for $i = 6, 8, 10$ and $b_i = 0$ for $i = 3, 18$.

The field redefinition, similarly to what was done in [24], was performed, and details are summarized in Appendix B. To get exactly the same results for the following constants, all 26 parameters denoted by stars in Tables I, II, III, IV, V, VI, and VII can be dropped, and for all others, a bar must then be added (bar parameters $\overline{\kappa_i^X}$ are defined in the last section of Appendix B). We prefer, however, to use the original parametrization, as it represents a direct connection with the resonance phenomenology and is thus simpler to use.

The explicit form of the resonance saturation generated by the resonance Lagrangian defined in (26) is

$$\begin{aligned}
& + \frac{c_d F_V \kappa_2^{SV}}{\sqrt{2} M_S^2 M_V^2} + \frac{F_V \kappa_1^V}{\sqrt{2} M_V^2} - \frac{\sqrt{2} F_V \kappa_5^V}{M_V^2} - \frac{F_V \kappa_6^V}{\sqrt{2} M_V^2} - \frac{F_V \kappa_8^V}{\sqrt{2} M_V^2} - \frac{F_V \kappa_9^V}{\sqrt{2} M_V^2} + \frac{\sqrt{2} G_V \kappa_{14}^V}{M_V^2} + \frac{F_A F_V \kappa_1^{VA}}{M_A^2 M_V^2} \\
& + \frac{F_A F_V \kappa_2^{VA}}{2 M_A^2 M_V^2} - \frac{2 F_V G_V \kappa_2^{VV}}{M_V^4} + \frac{\kappa^{VAS} c_d F_A F_V}{M_A^2 M_S^2 M_V^2} - \frac{\kappa^{VVP} d_m F_V G_V}{M_p^2 M_V^4}, \\
C_5^W &= \frac{F_A \kappa_{12}^A}{\sqrt{2} M_A^2} - \frac{d_m \kappa_2^P}{M_p^2} + \frac{d_m F_A \kappa_2^{PA}}{\sqrt{2} M_A^2 M_p^2} - \frac{d_m F_V \kappa_2^{PV}}{\sqrt{2} M_p^2 M_V^2} + \frac{F_V \kappa_{10}^V}{\sqrt{2} M_V^2} - \frac{G_V \kappa_{17}^V}{\sqrt{2} M_V^2} - \frac{F_V G_V \kappa_3^{VV}}{M_V^4}, \\
C_6^W &= -\frac{1}{192 M_0^2 \pi^2} + \frac{F_A \kappa_3^A}{3 \sqrt{2} M_A^2} - \frac{F_A F_V \kappa_3^{VA}}{3 M_A^2 M_V^2} - \frac{F_V G_V \kappa_3^{VV}}{3 M_V^4} - \frac{2 \sqrt{2} F_A \kappa_4^A}{3 M_A^2} + \frac{F_A \kappa_{10}^A}{\sqrt{2} M_A^2} \\
& - \frac{F_A \kappa_{15}^A}{3 \sqrt{2} M_A^2} + \frac{F_A^2 \kappa_4^{AA}}{6 M_A^4} - \frac{4 c_d \kappa_2^S}{3 M_S^2} + \frac{2 \sqrt{2} c_d F_A \kappa_1^{SA}}{3 M_A^2 M_S^2} - \frac{2 \sqrt{2} c_d F_V \kappa_1^{SV}}{3 M_S^2 M_V^2} - \frac{\sqrt{2} c_d F_V \kappa_2^{SV}}{3 M_S^2 M_V^2} \\
& - \frac{\sqrt{2} F_V \kappa_1^V}{3 M_V^2} + \frac{2 \sqrt{2} F_V \kappa_5^V}{3 M_V^2} + \frac{\sqrt{2} F_V \kappa_6^V}{3 M_V^2} + \frac{\sqrt{2} F_V \kappa_8^V}{3 M_V^2} + \frac{\sqrt{2} G_V \kappa_{13}^V}{M_V^2} - \frac{G_V \kappa_{17}^V}{3 \sqrt{2} M_V^2} - \frac{F_V \kappa_{18}^V}{\sqrt{2} M_V^2} \\
& - \frac{2 F_A F_V \kappa_1^{VA}}{3 M_A^2 M_V^2} - \frac{F_A F_V \kappa_2^{VA}}{3 M_A^2 M_V^2} - \frac{2 F_V G_V \kappa_1^{VV}}{M_V^4} - \frac{2 \kappa^{VAS} c_d F_A F_V}{3 M_A^2 M_S^2 M_V^2} - \frac{\sqrt{2} F_A d_{m0} \kappa_2^{PA}}{3 M_A^2 M_p^2} \\
& - \frac{2 d_{m0} \kappa_3^P}{3 M_p^2} + \frac{d_{m0} \kappa_2^P}{3 M_p^2} + \frac{d_{m0} F_V \kappa_2^{PV}}{3 \sqrt{2} M_p^2 M_V^2} + \frac{\sqrt{2} d_{m0} F_V \kappa_1^{PV}}{3 M_p^2 M_V^2} + \frac{2 \sqrt{2} d_{m0} G_V \kappa_3^{PV}}{3 M_p^2 M_V^2} - \frac{2 d_{m0} F_V G_V \kappa^{VVP}}{3 M_p^2 M_V^4}, \\
C_7^W &= \frac{2 d_m \kappa_5^P}{M_p^2} - \frac{\sqrt{2} d_m F_V \kappa_3^{PV}}{M_p^2 M_V^2} - \frac{F_V \kappa_{12}^V}{2 \sqrt{2} M_V^2} - \frac{\sqrt{2} F_V \kappa_{14}^V}{M_V^2} - \frac{F_V \kappa_{16}^V}{4 \sqrt{2} M_V^2} + \frac{F_V^2 \kappa_2^{VV}}{M_V^4} - \frac{F_V^2 \kappa_3^{VV}}{8 M_V^4} + \frac{\kappa^{VVP} d_m F_V^2}{2 M_p^2 M_V^4}, \\
C_8^W &= \frac{1}{256 M_0^2 \pi^2} + \frac{F_V \kappa_{12}^V}{6 \sqrt{2} M_V^2} - \frac{F_V \kappa_{13}^V}{\sqrt{2} M_V^2} + \frac{F_V \kappa_{16}^V}{12 \sqrt{2} M_V^2} + \frac{F_V^2 \kappa_1^{VV}}{2 M_V^4} + \frac{F_V^2 \kappa_3^{VV}}{24 M_V^4} \\
& - \frac{\sqrt{2} d_{m0} F_V \kappa_3^{PV}}{3 M_p^2 M_V^2} + \frac{d_{m0} F_V^2 \kappa^{VVP}}{6 M_p^2 M_V^4} + \frac{2 d_{m0} \kappa_5^P}{3 M_p^2}, \\
C_9^W &= -\frac{F_A \kappa_3^A}{4 \sqrt{2} M_A^2} - \frac{F_A^2 \kappa_3^{AA}}{8 M_A^4} - \frac{F_A \kappa_8^A}{2 \sqrt{2} M_A^2} - \frac{\sqrt{2} F_A \kappa_{11}^A}{M_A^2} - \frac{F_A \kappa_{12}^A}{\sqrt{2} M_A^2} - \frac{F_A \kappa_{15}^A}{4 \sqrt{2} M_A^2} \\
& + \frac{F_A^2 \kappa_2^{AA}}{M_A^4} + \frac{2 d_m \kappa_1^P}{M_p^2} - \frac{\sqrt{2} d_m F_A \kappa_1^{PA}}{M_A^2 M_p^2} - \frac{d_m F_A \kappa_2^{PA}}{\sqrt{2} M_A^2 M_p^2} + \frac{\kappa^{AAP} d_m F_A^2}{2 M_A^4 M_p^2}, \\
C_{10}^W &= \frac{1}{256 M_0^2 \pi^2} + \frac{F_A \kappa_3^A}{12 \sqrt{2} M_A^2} + \frac{F_A^2 \kappa_3^{AA}}{24 M_A^4} + \frac{F_A \kappa_8^A}{6 \sqrt{2} M_A^2} - \frac{F_A \kappa_9^A}{\sqrt{2} M_A^2} + \frac{F_A \kappa_{10}^A}{2 \sqrt{2} M_A^2} + \frac{F_A \kappa_{15}^A}{12 \sqrt{2} M_A^2} + \frac{F_A^2 \kappa_1^{AA}}{2 M_A^4} \\
& + \frac{F_A^2 \kappa^{AAP} d_{m0}}{6 M_A^4 M_p^2} - \frac{\sqrt{2} F_A d_{m0} \kappa_1^{PA}}{3 M_A^2 M_p^2} - \frac{F_A d_{m0} \kappa_2^{PA}}{3 \sqrt{2} M_A^2 M_p^2} + \frac{2 d_{m0} \kappa_1^P}{3 M_p^2}, \\
C_{11}^W &= \frac{F_A \kappa_{14}^A}{\sqrt{2} M_A^2} + \frac{c_m \kappa_2^S}{M_S^2} - \frac{c_m F_A \kappa_1^{SA}}{\sqrt{2} M_A^2 M_S^2} + \frac{c_m F_V \kappa_1^{SV}}{\sqrt{2} M_S^2 M_V^2} + \frac{c_m F_V \kappa_2^{SV}}{2 \sqrt{2} M_S^2 M_V^2} + \frac{F_V \kappa_4^V}{2 \sqrt{2} M_V^2} - \frac{F_V \kappa_{15}^V}{\sqrt{2} M_V^2} + \frac{F_A F_V \kappa_6^{VA}}{2 M_A^2 M_V^2} + \frac{\kappa^{VAS} c_m F_A F_V}{2 M_A^2 M_S^2 M_V^2},
\end{aligned}$$

$$\begin{aligned}
C_{12}^W &= \frac{\sqrt{2}G_V\kappa_1^V}{M_V^2} - \frac{\sqrt{2}G_V\kappa_2^V}{M_V^2} - \frac{\sqrt{2}G_V\kappa_3^V}{M_V^2} + \frac{G_V^2\kappa_3^{VV}}{M_V^4}, \\
C_{13}^W &= -\frac{F_A\kappa_3^A}{\sqrt{2}M_A^2} + \frac{F_AF_V\kappa_3^{VA}}{M_A^2M_V^2} + \frac{F_VG_V\kappa_3^{VV}}{M_V^4} + \frac{2\sqrt{2}F_A\kappa_4^A}{M_A^2} + \frac{F_A\kappa_{15}^A}{\sqrt{2}M_A^2} - \frac{F_A^2\kappa_4^{AA}}{2M_A^4} + \frac{4c_d\kappa_2^S}{M_S^2} - \frac{2\sqrt{2}c_dF_A\kappa_1^{SA}}{M_A^2M_S^2} \\
&\quad + \frac{2\sqrt{2}c_dF_V\kappa_1^{SV}}{M_S^2M_V^2} + \frac{\sqrt{2}c_dF_V\kappa_2^{SV}}{M_S^2M_V^2} + \frac{\sqrt{2}F_V\kappa_1^V}{M_V^2} - \frac{2\sqrt{2}F_V\kappa_5^V}{M_V^2} - \frac{\sqrt{2}F_V\kappa_6^V}{M_V^2} \\
&\quad - \frac{\sqrt{2}F_V\kappa_8^V}{M_V^2} - \frac{\sqrt{2}G_V\kappa_{12}^V}{M_V^2} - \frac{G_V\kappa_{16}^V}{\sqrt{2}M_V^2} + \frac{\sqrt{2}G_V\kappa_{17}^V}{M_V^2} + \frac{2F_AF_V\kappa_1^{VA}}{M_A^2M_V^2} + \frac{F_AF_V\kappa_2^{VA}}{M_A^2M_V^2} + \frac{2\kappa^{VAS}c_dF_AF_V}{M_A^2M_S^2M_V^2}, \\
C_{14}^W &= -\frac{F_A\kappa_3^A}{2\sqrt{2}M_A^2} - \frac{F_V\kappa_3^V}{\sqrt{2}M_V^2} + \frac{F_AF_V\kappa_3^{VA}}{2M_A^2M_V^2} + \frac{\sqrt{2}F_A\kappa_4^A}{M_A^2} + \frac{F_A\kappa_{15}^A}{2\sqrt{2}M_A^2} - \frac{F_A^2\kappa_4^{AA}}{4M_A^4} + \frac{2c_d\kappa_2^S}{M_S^2} - \frac{\sqrt{2}c_dF_A\kappa_1^{SA}}{M_A^2M_S^2} \\
&\quad + \frac{\sqrt{2}c_dF_V\kappa_1^{SV}}{M_S^2M_V^2} + \frac{c_dF_V\kappa_2^{SV}}{\sqrt{2}M_S^2M_V^2} + \frac{F_V\kappa_1^V}{\sqrt{2}M_V^2} - \frac{\sqrt{2}F_V\kappa_5^V}{M_V^2} - \frac{F_V\kappa_6^V}{\sqrt{2}M_V^2} \\
&\quad - \frac{F_V\kappa_8^V}{\sqrt{2}M_V^2} + \frac{F_AF_V\kappa_1^{VA}}{M_A^2M_V^2} + \frac{F_AF_V\kappa_2^{VA}}{2M_A^2M_V^2} + \frac{\kappa^{VAS}c_dF_AF_V}{M_A^2M_S^2M_V^2}, \\
C_{15}^W &= -\frac{F_A\kappa_3^A}{2\sqrt{2}M_A^2} + \frac{F_AF_V\kappa_3^{VA}}{2M_A^2M_V^2} - \frac{F_VG_V\kappa_3^{VV}}{M_V^4} + \frac{\sqrt{2}F_A\kappa_4^A}{M_A^2} + \frac{F_A\kappa_{15}^A}{2\sqrt{2}M_A^2} - \frac{F_A^2\kappa_4^{AA}}{4M_A^4} + \frac{2c_d\kappa_2^S}{M_S^2} - \frac{\sqrt{2}c_dF_A\kappa_1^{SA}}{M_A^2M_S^2} + \frac{\sqrt{2}c_dF_V\kappa_1^{SV}}{M_S^2M_V^2} \\
&\quad + \frac{c_dF_V\kappa_2^{SV}}{\sqrt{2}M_S^2M_V^2} + \frac{F_V\kappa_2^V}{\sqrt{2}M_V^2} - \frac{\sqrt{2}F_V\kappa_5^V}{M_V^2} - \frac{F_V\kappa_6^V}{\sqrt{2}M_V^2} - \frac{F_V\kappa_8^V}{\sqrt{2}M_V^2} - \frac{G_V\kappa_{17}^V}{\sqrt{2}M_V^2} + \frac{F_AF_V\kappa_1^{VA}}{M_A^2M_V^2} + \frac{F_AF_V\kappa_2^{VA}}{2M_A^2M_V^2} + \frac{\kappa^{VAS}c_dF_AF_V}{M_A^2M_S^2M_V^2}, \\
C_{16}^W &= \frac{\sqrt{2}F_A\kappa_2^A}{M_A^2} + \frac{F_AG_V\kappa_2^{VA}}{M_A^2M_V^2} - \frac{\sqrt{2}G_V\kappa_6^V}{M_V^2} + \frac{\sqrt{2}G_V\kappa_7^V}{M_V^2} - \frac{\sqrt{2}G_V\kappa_8^V}{M_V^2} + \frac{F_AG_V\kappa_3^{VA}}{M_A^2M_V^2} - \frac{F_AG_V\kappa_4^{VA}}{M_A^2M_V^2} - \frac{G_V^2\kappa_3^{VV}}{M_V^4}, \\
C_{17}^W &= \frac{F_A\kappa_1^A}{\sqrt{2}M_A^2} - \frac{c_d\kappa_1^S}{M_S^2} - \frac{\sqrt{2}c_dF_A\kappa_1^{SA}}{M_A^2M_S^2} + \frac{\sqrt{2}c_dF_V\kappa_1^{SV}}{M_S^2M_V^2} - \frac{\sqrt{2}c_dG_V\kappa_1^{SV}}{M_S^2M_V^2} + \frac{F_AF_V\kappa_1^{VA}}{M_A^2M_V^2} \\
&\quad - \frac{F_AG_V\kappa_1^{VA}}{M_A^2M_V^2} + \frac{F_A\kappa_2^A}{\sqrt{2}M_A^2} + \frac{\sqrt{2}F_A\kappa_4^A}{M_A^2} + \frac{F_A\kappa_{15}^A}{2\sqrt{2}M_A^2} - \frac{F_A^2\kappa_4^{AA}}{4M_A^4} + \frac{2c_d\kappa_2^S}{M_S^2} - \frac{c_dF_A\kappa_2^{SA}}{\sqrt{2}M_A^2M_S^2} + \frac{c_dF_V\kappa_2^{SV}}{2\sqrt{2}M_S^2M_V^2} - \frac{\sqrt{2}F_V\kappa_5^V}{M_V^2} + \frac{\sqrt{2}G_V\kappa_5^V}{M_V^2} \\
&\quad - \frac{F_V\kappa_6^V}{\sqrt{2}M_V^2} - \frac{F_V\kappa_8^V}{\sqrt{2}M_V^2} + \frac{F_AF_V\kappa_2^{VA}}{2M_A^2M_V^2} + \frac{F_AF_V\kappa_3^{VA}}{2M_A^2M_V^2} - \frac{F_VG_V\kappa_3^{VV}}{4M_V^4} + \frac{G_V^2\kappa_4^{VV}}{2M_V^4} - \frac{F_VG_V\kappa_4^{VV}}{4M_V^4} + \frac{\kappa^{VAS}c_dF_AF_V}{M_A^2M_S^2M_V^2} - \frac{\kappa^{VAS}c_dF_AG_V}{M_A^2M_S^2M_V^2}, \\
C_{18}^W &= 0, \\
C_{19}^W &= -\frac{\sqrt{2}F_A\kappa_5^A}{M_A^2} - \frac{F_AG_V\kappa_5^{VA}}{M_A^2M_V^2} - \frac{\sqrt{2}F_V\kappa_6^V}{M_V^2} - \frac{\sqrt{2}G_V\kappa_{11}^V}{M_V^2} + \frac{F_V\kappa_{16}^V}{\sqrt{2}M_V^2} - \frac{G_V\kappa_{16}^V}{\sqrt{2}M_V^2} + \frac{\sqrt{2}G_V\kappa_{17}^V}{M_V^2} + \frac{F_AF_V\kappa_3^{VA}}{M_A^2M_V^2} \\
&\quad + \frac{F_VG_V\kappa_3^{VV}}{M_V^4} - \frac{F_V^2\kappa_4^{VV}}{2M_V^4} + \frac{F_VG_V\kappa_4^{VV}}{M_V^4}, \\
C_{20}^W &= \frac{\sqrt{2}F_A\kappa_4^A}{M_A^2} - \frac{F_A^2\kappa_4^{AA}}{2M_A^4} - \frac{F_V^2\kappa_4^{VV}}{4M_V^4} + \frac{F_VG_V\kappa_4^{VV}}{2M_V^4} - \frac{F_A\kappa_5^A}{\sqrt{2}M_A^2} - \frac{F_A\kappa_6^A}{\sqrt{2}M_A^2} + \frac{F_A\kappa_{15}^A}{\sqrt{2}M_A^2} + \frac{2c_d\kappa_2^S}{M_S^2} - \frac{\sqrt{2}c_dF_A\kappa_1^{SA}}{M_A^2M_S^2} \\
&\quad + \frac{\sqrt{2}c_dF_V\kappa_1^{SV}}{M_S^2M_V^2} + \frac{c_dF_V\kappa_2^{SV}}{\sqrt{2}M_S^2M_V^2} - \frac{\sqrt{2}F_V\kappa_5^V}{M_V^2} - \frac{\sqrt{2}F_V\kappa_6^V}{M_V^2} - \frac{\sqrt{2}F_V\kappa_8^V}{M_V^2} + \frac{F_V\kappa_{16}^V}{2\sqrt{2}M_V^2} - \frac{G_V\kappa_{16}^V}{\sqrt{2}M_V^2} + \frac{F_AF_V\kappa_1^{VA}}{M_A^2M_V^2} \\
&\quad + \frac{F_AF_V\kappa_2^{VA}}{M_A^2M_V^2} + \frac{F_AF_V\kappa_3^{VA}}{M_A^2M_V^2} - \frac{F_VG_V\kappa_3^{VV}}{2M_V^4} + \frac{\kappa^{VAS}c_dF_AF_V}{M_A^2M_S^2M_V^2},
\end{aligned}$$

$$\begin{aligned}
C_{21}^W &= -\frac{\sqrt{2}F_A\kappa_4^A}{M_A^2} + \frac{F_A^2\kappa_4^{AA}}{2M_A^4} - \frac{F_A F_V \kappa_4^{VA}}{2M_A^2 M_V^2} + \frac{F_V^2 \kappa_4^{VV}}{4M_V^4} - \frac{F_V G_V \kappa_4^{VV}}{2M_V^4} + \frac{F_A \kappa_7^A}{\sqrt{2}M_A^2} - \frac{F_A \kappa_{15}^A}{\sqrt{2}M_A^2} - \frac{2c_d \kappa_2^S}{M_S^2} + \frac{\sqrt{2}c_d F_A \kappa_1^{SA}}{M_A^2 M_S^2} \\
&\quad - \frac{\sqrt{2}c_d F_V \kappa_1^{SV}}{M_S^2 M_V^2} - \frac{c_d F_V \kappa_2^{SV}}{\sqrt{2}M_S^2 M_V^2} + \frac{\sqrt{2}F_V \kappa_5^V}{M_V^2} + \frac{F_V \kappa_6^V}{\sqrt{2}M_V^2} + \frac{F_V \kappa_7^V}{\sqrt{2}M_V^2} + \frac{F_V \kappa_8^V}{\sqrt{2}M_V^2} - \frac{F_V \kappa_{16}^V}{2\sqrt{2}M_V^2} + \frac{G_V \kappa_{16}^V}{\sqrt{2}M_V^2} - \frac{G_V \kappa_{17}^V}{\sqrt{2}M_V^2} \\
&\quad - \frac{F_A F_V \kappa_1^{VA}}{M_A^2 M_V^2} - \frac{F_A F_V \kappa_2^{VA}}{2M_A^2 M_V^2} - \frac{F_A F_V \kappa_3^{VA}}{2M_A^2 M_V^2} - \frac{F_V G_V \kappa_3^{VV}}{2M_V^4} - \frac{\kappa^{VAS} c_d F_A F_V}{M_A^2 M_S^2 M_V^2}, \\
C_{22}^W &= -\frac{F_V \kappa_{17}^V}{\sqrt{2}M_V^2} - \frac{F_V^2 \kappa_3^{VV}}{2M_V^4}, \quad C_{23}^W = -\frac{F_A \kappa_{16}^A}{\sqrt{2}M_A^2} - \frac{F_A^2 \kappa_3^{AA}}{2M_A^4}. \tag{92}
\end{aligned}$$

The transformation established in Appendix B was employed as an independent check of the previous relations.

Apart from the already-mentioned $C_3^W = 0$ and $C_{18}^W = 0$, we have found one further relation free from κ_i^X ,

$$\frac{F_V^2}{2G_V} C_{12}^W = F_V (C_{14}^W - C_{15}^W) + G_V C_{22}^W. \tag{93}$$

VI. SUMMARY

In this paper we have studied the odd-intrinsic parity sector of the low-energy QCD. We have constructed the most general resonance Lagrangian that describes the interactions of the Goldstone bosons and the lowest-lying vector-, axial-, scalar-, and pseudoscalar-resonance multiplets. We worked in the large N_C approximation and considered only those terms that contribute to the $O(p^6)$ anomalous Lagrangian (i.e. to the first nontrivial order). This was the main aim of our work. We then demonstrated the use of this Lagrangian for three different applications. The first two represent calculations of two three-point Green functions (VVP) and (VAS). The third application is the complete integration out of the resonance fields, establishing the so-called saturation of LECs by resonance fields.

The first application VVP is the most important example of the odd-intrinsic sector, both from the theoretical and the phenomenological points of view. We have discussed different aspects of this Green function. First, after calculating this three-point correlator within our model and imposing a certain high-energy constraint, we ended up with the result which depends only on two parameters. They were further set using new *BABAR* data on $\pi\gamma\gamma$ off-shell form factors and the Belle Collaboration's limit on $\pi' \rightarrow \gamma\gamma$ decay. After setting these two parameters we can make further predictions. The outcome of our analysis is, for example, a very precise determination of the decay width of a process $\rho \rightarrow \pi\gamma$: $\Gamma_{\rho \rightarrow \pi\gamma} = 67(2.3)$ keV. We have also studied a relative dependence of the rare decays $\pi' \rightarrow \gamma\gamma$ and $\pi' \rightarrow \rho\gamma$. Based on the experimental upper limit of the former, one can set the lowest limit of the latter. The prediction of our model is the range $30 \text{ keV} \gtrsim \Gamma_{\pi' \rightarrow \rho\gamma} \gtrsim 4 \text{ keV}$ (based on Belle's $\Gamma_{\pi' \rightarrow \gamma\gamma} \lesssim 72 \text{ eV}$).

Next, we also evaluated the value of the C_7^W LEC, together with a short discussion on π^0 and η two-photon decays. Last but not least, a very precise determination of the off-shell π^0 -pole contribution to the muon $g-2$ factor was provided. Our final determination of this factor is $a_\mu^{\pi^0} = 65.8(1.2) \times 10^{-11}$. The $R\chi T$ approach has thus reduced the error of a similar determination based on the lowest-meson saturation ansatz by a factor of 10 and is in exact agreement with the most recent determination based on AdS/QCD assumptions. Let us note that the present theoretical error for the complete anomalous magnetic moment of the muon is around 50×10^{-11} , and the experimental error is around 60×10^{-11} [68] (with the well-known discrepancy above 3σ). A new proposed experiment at Fermilab E989 [69] plans to increase the precision to the preliminary value 16×10^{-11} and thus a reduction of the error in the theoretical light-by-light calculation is more than desirable.

If the VVP represents a very important and rich phenomenological example, the three-point correlator (VAS) is connected with very rare processes and represents an example of the odd sector which has so far not been studied. We have established its OPE behavior, which enabled us to reduce the dependence of the VAS Green function to one parameter. This opens the possibility of a future study of these rare but interesting processes.

In the last section we have studied the resonance saturation at low energies. We have integrated out the resonance fields to establish the dependence of LECs of odd-sector C_i^W on our parameters. As we are limited by large N_C , we cannot make predictions for C_3^W and C_{18}^W but we have set all other 21 LECs. We have found one relation which connects C_{12}^W , C_{14}^W , C_{15}^W , and C_{22}^W and is free from the $O(p^6)$ resonance parameters. It is interesting to notice that C_{22}^W gets only contributions from the vector resonances, and this can play an important role in the new AdS/QCD dual study (for details see [70,71]).

ACKNOWLEDGMENTS

We would especially like to thank Jarda Trnka for initiating this project and for his contribution at the early stages of this work. We also thank Hans Bijmans and Bachir Moussallam for valuable discussions and

KAROL KAMPF AND JIŘÍ NOVOTNÝ

comments. This work is supported in part by the European Community-Research Infrastructure Integrating Activity “Study of Strongly Interacting Matter” (HadronPhysics2, Grant Agreement No. 227431) and the Center for Particle Physics (Project No. LC 527) of the Ministry of Education of the Czech Republic.

APPENDIX A: THE LARGE N_C COUNTING

1. General considerations

Let us start with the $U_L(N_F) \times U_R(N_F)$ invariant Lagrangian for the nonet of the GB and resonances without using the equations of motion or the Cayley-Hamilton identities. Then the large N_C behavior of the couplings accompanying individual operators in the effective Lagrangian with octet GBs (after η' has been integrated out) can be understood as follows.

Let us write in the same way as in [24],

$$\tilde{u} = e^{i\phi^0 T^0/F\sqrt{2}} u, \quad (\text{A1})$$

where $T^0 = \sqrt{\frac{1}{N_F}} \mathbf{1}$ and

$$u = e^{i\phi^a T^a/F\sqrt{2}}$$

is the $SU_L(N_F) \times SU_R(N_F)$ basic building block, and therefore

$$\phi^0 = \frac{F}{i} \sqrt{\frac{2}{N_F}} \ln(\det \tilde{u}). \quad (\text{A2})$$

Let us also remind the reader [24] that ϕ^0 and ϕ^a do not mix under the nonlinearly realized $U_L(N_F) \times U_R(N_F)$ symmetry. For the construction of the $U_L(N_F) \times U_R(N_F)$ effective Lagrangian, we have the usual building blocks constructed from \tilde{u} and the usual external sources l_μ, r_μ, χ and χ^+ (now also with singlet components), e.g.

$$\begin{aligned} \tilde{u}_\mu &= u_\mu - D_\mu \phi^0 \frac{\sqrt{2} T^0}{F}, \\ \tilde{\chi}_\pm &= e^{-i\phi^0 \sqrt{2} T^0/F} u^\pm \chi u^\pm \pm e^{i\phi^0 \sqrt{2} T^0/F} u \chi^+ u \\ &= \chi_\pm - \frac{i}{F} \sqrt{\frac{2}{N_F}} \phi^0 \chi_\mp + \dots, \\ \langle l_\mu \rangle &= l_\mu^0 \sqrt{\frac{N_F}{2}}, \end{aligned} \quad (\text{A3})$$

etc., at our disposal. In the above formulas, the covariant (in fact invariant) derivative of ϕ^0 is defined as

$$D_\mu \phi^0 = \partial_\mu \phi^0 - 2a_\mu^0 F; \quad (\text{A4})$$

however, it does not represent an independent building block because of the identity

$$\langle \tilde{u}_\mu \rangle = \sqrt{\frac{N_F}{2}} \frac{D_\mu \phi^0}{F}. \quad (\text{A5})$$

PHYSICAL REVIEW D **84**, 014036 (2011)

The above set of building blocks has to be further enlarged, including also the external sources θ for the winding number density

$$\omega = \frac{g^2}{16\pi^2} \text{tr}_c G_{\mu\nu} \tilde{G}^{\mu\nu}, \quad (\text{A6})$$

with the covariant derivative

$$D_\mu \theta = \partial_\mu \theta + 2a_\mu^0.$$

We also have to include the following invariant combination,

$$X = \theta + \frac{\phi^0}{F}. \quad (\text{A7})$$

Let us remember the large N_C counting for the generating functional of the connected Green function of quark bilinears and winding number densities,

$$\begin{aligned} Z[l, r, \chi, \chi^+, \theta] &= N_C^2 Z_0[\theta/N_C] \\ &+ N_C Z_1[l, r, \chi, \chi^+, \theta/N_C] + \dots, \end{aligned} \quad (\text{A8})$$

where the ellipsis stands for the subleading terms in the $1/N_C$ expansion. This implies the usual N_C counting of the physical amplitudes with g glueballs and m mesons,

$$\mathcal{A}_{g,m} = O(N_C^{1+\delta_{m0}-g-(m/2)}). \quad (\text{A9})$$

This counting should be reflected within the construction of the effective chiral Lagrangian of $R\chi T$.

According to (A9), an explicit resonance field has to be counted as $O(N_C^{-1/2})$. As far as the GBs are concerned, within the tilded building blocks, each member of the pseudoscalar nonet is automatically accompanied by (minus) one power of the decay constant $F = O(N_C^{1/2})$, which ensures the right counting of the vertices with GBs, provided the corresponding fields are counted as $O(N_C^0)$. The only subtlety is connected with the field ϕ^0 .

The origin of the field ϕ^0 in the individual terms of the Lagrangian is twofold. It can either come from the tilded building blocks $Y = \tilde{u}_\mu, \tilde{h}_{\mu\nu}, \tilde{\chi}_\pm$ (and from their covariant derivatives $\tilde{D}_\mu Y$; note that it completely decouples from Γ_μ and $f_\pm^{\mu\nu}$) or from the X dependence of the Lagrangian. Each operator $\tilde{\mathcal{O}}$ constructed from the tilded building blocks only (and therefore including at least one flavor trace, the only exception being $\tilde{\mathcal{O}} = 1$) is, in general, accompanied by a potential $V_{\tilde{\mathcal{O}}}(X)$ which is a function of the variable X only,

$$\tilde{\mathcal{L}} = \sum_{\tilde{\mathcal{O}}} V_{\tilde{\mathcal{O}}}(X) \tilde{\mathcal{O}}. \quad (\text{A10})$$

While ϕ^0 originating from the tilded operators is counted as $O(N_C^0)$ as the other GB, however, the same field coming from the power expansion of the potentials counts as $O(1/N_C)$ within the large N_C expansion. Therefore, expanding the general operator $\tilde{\mathcal{O}}$ and the corresponding

RESONANCE SATURATION IN THE ODD-INTRINSIC ...

potential $V_{\tilde{O}}(X)$ in powers of ϕ^0 and its derivatives [and taking into account that $F = O(N_C^{1/2})$], we have the following natural rule for the order $O(N_C^n)$ of the resulting coupling constant at a term of this expansion with T flavor traces, R resonance fields, and n_0 fields ϕ^0 ,

$$2 - T - \frac{1}{2}R - \frac{3}{2}n_0 \leq n \leq 2 - T - \frac{1}{2}R - \frac{1}{2}n_0. \quad (\text{A11})$$

The lower or higher bounds are saturated when all ϕ^0 's come exclusively from either $V_{\tilde{O}}(X)$ or \tilde{O} .

Suppose that we had used the LO GB equations of motion prior to the expansion in powers of ϕ^0 . This allows us to eliminate the terms with derivatives, namely [24],

$$\nabla^\mu \tilde{u}_\mu = \tilde{\chi}_- + \frac{4}{\sqrt{2N_F}} M_0^2 \frac{\phi^0}{F}. \quad (\text{A12})$$

Such a transformation of the original tilded operator does not create any extra trace, in contrast to the octet case. Because the singlet mass $M_0^2 = O(1/N_C)$, the ϕ^0 dependence of the resulting operator brings about a factor of the order $O(N_C^{-3/2})$ (the same as if ϕ^0 came from the potential) and the above bounds on n therefore remain valid. On the other hand, a further simplification using the Cayley-Hamilton identity can destroy them, provided we use it in order to eliminate terms with less traces in favor of the terms with more traces.

The next step is to integrate out ϕ^0 , treating the mass M_0^2 as $O(p^0)$. This can be done using its equation of motion, derived from the corresponding part of the LO Lagrangian expanded in powers of ϕ^0 ,

$$\begin{aligned} \mathcal{L}_0^{(2)} &= \frac{1}{2} D\phi^0 \cdot D\phi^0 - \frac{1}{2} M_0^2 (\phi^0)^2 - i \frac{F}{2\sqrt{2N_F}} \langle \chi_- \rangle \phi^0 \\ &+ d_0 \langle P \rangle \phi^0 + \dots, \end{aligned} \quad (\text{A13})$$

where the d_0 term comes from the expansion of the potential and is therefore of the order $O(N_C^{-1})$. The solution for ϕ^0 reads, in the leading order of the p expansion,⁶

$$\begin{aligned} \phi^{(2)} &= \frac{1}{M_0^2} \left(-i \frac{F}{2\sqrt{2N_F}} \langle \chi_- \rangle + d_0 \langle P \rangle \right) \\ &= O(N_C^{3/2}) + O(N_C^0), \end{aligned} \quad (\text{A14})$$

where we have depicted the orders of both terms. $\phi^{(2)}$ should then be inserted into the original Lagrangian expanded in powers of ϕ^0 . As a result, taking (A11) into account, the orders of the multiple trace operators within the $SU_L(N_F) \times SU_R(N_F)$ operator basis are enhanced. Namely, we have the following bound for the corresponding couplings,

⁶Here we have taken into account that the resonance fields should be counted as $O(p^2)$.

PHYSICAL REVIEW D **84**, 014036 (2011)

$$\begin{aligned} 2 - T_0 - \frac{1}{2}R_0 - \frac{3}{2}n_{(P)} &\leq n \\ &\leq 2 - T_0 - \frac{1}{2}R_0 + n_{\langle \chi_- \rangle} - \frac{1}{2}n_{(P)}, \end{aligned} \quad (\text{A15})$$

where T_0 and R_0 are the numbers of the traces and resonance fields before elimination of ϕ^0 and $n_{\langle \chi_- \rangle}$, and $n_{(P)}$ are the numbers of the new factors $\langle \chi_- \rangle$ and $\langle P \rangle$ (which appear after ϕ^0 is integrated out), respectively. More conveniently, this can be expressed in terms of the actual number of traces $T = T_0 + n_{(P)} + n_{\langle \chi_- \rangle}$ and resonances $R = R_0 + n_{(P)}$ as

$$2 - T - \frac{1}{2}R + n_{\langle \chi_- \rangle} \leq n \leq 2 - T - \frac{1}{2}R + n_{(P)} + 2n_{\langle \chi_- \rangle}. \quad (\text{A16})$$

The loophole of this formula is that, for its application, one has to trace back which of the factors $\langle P \rangle$ and $\langle \chi_- \rangle$ originate in the ϕ^0 dependence of the tilded Lagrangian. The extreme cases are either none or all of them, which gives a very raw estimate,

$$2 - T - \frac{1}{2}R \leq n \leq 2 - T - \frac{1}{2}R + N_{(P)} + 2N_{\langle \chi_- \rangle}, \quad (\text{A17})$$

where now $N_{\langle \chi_- \rangle}$ and $N_{(P)}$ are the total numbers of $\langle P \rangle$ and $\langle \chi_- \rangle$ traces in the operator, and the lower bound now corresponds to the usual trace and resonance counting.

2. Explicit examples

Let us illustrate the above statements by means of explicit examples. For instance, the coupling at the term $\langle S\chi_- \rangle \langle \chi_- \rangle$, at first sight of the order $O(N_C^{-1/2})$, might be of the order $O(N_C^{1/2})$ or even $O(N_C^{3/2})$, because it can originate either from the term

$$\begin{aligned} i \langle S\tilde{\chi}_- \rangle W_{(S\chi_-)}(X) &= i \langle S(\chi_- + \dots) \rangle (w_{(S\chi_-)}^1 X + \dots) \rightarrow -\langle S\chi_- \rangle \\ &\times \frac{1}{M_0^2} \left(w_{(S\chi_-)}^1 \frac{1}{2\sqrt{2N_F}} \langle \chi_- \rangle + \dots \right), \end{aligned} \quad (\text{A18})$$

which has the constant $w_{(S\chi_-)}^1 = O(N_C^{-1/2})$ [this corresponds to the lower bound (A16)], or from the term

$$\begin{aligned} \langle S\tilde{\chi}_+ \rangle W_{(S\chi_+)}(X) &= \langle S \left(\chi_+ - \frac{i}{F} \sqrt{\frac{2}{N_F}} \phi^0 \chi_- + \dots \right) \rangle (w_{(S\chi_+)}^0 + \dots) \\ &= -w_{(S\chi_+)}^0 \frac{i}{F} \sqrt{\frac{2}{N_F}} \phi^0 \langle S\chi_- \rangle + \dots \\ &\rightarrow \frac{1}{M_0^2} w_{(S\chi_+)}^0 \left(\frac{1}{2N_F} \right) \langle S\chi_- \rangle \langle \chi_- \rangle + \dots, \end{aligned} \quad (\text{A19})$$

where $w_{(S\chi_+)}^0 = O(N_C^{1/2})$ [this corresponds to the upper bound (A16)].

Similarly, the coupling d_{m0} at the operator $i \langle P \rangle \langle \chi_- \rangle$ [see (14)], naively of the order $O(N_C^{-1/2})$, can be enhanced by

KAROL KAMPF AND JIŘÍ NOVOTNÝ

the ϕ^0 exchange. Indeed, inserting (14) into the term $d_0\langle P\rangle\phi^0$ of the Lagrangian (13), we get the following contribution to d_{m0} :

$$d_{m0} = -\frac{d_0}{M_0^2} \frac{F\sqrt{N_F}}{2\sqrt{2}} = O(N_C^{-1/2}), \quad (\text{A20})$$

where we have taken into account that $d_0 = O(N_C^{-1})$.

Let us also give some examples of the odd-intrinsic parity terms with resonances, which, similar to the previous example, lead to N_C enhanced multiple trace terms when ϕ^0 is integrated out. Some terms with one resonance are, for example,

$$\begin{aligned} \tilde{\mathcal{L}}_R &= \varepsilon_{\mu\nu\alpha\beta} \langle V^{\mu\nu} [\tilde{u}^\alpha, \tilde{u}^\beta] \rangle W_{R1}(X) \\ &+ \varepsilon_{\mu\nu\alpha\beta} \langle V^{\mu\nu} f_+^{\alpha\beta} \rangle W_{R2}(X) \\ &+ \varepsilon_{\mu\nu\alpha\beta} \langle A^{\mu\nu} f_+^{\alpha\beta} \rangle W_{R3}(X), \end{aligned} \quad (\text{A21})$$

where

$$W_{Ri}(X) = \sum_k w_{Ri}^{(k)} X^k \quad (\text{A22})$$

and where

$$w_{Ri}^{(0)} = 0, \quad w_{Ri}^{(1)} = O(N_C^{-1/2}), \quad \text{for } i = 1, 2, 3. \quad (\text{A23})$$

These generate the operators

$$\begin{aligned} \hat{\mathcal{O}}_{18}^V &= \varepsilon_{\mu\nu\alpha\beta} \langle V^{\mu\nu} [u^\alpha, u^\beta] \rangle \langle \chi_- \rangle, \\ \hat{\mathcal{O}}_{13}^V &= i\varepsilon_{\mu\nu\alpha\beta} \langle V^{\mu\nu} f_+^{\alpha\beta} \rangle \langle \chi_- \rangle, \\ \hat{\mathcal{O}}_9^A &= i\langle A^{\mu\nu} f_+^{\alpha\beta} \rangle \langle \chi_- \rangle \end{aligned} \quad (\text{A24})$$

with the couplings of the order $O(N_C^{-1/2})$ (i.e. of the same order as analogous single trace operators and therefore included in our basis) and

$$\begin{aligned} \varepsilon_{\mu\nu\alpha\beta} \langle V^{\mu\nu} [u^\alpha, u^\beta] \rangle \langle P \rangle, \quad \varepsilon_{\mu\nu\alpha\beta} \langle V^{\mu\nu} f_+^{\alpha\beta} \rangle \langle P \rangle, \\ \langle A^{\mu\nu} f_+^{\alpha\beta} \rangle \langle P \rangle \end{aligned} \quad (\text{A25})$$

with the couplings of the order $O(N_C^{-1})$ suppressed with respect to the single trace operators.

The two-resonance example is

$$\begin{aligned} \tilde{\mathcal{L}}_{RR} &= \varepsilon_{\mu\nu\alpha\beta} \langle V^{\mu\nu} V^{\alpha\beta} \rangle W_{RR1}(X) \\ &+ \varepsilon_{\mu\nu\alpha\beta} \langle A^{\mu\nu} A^{\alpha\beta} \rangle W_{RR1}(X), \end{aligned} \quad (\text{A26})$$

where

$$\begin{aligned} W_{RRi}(X) &= \sum_k w_{RRi}^{(k)} X^k \quad \text{with } w_{RRi}^{(0)} = 0, \\ w_{RRi}^{(1)} &= O(N_C^{-1}), \quad \text{for } i = 1, 2. \end{aligned}$$

It gives rise to the operators

$$\begin{aligned} \hat{\mathcal{O}}_1^{VV} &= i\varepsilon_{\mu\nu\alpha\beta} \langle V^{\mu\nu} V^{\alpha\beta} \rangle \langle \chi_- \rangle, \\ \hat{\mathcal{O}}_1^{AA} &= i\varepsilon_{\mu\nu\alpha\beta} \langle A^{\mu\nu} A^{\alpha\beta} \rangle \langle \chi_- \rangle \end{aligned} \quad (\text{A27})$$

PHYSICAL REVIEW D **84**, 014036 (2011)

with the couplings of the order $O(N_C^0)$ (the same order as the analogous single trace operators and therefore included in our basis), and $O(N_C^{-3/2})$ operators

$$\varepsilon_{\mu\nu\alpha\beta} \langle V^{\mu\nu} V^{\alpha\beta} \rangle \langle P \rangle, \quad \varepsilon_{\mu\nu\alpha\beta} \langle A^{\mu\nu} A^{\alpha\beta} \rangle \langle P \rangle, \quad (\text{A28})$$

which are suppressed with respect to the single trace ones.

As the last step, we integrate out the resonance fields in order to get the resonance contribution to the odd parity sector LECs of the resulting ChPT Lagrangian. This can be done using the $O(p^2)$ equation of motion for the resonance fields and inserting their solution $R^{(2)}$ back into the $R\chi T$ Lagrangian. The general form reads

$$R^{(2)} = \frac{1}{M_R^2} J_R^{(2)}, \quad (\text{A29})$$

where $J_R^{(2)} = O(p^2)$ comes from the LO resonance Lagrangian (14). Because $J_R^{(2)} = O(N_C^{1/2})$, the order of the contribution of the individual terms of the $R\chi T$ Lagrangian (with ϕ^0 integrated out) can be obtained, counting the resonance fields as $O(N_C^{1/2})$. This gives, finally, the following simple bound on the order of the contribution of the operator with T traces, total $N_{\langle P \rangle}$ factors $\langle P \rangle$, and total $N_{\langle \chi_- \rangle}$ factors $\langle \chi_- \rangle$ originating in the LECs,

$$2 - T \leq n \leq 2 - T + N_{\langle P \rangle} + 2N_{\langle \chi_- \rangle}. \quad (\text{A30})$$

The lower bound represents the usual trace counting. Note, however, that the upper bound has to be taken with some caution, because it can be saturated only in the case when all $\langle P \rangle$ and $\langle \chi_- \rangle$ traces appear as a consequence of the ϕ^0 dependence, where this ϕ^0 dependence comes solely from the tilded operators and not from the potentials. For a given operator these two conditions need not be satisfied simultaneously.

The fact that the N_C order of some operators can be enhanced could further complicate the usual way of the saturation of the ChPT LECs. Namely, in the process of integrating out the resonances, it is assumed that loops can give only NLO contributions suppressed by the factor $1/N_C$ for each loop. This counting could apparently be complicated by the enhanced operators. Let us illustrate this point, assuming the contribution of the following term of the odd $R\chi T$ Lagrangian $\tilde{\mathcal{L}}$,

$$\begin{aligned} \tilde{\mathcal{L}} &= \dots + W_2^{AP}(X) \varepsilon_{\mu\nu\alpha\beta} \langle \{A^{\mu\nu}, \nabla^\alpha P\} \tilde{u}^\beta \rangle + \dots \\ &= \dots - 2W_2^{AP} \varepsilon_{\mu\nu\alpha\beta} \langle A^{\mu\nu} \nabla^\alpha P \rangle \sqrt{\frac{2}{N_F}} \frac{D^\beta \phi^0}{F} + \dots \end{aligned} \quad (\text{A31})$$

with $w_2^{AP} = O(N_C^0)$. This gives rise to the following enhanced N_C term,

$$-\frac{i}{N_F} w_2^{AP} \frac{1}{M_0^2} \varepsilon_{\mu\nu\alpha\beta} \langle A^{\mu\nu} \nabla^\alpha P \rangle \partial^\beta \langle \chi_- \rangle = O(N_C). \quad (\text{A32})$$

Apparently, this term contributes to the $O(p^8)$ LECs, when the resonances are integrated out at the *tree level*. However,

RESONANCE SATURATION IN THE ODD-INTRINSIC ...

the bubble with two such vertices gives a contribution to the $O(p^6)$ operator $\partial_\alpha \langle \chi_- \rangle \partial^\alpha \langle \chi_- \rangle$ of the enhanced order $O(N_C^2)$. The same is true also for analogous operators from the even sector, e.g.

$$V_1^{SP}(X) \langle \{D_\mu S, P\} \tilde{u}^\mu \rangle = 2v_1^{SP} \langle PD_\mu S \rangle \sqrt{\frac{2}{N_F}} \frac{D^\mu \phi^0}{F} + \dots \quad (\text{A33})$$

with $v_1^{SP} = O(N_C)$, which leads to the enhanced operator

$$\frac{i}{N_F} v_1^{SP} \frac{1}{M_0^2} \langle P \nabla_\mu S \rangle \partial^\mu \langle \chi_- \rangle = O(N_C) \quad (\text{A34})$$

counted as $O(p^8)$ in the tree-level saturation process. The bubble with two vertices,

$$\frac{i}{N_F} v_1^{SP} \frac{1}{M_0^2} \langle P \partial_\mu S \rangle \partial^\mu \langle \chi_- \rangle, \quad (\text{A35})$$

leads to the expression

$$\begin{aligned} & \frac{N_F^2}{2} \left(\frac{i}{N_F} v_1^{SP} \frac{1}{M_0^2} \right)^2 \int d^d x d^d y \partial^\mu \langle \chi_-(x) \rangle \partial^\nu \langle \chi_-(y) \rangle \\ & \times \int \frac{d^d k}{(2\pi)^d} e^{ik \cdot (x-y)} \frac{d^d p}{(2\pi)^d} \\ & \times \frac{P_\mu P_\nu}{(p^2 - M_S^2 + i0)((p-k)^2 - M_P^2 + i0)} \\ & = \frac{i}{2} \left(\frac{v_1^{SP}}{M_0^2} \right)^2 \int d^d x \partial^\mu \langle \chi_-(x) \rangle \partial_\mu \langle \chi_-(x) \rangle \\ & \times \frac{(M_P^2)^{2-\varepsilon} - (M_S^2)^{2-\varepsilon}}{M_P^2 - M_S^2} \frac{1}{32\pi^2} \Gamma(\varepsilon - 2) (4\pi)^\varepsilon + O(p^8) \end{aligned} \quad (\text{A36})$$

and (after the addition of an appropriate counterterm) results in the following $O(N_C^2)$ contribution to the coupling $C_{\partial_\alpha \langle \chi_- \rangle \partial^\alpha \langle \chi_- \rangle}$ associated with the $O(p^6)$ operator $\partial_\alpha \langle \chi_- \rangle \partial^\alpha \langle \chi_- \rangle$,

$$\begin{aligned} C_{\partial_\alpha \langle \chi_- \rangle \partial^\alpha \langle \chi_- \rangle}^{PS\text{-loop}} & = -\frac{1}{64\pi^2} \left(\frac{v_1^{SP}}{M_0^2} \right)^2 \\ & \times \frac{M_P^4 (\ln \frac{M_P^2}{\mu^2} + \gamma - \frac{1}{2}) - M_S^4 (\ln \frac{M_S^2}{\mu^2} + \gamma - \frac{1}{2})}{M_P^2 - M_S^2}. \end{aligned} \quad (\text{A37})$$

Though the above loop contributions are enhanced by the factor N_C^2 with respect to the naive trace counting, this does not mean that loop counting fails. The reason is that the LO contribution to $C_{\partial_\alpha \langle \chi_- \rangle \partial^\alpha \langle \chi_- \rangle}$ that comes from the tree level and originates in the kinetic term of the field ϕ^0

$$\frac{1}{2} \partial_\mu \phi^0 \cdot \partial^\mu \phi^0 \rightarrow -\frac{1}{2} \left(\frac{F}{2M_0^2 \sqrt{2N_F}} \right)^2 \partial_\alpha \langle \chi_- \rangle \partial^\alpha \langle \chi_- \rangle = O(N_C^3) \quad (\text{A38})$$

PHYSICAL REVIEW D **84**, 014036 (2011)

so that the loop contribution is suppressed by $1/N_C$ as usual.

Let us finally comment briefly on one point, which also might lead to confusion. In [24], the following operators are abandoned, using the large N_C arguments, namely,

$$i \langle P u_\mu u^\mu \rangle \langle \chi_- \rangle, \quad i \langle SP \rangle \langle \chi_- \rangle, \quad i \langle \nabla_\mu \nabla^\mu \chi_- \rangle \langle P \rangle. \quad (\text{A39})$$

These can be, however, derived from the operators (before doing any transformations)

$$i \langle P \tilde{u}_\mu \tilde{u}^\mu \rangle V(X), \quad i \langle SP \rangle V(X), \quad i \langle \nabla_\mu \nabla^\mu \tilde{\chi}_+ \rangle V(X), \quad (\text{A40})$$

by means of integrating out the field ϕ^0 , which appears from the potential for the first two operators [and saturates, therefore, the lower bound of (A16)] and from the building block $\tilde{\chi}_+$ for the last one [and corresponds, therefore, to the upper bound of (A16)]. According to our rules the operators are of the orders $O(N_C^{1/2})$, $O(N_C^0)$, and $O(N_C^{1/2})$, respectively (as similar operators without an additional trace), and all of them contribute, therefore, at the $O(N_C)$ order of the LECs of the effective chiral Lagrangian staying at the operators

$$\langle \chi_- u_\mu u^\mu \rangle \langle \chi_- \rangle, \quad \langle \chi_+ \chi_- \rangle \langle \chi_- \rangle, \quad \langle \nabla_\mu \nabla^\mu \chi_- \rangle \langle \chi_- \rangle. \quad (\text{A41})$$

However, these operators can be derived analogously from

$$\langle \tilde{\chi}_+ \tilde{u}_\mu \tilde{u}^\mu \rangle, \quad \langle \tilde{\chi}_+ \tilde{\chi}_+ \rangle, \quad \langle \nabla_\mu \nabla^\mu \tilde{\chi}_+ \rangle, \quad (\text{A42})$$

by the process which saturates the upper bound of (A16) and results in the order $O(N_C^2)$. The abandoned operators lead, therefore, to the NLO contribution to the corresponding LECs.

APPENDIX B: FIELD REDEFINITION

As we have discussed in detail in Sec. III, by means of an appropriate field redefinition we can effectively eliminate a subset of the $O(p^6)$ operators from the Lagrangian $\mathcal{L}_{R\chi T}^{(6, \text{odd})}$ and shift their influence on the ChPT LECs into the effective coefficients $\bar{\kappa}_i^X$ which stay at the remaining operators of the chiral order $O(p^6)$ and higher. As a consequence, the $O(p^6)$ LECs resulting from the process of integrating out the resonance fields from the Lagrangian $\mathcal{L}_{R\chi T}$ depend only on these effective couplings $\bar{\kappa}_i^X$ which are particular linear combinations of the original resonance couplings κ_i^X . In order to identify these relevant combinations and the redundant operators, we can proceed in several steps.

1. Elimination of $\mathcal{O}_{1,2}^{VV}$, $\mathcal{O}_{1,2}^{AA}$, \mathcal{O}^{VVP} , and \mathcal{O}^{AAP}

By the elimination of $\mathcal{O}_{1,2}^{VV}$, $\mathcal{O}_{1,2}^{AA}$, \mathcal{O}^{VVP} , and \mathcal{O}^{AAP} with the field redefinitions

$$\begin{aligned}
V_{\mu\nu} &\rightarrow V_{\mu\nu} - \frac{2}{M_V^2} \varepsilon_{\mu\nu\alpha\beta} \left(i\kappa_1^{VV} \langle \chi_- \rangle V^{\alpha\beta} + i\kappa_2^{VV} \{ \chi_-, V^{\alpha\beta} \} + \frac{1}{2} \kappa^{VVP} \{ P, V^{\alpha\beta} \} \right), \\
A_{\mu\nu} &\rightarrow A_{\mu\nu} - \frac{2}{M_A^2} \varepsilon_{\mu\nu\alpha\beta} \left(i\kappa_1^{AA} \langle \chi_- \rangle A^{\alpha\beta} + i\kappa_2^{AA} \{ \chi_-, A^{\alpha\beta} \} + \frac{1}{2} \kappa^{AAP} \{ P, A^{\alpha\beta} \} \right),
\end{aligned}$$

we get, for the $O(p^4)$ part of the Lagrangian,

$$\begin{aligned}
&\mathcal{L}_{RR,\text{kin}}^{(4)} + \mathcal{L}_R^{(4)} \rightarrow \mathcal{L}_{RR,\text{kin}}^{(4)} + \mathcal{L}_R^{(4)} \\
&= \mathcal{L}_{RR,\text{kin}}^{(4)} + \mathcal{L}_R^{(4)} - \kappa_1^{VV} \mathcal{O}_1^{VV} - \kappa_2^{VV} \mathcal{O}_2^{VV} - \kappa^{VVP} \mathcal{O}^{VVP} - \kappa_1^{AA} \mathcal{O}_1^{AA} - \kappa_2^{AA} \mathcal{O}_2^{AA} - \kappa^{AAP} \mathcal{O}^{AAP} \\
&\quad - \frac{F_V}{\sqrt{2}M_V^2} \left(\kappa_1^{VV} \mathcal{O}_{13}^V + \kappa_2^{VV} \mathcal{O}_{14}^V + \frac{1}{2} \kappa^{VVP} \mathcal{O}_3^{PV} \right) - \frac{iG_V}{\sqrt{2}M_V^2} (2i\kappa_1^{VV} \mathcal{O}_{18}^V + 2i\kappa_2^{VV} \mathcal{O}_9^V - i\kappa^{VVP} \mathcal{O}_1^{PV}) \\
&\quad - \frac{F_A}{\sqrt{2}M_A^2} \left(\kappa_1^{AA} \mathcal{O}_9^A + \kappa_2^{AA} \mathcal{O}_{11}^A + \frac{1}{2} \kappa^{AAP} \mathcal{O}_1^{PA} \right) + O(p^8).
\end{aligned}$$

At the same time, the same redefinition applied to $\mathcal{L}_{R\chi T}^{(6,\text{odd})}$ generates only the additional terms of the order $O(p^8)$ and higher, which can be neglected as described above. We can thus eliminate the operators $\mathcal{O}_{1,2}^{VV}$, \mathcal{O}^{VVP} , $\mathcal{O}_{1,2}^{AA}$, and \mathcal{O}^{AAP} and include their influence on the $O(p^6)$ LECs effectively into the constants $\overline{\kappa}_{13}^V$, $\overline{\kappa}_{14}^V$, $\overline{\kappa}_3^{PV}$, $\overline{\kappa}_{18}^V$, $\overline{\kappa}_9^V$, $\overline{\kappa}_1^{PV}$ and $\overline{\kappa}_9^A$, $\overline{\kappa}_{11}^A$, $\overline{\kappa}_1^{PA}$.

2. Elimination of \mathcal{O}_i^{VA} and \mathcal{O}^{VAS}

In the same way, we can also eliminate the mixed bilinear terms using the field redefinition

$$\begin{aligned}
V_{\mu\nu} &\rightarrow V_{\mu\nu} - \frac{1}{M_V^2} \varepsilon_{\mu\nu\alpha\sigma} (i\kappa_1^{VA} g_\beta^\sigma [A^{\alpha\beta}, u^\rho u_\rho] + i\kappa_2^{VA} (A^{\alpha\beta} u_\beta u^\sigma - u^\sigma u_\beta A^{\alpha\beta}) + i\kappa_3^{VA} (A^{\alpha\beta} u^\sigma u_\beta - u_\beta u^\sigma A^{\alpha\beta}) \\
&\quad + i\kappa_4^{VA} (u_\beta A^{\alpha\beta} u^\sigma - u^\sigma A^{\alpha\beta} u_\beta) + \kappa_5^{VA} \{ A^{\alpha\beta}, f_+^{\sigma\rho} \} g_{\beta\rho} + i\kappa_6^{VA} [A^{\alpha\beta}, \chi_+] g_\beta^\sigma + i\kappa^{VAS} [A^{\alpha\beta}, S] g_\beta^\sigma), \\
A_{\mu\nu} &\rightarrow A_{\mu\nu} - \frac{1}{M_A^2} \varepsilon_{\alpha\beta\mu\sigma} (i\kappa_1^{VA} g_\nu^\sigma [u^\rho u_\rho, V^{\alpha\beta}] + i\kappa_2^{VA} (u^\nu u^\sigma V^{\alpha\beta} - V^{\alpha\beta} u^\sigma u^\nu) + i\kappa_3^{VA} (u^\sigma u^\nu V^{\alpha\beta} - V^{\alpha\beta} u^\nu u^\sigma) \\
&\quad + i\kappa_4^{VA} (u^\sigma V^{\alpha\beta} u^\nu - u^\nu V^{\alpha\beta} u^\sigma) + \kappa_5^{VA} \{ V^{\alpha\beta}, f_+^{\sigma\rho} \} g_{\rho\nu} + i\kappa_6^{VA} [\chi_+, V^{\alpha\beta}] g_\nu^\sigma + i\kappa^{VAS} [S, V^{\alpha\beta}] g_\nu^\sigma).
\end{aligned}$$

We then get

$$\begin{aligned}
\frac{1}{4} M_V^2 \langle V^{\mu\nu} V_{\mu\nu} \rangle + \frac{1}{4} M_A^2 \langle A^{\mu\nu} A_{\mu\nu} \rangle &\rightarrow \frac{1}{4} M_V^2 \langle V^{\mu\nu} V_{\mu\nu} \rangle + \frac{1}{4} M_A^2 \langle A^{\mu\nu} A_{\mu\nu} \rangle - \kappa_1^{VA} \mathcal{O}_1^{VA} - \kappa_2^{VA} \mathcal{O}_2^{VA} \\
&\quad - \kappa_3^{VA} \mathcal{O}_3^{VA} - \kappa_4^{VA} \mathcal{O}_4^{VA} - \kappa_5^{VA} \mathcal{O}_5^{VA} - \kappa_6^{VA} \mathcal{O}_6^{VA} - \kappa^{VAS} \mathcal{O}^{VAS},
\end{aligned}$$

and the operators \mathcal{O}_i^{VA} and \mathcal{O}^{VAS} are thus eliminated. The only relevant additional effect of the redefinition comes from the transformation of $\mathcal{L}_R^{(4)}$,

$$\begin{aligned}
\frac{F_V}{2\sqrt{2}} \langle V_{\mu\nu} f_+^{\mu\nu} \rangle &\rightarrow \frac{F_V}{2\sqrt{2}} \langle V_{\mu\nu} f_+^{\mu\nu} \rangle - \frac{F_V}{2\sqrt{2}M_V^2} \left[-\kappa_1^{VA} \mathcal{O}_4^A + \kappa_2^{VA} \left(\mathcal{O}_6^A - \frac{1}{2} \mathcal{O}_4^A \right) \right. \\
&\quad \left. + \kappa_3^{VA} \left(\mathcal{O}_5^A - \frac{1}{2} \mathcal{O}_4^A \right) + \kappa_4^{VA} \mathcal{O}_7^A - \kappa_6^{VA} \mathcal{O}_{14}^A + \kappa^{VAS} \mathcal{O}_1^{SA} \right], \\
\frac{F_A}{2\sqrt{2}} \langle A_{\mu\nu} f_+^{\mu\nu} \rangle &\rightarrow \frac{F_A}{2\sqrt{2}} \langle A_{\mu\nu} f_+^{\mu\nu} \rangle - \frac{F_A}{2\sqrt{2}M_A^2} \left[\kappa_1^{VA} \mathcal{O}_3^V + \kappa_2^{VA} \mathcal{O}_8^V + \kappa_3^{VA} \mathcal{O}_6^V + \kappa_4^{VA} \mathcal{O}_7^V - \kappa_5^{VA} \mathcal{O}_{11}^V + \kappa_6^{VA} \mathcal{O}_{15}^V - \kappa^{VAS} \mathcal{O}_1^{SV} \right], \\
\frac{iG_V}{2\sqrt{2}} \langle V_{\mu\nu} [u^\mu, u^\nu] \rangle &\rightarrow \frac{iG_V}{2\sqrt{2}} \langle V_{\mu\nu} [u^\mu, u^\nu] \rangle + \frac{G_V}{2\sqrt{2}M_V^2} \left[-2\kappa_1^{VA} \mathcal{O}_1^A + \kappa_2^{VA} (\mathcal{O}_2^A - \mathcal{O}_1^A) + \kappa_3^{VA} (\mathcal{O}_2^A - \mathcal{O}_1^A) \right. \\
&\quad \left. + \kappa_4^{VA} (\mathcal{O}_1^A - \mathcal{O}_2^A) + \kappa_5^{VA} (\mathcal{O}_5^A - \mathcal{O}_6^A) + 2\kappa_6^{VA} \mathcal{O}_{13}^A + 2\kappa^{VAS} \mathcal{O}_2^{SA} \right].
\end{aligned}$$

Here we have used

$$\langle \{ A^{\alpha\beta}, f_+^{\sigma\rho} \} f_+^{\mu\nu} \rangle g_{\beta\rho} \varepsilon_{\mu\nu\alpha\sigma} = 0$$

and other similar consequences of the Shouten identity.

3. Elimination of \mathcal{O}_1^{PA} , \mathcal{O}_i^{SV} , \mathcal{O}_i^{PV} , and \mathcal{O}_i^{SA}

Finally, we can further eliminate other terms by the redefinitions

$$\begin{aligned}
S &\rightarrow S + \frac{1}{2M_S^2} \varepsilon_{\mu\nu\alpha\beta} (i\kappa_1^{SA} [f_+^{\alpha\beta}, A^{\mu\nu}] + \kappa_2^{SA} [u^\alpha u^\beta, A^{\mu\nu}]), \\
P &\rightarrow P + \frac{1}{2M_P^2} \varepsilon_{\mu\nu\alpha\beta} (\kappa_1^{PA} \{A^{\mu\nu}, f_+^{\alpha\beta}\} + i\kappa_1^{PV} \{V^{\mu\nu}, u^\alpha u^\beta\} + i\kappa_2^{PV} u^\beta V^{\mu\nu} u^\alpha + \kappa_3^{PV} \{V^{\mu\nu}, f_+^{\alpha\beta}\}), \\
A_{\mu\nu} &\rightarrow A_{\mu\nu} - \frac{1}{M_A^2} \varepsilon_{\mu\nu\alpha\beta} (i\kappa_1^{SA} [S, f_+^{\alpha\beta}] + \kappa_2^{SA} [S, u^\alpha u^\beta] + \kappa_1^{PA} \{P, f_+^{\alpha\beta}\}), \\
V_{\mu\nu} &\rightarrow V_{\mu\nu} - \frac{1}{M_V^2} \varepsilon_{\mu\nu\alpha\beta} (i\kappa_1^{PV} \{P, u^\alpha u^\beta\} + i\kappa_2^{PV} u^\alpha P u^\beta + \kappa_3^{PV} \{P, f_+^{\alpha\beta}\}).
\end{aligned}$$

We then get

$$\begin{aligned}
& -\frac{1}{2}M_P^2 \langle PP \rangle - \frac{1}{2}M_S^2 \langle SS \rangle + \frac{1}{4}M_A^2 \langle A^{\mu\nu} A_{\mu\nu} \rangle + \frac{1}{4}M_V^2 \langle V^{\mu\nu} V_{\mu\nu} \rangle \\
& \rightarrow -\frac{1}{2}M_P^2 \langle PP \rangle - \frac{1}{2}M_S^2 \langle SS \rangle + \frac{1}{4}M_A^2 \langle A^{\mu\nu} A_{\mu\nu} \rangle + \frac{1}{4}M_V^2 \langle V^{\mu\nu} V_{\mu\nu} \rangle - \kappa_1^{PA} \mathcal{O}_1^{PA} - \kappa_1^{PV} \mathcal{O}_1^{PV} - \kappa_2^{PV} \mathcal{O}_2^{PV} \\
& - \kappa_3^{PV} \mathcal{O}_3^{PV} - \kappa_1^{SA} \mathcal{O}_1^{SA} - \kappa_2^{SA} \mathcal{O}_2^{SA} - \kappa_1^{SV} \mathcal{O}_1^{SV},
\end{aligned}$$

and therefore the operators \mathcal{O}_i^{SA} , \mathcal{O}_i^{PV} , and \mathcal{O}_i^{PA} are eliminated. We get the additional contributions

$$\begin{aligned}
c_d \langle S u^\mu u_\mu \rangle &\rightarrow c_d \langle S u^\mu u_\mu \rangle + \frac{c_d}{2M_S^2} (-\kappa_1^{SA} \mathcal{O}_4^A - \kappa_2^{SA} \mathcal{O}_1^A - \kappa_1^{SV} \mathcal{O}_5^V), \\
c_m \langle S \chi_+ \rangle &\rightarrow c_m \langle S \chi_+ \rangle + \frac{c_m}{2M_S^2} (-\kappa_1^{SA} \mathcal{O}_{14}^A + \kappa_2^{SA} \mathcal{O}_{13}^A - \kappa_1^{SV} \mathcal{O}_{15}^V),
\end{aligned}$$

$$id_m \langle P \chi_- \rangle \rightarrow id_m \langle P \chi_- \rangle + \frac{d_m}{2M_P^2} (\kappa_1^{PA} \mathcal{O}_{11}^A - \kappa_1^{PV} \mathcal{O}_9^V - \kappa_2^{PV} \mathcal{O}_{10}^V + \kappa_3^{PV} \mathcal{O}_{14}^V),$$

$$i \frac{d_{m0}}{N_F} \langle P \rangle \langle \chi_- \rangle \rightarrow i \frac{d_{m0}}{N_F} \langle P \rangle \langle \chi_- \rangle + \frac{d_{m0}}{N_F M_P^2} (\kappa_1^{PA} \mathcal{O}_9^A - \kappa_1^{PV} \mathcal{O}_{18}^V - \frac{1}{2} \kappa_2^{PV} \mathcal{O}_{18}^V + \kappa_3^{PV} \mathcal{O}_{13}^V),$$

$$\frac{F_A}{2\sqrt{2}} \langle A_{\mu\nu} f^{\mu\nu} \rangle \rightarrow \frac{F_A}{2\sqrt{2}} \langle A_{\mu\nu} f^{\mu\nu} \rangle - \frac{F_A}{2\sqrt{2} M_A^2} (\kappa_1^{SA} \mathcal{O}_2^S - \kappa_2^{SA} \mathcal{O}_1^S + \kappa_1^{PA} \mathcal{O}_1^P),$$

$$\frac{F_V}{2\sqrt{2}} \langle V_{\mu\nu} f_+^{\mu\nu} \rangle \rightarrow \frac{F_V}{2\sqrt{2}} \langle V_{\mu\nu} f_+^{\mu\nu} \rangle - \frac{F_V}{2\sqrt{2} M_V^2} (\kappa_1^{PV} \mathcal{O}_3^P - \kappa_2^{PV} \mathcal{O}_2^P + \kappa_3^{PV} \mathcal{O}_5^P - \kappa_1^{SV} \mathcal{O}_2^S),$$

$$\frac{iG_V}{2\sqrt{2}} \langle V_{\mu\nu} [u^\mu, u^\nu] \rangle \rightarrow \frac{iG_V}{2\sqrt{2}} \langle V_{\mu\nu} [u^\mu, u^\nu] \rangle + \frac{G_V}{\sqrt{2} M_V^2} (2\kappa_1^{PV} \mathcal{O}_4^P - \kappa_2^{PV} \mathcal{O}_4^P - \kappa_3^{PV} \mathcal{O}_3^P + \kappa_1^{SV} \mathcal{O}_1^S).$$

4. Elimination of $\mathcal{O}_{2,3}^{AA}$, $\mathcal{O}_{2,3}^{VV}$, \mathcal{O}_2^{PA} , and \mathcal{O}_2^{SV}

The operators with derivatives acting on the resonance fields can also be eliminated by means of a suitable field redefinition; however, contrary to previous cases, one has to use integration by parts and the equations of motion for the GB fields.

Let us assume the following redefinitions for $R = V, A$,

$$R_{\mu\nu} \rightarrow R_{\mu\nu} - \frac{\kappa_3^{RR}}{M_R^2} (g_{\nu\sigma} \varepsilon_{\alpha\rho\nu\beta} \{\nabla^\sigma R^{\alpha\rho}, u^\beta\} - (\mu \leftrightarrow \nu)) + \frac{\kappa_4^R}{M_R^2} \varepsilon_{\mu\nu\alpha\beta} \nabla^\beta \{R^{\alpha\sigma}, u_\sigma\}.$$

We then get, modulo integration by parts,

$$\frac{1}{4} M_R^2 \langle R_{\mu\nu} R^{\mu\nu} \rangle \rightarrow \frac{1}{4} M_R^2 \langle R_{\mu\nu} R^{\mu\nu} \rangle - \kappa_3^{RR} \mathcal{O}_3^{RR} - \kappa_4^{RR} \mathcal{O}_4^{RR}$$

and (again up to the integration by parts and GB equations of motion)

$$\begin{aligned}
& \frac{F_V}{2\sqrt{2}} \langle V_{\mu\nu} f_+^{\mu\nu} \rangle + \frac{G_V}{2\sqrt{2}} \langle V_{\mu\nu} [u^\mu, u^\nu] \rangle \\
& \rightarrow \frac{F_V}{2\sqrt{2}} \langle V_{\mu\nu} f_+^{\mu\nu} \rangle + \frac{G_V}{2\sqrt{2}} \langle V_{\mu\nu} [u^\mu, u^\nu] \rangle + \frac{F_V \kappa_3^{VV}}{2\sqrt{2} M_V^2} (\mathcal{O}_{11}^V + \mathcal{O}_{12}^V + 2\mathcal{O}_{17}^V) \\
& \quad + \frac{G_V \kappa_3^{VV}}{2\sqrt{2} M_V^2} (2\mathcal{O}_1^V - \mathcal{O}_2^V + \mathcal{O}_3^V - \mathcal{O}_6^V - \mathcal{O}_7^V + 2\mathcal{O}_8^V + \mathcal{O}_9^V - 2\mathcal{O}_{10}^V) + \frac{F_V \kappa_4^{VV}}{2\sqrt{2} M_V^2} (-\mathcal{O}_{11}^V + \mathcal{O}_{12}^V - 2\mathcal{O}_{16}^V) \\
& \quad + \frac{G_V \kappa_4^{VV}}{2\sqrt{2} M_V^2} (\mathcal{O}_1^V + \mathcal{O}_2^V + \mathcal{O}_5^V - \mathcal{O}_7^V - \mathcal{O}_8^V) \frac{F_A}{2\sqrt{2}} \langle A_{\mu\nu} f^{\mu\nu} \rangle \\
& \rightarrow \frac{F_A}{2\sqrt{2}} \langle A_{\mu\nu} f^{\mu\nu} \rangle + \frac{F_A \kappa_3^{AA}}{2\sqrt{2} M_A^2} (\mathcal{O}_8^A + 2\mathcal{O}_{16}^A) + \frac{F_A \kappa_4^{AA}}{2\sqrt{2} M_A^2} (\mathcal{O}_8^A - 2\mathcal{O}_{15}^A).
\end{aligned}$$

Analogously, for the redefinition of the S and P fields

$$S \rightarrow S - \frac{i}{M_S^2} \kappa_2^{SV} \varepsilon_{\mu\nu\alpha\beta} \nabla^\alpha [u^\beta, V^{\mu\nu}], \quad P \rightarrow P - \frac{1}{M_P^2} \kappa_2^{PA} \varepsilon_{\mu\nu\alpha\beta} \nabla^\alpha \{A^{\mu\nu}, u^\beta\},$$

we get, on one hand,

$$-\frac{1}{2} M_S^2 \langle SS \rangle - \frac{1}{2} M_P^2 \langle PP \rangle \rightarrow -\frac{1}{2} M_S^2 \langle SS \rangle - \frac{1}{2} M_P^2 \langle PP \rangle - \kappa_2^{SV} \mathcal{O}_2^{SV} - \kappa_2^{PA} \mathcal{O}_2^{PA}$$

and, on the other hand,

$$\begin{aligned}
c_m \langle S \chi_+ \rangle + c_d \langle S u^\sigma u_\sigma \rangle & \rightarrow c_m \langle S \chi_+ \rangle + c_d \langle S u^\sigma u_\sigma \rangle + \frac{c_m}{M_S^2} \kappa_2^{SV} \mathcal{O}_4^V + \frac{c_d}{2M_S^2} \kappa_2^{SV} (\mathcal{O}_1^V + \mathcal{O}_2^V - \mathcal{O}_7^V - \mathcal{O}_8^V) + d_m \langle P \chi_- \rangle + \frac{d_{m0}}{N_F} \langle P \rangle \langle \chi_- \rangle \\
& \rightarrow d_m \langle P \chi_- \rangle + \frac{d_{m0}}{N_F} \langle P \rangle \langle \chi_- \rangle + \frac{d_m}{M_P^2} \kappa_2^{PA} \mathcal{O}_{12}^A - \frac{2d_{m0}}{N_F} \kappa_2^{PA} \mathcal{O}_{10}^A.
\end{aligned}$$

This completes the elimination of the operators which are bilinear and trilinear in the resonance fields from the Lagrangian $\mathcal{L}_{R\chi T}^{(6, \text{odd})}$.

5. The effective couplings $\overline{\kappa}_i^X$

Putting the results of the previous subsections together, we get the parameters $\overline{\kappa}_i^X$ of the reparametrized and truncated Lagrangian $\mathcal{L}_{R\chi T}^{(6, \text{odd})}$, which is relevant for the saturation of ChPT LECs, as functions of the parameters κ_i^X . As we have discussed above, the LECs have to depend on the couplings κ_i^X of the original Lagrangian $\mathcal{L}_{R\chi T}^{(6, \text{odd})}$ only through their particular combinations $\overline{\kappa}_i^X$. We have proved this by means of direct calculation as a nontrivial check of the formulas (92).

$$\overline{\kappa}_1^V = \kappa_1^V + \frac{c_d}{2M_S^2} \kappa_2^{SV} + \frac{G_V}{\sqrt{2}M_V^2} \kappa_3^{VV} + \frac{G_V}{2\sqrt{2}M_V^2} \kappa_4^{VV},$$

$$\overline{\kappa}_2^V = \kappa_2^V + \frac{c_d}{2M_S^2} \kappa_2^{SV} - \frac{G_V}{2\sqrt{2}M_V^2} \kappa_3^{VV} + \frac{G_V}{2\sqrt{2}M_V^2} \kappa_4^{VV},$$

$$\overline{\kappa}_3^V = \kappa_3^V + \frac{G_V}{2\sqrt{2}M_V^2} \kappa_3^{VV},$$

$$\overline{\kappa}_4^V = \kappa_4^V + \frac{c_m}{M_S^2} \kappa_2^{SV},$$

$$\begin{aligned}
\overline{\kappa}_5^V &= \kappa_5^V - \frac{c_d}{2M_S^2} \left(\kappa_1^{SV} + \frac{F_A}{2\sqrt{2}M_A^2} \kappa^{VAS} \right) \\
& \quad - \frac{F_A}{2\sqrt{2}M_A^2} \kappa_1^{VA} + \frac{G_V}{2\sqrt{2}M_V^2} \kappa_4^{VV},
\end{aligned}$$

$$\overline{\kappa}_6^V = \kappa_6^V - \frac{F_A}{2\sqrt{2}M_A^2} \kappa_3^{VA} - \frac{G_V}{2\sqrt{2}M_V^2} \kappa_3^{VV},$$

$$\begin{aligned}
\overline{\kappa}_7^V &= \kappa_7^V - \frac{F_A}{2\sqrt{2}M_A^2} \kappa_4^{VA} - \frac{c_d}{2M_S^2} \kappa_2^{SV} \\
& \quad - \frac{G_V}{2\sqrt{2}M_V^2} \kappa_3^{VV} - \frac{G_V}{2\sqrt{2}M_V^2} \kappa_4^{VV},
\end{aligned}$$

$$\overline{\kappa}_8^V = \kappa_8^V - \frac{F_A}{2\sqrt{2}M_A^2} \kappa_2^{VA} - \frac{c_d}{2M_S^2} \kappa_2^{SV} + \frac{G_V}{\sqrt{2}M_V^2} \kappa_3^{VV} - \frac{G_V}{2\sqrt{2}M_V^2} \kappa_4^{VV},$$

$$\overline{\kappa}_9^V = \kappa_9^V + \frac{2G_V \kappa_2^{VV}}{\sqrt{2}M_V^2} - \frac{d_m}{2M_P^2} \left(\kappa_1^{PV} - \frac{G_V \kappa^{VVP}}{\sqrt{2}M_V^2} \right) + \frac{G_V}{2\sqrt{2}M_V^2} \kappa_3^{VV},$$

$$\overline{\kappa}_{10}^V = \kappa_{10}^V - \frac{d_m}{2M_P^2} \kappa_2^{PV} - \frac{G_V}{\sqrt{2}M_V^2} \kappa_3^{VV},$$

$$\overline{\kappa}_{11}^V = \kappa_{11}^V + \frac{F_A}{2\sqrt{2}M_A^2} \kappa_5^{VA} + \frac{F_V}{2\sqrt{2}M_V^2} \kappa_3^{VV} - \frac{F_V}{2\sqrt{2}M_V^2} \kappa_4^{VV},$$

RESONANCE SATURATION IN THE ODD-INTRINSIC ...

$$\begin{aligned}\overline{\kappa}_{12}^V &= \kappa_{12}^V + \frac{F_V}{2\sqrt{2}M_V^2} \kappa_3^{VV} + \frac{F_V}{2\sqrt{2}M_V^2} \kappa_4^{VV}, \\ \overline{\kappa}_{13}^V &= \kappa_{13}^V + \frac{d_{m0}}{N_F M_P^2} \left(\kappa_3^{PV} - \frac{F_V \kappa^{VVP}}{2\sqrt{2}M_V^2} \right) - \frac{F_V \kappa_1^{VV}}{\sqrt{2}M_V^2}, \\ \overline{\kappa}_{14}^V &= \kappa_{14}^V - \frac{F_V \kappa_2^{VV}}{\sqrt{2}M_V^2} + \frac{d_m}{2M_P^2} \left(\kappa_3^{PV} - \frac{F_V \kappa^{VVP}}{2\sqrt{2}M_V^2} \right), \\ \overline{\kappa}_{15}^V &= \kappa_{15}^V - \frac{c_m}{2M_S^2} \left(\kappa_1^{SV} + \frac{F_A}{2\sqrt{2}M_A^2} \kappa^{VAS} \right) - \frac{F_A}{2\sqrt{2}M_A^2} \kappa_6^{VA}, \\ \overline{\kappa}_{16}^V &= \kappa_{16}^V - \frac{F_V}{\sqrt{2}M_V^2} \kappa_4^{VV}, \\ \overline{\kappa}_{17}^V &= \kappa_{17}^V + \frac{F_V}{\sqrt{2}M_V^2} \kappa_3^{VV}, \\ \overline{\kappa}_{18}^V &= \kappa_{18}^V - \frac{d_{m0}}{N_F M_P^2} \left(\kappa_1^{PV} + \frac{1}{2} \kappa_2^{PV} - \frac{G_V \kappa^{VVP}}{\sqrt{2}M_V^2} \right) + \frac{2G_V \kappa_1^{VV}}{\sqrt{2}M_V^2}, \\ \overline{\kappa}_1^A &= \kappa_1^A - \frac{c_d}{2M_S^2} \left(\kappa_2^{SA} + \frac{G_V}{\sqrt{2}M_V^2} \kappa^{VAS} \right) \\ &\quad - \frac{G_V}{2\sqrt{2}M_V^2} (2\kappa_1^{VA} + \kappa_2^{VA} + \kappa_3^{VA} - \kappa_4^{VA}), \\ \overline{\kappa}_2^A &= \kappa_2^A + \frac{G_V}{2\sqrt{2}M_V^2} (\kappa_2^{VA} + \kappa_3^{VA} - \kappa_4^{VA}), \\ \overline{\kappa}_3^A &= \kappa_3^A, \\ \overline{\kappa}_4^A &= \kappa_4^A - \frac{c_d}{2M_S^2} \left(\kappa_1^{SA} - \frac{F_V}{2\sqrt{2}M_V^2} \kappa^{VAS} \right) \\ &\quad + \frac{F_V}{2\sqrt{2}M_V^2} \left(\kappa_1^{VA} + \frac{1}{2} \kappa_2^{VA} + \frac{1}{2} \kappa_3^{VA} \right), \\ \overline{\kappa}_5^A &= \kappa_5^A - \frac{F_V}{2\sqrt{2}M_V^2} \kappa_3^{VA} + \frac{G_V}{2\sqrt{2}M_V^2} \kappa_5^{VA}, \\ \overline{\kappa}_6^A &= \kappa_6^A - \frac{F_V}{2\sqrt{2}M_V^2} \kappa_2^{VA} - \frac{G_V}{2\sqrt{2}M_V^2} \kappa_5^{VA}, \\ \overline{\kappa}_7^A &= \kappa_7^A - \frac{F_V}{2\sqrt{2}M_V^2} \kappa_4^{VA}, \\ \overline{\kappa}_8^A &= \kappa_8^A + \frac{F_A \kappa_3^{AA}}{2\sqrt{2}M_A^2} + \frac{F_A \kappa_4^{AA}}{2\sqrt{2}M_A^2},\end{aligned}$$

PHYSICAL REVIEW D **84**, 014036 (2011)

$$\begin{aligned}\overline{\kappa}_9^A &= \kappa_9^A + \frac{d_{m0}}{N_F M_P^2} \left(\kappa_1^{PA} - \frac{F_A \kappa^{AAP}}{2\sqrt{2}M_A^2} \right) - \frac{F_A \kappa_1^{AA}}{\sqrt{2}M_A^2}, \\ \overline{\kappa}_{10}^A &= \kappa_{10}^A - \frac{2d_{m0}}{N_F M_P^2} \kappa_2^A, \\ \overline{\kappa}_{11}^A &= \kappa_{11}^A - \frac{F_A \kappa_2^{AA}}{\sqrt{2}M_A^2} + \frac{d_m}{2M_P^2} \left(\kappa_1^{PA} - \frac{F_A \kappa^{AAP}}{2\sqrt{2}M_A^2} \right), \\ \overline{\kappa}_{12}^A &= \kappa_{12}^A + \frac{d_m}{M_P^2} \kappa_2^{PA}, \\ \overline{\kappa}_{13}^A &= \kappa_{13}^A + \frac{G_V}{\sqrt{2}M_V^2} \kappa_6^{VA} + \frac{c_m}{2M_S^2} \left(\kappa_2^{SA} + \frac{G_V}{\sqrt{2}M_V^2} \kappa^{VAS} \right), \\ \overline{\kappa}_{14}^A &= \kappa_{14}^A + \frac{F_V}{2\sqrt{2}M_V^2} \kappa_6^{VA} - \frac{c_m}{2M_S^2} \left(\kappa_1^{SA} - \frac{F_V}{2\sqrt{2}M_V^2} \kappa^{VAS} \right), \\ \overline{\kappa}_{15}^A &= \kappa_{15}^A - \frac{F_A \kappa_4^{AA}}{\sqrt{2}M_A^2}, \\ \overline{\kappa}_{16}^A &= \kappa_{16}^A + \frac{F_A \kappa_3^{AA}}{\sqrt{2}M_A^2}, \\ \overline{\kappa}_1^S &= \kappa_1^S + \frac{F_A}{2\sqrt{2}M_A^2} \left(\kappa_2^{SA} + \frac{G_V}{\sqrt{2}M_V^2} \kappa^{VAS} \right) \\ &\quad + \frac{G_V}{\sqrt{2}M_V^2} \left(\kappa_1^{SV} + \frac{F_A}{2\sqrt{2}M_A^2} \kappa^{VAS} \right), \\ \overline{\kappa}_2^S &= \kappa_2^S - \frac{F_A}{2\sqrt{2}M_A^2} \left(\kappa_1^{SA} - \frac{F_V}{2\sqrt{2}M_V^2} \kappa^{VAS} \right) \\ &\quad + \frac{F_V}{2\sqrt{2}M_V^2} \left(\kappa_1^{SV} + \frac{F_A}{2\sqrt{2}M_A^2} \kappa^{VAS} \right), \\ \overline{\kappa}_1^P &= \kappa_1^P - \frac{F_A}{2\sqrt{2}M_A^2} \left(\kappa_1^{PA} - \frac{F_A \kappa^{AAP}}{2\sqrt{2}M_A^2} \right), \\ \overline{\kappa}_2^P &= \kappa_2^P + \frac{F_V}{2\sqrt{2}M_V^2} \kappa_2^{PV}, \\ \overline{\kappa}_3^P &= \kappa_3^P - \frac{F_V}{2\sqrt{2}M_V^2} \left(\kappa_1^{PV} - \frac{G_V \kappa^{VVP}}{\sqrt{2}M_V^2} \right) \\ &\quad - \frac{G_V}{\sqrt{2}M_V^2} \left(\kappa_3^{PV} - \frac{F_V \kappa^{VVP}}{2\sqrt{2}M_V^2} \right), \\ \overline{\kappa}_4^P &= \kappa_4^P + \frac{2G_V}{\sqrt{2}M_V^2} \left(\kappa_1^{PV} - \frac{1}{2} \kappa_2^{PV} - \frac{G_V \kappa^{VVP}}{\sqrt{2}M_V^2} \right), \\ \overline{\kappa}_5^P &= \kappa_5^P - \frac{F_V}{2\sqrt{2}M_V^2} \left(\kappa_3^{PV} - \frac{F_V \kappa^{VVP}}{2\sqrt{2}M_V^2} \right).\end{aligned}$$

KAROL KAMPF AND JIŘÍ NOVOTNÝ

PHYSICAL REVIEW D **84**, 014036 (2011)

- [1] S. Weinberg, *Physica A (Amsterdam)* **96**, 327 (1979).
- [2] J. Gasser and H. Leutwyler, *Ann. Phys. (N.Y.)* **158**, 142 (1984).
- [3] J. Gasser and H. Leutwyler, *Nucl. Phys.* **B250**, 465 (1985).
- [4] J. Bijnens, *Prog. Part. Nucl. Phys.* **58**, 521 (2007).
- [5] J. Bijnens, G. Colangelo, and G. Ecker, *J. High Energy Phys.* **02** (1999) 020.
- [6] J. Bijnens, G. Colangelo, and G. Ecker, *Ann. Phys. (N.Y.)* **280**, 100 (2000).
- [7] T. Ebertshäuser, H. W. Fearing, and S. Scherer, *Phys. Rev. D* **65**, 054033 (2002).
- [8] J. Bijnens, L. Girlanda, and P. Talavera, *Eur. Phys. J. C* **23**, 539 (2002).
- [9] J.F. Donoghue and E. Golowich, *Phys. Rev. D* **49**, 1513 (1994).
- [10] M. Davier, L. Girlanda, A. Hocker, and J. Stern, *Phys. Rev. D* **58**, 096014 (1998).
- [11] B. Moussallam, *Phys. Rev. D* **51**, 4939 (1995).
- [12] M. Knecht and A. Nyffeler, *Eur. Phys. J. C* **21**, 659 (2001).
- [13] P. Masjuan and S. Peris, *J. High Energy Phys.* **05** (2007) 040.
- [14] M. Golterman and S. Peris, *Phys. Rev. D* **74**, 096002 (2006).
- [15] G. 't Hooft, *Nucl. Phys.* **B72**, 461 (1974).
- [16] S. Peris, B. Phily, and E. de Rafael, *Phys. Rev. Lett.* **86**, 14 (2001).
- [17] J. Bijnens, E. Gamiz, E. Lipartia, and J. Prades, *J. High Energy Phys.* **04** (2003) 055.
- [18] I. Rosell, P. Ruiz-Femenia, and J. Portoles, *J. High Energy Phys.* **12** (2005) 020.
- [19] I. Rosell, J.J. Sanz-Cillero, and A. Pich, *J. High Energy Phys.* **01** (2007) 039.
- [20] A. Pich, I. Rosell, and J. Sanz-Cillero, *J. High Energy Phys.* **07** (2008) 014.
- [21] I. Rosell, P. Ruiz-Femenia, and J.J. Sanz-Cillero, *Phys. Rev. D* **79**, 076009 (2009).
- [22] A. Pich, I. Rosell, and J.J. Sanz-Cillero, *J. High Energy Phys.* **02** (2011) 109.
- [23] G. Ecker, J. Gasser, A. Pich, and E. de Rafael, *Nucl. Phys.* **B321**, 311 (1989).
- [24] V. Cirigliano *et al.*, *Nucl. Phys.* **B753**, 139 (2006).
- [25] J. Portoles, *AIP Conf. Proc.* **1322**, 178 (2010).
- [26] E. Pallante and R. Petronzio, *Nucl. Phys.* **B396**, 205 (1993).
- [27] J. Prades, *Z. Phys. C* **63**, 491 (1994).
- [28] P.D. Ruiz-Femenia, A. Pich, and J. Portoles, *J. High Energy Phys.* **07** (2003) 003.
- [29] B. Ananthanarayan and B. Moussallam, *J. High Energy Phys.* **05** (2002) 052.
- [30] K. Kampf and B. Moussallam, *Phys. Rev. D* **79**, 076005 (2009).
- [31] S.R. Coleman, J. Wess, and B. Zumino, *Phys. Rev.* **177**, 2239 (1969).
- [32] C.G. Callan, Jr., S.R. Coleman, J. Wess, and B. Zumino, *Phys. Rev.* **177**, 2247 (1969).
- [33] G. Ecker, J. Gasser, H. Leutwyler, A. Pich, and E. de Rafael, *Phys. Lett. B* **223**, 425 (1989).
- [34] K. Kampf, J. Novotny, and J. Trnka, *Eur. Phys. J. C* **50**, 385 (2007).
- [35] K. Kampf, J. Novotny, and J. Trnka, *Phys. Rev. D* **81**, 116004 (2010).
- [36] E. Witten, *Nucl. Phys.* **B223**, 422 (1983).
- [37] J. A. Schouten, *Proc. K. Ned. Akad. Wet.* **41**, 709 (1938).
- [38] V. Mateu and J. Portoles, *Eur. Phys. J. C* **52**, 325 (2007).
- [39] M. Jamin and V. Mateu, *J. High Energy Phys.* **04** (2008) 040.
- [40] A. Nyffeler, *Phys. Rev. D* **79**, 073012 (2009).
- [41] A. Nyffeler, *Proc. Sci.*, CD09 (2009) 080.
- [42] E.R. Arriola and W. Broniowski, *Phys. Rev. D* **81**, 094021 (2010).
- [43] G.P. Lepage and S.J. Brodsky, *Phys. Rev. D* **22**, 2157 (1980).
- [44] S.J. Brodsky and G.P. Lepage, *Phys. Rev. D* **24**, 1808 (1981).
- [45] B. Aubert *et al.* (BABAR Collaboration), *Phys. Rev. D* **80**, 052002 (2009).
- [46] S.S. Agaev, V.M. Braun, N. Offen, and F.A. Porkert, *Phys. Rev. D* **83**, 054020 (2011).
- [47] A.E. Dorokhov, [arXiv:1003.4693](https://arxiv.org/abs/1003.4693).
- [48] K. Kampf and B. Moussallam, *Eur. Phys. J. C* **47**, 723 (2006).
- [49] I. Larin *et al.* (PrimEx), *Phys. Rev. Lett.* **106**, 162303 (2011).
- [50] K. Abe *et al.* (Belle Collaboration), [arXiv:hep-ex/0610022](https://arxiv.org/abs/hep-ex/0610022).
- [51] K. Nakamura *et al.* (Particle Data Group), *J. Phys. G* **37**, 075021 (2010).
- [52] J.F. Donoghue, B.R. Holstein, and Y.C.R. Lin, *Phys. Rev. Lett.* **55**, 2766 (1985).
- [53] J. Bijnens, A. Bramon, and F. Cornet, *Phys. Rev. Lett.* **61**, 1453 (1988).
- [54] J. Bijnens and K. Kampf, *Nucl. Phys. B, Proc. Suppl.* **207–208**, 220 (2010).
- [55] K. Kampf, M. Knecht, J. Novotny, and M. Zdrahal, [arXiv:1103.0982](https://arxiv.org/abs/1103.0982).
- [56] F. Jegerlehner and A. Nyffeler, *Phys. Rep.* **477**, 1 (2009).
- [57] J. Bijnens, E. Pallante, and J. Prades, *Phys. Rev. Lett.* **75**, 1447 (1995).
- [58] J. Bijnens, E. Pallante, and J. Prades, *Nucl. Phys.* **B474**, 379 (1996).
- [59] M. Knecht and A. Nyffeler, *Phys. Rev. D* **65**, 073034 (2002).
- [60] A. Bertin *et al.* (OBELIX Collaboration), *Phys. Lett. B* **414**, 220 (1997).
- [61] T. Gherghetta, J.I. Kapusta, and T.M. Kelley, *Phys. Rev. D* **79**, 076003 (2009).
- [62] L. Cappiello, O. Cata, and G. D'Ambrosio, *Phys. Rev. D* **83**, 093006 (2011).
- [63] S.-Z. Jiang and Q. Wang, *Phys. Rev. D* **81**, 094037 (2010).
- [64] R. Unterdorfer and H. Pichl, *Eur. Phys. J. C* **55**, 273 (2008).
- [65] O. Strandberg, [arXiv:hep-ph/0302064](https://arxiv.org/abs/hep-ph/0302064).
- [66] A.A. Poblaguev *et al.*, *Phys. Rev. Lett.* **89**, 061803 (2002).
- [67] R. Kaiser and H. Leutwyler, *Eur. Phys. J. C* **17**, 623 (2000).
- [68] G.W. Bennett *et al.* (Muon $g - 2$ Collaboration), *Phys. Rev. D* **73**, 072003 (2006).
- [69] The Muon $g - 2$ Experiment at Fermilab, <http://gm2.fnal.gov/>.
- [70] D.T. Son and N. Yamamoto, [arXiv:1010.0718](https://arxiv.org/abs/1010.0718).
- [71] M. Knecht, S. Peris, and E. de Rafael, [arXiv:1101.0706](https://arxiv.org/abs/1101.0706).

2.4 Leading logarithms in the anomalous sector of two-flavour QCD

J. Bijens, K. Kampf and S. Lanz, *Leading logarithms in the anomalous sector of two-flavour QCD*, Nucl. Phys. B **860** (2012) 245 [arXiv:1201.2608 [hep-ph]].

Available online at www.sciencedirect.com**SciVerse ScienceDirect**

Nuclear Physics B 860 (2012) 245–266

**NUCLEAR
PHYSICS B**www.elsevier.com/locate/nuclphysb

Leading logarithms in the anomalous sector of two-flavour QCD

Johan Bijnens^a, Karol Kampf^{b,a}, Stefan Lanz^{a,*}^a *Department of Astronomy and Theoretical Physics, Lund University, Sölvegatan 14A, S 223 62 Lund, Sweden*^b *Institute of Particle and Nuclear Physics, Faculty of Mathematics and Physics, Charles University, 18000 Prague, Czech Republic*

Received 13 January 2012; accepted 23 February 2012

Available online 28 February 2012

Abstract

We add the Wess–Zumino–Witten term to the $N = 3$ massive nonlinear sigma model and study the leading logarithms in the anomalous sector. We obtain the leading logarithms to six loops for $\pi^0 \rightarrow \gamma^* \gamma^*$ and to five loops for $\gamma^* \pi \pi \pi$. In addition we extend the earlier work on the mass and decay constant to six loops and the vector form factor to five loops. We present numerical results for the anomalous processes and the vector form factor. In all cases the series are found to converge rapidly.

© 2012 Elsevier B.V. All rights reserved.

Keywords: Renormalization group evolution of parameters; Spontaneous and radiative symmetry breaking; Chiral Lagrangians; Anomalous processes

1. Introduction

Obtaining exact results in quantum field theory is rather difficult. One of the few things which can be easily calculated to all orders in renormalizable theories are the leading logarithms of the type $(g^2 \log \mu^2)^n$ where μ is the subtraction scale and g the coupling constant. The analogue of this in effective field theories is not so simple since at each order in the expansion new terms in the Lagrangian appear and the recursive argument embedded in the renormalization group equations for renormalizable theories no longer applies. Nonetheless, one can calculate the leading

* Corresponding author.

E-mail address: stefan.lanz@thep.lu.se (S. Lanz).

logarithms in effective field theories using only one-loop calculations. This was suggested at two-loop order by Weinberg [1] and proven to all orders in [2].

In the massless case this has been used to very high orders in [3–5] for meson–meson scattering and form factors. In the massive case, many more terms contribute but in [6,7] a method was developed for handling those, and the leading logarithms in the massive nonlinear sigma model were obtained to five-loop order for the mass, decay constant and the vacuum expectation value and to four-loop order for the vector and scalar form factors and the meson–meson scattering amplitude. A natural continuation of that program is to extend it to other sectors as well. We therefore add to the massive nonlinear sigma model for $N = 3$ the anomalous part via the Wess–Zumino–Witten (WZW) term. This allows us to study the leading logarithms for anomalous processes in two-flavour Chiral Perturbation Theory (ChPT). In addition one can hope that in this sector with its many nonrenormalization theorems it might be easier to guess the all order results when the first terms in the series are known. The WZW term only makes sense for $N = 3$ so we do not work out the results for general N in this case.

We have also improved the programs used in [6,7] so that they now can be used to arbitrarily high orders given enough computing power. So, at least in principle, the problem of the leading logarithms is solved. In practice we obtained one order more than in the earlier work.

The main part of the paper is devoted to the calculations of the leading logarithms (LL) for the two main anomalous processes in the pion sector, the full $\pi^0\gamma^*\gamma^*$ and $\gamma^*\pi\pi\pi$ vertices. For the former we obtained the LL to six loops and for the latter to five. The results indicate that in all cases the chiral expansion converges fast but we did not find a simple all-order conjecture.

The results agree with all known relevant earlier calculations. As an additional check we have used several different parametrizations of the fields.

In Section 2.1 we introduce shortly the massive nonlinear sigma model and in Section 2.2 the two-flavour Wess–Zumino–Witten term. Section 3 contains the discussion of LL in the nonanomalous sector where we present our new results and show some numerical results. Here we also explain briefly the principles of the calculation. More details on the method can be found in [6,7]. Sections 4 and 5 are the main part of this paper. The LL are calculated in Section 4. We did not find a simple all-order conjecture but the LL indicate for example that the nonfactorizable part in $\pi^0\gamma^*\gamma^*$ with both photons off shell should be small. We present numerical results in Section 5. In all cases we find good convergence. Section 6 shortly recapitulates our results. Appendix A contains a dispersive argument to clarify the discrepancy with [4] for the vector form factor.

2. The model

2.1. Massive nonlinear $O(N + 1)/O(N)$ sigma model

The $O(N + 1)/O(N)$ nonlinear sigma model, including external sources, is given by the Lagrangian

$$\mathcal{L}_{n\sigma} = \frac{F^2}{2} D_\mu \Phi^T D^\mu \Phi + F^2 \chi^T \Phi. \quad (1)$$

Φ is a real $N + 1$ vector, $\Phi^T = (\Phi^0 \ \Phi^1 \ \dots \ \Phi^N)$, which satisfies the constraint $\Phi^T \Phi = 1$ and transforms under the fundamental representation of $O(N + 1)$. The covariant derivative is

$$D_\mu \Phi^0 = \partial_\mu \Phi^0 + a_\mu^a \Phi^a,$$

$$D_\mu \Phi^a = \partial_\mu \Phi^a + v_\mu^{ab} \Phi^b - a_\mu^a \Phi^0. \quad (2)$$

The vector sources are antisymmetric, $v_\mu^{ab} = -v_\mu^{ba}$, and correspond to the unbroken group generators. The axial sources a_μ^a correspond to the broken generators. Lower-case Latin indices a, b, \dots run over $1, \dots, N$ in the remainder and are referred to as flavour indices. The mass term $\chi^T \Phi$ contains the scalar, s^0 , and pseudoscalar, p^a , external sources as well as the explicit symmetry breaking term M^2 :

$$\chi^T = ((2Bs^0 + M^2)p^1 \dots p^N). \quad (3)$$

The vacuum condensate

$$\langle \Phi^T \rangle = (1 \ 0 \ \dots \ 0) \quad (4)$$

breaks $O(N+1)$ spontaneously to $O(N)$. We thus have in principle N Goldstone bosons represented by ϕ . The explicit symmetry breaking term, the part containing M^2 , breaks the $O(N+1)$ symmetry to $O(N)$, enforcing the vacuum condensate to be in the direction (4) and gives a mass to the Goldstone bosons which at tree level is exactly M .

This particular model is the same as lowest-order two-flavour ChPT for $N=3$ [8,9] and has been used as a model for strongly interacting Higgs sectors in several scenarios; see, e.g., [10,11].

The terminology for the external sources or fields is taken from two-flavour ChPT. The vector currents for $N=3$ are given by $v^{ab} = -\varepsilon^{abc} v^c$ with ε^{abc} the Levi-Civita tensor. The electromagnetic current at lowest order is associated with v^3 .

We write Φ in terms of a real N -component vector ϕ , which transforms linearly under the unbroken part of the symmetry group $O(N)$. We have made use of five different parametrizations in order to check the validity of our results. They are

$$\begin{aligned} \Phi_1 &= \begin{pmatrix} \sqrt{1 - \frac{\phi^T \phi}{F^2}} \\ \frac{\phi}{F} \end{pmatrix}, & \Phi_2 &= \frac{1}{\sqrt{1 + \frac{\phi^T \phi}{F^2}}} \begin{pmatrix} 1 \\ \frac{\phi}{F} \end{pmatrix}, \\ \Phi_3 &= \begin{pmatrix} 1 - \frac{1}{2} \frac{\phi^T \phi}{F^2} \\ \sqrt{1 - \frac{1}{4} \frac{\phi^T \phi}{F^2}} \frac{\phi}{F} \end{pmatrix}, & \Phi_4 &= \begin{pmatrix} \cos \sqrt{\frac{\phi^T \phi}{F^2}} \\ \sin \sqrt{\frac{\phi^T \phi}{F^2}} \frac{\phi}{\sqrt{\phi^T \phi}} \end{pmatrix}, \\ \Phi_5 &= \frac{1}{1 + \frac{\phi^T \phi}{4F^2}} \begin{pmatrix} 1 - \frac{\phi^T \phi}{4F^2} \\ \frac{\phi}{F} \end{pmatrix}. \end{aligned} \quad (5)$$

Φ_1 is the parametrization used in [8], Φ_2 a simple variation. Φ_3 is such that the explicit symmetry breaking term in (1) only gives a mass term to the ϕ field but no vertices. Φ_4 is the parametrization one ends up with if using the general prescription of [12]. Finally, Φ_5 has been used by Weinberg in, e.g., [1,9]. The reason for using different parametrizations is that for each one of them, the contributions are distributed very differently between the diagrams and obtaining the same result thus provides a thorough check on our calculations.

2.2. *Wess–Zumino–Witten Lagrangian*

For $N=3$, the massive nonlinear $O(N+1)/O(N)$ sigma model corresponds to two-flavour ChPT, which is an effective field theory for QCD. It is well known that the chiral axial current

of the latter is anomalous [13–16], leading to the occurrence of processes such as $\pi^0 \rightarrow \gamma\gamma$ or $\pi\gamma \rightarrow \pi\pi$. The Lagrangian that we have introduced above does, however, not account for this. The necessary interaction terms are contained in the Wess–Zumino–Witten term [17,18], which must be added to the effective Lagrangian. It is constructed such that it reproduces the anomalous Ward identities. Kaiser derived the WZW term for two-flavour ChPT [19], where it is considerably simpler than in the case of three flavours. His result can be re-expressed in terms of the field Φ as

$$\begin{aligned} \mathcal{L}_{\text{WZW}} = & -\frac{N_c}{8\pi^2} \epsilon^{\mu\nu\rho\sigma} \left\{ \epsilon^{abc} \left(\frac{1}{3} \Phi^0 \partial_\mu \Phi^a \partial_\nu \Phi^b \partial_\rho \Phi^c - \partial_\mu \Phi^0 \partial_\nu \Phi^a \partial_\rho \Phi^b \Phi^c \right) v_\sigma^0 \right. \\ & \left. + (\partial_\mu \Phi^0 \Phi^a - \Phi^0 \partial_\mu \Phi^a) v_\nu^a \partial_\rho v_\sigma^0 + \frac{1}{2} \epsilon^{abc} \Phi^0 \Phi^a v_\mu^b v_\nu^c \partial_\rho v_\sigma^0 \right\}. \end{aligned} \quad (6)$$

The interaction with the axial current coming from the WZW term has been omitted. Note that the normalization of the vector field differs from the one used in [19]. The Lagrangian depends on the Levi-Civita tensor ϵ^{abc} in the $SO(3)$ flavour indices. This is an object specific to $N = 3$. There is no obvious simple generalization¹ to different N so for anomalous processes we restrict the calculation to $N = 3$.

The Lagrangian in (6) is of chiral order p^4 implying that anomalous processes are of the same order at leading order, while one-loop corrections are already $\mathcal{O}(p^6)$. This is immediately clear from the presence of the epsilon tensor with four Lorentz indices: each one of them must be combined with either a derivative or an external vector field, both of which are $\mathcal{O}(p)$.

The interaction of the pseudoscalars with the photon field \mathcal{A}_μ can be obtained from the WZW Lagrangian by setting the vector current to

$$v_\mu^0 = \frac{e}{3} \mathcal{A}_\mu, \quad v_\mu^a = e \mathcal{A}_\mu \delta^{a3}. \quad (7)$$

The Lagrangian of (1) has also a symmetry that QCD does not have [18]. The fields under this extra symmetry, called intrinsic parity, transform as

$$\Phi^0 \rightarrow \Phi^0, \quad \Phi^a \rightarrow -\Phi^a, \quad v_\mu^{ab} \rightarrow v_\mu^{ab}, \quad a_\mu^a \rightarrow -a_\mu^a, \quad s \rightarrow s, \quad p \rightarrow -p. \quad (8)$$

The Lagrangian (1) and higher orders are even under this symmetry while (6) is odd.

As in the even sector, we have used several of the parametrizations given in (5). Intrinsic parity for the different ϕ is such that it is always odd, $\phi^a \rightarrow -\phi^a$. The WZW term leads to interactions of one, two, or three photons with an odd number of pions. The anomaly also generates purely mesonic interactions among an odd number of five or more Goldstone bosons. However, for two flavours the purely mesonic odd intrinsic parity processes vanish to all orders.

We use anomalous and odd intrinsic parity as synonyms and refer to the $N = 3$ case here occasionally as the two-flavour case since it corresponds to two light quark flavours.

3. Leading logarithms in the even sector

In this section we recapitulate and extend some results of the even intrinsic parity sector of [6,7]. We focus on those results that will be needed for the later calculations in the anomalous sector.

¹ The generalization to different n for the $SU(n) \times SU(n)/SU(n)$ case is easy but that is a different case than the $O(N+1)/O(N)$ considered here.

The leading dependence on $\log \mu$ at each order, with μ the subtraction scale, is what we call the leading logarithm. It can in principle always be obtained from one-loop calculations as was proven using β -functions in [2] and in a simpler diagrammatic way in [6]. We will discuss some of those results in the sections on the explicit calculation of the mass and $\gamma\pi \rightarrow \pi\pi$.

In effective field theories there is a new Lagrangian at every order. The observation of [6] that the needed parts of those Lagrangians can be generated automatically from the one-loop diagrams allowed to perform the calculations. The actual calculations were performed by using FORM [20] extensively.

We have extended the programs used in [6,7] so that they can in principle run to an arbitrary order.² The only limit is set by computing time, which grows rapidly with the order. The necessary additions include routines that generate the required diagrams at a given order and calculate one-loop diagrams with an arbitrary number of propagators. In this way, we have verified some of the earlier results and obtained the coefficient of one more order for the mass, decay constant and vector form factor.

In effective field theories writing the expansion in terms of lowest order or physical quantities can make quite a big difference in the rate of convergence. We therefore follow [7] in using two different expansions in terms of leading logarithms. A given observable O_{phys} can be written in different ways:

$$O_{\text{phys}} = O_0(1 + a_1 L + a_2 L^2 + \dots), \quad (9)$$

$$O_{\text{phys}} = O_0(1 + c_1 L_{\text{phys}} + c_2 L_{\text{phys}}^2 + \dots), \quad (10)$$

where the chiral logarithms are defined either from the lowest-order parameters M and F as

$$L \equiv \frac{M^2}{16\pi^2 F^2} \log \frac{\mu^2}{M^2}, \quad (11)$$

or from the physical decay constant F_π and mass M_π as

$$L_{\text{phys}} \equiv \frac{M_\pi^2}{16\pi^2 F_\pi^2} \log \frac{\mu^2}{M_\pi^2}. \quad (12)$$

3.1. Mass

In this subsection we will present the first few coefficients a_i and c_i of the expansions in (9) and (10) with $O_{\text{phys}} = M_\pi^2$ and $O_0 = M^2$. In addition, we have also calculated the generic two-point function, which is needed for the wave-function renormalization. We extend the result from [6] by giving the expansion coefficients a_i and c_i also at sixth order.

Let us briefly recapitulate the strategy that is followed to obtain the expansion coefficients. The starting point is the Lagrangian (1) which generates vertices with an arbitrary even number of pion legs. These lowest-order vertices are diagrammatically denoted by $\boxed{0}$ with the corresponding number of legs appended. The zero in this symbol refers to the order in the expansion. If we want to calculate the leading logarithm for the two-point function at one-loop level, we must evaluate the tadpole diagram with one insertion of the leading-order four-pion vertex. Its divergence must be canceled by a counter term from the next order. This can be depicted schematically as

² In [6,7], a different program was used for each diagram with a given number of vertices/propagators and the list of possible diagrams was constructed by hand.

$$\text{Diagram (13)} \quad (13)$$

Also at the next order, divergences must cancel, but the situation is somewhat more complicated. There are two one-loop diagrams from which, using the results of [2,6], the leading divergence can be determined. This thus determines the relevant part of the second-order Lagrangian:

$$\text{Diagram (14)} \quad (14)$$

We already have all information ready in order to calculate the second diagram: the tree-level vertex follows directly from the lowest-order Lagrangian and the next-to-leading-order vertex has been determined in (13). The first diagram, however, contains the next-to-leading-order vertex with four pion legs, which we do not know yet. In order to obtain its divergence, we must calculate two more diagrams:

$$\text{Diagram (15)} \quad (15)$$

The algorithm continues to higher orders in exactly the same way. All the diagrams needed for the two-point function up to third order are shown in [6], Figs. 3–5. The total number of diagrams needed for the mass up to order n is 1, 5, 16, 45, 116, 303, ...

We did not find a simple formula to estimate the total number of diagrams needed. We did find a conjecture, verified up to 12th order, about the number of diagrams needed with only two external legs at each order:

$$\# \text{ two-point diagrams} = \begin{cases} 2^{n-2} + 3 \times 2^{\frac{n-3}{2}} - 1 & \text{for } n \text{ odd,} \\ 2^{n-2} + 2^{\frac{n}{2}} - 1 & \text{for } n \text{ even,} \end{cases} \quad (16)$$

that is: 1, 2, 4, 7, 13, 23, 43, 79, 151, ... diagrams with two external legs at order n .

The coefficients a_i and c_i in the expansion of the physical mass are listed up to sixth order in Tables 1 and 2. The sixth-order results are new. We can use these results to check the expansions and how fast they converge. We chose $F = 0.090$ GeV, $F_\pi = 0.0922$ GeV and $\mu = 0.77$ GeV for the plots presented here in Fig. 1.

3.2. Decay constant

The decay constant F_π is defined by

$$\langle 0 | j_{a,\mu}^b | \phi^c(p) \rangle = i F_\pi p_\mu \delta^{bc}. \quad (17)$$

Table 1

The coefficients a_i of the leading logarithm L^i up to $i = 6$ for the physical meson mass.

i	a_i for $N = 3$	a_i for general N
1	$-1/2$	$1 - 1/2N$
2	$17/8$	$7/4 - 7/4N + 5/8N^2$
3	$-103/24$	$37/12 - 113/24N + 15/4N^2 - N^3$
4	$24367/1152$	$839/144 - 1601/144N + 695/48N^2 - 135/16N^3 + 231/128N^4$
5	$-8821/144$	$33661/2400 - 1151407/43200N + 197587/4320N^2 - 12709/300N^3 + 6271/320N^4 - 7/2N^5$
6	$\frac{1922964667}{6220800}$	$158393809/3888000 - 182792131/2592000N + 1046805817/7776000N^2 - 17241967/103680N^3 + 70046633/576000N^4 - 23775/512N^5 + 7293/1024N^6$

Table 2

The coefficients c_i of the leading logarithm L_{phys}^i up to $i = 6$ for the physical meson mass.

i	c_i for $N = 3$	c_i for general N
1	$-1/2$	$1 - 1/2N$
2	$7/8$	$-1/4 + 3/4N - 1/8N^2$
3	$211/48$	$-5/12 + 7/24N + 5/8N^2 - 1/16N^3$
4	$21547/1152$	$347/144 - 587/144N + 47/24N^2 + 25/48N^3 - 5/128N^4$
5	$179341/2304$	$-6073/1800 + 32351/2400N - 59933/4320N^2 + 224279/43200N^3 + 761/1920N^4 - 7/256N^5$
6	$\frac{2086024177}{6220800}$	$-17467151/3888000 - 10487351/2592000N + 68244763/1944000N^2 - 5630053/172800N^3 + 18673489/1728000N^4 + 583/2560N^5 - 21/1024N^6$

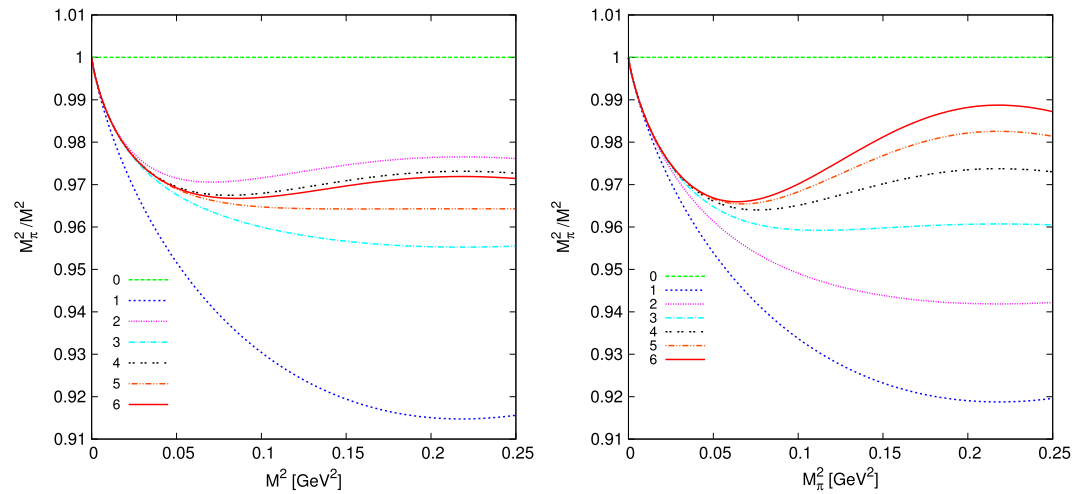


Fig. 1. The contribution of the leading logarithms to M_π^2/M^2 order by order for $F = 0.090$ GeV, $F_\pi = 0.0922$ GeV, $\mu = 0.77$ GeV and $N = 3$. The left panel shows the expansion in L keeping F fixed, the right panel the expansion in L_{phys} keeping F_π fixed.

We thus need to evaluate a matrix-element with one external axial field and one incoming meson. The diagrams needed for the wave function renormalization were already evaluated in the calculation for the mass in the previous subsection. What remains is thus the evaluation of all relevant one-particle-irreducible (1PI) diagrams with an external a_μ^a . At one-loop order there is only a

252

J. Bijnens et al. / Nuclear Physics B 860 (2012) 245–266

Table 3

The coefficients a_i of the leading logarithm L^i for the decay constant F_π in the case $N = 3$ and in the generic N case.

i	a_i for $N = 3$	a_i for general N
1	1	$-1/2 + 1/2N$
2	$-5/4$	$-1/2 + 7/8N - 3/8N^2$
3	$83/24$	$-7/24 + 21/16N - 73/48N^2 + 1/2N^3$
4	$-3013/288$	$47/576 + 1345/864N - 14077/3456N^2 + 625/192N^3 - 105/128N^4$
5	$2060147/51840$	$-23087/64800 + 459413/172800N - 189875/20736N^2 + 546941/43200N^3 - 1169/160N^4 + 3/2N^5$
6	$-\frac{69228787}{466560}$	$-277079063/93312000 + 1680071029/186624000N - 686641633/31104000N^2 + 813791909/20736000N^3 - 128643359/3456000N^4 + 260399/15360N^5 - 3003/1024N^6$

Table 4

The coefficients c_i of the leading logarithm L_{phys}^i for the decay constant F_π in the case $N = 3$ and in the generic N case.

i	c_i for $N = 3$	c_i for general N
1	1	$-1/2 + 1/2N$
2	$5/4$	$1/2 - 7/8N + 3/8N^2$
3	$13/12$	$-1/24 + 13/16N - 13/12N^2 + 5/16N^3$
4	$-577/288$	$-913/576 + 2155/864N - 361/3456N^2 - 69/64N^3 + 35/128N^4$
5	$-14137/810$	$535901/129600 - 2279287/172800N + 273721/20736N^2 - 11559/3200N^3 - 997/1280N^4 + 63/256N^5$
6	$-\frac{37737751}{466560}$	$-112614143/93312000 + 3994826029/186624000N - 1520726023/31104000N^2 + 276971363/6912000N^3 - 39882839/3456000N^4 - 979/15360N^5 + 231/1024N^6$

single diagram, but at higher orders, we must calculate 2, 4, 7, 13, 23, ... diagrams, not counting the auxiliary diagrams required for the renormalization of higher-order vertices with more than two legs. We do not show these diagrams here, but they can be found up to third order in [7]. The total number of diagrams with an axial current that needs to be calculated for the decay constant to order n is 1, 5, 18, 56, 169, 511, ...

We give the coefficients for both leading logarithm series with $O_{\text{phys}} = F_\pi$ and $O_0 = F$ in Tables 3 and 4. The sixth order is again a new result. Note that once the expression of F_π as a function of F is known one may express the remaining observables as a function of the physical M_π^2 and F_π . This has already been used to calculate the coefficients c_i in Tables 2 and 4 from the corresponding a_i .

We have plotted in Fig. 2 the expansion in terms of the unrenormalized quantities and in terms of the physical quantities. In both cases we get a good convergence but it is excellent for the expansion in physical quantities.

3.3. Vector form factor

Before we proceed to the discussion of anomalous processes, we turn to the last ingredient from the even intrinsic parity sector which will be used later: the vertex involving a single photon and an even number of pions. It is directly connected to the vector form factor, which is defined by

$$\langle \phi^a(p_f) | j_{V,\mu}^{cd} - j_{V,\mu}^{dc} | \phi^b(p_i) \rangle = (\delta^{ac}\delta^{db} - \delta^{ad}\delta^{bc}) i(p_f + p_i)_\mu F_V [(p_f - p_i)^2]. \quad (18)$$

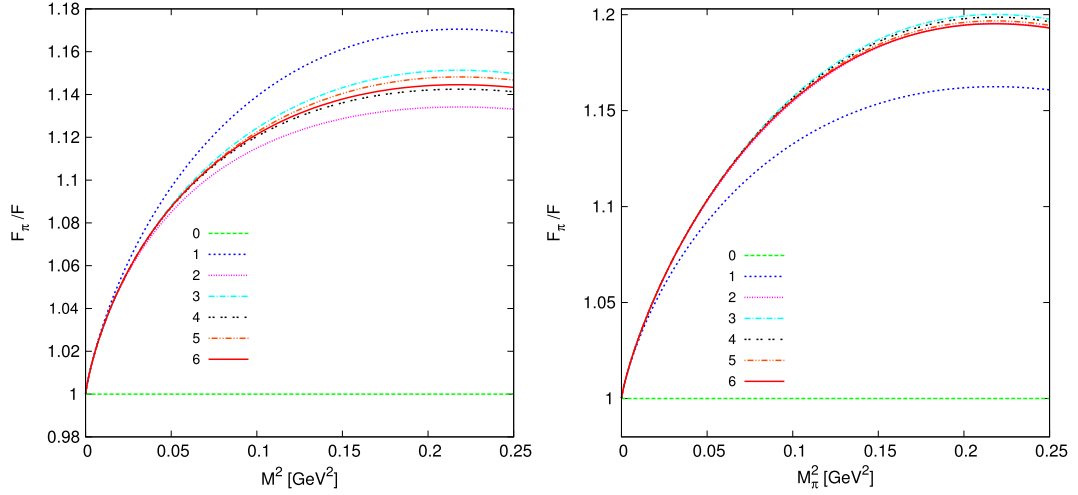


Fig. 2. The contribution of the leading logarithms to F_π/F order by order for $\mu = 0.77$ GeV and $N = 3$. The left panel shows the expansion in L with $F = 0.090$ GeV fixed, the right panel the expansion in L_{phys} with $F_\pi = 0.0922$ MeV fixed.

The procedure to find the leading logarithm for this observable follows the lines of the one for the decay constant. For the wave function renormalization one may again use the results obtained in the mass calculation. We express here the results in terms of $\tilde{t} = t/M_\pi^2$ and

$$L_{\mathcal{M}} = \frac{M_\pi^2}{16\pi^2 F_\pi^2} \log \frac{\mu^2}{\mathcal{M}^2} \quad (19)$$

with a scale \mathcal{M}^2 that is some combination of t and M_π^2 . Again we have added one more order compared to the result in [7]. To fifth order we find

$$\begin{aligned} F_V(t) = & 1 + L_{\mathcal{M}}[1/6\tilde{t}] + L_{\mathcal{M}}^2[\tilde{t}(-11/12 + 5/12N) + \tilde{t}^2(5/36 - 1/24N)] \\ & + L_{\mathcal{M}}^3[\tilde{t}(+1387/648 - 845/324N + 7/9N^2) \\ & + \tilde{t}^2(-4007/6480 + 3521/6480N - 29/180N^2) \\ & + \tilde{t}^3(+721/12960 - 47/1440N + 1/80N^2)] \\ & + L_{\mathcal{M}}^4[\tilde{t}(-44249/15552 + 222085/31104N \\ & - 55063/10368N^2 + 127/96N^3) \\ & + \tilde{t}^2(+349403/155520 - 15139/4860N + 86719/51840N^2 - 199/480N^3) \\ & + \tilde{t}^3(-85141/155520 + 885319/1555200N - 5303/19200N^2 + 21/320N^3) \\ & + \tilde{t}^4(+4429/103680 - 57451/1555200N + 289/14400N^2 - 1/240N^3)] \\ & + L_{\mathcal{M}}^5[\tilde{t}(-2278099/777600 - 2377637/466560N \\ & + 64763783/4665600N^2 - 178063/19200N^3 + 69/32N^4) \\ & + \tilde{t}^2(-62212433/11664000 + 27685279/2332800N \\ & - 376597697/38880000N^2 + 53519593/12960000N^3 - 361/400N^4) \\ & + \tilde{t}^3(74033879/30240000 - 2247054421/544320000N \end{aligned}$$

$$\begin{aligned}
& + 32\,125\,153/11\,340\,000N^2 - 13\,264\,877/12\,096\,000N^3 + 1209/5600N^4) \\
& + \tilde{t}^4(-299\,603\,257/816\,480\,000 + 213\,192\,107/408\,240\,000N \\
& - 98\,330\,371/272\,160\,000N^2 + 546\,331/3\,780\,000N^3 - 233/8400N^4) \\
& + \tilde{t}^5(3\,090\,331/163\,296\,000 - 36\,097\,349/1\,632\,960\,000N \\
& + 28\,441\,883/1\,632\,960\,000N^2 - 15\,971/2\,268\,000N^3 + 1/672N^4)]. \quad (20)
\end{aligned}$$

Note that $F_V(0) = 1$ as it should be.

The vector form factor was also calculated in the massless case in [4]. In order to transform our result into this limit, we define

$$K_t \equiv \frac{t}{16\pi^2 F^2} \log\left(-\frac{\mu^2}{t}\right). \quad (21)$$

Replacing $\mathcal{M}^2 \rightarrow t$ and then performing the limit $M_\pi^2 \rightarrow 0$ (which implies $F_\pi \rightarrow F$), we get

$$\begin{aligned}
F_V^0(t) &= 1 + K_t/6 + K_t^2(5/36 - N/24) \\
& + K_t^3(721/12\,960 - 47/1440N + N^2/80) \\
& + K_t^4(4429/103\,680 - 57\,451/1\,555\,200N + 289/14\,400N^2 - N^3/240) \\
& + K_t^5(3\,090\,331/163\,296\,000 - 36\,097\,349/1\,632\,960\,000N \\
& + 28\,441\,883/1\,632\,960\,000N^2 - 15\,971/2\,268\,000N^3 + N^4/672). \quad (22)
\end{aligned}$$

This differs from the result of [4]. The difference is discussed in Appendix A using a dispersive approach as an alternative check, which agrees with [7] and (22). Up to the given order, the coefficient of the highest power in N in (22) at each order is of the form

$$f_V^n = \frac{(-1)^{n-1}}{(n+1)(n+2)} \left(\frac{N}{2}\right)^{n-1}, \quad (23)$$

such that, assuming this representation of f_V^n to be valid also at higher orders, we can write

$$F_V^0(t) = 1 + \sum_{n=1}^{\infty} f_V^n K_t^n (1 + O(1/N)). \quad (24)$$

The summation can be performed explicitly and we obtain the next-to-large N result in the chiral limit in a closed form:

$$F_V^{0NLN}(t) = 1 + \frac{1}{N} + \frac{4}{K_t N^2} \left[1 - \left(1 + \frac{2}{K_t N} \right) \log\left(1 + \frac{K_t N}{2} \right) \right]. \quad (25)$$

These large N formulas are also present in [4] up to a sign mistake. In that article, the large N has been explicitly calculated to all orders.

We close this section with giving the expansion for the radius and curvature of the vector form factor defined by

$$F_V(t) = 1 + \frac{1}{6} \langle r^2 \rangle_V t + c_V t^2 + \dots \quad (26)$$

The coefficients c_i for the expansion in physical quantities are given in Tables 5 and 6 in units of M_π^2 , again adding one order compared to [7]. The result up to two-loop order agrees with the

Table 5

The coefficients c_i of the leading logarithm L_{phys} in the expansion of the radius $\langle r^2 \rangle_V$ in the case $N = 3$ and for general N .

i	c_i for $N = 3$	c_i for general N
1	1	1
2	2	$-11/2 + 5/2N$
3	853/108	$1387/108 - 845/54N + 14/3N^2$
4	50513/1296	$-44\,249/2592 + 222\,085/5184N - 55\,063/1728N^2 + 127/16N^3$
5	120401/648	$-2\,278\,099/129\,600 - 2\,377\,637/77\,760N + 64\,763\,783/777\,600N^2 - 178\,063/3200N^3 + 207/16N^4$

Table 6

The coefficients c_i of the leading logarithm L_{phys} in the expansion of the curvature c_V in the case $N = 3$ and for general N .

i	c_i for $N = 3$	c_i for general N
1	0	0
2	1/72	$5/36 - 1/24N$
3	-71/162	$-4007/6480 + 3521/6480N - 29/180N^2$
4	-25169/7776	$349\,403/155\,520 - 15\,139/4860N + 86\,719/51\,840N^2 - 199/480N^3$
5	-1349303/72900	$-62\,212\,433/11\,664\,000 + 27\,685\,279/2\,332\,800N - 376\,597\,697/38\,880\,000N^2 + 53\,519\,593/12\,960\,000N^3 - 361/400N^4$

LL extracted from the full two-loop calculation [21]. We do not present numerical results for the vector form factor since these are dominated in the physical case $N = 3$ by the large higher-order coefficient contributions, see, e.g., [8,21].

4. Leading logarithms in the anomalous sector

4.1. $\pi\gamma \rightarrow \pi\pi$

The process $\pi^0\gamma \rightarrow \pi^0\pi^0$ is forbidden by C -symmetry and we will therefore concentrate on $\pi^-\gamma \rightarrow \pi^-\pi^0$. The latter can be represented by the anomalous VAAA quadrangle diagram at quark level. We follow the notation introduced in [22] where the one-loop order was calculated. At tree-level, the amplitude for $\pi^-(p_1)\gamma(k) \rightarrow \pi^-(p_2)\pi^0(p_0)$ can be obtained from the Wess–Zumino–Witten Lagrangian (6):

$$A_0 = \frac{ie}{4\pi^2 F^3} \epsilon_{\mu\nu\alpha\beta} \epsilon^\mu(k) p_1^\nu p_2^\alpha p_0^\beta. \quad (27)$$

For higher orders we express the results in terms of physical variables only as

$$A = i F^{3\pi}(s, t, u) \epsilon_{\mu\nu\alpha\beta} \epsilon^\mu(k) p_1^\nu p_2^\alpha p_0^\beta, \quad (28)$$

with the Mandelstam variables

$$s = (p_1 + k)^2, \quad t = (p_1 - p_2)^2, \quad u = (p_1 - p_0)^2, \quad s + t + u = 3M_\pi^2 + k^2. \quad (29)$$

The function $F^{3\pi}(s, t, u)$ for $\gamma\pi \rightarrow \pi\pi$ is fully symmetric in s, t, u . We write it in terms of F_π as

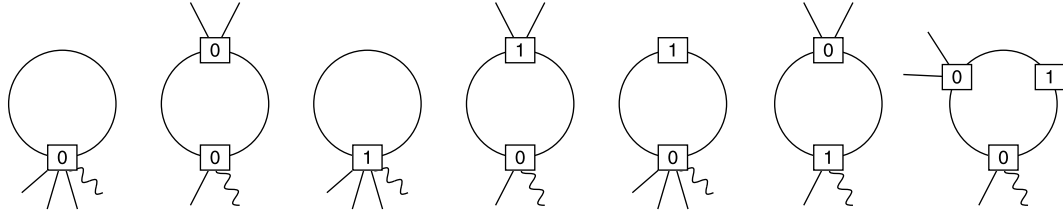


Fig. 3. The irreducible diagrams for the process $\pi\gamma \rightarrow \pi\pi$ up to two-loop level. The first two diagrams are the one-loop level.

$$F^{3\pi}(s, t, u) = F_0^{3\pi} f(s, t, u), \quad F_0^{3\pi} = \frac{e}{4\pi^2 F_\pi^3}. \quad (30)$$

If one expands $f(s, t, u)$ as a polynomial in s, t, u one can use the relation in (29) to see how many new independent kinematical quantities can appear at each order. Up to fifth order in s, t, u there is only one at each order. At sixth order there are two. For the first five orders we choose as independent quantities³

$$\Delta_n = s^n + t^n + u^n. \quad (31)$$

We also define $\tilde{k}^2 = k^2/M_\pi^2$ and $\tilde{\Delta}_n = \Delta_n/M_\pi^{2n}$. In the end we write $f(s, t, u)$ in terms of $\tilde{k}^2, M_\pi^2, \tilde{\Delta}_2, \dots, \tilde{\Delta}_5$.

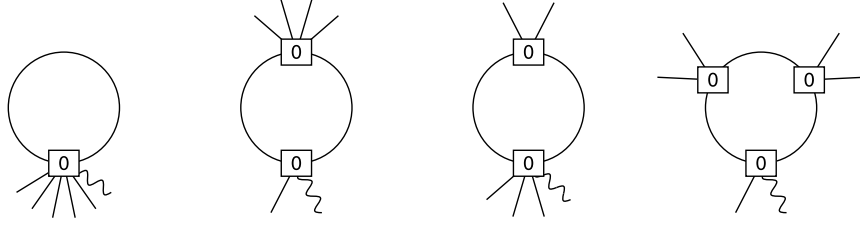
The main focus of this article is calculating the leading logarithms in the anomalous sector. The procedure follows very similar steps as in the even sector. From the even sector we will need the wave function renormalization and the expressions for the higher-order purely mesonic vertices as well as the decay constant and mass when using an expansion in terms of physical quantities. Vertices coupling an even number of pions to a single photon are not needed at this point, because the two-flavour anomaly does not contain interaction terms involving an odd number of pions and no photon. What remains to be calculated are the irreducible diagrams with three external pions and one external photon. The required diagrams up to two-loop order are depicted in Fig. 3. As in Section 3, a box with n inside, \boxed{n} , means a vertex of order n . To reach the one-loop level, we must calculate the first two of these diagrams. Inspection of the remaining diagrams for the two-loop level shows that all vertices are already known except the one with five pions and one photon in the third diagram. The diagrams that are needed in order to obtain its divergence are shown in Fig. 4. Note that the vertex with three pions and one photon in the sixth diagram of Fig. 3 is fixed by the one-loop calculation, the first two diagrams in the same figure.

To go to higher orders we rapidly need vertices with many more legs. We have generated all diagrams needed and calculated them up to fifth order. We agree with the logarithm determined from the full one-loop result [22]. The results were obtained in several different parametrizations with consistent results.

We have calculated the amplitude for $\pi^- \gamma \rightarrow \pi^- \pi^0$ up to five-loop level. In the general case, i.e., for $k^2, M_\pi^2 \neq 0$, we obtain

$$f^{LL}(s, t, u) = 1 + L\mathcal{M} \frac{1}{6} (3 + \tilde{k}^2) + L^2\mathcal{M} \frac{1}{72} (\tilde{k}^2 - 3)(\tilde{k}^2 + 33)$$

³ The same arguments can be applied to any process fully symmetric in s, t , and u . A prominent example is $\eta \rightarrow 3\pi^0$, where $s + t + u = 3M_\pi^2 + M_\eta^2$.

Fig. 4. The irreducible (auxiliary) diagrams needed for the vertex $5\pi\gamma$ up to one-loop level.

$$\begin{aligned}
& + L_{\mathcal{M}}^3 \frac{1}{1296} (90\tilde{\Delta}_3 - 640\tilde{\Delta}_2 - 8157 + 2105\tilde{k}^2 + 81\tilde{k}^4 + \tilde{k}^6) \\
& + L_{\mathcal{M}}^4 \frac{1}{155\,520} [-1532\tilde{\Delta}_4 + \tilde{\Delta}_3(88\,538 + 1890\tilde{k}^2) \\
& - \tilde{\Delta}_2(577\,760 + 12\,240\tilde{k}^2 + 540\tilde{k}^4) \\
& - 2\,433\,375 + 1\,296\,190\tilde{k}^2 + 57\,430\tilde{k}^4 + 480\tilde{k}^6 + 185\tilde{k}^8] \\
& + L_{\mathcal{M}}^5 \frac{1}{326\,592\,000} [\tilde{\Delta}_5 13\,252\,156 - \tilde{\Delta}_4(160\,744\,570 + 518\,350\tilde{k}^2) \\
& + \tilde{\Delta}_3(1\,465\,187\,530 + 39\,593\,272\tilde{k}^2 + 247\,260\tilde{k}^4) \\
& - \tilde{\Delta}_2(6\,756\,522\,937 + 257\,781\,206\tilde{k}^2 + 11\,188\,776\tilde{k}^4 - 9160\tilde{k}^6) \\
& - 6\,498\,695\,163 + 12\,675\,091\,794\tilde{k}^2 + 801\,259\,373\tilde{k}^4 + 4\,780\,240\tilde{k}^6 \\
& + 2\,948\,600\tilde{k}^8 - 1832\tilde{k}^{10}]. \tag{32}
\end{aligned}$$

The symmetry in s , t and u is obvious in this expression. Note that at second order $\tilde{\Delta}_2$ does not appear even though it could be present a priori.

We can check whether we find a simpler expression in the massless limit and for an on-shell photon, $k^2 = 0$. In this case we need to express the result in terms of the logarithm

$$L_{\Delta} = \frac{1}{16\pi^2 F^2} \log\left(\frac{\mu^2}{\hat{\Delta}}\right), \tag{33}$$

where $\hat{\Delta}$ is some combination of s , t , and u :

$$f^{LL0}(s, t, u) = 1 + \frac{5}{72} \Delta_3 L_{\Delta}^3 - \frac{383}{19\,440} \Delta_4 L_{\Delta}^4 + \frac{3\,313\,039}{81\,648\,000} \Delta_5 L_{\Delta}^5. \tag{34}$$

It is clear from symmetry considerations that there should be no term linear in L_{Δ} . We do however not know why the quadratic term is also absent.

4.2. $\pi^0 \rightarrow \gamma\gamma$

This is the most important process in the odd-intrinsic parity sector of QCD, since it is the process in which the chiral anomaly was discovered. It remains the main experimental test thereof.

We started our discussion of anomalous processes with $\pi\gamma \rightarrow \pi\pi$ because the leading logarithms for this process could be calculated from our results in the even intrinsic parity sector and just one type of anomalous vertex.

We define the reduced amplitude $F_{\pi\gamma\gamma}$ for $\pi^0 \rightarrow \gamma(k_1)\gamma(k_2)$

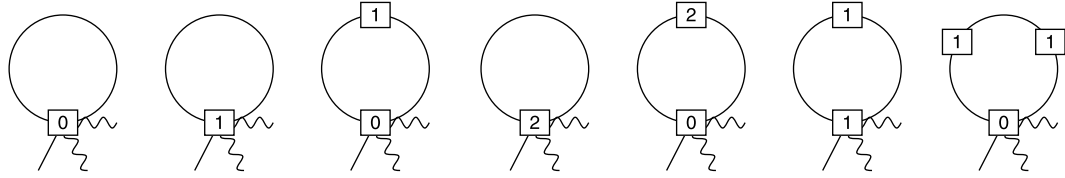


Fig. 5. First type of the irreducible diagrams contributing to $\pi^0 \rightarrow \gamma\gamma$ up to three-loop order.

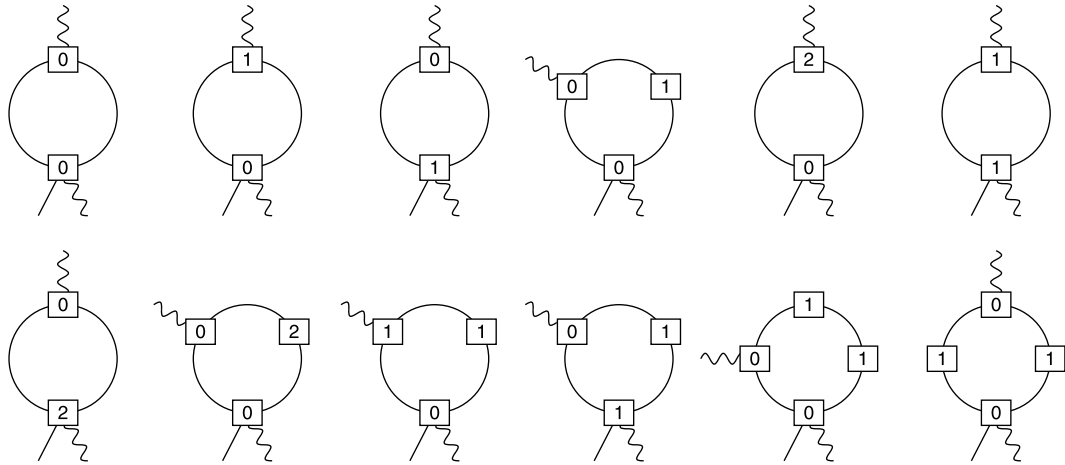


Fig. 6. Second type of the irreducible diagrams contributing to $\pi^0 \rightarrow \gamma\gamma$ up to three-loop order.

$$A = \epsilon_{\mu\nu\alpha\beta} \varepsilon_1^{*\mu}(k_1) \varepsilon_2^{*\nu}(k_2) k_1^\alpha k_2^\beta F_{\pi\gamma\gamma}(k_1^2, k_2^2). \quad (35)$$

$F_{\pi\gamma\gamma}(k_1^2, k_2^2)$ is symmetric under the interchange of the two photons.

The irreducible diagrams contributing to $\pi^0 \rightarrow \gamma\gamma$ consist of two different types of one-loop diagrams. The first type contains the diagrams where both photons are attached to the *same* vertex, while in the diagrams of the second type, the two photons connect to two different vertices, only one of which is anomalous. We show here the diagrams needed for the calculation of the leading logarithms up to third order. Those of the first type are depicted in Fig. 5. There is one diagram at one-loop order, there are two at two-loop order, and four at three-loop order. The diagrams of the second type are depicted in Fig. 6. This time, there is one diagram at one-loop order, there are three at two-loop, and eight at three-loop order. The figures do not contain the auxiliary diagrams that are needed in order to determine the higher-order vertices with more than one pion leg. We only mention that up to three-loop order, one needs to calculate 11 and 23 diagrams for the first and second type of topologies, respectively.

The first type of diagrams is a consistent subset if we only keep the terms with two vector sources in the Lagrangian (6). That this leads to identical results for several different parametrizations provides a thorough check on the correctness of our programs for this class of diagrams separately.

We write the result with $\tilde{k}_i^2 = k_i^2/M_\pi^2$ in the form

$$F_{\pi\gamma\gamma}(k_1^2, k_2^2) = \frac{e^2}{4\pi^2 F_\pi} F_\gamma(k_1^2) F_\gamma(k_2^2) F_{\gamma\gamma}(k_1^2, k_2^2) \hat{F}. \quad (36)$$

The functions $F_\gamma(k_i^2)$ and $F_{\gamma\gamma}(k_1^2, k_2^2)$ are defined to be equal to one for $k_i^2 = 0$. $F_{\gamma\gamma}(k_1^2, k_2^2)$ contains only those parts that cannot be absorbed in the F_γ and thus gives the part that cannot be obtained as a product of single photon form factors. Finally \hat{F} gives the corrections for the on-shell decay $\pi^0 \rightarrow \gamma\gamma$.

We have calculated all contributions needed for the LLs up to six-loop order and obtained

$$\begin{aligned}
\hat{F} &= 1 - 1/6L_{\mathcal{M}}^2 + 5/6L_{\mathcal{M}}^3 + 56\,147/7776L_{\mathcal{M}}^4 + 446\,502\,199/11\,664\,000L_{\mathcal{M}}^5 \\
&\quad + 65\,694\,012\,997/367\,416\,000L_{\mathcal{M}}^6, \\
F_\gamma(k^2) &= 1 + L_{\mathcal{M}}(1/6\tilde{k}^2) + L_{\mathcal{M}}^2(5/24\tilde{k}^2 + 1/72\tilde{k}^4) \\
&\quad + L_{\mathcal{M}}^3(71/432\tilde{k}^2 + 1/24\tilde{k}^4 + 1/1296\tilde{k}^6) \\
&\quad + L_{\mathcal{M}}^4(-24\,353/31\,104\tilde{k}^2 + 4873/10\,368\tilde{k}^4 \\
&\quad - 2357/31\,104\tilde{k}^6 + 145/31\,104\tilde{k}^8) \\
&\quad + L_{\mathcal{M}}^5(-548\,440\,741/81\,648\,000\tilde{k}^2 + 9\,793\,363/3\,024\,000\tilde{k}^4 \\
&\quad - 32\,952\,389/54\,432\,000\tilde{k}^6 + 487\,493/13\,608\,000\tilde{k}^8 - 2069/10\,886\,400\tilde{k}^{10}) \\
&\quad + L_{\mathcal{M}}^6(-3\,519\,465\,627\,493/102\,876\,480\,000\tilde{k}^2 \\
&\quad + 3\,560\,724\,235\,307/205\,752\,960\,000\tilde{k}^4 \\
&\quad - 1\,524\,042\,680\,197/411\,505\,920\,000\tilde{k}^6 \\
&\quad + 4\,741\,599\,089/11\,757\,312\,000\tilde{k}^8 - 510\,932\,327/13\,716\,864\,000\tilde{k}^{10} \\
&\quad + 1\,775\,869/914\,457\,600\tilde{k}^{12}), \\
F_{\gamma\gamma}(k_1^2, k_2^2) &= 1 + L_{\mathcal{M}}^3\tilde{k}_1^2\tilde{k}_2^2\frac{1}{72} \\
&\quad + L_{\mathcal{M}}^4\tilde{k}_1^2\tilde{k}_2^2[-203/7776 + 29/10\,368(\tilde{k}_1^2 + \tilde{k}_2^2) \\
&\quad + 1/216(\tilde{k}_1^4 + \tilde{k}_2^4) - 1/144\tilde{k}_1^2\tilde{k}_2^2] \\
&\quad + L_{\mathcal{M}}^5\tilde{k}_1^2\tilde{k}_2^2[-5\,983\,633/10\,206\,000 + 46\,103/1\,632\,960(\tilde{k}_1^2 + \tilde{k}_2^2) \\
&\quad + 372\,113/11\,664\,000(\tilde{k}_1^4 + \tilde{k}_2^4) - 211/5\,443\,200(\tilde{k}_1^6 + \tilde{k}_2^6) \\
&\quad - 394\,157/9\,072\,000\tilde{k}_1^2\tilde{k}_2^2 - 4/25\,515\tilde{k}_1^2\tilde{k}_2^2(\tilde{k}_1^2 + \tilde{k}_2^2)] \\
&\quad + L_{\mathcal{M}}^6\tilde{k}_1^2\tilde{k}_2^2[-1\,072\,421\,939\,773/205\,752\,960\,000 \\
&\quad + 1\,444\,445\,383/6\,531\,840\,000(\tilde{k}_1^2 + \tilde{k}_2^2) \\
&\quad + 10\,840\,553\,807/102\,876\,480\,000(\tilde{k}_1^4 + \tilde{k}_2^4) \\
&\quad + 282\,016\,297/205\,752\,960\,000(\tilde{k}_1^6 + \tilde{k}_2^6) \\
&\quad + 6\,157\,391/4\,115\,059\,200(\tilde{k}_1^8 + \tilde{k}_2^8) \\
&\quad - 3\,852\,620\,057/29\,393\,280\,000\tilde{k}_1^2\tilde{k}_2^2 - 154\,739/58\,320\,000\tilde{k}_1^2\tilde{k}_2^2(\tilde{k}_1^2 + \tilde{k}_2^2) \\
&\quad - 75\,041\,473/20\,575\,296\,000\tilde{k}_1^2\tilde{k}_2^2(\tilde{k}_1^4 + \tilde{k}_2^4) \\
&\quad + 174\,329/35\,721\,000\tilde{k}_1^4\tilde{k}_2^4]. \tag{37}
\end{aligned}$$

The absence of the linear term in \hat{F} agrees with the statement from [23,24] that the contribution from one-loop diagrams at NLO can be absorbed into F_π . The quadratic term also coincides

with the two-loop calculation of [25] and the complete one-loop expression for off-shell photons is the same as in [24].

Note that the nonfactorizable contribution $F_{\gamma\gamma}$ only starts at three-loop order and that the part surviving in the chiral limit only starts at four-loop level. The leading logarithms thus predict this part to be fairly small.

The lowest-order results for the two anomalous processes are connected via the current algebra relation [26,27]

$$F^{3\pi}(0, 0, 0) = \frac{1}{eF_\pi^2} F_{\pi\gamma\gamma}(0, 0), \quad (38)$$

which holds exactly in the chiral limit. Even beyond this limit it is valid also at the one-loop level for the leading logarithms as can be seen by comparing (32) and (37). The current algebra relation remains true, if in both amplitudes one of the photons is allowed to be off-shell, i.e.

$$F^{3\pi}(s, t, u)|_{s+t+u=3M_\pi^2+k^2} = \frac{1}{eF_\pi^2} F_{\pi\gamma\gamma}(k^2, 0). \quad (39)$$

It turns out that in the chiral limit, this relation holds for the leading logarithms up to two loops, as can again be checked from (32) and (37).

5. Phenomenology of the anomalous sector

5.1. $\pi\gamma \rightarrow \pi\pi$

The only direct measurement of the $\pi\gamma \rightarrow \pi\pi$ vertex has been performed at the IHEP accelerator in Serpukhov [28] using $\pi^-\gamma \rightarrow \pi^-\pi^0$, where the γ comes from the electromagnetic field of a nucleus via the Primakoff effect. The relevant cross-section was measured with a pion beam of $E = 40$ GeV and the photons' virtuality was in the region $k^2 < 2 \times 10^{-3}$ GeV², which can be neglected at the present precision. The analysis is for values of $s < 10M_\pi^2$ and thus within the region where ChPT is applicable. Assuming the function $F^{3\pi}(s, t, u)$ of (30) to be approximately constant, $F^{3\pi}(s, t, u) \approx \bar{F}^{3\pi}$, they find

$$\bar{F}_{\text{exp}}^{3\pi} = 12.9 \pm 0.9 \pm 0.5 \text{ GeV}^{-3}. \quad (40)$$

Another derivation used the data on $\pi^-e^- \rightarrow \pi^-e^-\pi^0$ [29] to determine $F_0^{3\pi}$ [30]. They obtained

$$F_{0,\text{exp}}^{3\pi} = 9.9 \pm 1.1 \text{ GeV}^{-3} \quad \text{or} \quad 9.6 \pm 1.1 \text{ GeV}^{-3}, \quad (41)$$

depending on the way electromagnetic corrections are included.

The value in (40) needs to be corrected for extrapolation to the point $s = t = u = 0$. The one-loop ChPT corrections were evaluated in [22] and a possibly large electromagnetic correction identified in [31]. The main conclusion is that the experimental values are in fairly good agreement with the theoretical result of (30) which gives $F_0^{3\pi} = 9.8 \text{ GeV}^{-3}$ as discussed further below.

The comparison with [28] goes via their result $\sigma/Z^2 = 1.63 \pm 0.23 \pm 0.13$ nb and [28,31]

$$\frac{\sigma}{Z^2} = \frac{\alpha}{\pi} \int_{4M_\pi^2}^{10M_\pi^2} ds \left(\ln \frac{q_{\text{max}}^2}{q_{\text{min}}^2} + \frac{q_{\text{min}}^2}{q_{\text{max}}^2} - 1 \right) \frac{\sigma_{\gamma\pi \rightarrow \pi\pi}}{s - M_\pi^2},$$

Table 7

The extraction of the anomalous $\gamma 3\pi$ factor $F_0^{3\pi}$ (in GeV^{-3}) from experiment using various estimates of the higher-order corrections. LO includes no higher-order corrections and thus coincides with (40). The next column contains the QED correction f_0^{EM} . Then come the values including in addition the leading logarithm and the complete correction from f_1^{loop} . The last three columns also contain f_1^{tree} using the model estimates in (47).

	LO	f_0^{EM}	f_1^{loop} (LL)	f_1^{loop}	f_1^{tree} (HLS)	f_1^{tree} (CQM)	f_1^{tree} (SDE)
$F_0^{3\pi}$	12.9	12.3	12.0	11.9	11.4	10.1	12.0

$$\sigma_{\gamma\pi\rightarrow\pi\pi} = \frac{1}{1024\pi} s(s - M_\pi^2) \left(1 - \frac{4M_\pi^2}{s}\right)^{3/2} \int_0^\pi d\theta \sin^3 \theta |F_0^{3\pi} f(s, t, u)|^2. \quad (42)$$

Inserting the charged pion mass, $q_{\text{max}}^2 = 2 \cdot 10^{-3} \text{ GeV}^2$, $q_{\text{min}}^2 = ((s - M_\pi^2)/(2E))^2$, and $f(s, t, u) = 1$ in (42) leads to the value in (40).

The various known higher-order corrections can now be included via $f(s, t, u)$:

$$f(s, t, u) = 1 + f_0^{\text{EM}} + f_1^{\text{loop}} + f_1^{\text{tree}} + \dots \quad (43)$$

The dependence on s, t, u is tacitly assumed for all functions f_i . The index i refers to the \hbar order. The leading-order electromagnetic correction f_0^{EM} was determined in [31] as $f_0^{\text{EM}} = -2e^2 F_\pi^2/t$ and higher-order electromagnetic corrections were found to be small. The next-to-leading-order correction coming from one-loop graphs is, in the isospin limit, given by [22]

$$f_1^{\text{loop}} = \frac{1}{6F_\pi^2} \left[-\frac{M_\pi^2}{(4\pi)^2} \left(1 + 3 \log \frac{M_\pi^2}{\mu^2}\right) + I(s) + I(t) + I(u) \right], \quad (44)$$

with $I(s) = (s - 4M_\pi^2)\bar{J}(s)$, where $\bar{J}(s)$ is the standard subtracted two-point function

$$16\pi^2 \bar{J}(q^2) = \sigma \log \frac{\sigma - 1}{\sigma + 1} + 2, \quad \sigma = \sqrt{1 - 4M_\pi^2/q^2}. \quad (45)$$

The logarithmic term in (44) agrees with our LL calculation. The full expression accounting for the pion mass difference can be found in [31].

The contribution from the NLO Lagrangian can be expressed in terms of the low-energy constants introduced in [32] as

$$f_1^{\text{tree}} = 128\pi^2 M_\pi^2 (c_2^{Wr} + c_6^{Wr}). \quad (46)$$

In order to estimate the value of f_1^{tree} , several methods exist in the literature: hidden local symmetry (HLS) [22], phenomenology [33], the constituent quark model (CQM) [33,34], Schwinger–Dyson equation (SDE) [35], or resonance saturation [36], to name a few. The spread in results can be seen from the estimates following from three of these methods

$$f_1^{\text{tree}} = \frac{3M_\pi^2}{2M_\rho^2} = 0.048 \text{ (HLS)}, \quad = 0.19 \text{ (CQM)}, \quad = -0.01 \text{ (SDE)}. \quad (47)$$

The two-loop corrections, estimated using dispersive techniques [37], are found to be small.

These corrections can now be incorporated in the calculation of $F_0^{3\pi}$ from the cross section measured at Serpukhov using (42). Turning them on one by one, we find the results listed in Table 7. Comparison of the third and fourth column shows that at the one-loop order, the leading logarithm provides a good estimate for the size of the complete correction: it accounts for 60% of

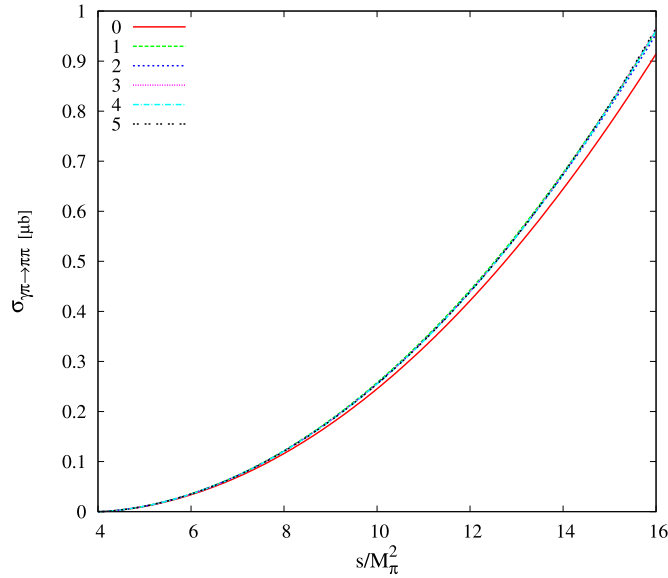


Fig. 7. The leading logarithm contribution to the total cross section for $\pi^- \gamma \rightarrow \pi^- \pi^0$ as a function of s .

the shift. The uncertainty on the listed values has two main sources: the experimental uncertainty of about $\pm 1 \text{ GeV}^{-3}$ and the model dependence of the c_i^{Wr} . From the spread of the estimates in Table 7, the latter also is about $\pm 1 \text{ GeV}^{-3}$. The total error, adding quadratically, is thus about $\pm 1.5 \text{ GeV}^{-3}$, such that the theoretical result $F_0^{3\pi} = 9.8 \text{ GeV}^{-3}$ agrees reasonably with the final values at the one-loop level.

Let us now return to the discussion of the expansion f^{LL} in (32). The one-loop LL shifts the result by -0.3 as already shown. Adding the LL contributions up to five-loop order in (42) leads to

$$F_0^{3\pi LL} = (12.9 - 0.3 + 0.04 + 0.02 + 0.006 + 0.001 + \dots) \text{ GeV}^{-3}. \quad (48)$$

Clearly, the series converges rather well. The small size of the LLs beyond one loop indicates that the full corrections at higher orders are negligible.

The total cross section obtained from only the LL contributions as a function of the center-of-mass energy is depicted in Fig. 7.

5.2. $\pi^0 \rightarrow \gamma\gamma$

For the decay $\pi^0 \rightarrow \gamma\gamma$, there is more experimental information available. For a recent review, see [38]. The current PDG average ([39], updated 2011) for the lifetime of the neutral pion is based on six experiments: three relying on the Primakoff effect [40–42], a direct measurement [43], an e^+e^- collider measurement [44], and a measurement of the weak form factor in $\pi^+ \rightarrow e^+\nu\gamma$ [45], which is related to the π^0 lifetime via the conserved vector current hypothesis. This leads to the average lifetime $\tau_{\pi^0} = (8.4 \pm 0.4) \times 10^{-17} \text{ s}$. Including the recent precise measurement by PrimEx at JLab [46],

$$\Gamma(\pi^0 \rightarrow \gamma\gamma)_{\text{PrimEx}} = 7.82 \pm 0.14 \pm 0.17 \text{ eV}, \quad (49)$$

leads to a smaller uncertainty, $\tau_{\pi^0} = (8.35 \pm 0.31) \times 10^{-17}$ s. Ongoing efforts by the PrimEx Collaboration are expected to decrease the error by a factor two.

The partial decay width is related to the decay amplitude by

$$\Gamma_{\gamma\gamma} = \frac{M_\pi^3}{64\pi} |F_{\pi\gamma\gamma}|^2. \quad (50)$$

At lowest order we find from the Wess–Zumino–Witten Lagrangian

$$F_{\pi\gamma\gamma}^{\text{LO}} = \frac{e^2}{4\pi^2 F_\pi} \Rightarrow \Gamma(\pi^0 \rightarrow \gamma\gamma)_{\text{LO}} \approx 7.76 \text{ eV}, \quad (51)$$

which is in perfect agreement with the PDG average as well as with the PrimEx result (49). Higher-order corrections might still destroy the agreement and we can use the leading logarithms to estimate the size of these contributions and to examine the convergence of the chiral series. Notice that no chiral logarithms are present at the one-loop level once everything is expressed in terms of the physical quantities F_π and M_π [23,24]. At the two-loop level, leading logarithms start to contribute [25]. At present the best prediction including electromagnetic and two-loop effects is [25]

$$\Gamma_{\pi^0 \rightarrow \gamma\gamma} = (8.09 \pm 0.11) \text{ eV}, \quad (52)$$

which leads to the lifetime $\tau_{\pi^0} = (8.04 \pm 0.11) 10^{-17}$ s.

Our result for \hat{F} in (37) indicates that the convergence is fast and higher orders are small. Putting in $\mu = 0.77$ GeV we obtain

$$\hat{F} = 1 + 0 - 0.000372 + 0.000088 + 0.000036 + 0.000009 + 0.000002 + \dots, \quad (53)$$

which clearly shows a fast convergence.

We now turn to the discussion of the meson–photon transition form factor $F_\gamma(-Q^2)$, normalized to the value at $Q^2 = 0$, which has been given in (37). It was measured by CELLO [47], CLEO [48], and recently by BaBar [49] mainly in the range $1 \leq Q^2 \leq 40$ GeV². New activity is expected for very low Q^2 by KLOE-2 at DAΦNE [50] which should directly test the prediction.

The LL contribution up to fifth order has been given in (37). Our result for the LL contribution to this quantity is depicted in Fig. 8 together with the VMD prediction

$$F_\gamma^{\text{VMD}}(-Q^2) = \frac{m_V^2}{m_V^2 + Q^2}. \quad (54)$$

6. Conclusion

In this paper we have extended the earlier work on leading logarithms in effective field theories to the anomalous sector. First we improved the programs used in the earlier work on the massive nonlinear sigma model [6,7]. This allowed us to compute one order higher than in those papers and we presented results for the mass, decay constant and the vector form factor. For the latter we clarified the discrepancy with the chiral limit work of [4] and we presented some numerical results as well.

The main part of this paper is the extension to the anomalous sector. We thus added the Wess–Zumino–Witten term to the massive nonlinear sigma model for $N = 3$ and computed the leading logarithms to six-loop order for $\pi^0 \rightarrow \gamma^* \gamma^*$ and five-loop order for the $\gamma^* \pi \pi \pi$ vertex. We did

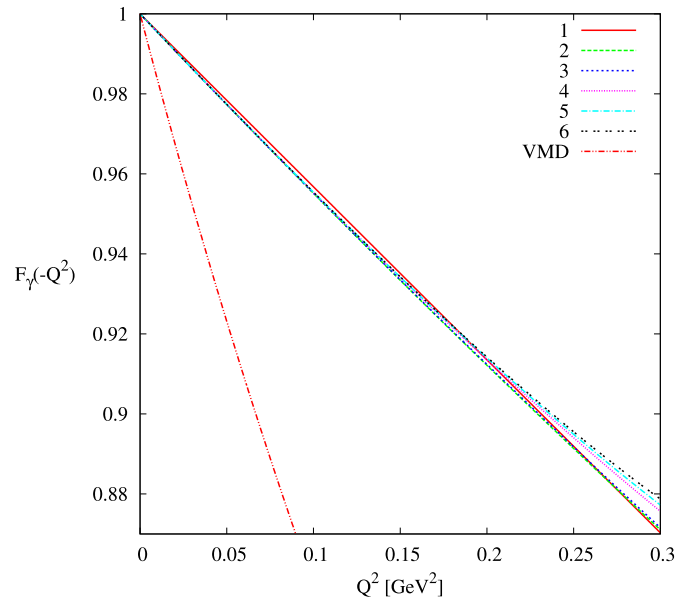


Fig. 8. The LL contribution to $F_\gamma(-Q^2)$ at different orders. Also shown is the VMD prediction as a comparison.

not find a simple guess for the coefficients which was one of the hopes when starting this work. In both cases the leading logarithms indicate that the chiral series converges fast and we presented some numerical results for the pion lifetime, the transition form factor and the $\gamma^* \pi \pi \pi$ vertex.

Acknowledgements

S.L. is supported by a grant from the Swiss National Science Foundation and K.K. by the Center for Particle Physics (project No. LC 527) of the Ministry of Education of the Czech Republic. This work is supported in part by the European Community – Research Infrastructure Integrating Activity “Study of Strongly Interacting Matter” (HadronPhysics2, Grant Agreement No. 227431) and the Swedish Research Council grants 621-2008-4074 and 621-2010-3326.

Appendix A. Dispersive approach for the pion form factor

Since the leading logarithms for the vector form factor in the chiral limit obtained in [7] and here do not agree with the corresponding result from Kivel et al. [4], another check of our result is in order. In [5], it was found that the partial wave amplitudes for $\pi\pi$ scattering are given by

$$t_l^I(s) = \frac{\pi}{2} \sum_{n=1}^{\infty} \omega_{nl}^I \frac{\hat{S}(s)^n}{2l+1} \ln^{n-1} \left(\frac{\mu^2}{s} \right) + \mathcal{O}(\text{NLL}), \quad (55)$$

with the dimensionless function $\hat{S}(s) = \frac{s}{(4\pi F)^2}$. The coefficients ω_{nl}^I can be found in Tables I and II in [5].

The leading logarithms for the scalar form factor are

$$F_S(s) = \sum_{n=0}^{\infty} f_n^S \hat{S}(s)^n \ln^n \left(-\frac{\mu^2}{s} \right). \quad (56)$$

In this case, the results from [4] and [7] for the coefficients f_0^S are in agreement. The discontinuity across the cut of the scalar form factor must satisfy

$$\text{disc } F_S(s) = t_0^0 F_S(s), \quad (57)$$

which can be easily verified to hold for the coefficients f_n^S given in [4,7].

A similar expansion holds for the vector form factor:

$$F_V(s) = \sum_{n=0}^{\infty} f_n^V \hat{S}(s)^n \ln^n \left(-\frac{\mu^2}{s} \right) + \mathcal{O}(\text{NLL}). \quad (58)$$

This time, however, the results from [4] disagree with ours and [7] for $n > 2$. The discontinuity across the cut of the vector form factor must hold

$$\text{disc } F_V(s) = t_1^1 F_V(s), \quad (59)$$

which is only given for the f_n^V from us and [7]. We therefore conclude that this is the correct result.

Dropping the factor $(-1)^{p+1}$ in (12) of [4] brings that result in agreement with ours. That there is indeed a misprint in [4] was confirmed to us by the authors and was stated in the PhD thesis of A.A. Vladimirov.

References

- [1] S. Weinberg, Phenomenological Lagrangians, Festschrift honoring Julian Schwinger on his 60th birthday, *Physica A* 96 (1979) 327.
- [2] M. Büchler, G. Colangelo, Renormalization group equations for effective field theories, *Eur. Phys. J. C* 32 (2003) 427–442, hep-ph/0309049.
- [3] N. Kivel, M. Polyakov, A. Vladimirov, Chiral logarithms in the massless limit tamed, *Phys. Rev. Lett.* 101 (2008) 262001, arXiv:0809.3236.
- [4] N. Kivel, M. Polyakov, A. Vladimirov, Leading chiral logarithms for pion form factors to arbitrary number of loops, *JETP Lett.* 89 (2009) 529–534, arXiv:0904.3008.
- [5] J. Koschinski, M.V. Polyakov, A.A. Vladimirov, Leading infrared logarithms from unitarity, analyticity and crossing, *Phys. Rev. D* 82 (2010) 014014, arXiv:1004.2197.
- [6] J. Bijnens, L. Carloni, Leading logarithms in the massive $O(N)$ nonlinear sigma model, *Nucl. Phys. B* 827 (2010) 237–255, arXiv:0909.5086.
- [7] J. Bijnens, L. Carloni, The massive $O(N)$ non-linear sigma model at high orders, *Nucl. Phys. B* 843 (2011) 55–83, arXiv:1008.3499.
- [8] J. Gasser, H. Leutwyler, Chiral perturbation theory to one loop, *Annals Phys.* 158 (1984) 142.
- [9] S. Weinberg, Nonlinear realizations of chiral symmetry, *Phys. Rev.* 166 (1968) 1568–1577.
- [10] M.B. Einhorn, Speculations on a strongly interacting Higgs sector, *Nucl. Phys. B* 246 (1984) 75.
- [11] F. Sannino, Dynamical stabilization of the Fermi scale: Phase diagram of strongly coupled theories for (minimal) walking technicolor and unparticles, arXiv:0804.0182.
- [12] S.R. Coleman, J. Wess, B. Zumino, Structure of phenomenological Lagrangians. 1, *Phys. Rev.* 177 (1969) 2239–2247.
- [13] S.L. Adler, Axial vector vertex in spinor electrodynamics, *Phys. Rev.* 177 (1969) 2426–2438.
- [14] S.L. Adler, W.A. Bardeen, Absence of higher order corrections in the anomalous axial vector divergence equation, *Phys. Rev.* 182 (1969) 1517–1536.
- [15] W.A. Bardeen, Anomalous Ward identities in spinor field theories, *Phys. Rev.* 184 (1969) 1848–1857.
- [16] J. Bell, R. Jackiw, A PCAC puzzle: $\pi^0 \rightarrow \gamma\gamma$ in the sigma model, *Nuovo Cim. A* 60 (1969) 47–61.
- [17] J. Wess, B. Zumino, Consequences of anomalous Ward identities, *Phys. Lett. B* 37 (1971) 95.
- [18] E. Witten, Global aspects of current algebra, *Nucl. Phys. B* 223 (1983) 422–432.
- [19] R. Kaiser, Anomalies and WZW term of two flavor QCD, *Phys. Rev. D* 63 (2001) 076010, hep-ph/0011377.
- [20] J. Vermaseren, New features of FORM, math-ph/0010025.

- [21] J. Bijnens, G. Colangelo, P. Talavera, The vector and scalar form-factors of the pion to two loops, JHEP 9805 (1998) 014, hep-ph/9805389.
- [22] J. Bijnens, A. Bramon, F. Cornet, Three pseudoscalar photon interactions in chiral perturbation theory, Phys. Lett. B 237 (1990) 488.
- [23] J. Donoghue, B.R. Holstein, Y. Lin, Chiral loops in π^0 , $\eta^0 \rightarrow \gamma\gamma$ and η - η' mixing, Phys. Rev. Lett. 55 (1985) 2766–2769.
- [24] J. Bijnens, A. Bramon, F. Cornet, Pseudoscalar decays into two photons in chiral perturbation theory, Phys. Rev. Lett. 61 (1988) 1453.
- [25] K. Kampf, B. Moussallam, Chiral expansions of the π^0 lifetime, Phys. Rev. D 79 (2009) 076005, arXiv:0901.4688.
- [26] S.L. Adler, B.W. Lee, S. Treiman, A. Zee, Low-energy theorem for $\gamma + \gamma \rightarrow \pi + \pi + \pi$, Phys. Rev. D 4 (1971) 3497–3501.
- [27] M. Terent'ev, Process $\pi^\pm \rightarrow \pi^0\pi^\pm$ in Coulomb field and anomalous divergence of neutral axial vector current, Phys. Lett. B 38 (1972) 419.
- [28] Y. Antipov, V. Batarin, V. Bezzubov, N. Budanov, Y. Gorin, et al., Investigation of the chiral anomaly $\gamma \rightarrow 3\pi$ in pion pair production by pion in the nuclear Coulomb field, Phys. Rev. D 36 (1987) 21.
- [29] S. Amendolia, M. Arik, B. Badelek, G. Batignani, G. Beck, et al., First measurement of the reaction $\pi^- e \rightarrow \pi^- \pi^0 e$, Phys. Lett. B 155 (1985) 457.
- [30] I. Giller, A. Ocherashvili, T. Ebertshauser, M. Moinester, S. Scherer, A new determination of the $\gamma\pi \rightarrow \pi\pi$ anomalous amplitude via $\pi^- e^- \rightarrow \pi^- e^- \pi^0$ data, Eur. Phys. J. A 25 (2005) 229–240, hep-ph/0503207.
- [31] L. Ametller, M. Knecht, P. Talavera, Electromagnetic corrections to $\gamma\pi^\pm \rightarrow \pi^0\pi^\pm$, Phys. Rev. D 64 (2001) 094009, hep-ph/0107127.
- [32] J. Bijnens, L. Girlanda, P. Talavera, The anomalous chiral Lagrangian of order p^6 , Eur. Phys. J. C 23 (2002) 539–544, hep-ph/0110400.
- [33] O. Strandberg, Determination of the anomalous chiral coefficients of order p^6 , Masters Thesis (Advisor: Johan Bijnens), hep-ph/0302064.
- [34] J. Bijnens, The anomalous sector of the QCD effective Lagrangian, Nucl. Phys. B 367 (1991) 709–730.
- [35] S.-Z. Jiang, Q. Wang, Computation of the coefficients for p^6 order anomalous chiral Lagrangian, Phys. Rev. D 81 (2010) 094037, arXiv:1001.0315.
- [36] K. Kampf, J. Novotny, Resonance saturation in the odd-intrinsic parity sector of low-energy QCD, Phys. Rev. D 84 (2011) 014036, arXiv:1104.3137.
- [37] T. Hannah, The anomalous process $\gamma\pi \rightarrow \pi\pi$ to two loops, Nucl. Phys. B 593 (2001) 577–595, hep-ph/0102213.
- [38] A. Bernstein, B.R. Holstein, Neutral pion lifetime measurements and the QCD chiral anomaly, arXiv:1112.4809.
- [39] Particle Data Group Collaboration, K. Nakamura, et al., Review of particle physics, J. Phys. G 37 (2010) 075021.
- [40] V. Kryshkin, A. Sterligov, Y. Usov, Measurement of lifetime of the π^0 meson, Zh. Eksp. Teor. Fiz. 57 (1969) 1917–1922.
- [41] G. Bellettini, C. Bemporad, P. Braccini, C. Bradaschia, L. Foa, et al., A new measurement of the π^0 lifetime through the Primakoff effect in nuclei, Nuovo Cim. A 66 (1970) 243–252.
- [42] A. Browman, J. DeWire, B. Gittelman, K. Hanson, D. Larson, et al., The decay width of the neutral π meson, Phys. Rev. Lett. 33 (1974) 1400.
- [43] H. Atherton, C. Bovet, P. Coet, R. Desalvo, N. Doble, et al., Direct measurement of the lifetime of the neutral pion, Phys. Lett. B 158 (1985) 81–84.
- [44] Crystal Ball Collaboration, D. Williams, et al., Formation of the pseudoscalars π^0 , η and η' in the reaction $\gamma\gamma \rightarrow \gamma\gamma$, Phys. Rev. D 38 (1988) 1365.
- [45] M. Bychkov, D. Pocanic, B. VanDevender, V. Baranov, W.H. Bertl, et al., New precise measurement of the pion weak form factors in $\pi^+ \rightarrow e^+ \nu\gamma$ decay, Phys. Rev. Lett. 103 (2009) 051802, arXiv:0804.1815.
- [46] PrimEx Collaboration, I. Larin, et al., A new measurement of the π^0 radiative decay width, Phys. Rev. Lett. 106 (2011) 162303, arXiv:1009.1681.
- [47] CELLO Collaboration, H. Behrend, et al., A measurement of the π^0 , η and η' electromagnetic form factors, Z. Phys. C 49 (1991) 401–410.
- [48] CLEO Collaboration, J. Gronberg, et al., Measurements of the meson–photon transition form factors of light pseudoscalar mesons at large momentum transfer, Phys. Rev. D 57 (1998) 33–54, hep-ex/9707031.
- [49] BaBar Collaboration, B. Aubert, et al., Measurement of the $\gamma\gamma^* \rightarrow \pi^0$ transition form factor, Phys. Rev. D 80 (2009) 052002, arXiv:0905.4778.
- [50] G. Amelino-Camelia, F. Archilli, D. Babusci, D. Badoni, G. Bencivenni, et al., Physics with the KLOE-2 experiment at the upgraded DAΦNE, Eur. Phys. J. C 68 (2010) 619–681, arXiv:1003.3868.

2.5 Tree-level Amplitudes in the Nonlinear Sigma Model

K. Kampf, J. Novotny and J. Trnka, *Tree-level Amplitudes in the Nonlinear Sigma Model*, JHEP **1305** (2013) 032 [arXiv:1304.3048 [hep-th]].



PUBLISHED FOR SISSA BY SPRINGER

RECEIVED: April 12, 2013

ACCEPTED: April 22, 2013

PUBLISHED: May 7, 2013

Tree-level amplitudes in the nonlinear sigma model

Karol Kampf,^a Jiří Novotný^a and Jaroslav Trnka^{a,b}

^a*Institute of Particle and Nuclear Physics,
Faculty of Mathematics and Physics, Charles University in Prague,
CZ-18000 Prague, Czech Republic*

^b*Department of Physics, Princeton University,
Princeton, New Jersey 08544, U.S.A.*

E-mail: karol.kampf@mff.cuni.cz, jiri.novotny@mff.cuni.cz,
jtrnka@princeton.edu

ABSTRACT: We study in detail the general structure and further properties of the tree-level amplitudes in the $SU(N)$ nonlinear sigma model. We construct the flavor-ordered Feynman rules for various parameterizations of the $SU(N)$ fields $U(x)$, write down the Berends-Giele relations for the semi-on-shell currents and discuss their efficiency for the amplitude calculation in comparison with those of renormalizable theories. We also present an explicit form of the partial amplitudes up to ten external particles. It is well known that the standard BCFW recursive relations cannot be used for reconstruction of the on-shell amplitudes of effective theories like the $SU(N)$ nonlinear sigma model because of the inappropriate behavior of the deformed on-shell amplitudes at infinity. We discuss possible generalization of the BCFW approach introducing “BCFW formula with subtractions” and with help of Berends-Giele relations we prove particular scaling properties of the semi-on-shell amplitudes of the $SU(N)$ nonlinear sigma model under specific shifts of the external momenta. These results allow us to define alternative deformation of the semi-on-shell amplitudes and derive BCFW-like recursion relations. These provide a systematic and effective tool for calculation of Goldstone bosons scattering amplitudes and it also shows the possible applicability of on-shell methods to effective field theories. We also use these BCFW-like relations for the investigation of the Adler zeroes and double soft limit of the semi-on-shell amplitudes.

KEYWORDS: Scattering Amplitudes, Sigma Models, Global Symmetries

ARXIV EPRINT: [1304.3048](https://arxiv.org/abs/1304.3048)

Contents

1	Introduction	2
2	Nonlinear sigma model	3
2.1	Leading order Lagrangian	3
2.2	General properties of the tree-level scattering amplitudes	5
2.3	Tree-level amplitudes for $G = \text{SU}(N)$	6
2.3.1	Flavor ordered Feynman rules	6
2.3.2	Dependence on the parametrization	7
2.3.3	Interrelation of the cases $G = \text{U}(N)$ and $G = \text{SU}(N)$	8
2.4	Explicit examples of $\text{SU}(N)$ on-shell amplitudes	9
3	Recursive methods for scattering amplitudes	10
3.1	BCFW recursion relations	10
3.2	Reconstruction formula with subtractions	12
4	BCFW-like relations for semi-on-shell amplitudes	14
4.1	Semi-on-shell amplitudes and Berends-Giele relations	14
4.2	Cayley parametrization	17
4.3	Scaling properties of semi-on-shell amplitudes	18
4.4	BCFW reconstruction	21
4.5	Explicit example of application of BCFW relations: 6pt amplitude	25
5	More properties of stripped semi-on-shell amplitudes	26
5.1	Adler zeroes	28
5.2	Double-soft limit	31
6	Summary and conclusion	36
A	General parametrization	37
B	More examples of amplitudes	42
C	Relative efficiency of Feynman diagrams and Berends-Giele relations	42
C.1	Number of the Feynman graphs	43
C.2	Efficiency of the Berends-Giele relations	46
D	Other example of scaling properties of the semi-on-shell amplitudes	46
E	Double soft limit of Goldstone boson amplitudes	47
E.1	Vector WI and symmetry with respect to H	48
E.2	Soft vector current singularity	49
E.3	Axial WI and Adler zero	50
E.4	Double soft limit	51

1 Introduction

The chiral nonlinear sigma model is a widely used tool for description of many phenomena in theoretical particle physics. It is based on a simple Lie Group G and the spontaneous symmetry breaking $G \times G \rightarrow G$ gives rise to massless excitations - Goldstone bosons. For instance, in the theory of strong interactions, the group G is $SU(N_f)$ where $N_f = 2, 3$ is a number of light quark flavors and Goldstone bosons are associated with the triplet of pions (for $N_f = 2$) or octet of pseudoscalar mesons π , K and η (for $N_f = 3$). The interactions of these degrees of freedom dominate the hadronic world at low energies. In this context, the leading order nonlinear $U(3) \times U(3)$ chiral invariant effective Lagrangian, the kinetic part of which corresponds to the chiral nonlinear $U(3)$ sigma model, was constructed in the late sixties by Cronin [1] while the $SU(2)$ case was studied by Weinberg [2, 3], Brown [4] and Chang and Gürsey [5]. Further generalization lead to the invention of Chiral Perturbation Theory as a low energy effective theory of Quantum Chromodynamics by Weinberg [6] and by Gasser and Leutwyler [7, 8]. Chiral Perturbation Theory became a very useful tool for the investigation of the low energy hadron physics.

The focus of this paper is on scattering amplitudes of Goldstone bosons within the $SU(N)$ nonlinear sigma model described by the leading order Lagrangian. In principle, the standard Feynman diagram approach allows us to calculate arbitrary amplitude. Because the model is effective, and the Lagrangian contains an infinite tower of terms the calculation becomes very complicated for amplitudes of many external Goldstone bosons even at tree-level. It would be therefore desirable to find alternative non-diagrammatic methods which could save the computational effort and provide us with a tool to get the amplitudes more efficiently. In the past an attempt to formulate the calculation of the tree-level without any reference to the Lagrangian was made by Susskind and Frye [9]. They postulated recursive procedure for pion amplitudes based on certain algebraic duality assumptions supplemented with the requirement of Adler zero condition which should have to be satisfied separately for group-factor free kinematical functions recently known as the partial or stripped amplitudes. Such a condition had been proven in the special case of pion amplitudes described by the $SU(2)$ nonlinear sigma model by Osborn [10]. In [9] the authors successively calculated the amplitudes up to eight pions and showed that these results are equivalent to the diagrammatic calculation based on the $SU(2)$ nonlinear sigma model. The full equivalence for all amplitudes has been proven by Ellis and Renner in [11].

Over the past two decades there has been a huge progress in understanding scattering amplitudes using *on-shell methods* (for a review see e.g. [12–15]). They do not use explicitly the Lagrangian description of the theory and all on-shell quantities are calculated using on-shell data only with no access to off-shell physics (unlike virtual particles in Feynman diagrams). This has lead to many new theoretical tools (e.g. unitary methods [16, 17], BCFW recursion relations for tree-level amplitudes [18, 19] and the loop integrand [20]) as well as practical applications of on-shell methods to LHC processes (for recent results of the next-to-leading order QCD corrections for $W + 4$ -jets see [21]). Most of the recent theoretical developments have been driven by an intensive exploration of $\mathcal{N} = 4$ super Yang-Mills theory in the planar limit both at weak and strong couplings (see e.g. [22–33]).

There have been several attempts to extend some of these methods to other theories. The most natural starting point are the recursion relations for on-shell tree-level amplitudes, originally found by Britto, Cachazo, Feng and Witten for Yang-Mills theory [18, 19] and later also for gravity [34, 35]. The main idea is to perform a complex shift on external momenta and reconstruct the amplitude recursively using analytic properties of the S-matrix. More recently, this recursive approach was extended to Yang-Mills and gravity theories coupled to matter, as well as more general class of renormalizable theories [36].

In this paper, we find the new recursion relations for all on-shell tree-level amplitudes of Goldstone bosons within $SU(N)$ nonlinear sigma model. This shows that on-shell methods can be applied also for effective field theories and it gives new computational tool in this model. Using these recursion relations we are also able to prove more properties of tree-level amplitudes that are invisible in the Feynman diagram approach.

The paper is organized as follows: in section 2 we discuss $SU(N)$ nonlinear sigma model, introduce *stripped amplitudes* and using *minimal* parametrization (the convenient properties of which has been discussed in [11]) we calculate tree-level amplitudes up to 10 points. In section 3 we review BCFW recursion relations and their generalization to theories that do not vanish at infinity at large momentum shift. Section 4 is the main part of the paper, we first introduce semi-on-shell amplitudes, ie. amplitudes with $n - 1$ on-shell and one off-shell external legs. Then we prove scaling properties under particular momentum shifts which allows us to construct BCFW-like recursion relations. Finally, we show explicit 6pt example. In section 5 we use previous results to prove Adler zeroes and double-soft limit formula for stripped amplitudes. Additional results and technical details are postponed to appendices: in appendix A, we describe the general parametrization of the $SU(N)$ nonlinear sigma model. In appendix B we give the results of the amplitudes up to 10p. Appendix C is devoted to the counting of flavor-ordered Feynman graphs needed for the calculations of the amplitudes in nonlinear sigma models and other theories. In appendix D we present additional scaling properties of the semi-on-shell amplitudes. In appendix E, we study the double soft-limit for more general class of spontaneously broken theories for complete (not stripped) amplitudes.

2 Nonlinear sigma model

2.1 Leading order Lagrangian

Let us first assume a most general case of the principal chiral nonlinear sigma model based on a simple compact Lie group G . Such a model corresponds to the spontaneous symmetry breaking of the chiral group $G_L \times G_R$ where $G_{L,R} = G$ to its diagonal subgroup $G_V = G$, i.e. to the subgroup of the elements $h = (g_L, g_R)$ where $g_L = g_R$. The vacuum little group G_V is invariant with respect to the involutive automorphism $(g_L, g_R) \rightarrow (g_R, g_L)$ and the homogeneous space $G_L \times G_R / G_V$ is a symmetric space which is isomorphic to the group space G . A canonical realization of such an isomorphism is via restriction of the mapping

$$(g_L, g_R) \rightarrow g_R g_L^{-1} \equiv U \tag{2.1}$$

(which is constant on the right cosets of G_V in $G_L \times G_R$) to $G_L \times G_R/G_V$. Provided we induce the action of the chiral group on $G_L \times G_R/G_V$ by means of the left multiplication, the transformation of U under general element (V_L, V_R) of the chiral group is linear

$$U \rightarrow V_R U V_L^{-1}. \quad (2.2)$$

This can be used to construct the most general chiral invariant leading order effective Lagrangian in general number d of space-time dimensions describing the dynamics of the Goldstone bosons corresponding to the spontaneous symmetry breaking $G_L \times G_R \rightarrow G_V$ as

$$\mathcal{L}^{(2)} = \frac{F^2}{4} \langle \partial_\mu U \partial^\mu U^{-1} \rangle = -\frac{F^2}{4} \langle (U^{-1} \partial_\mu U) (U^{-1} \partial^\mu U) \rangle, \quad (2.3)$$

where F is a constant¹ with the canonical dimension $d/2 - 1$. Here and in what follows we use the notation $\langle \cdot \rangle = \text{Tr}(\cdot)$ and the trace is taken in the defining representation of G . The overall normalization factor is dictated by the form of the parametrization of the matrix U in terms of the Goldstone boson fields ϕ^a which we write for the purposes of this subsection² as

$$U = \exp \left(\sqrt{2} \frac{i}{F} \phi \right) \quad (2.4)$$

where $\phi = \phi^a t^a$ and t^a , $a = 1, \dots, \dim G$ are generators of G satisfying

$$\langle t^a t^b \rangle = \delta^{ab} \quad (2.5)$$

$$[t^a, t^b] = i\sqrt{2} f^{abc} t^c. \quad (2.6)$$

Here f^{abc} are totally antisymmetric structure constants of the group G . According to (2.2), the fields ϕ^a transform linearly under the little group G_V as the vector in the adjoint representation of G while the general chiral transformations of ϕ^a are nonlinear.

The Lagrangian $\mathcal{L}^{(2)}$ can be rewritten in terms of the Goldstone boson fields as follows. We have

$$U^{-1} \partial_\mu U = -\frac{\exp(-\sqrt{2} \frac{i}{F} \text{Ad}(\phi)) - 1}{\text{Ad}(\phi)} \partial_\mu \phi = -\frac{1}{\sqrt{2}} t \cdot \frac{\exp(-\frac{2i}{F} D_\phi) - 1}{D_\phi} \cdot \partial \phi \quad (2.7)$$

where

$$\text{Ad}(\phi) \partial_\mu \phi = [\phi, \partial_\mu \phi] = \sqrt{2} t^a D_\phi^{ab} \partial_\mu \phi^b \equiv \sqrt{2} t \cdot D_\phi \cdot \partial \phi, \quad (2.8)$$

the matrix D_ϕ^{ab} is given as

$$D_\phi^{ab} = -i f^{cab} \phi^c \quad (2.9)$$

and the dot means contraction of the indices in the adjoint representation. Inserting this in (2.3) we get finally

$$\mathcal{L}^{(2)} = \frac{F^2}{4} \partial \phi^T \cdot \frac{1 - \cos(\frac{2}{F} D_\phi)}{D_\phi^2} \cdot \partial \phi = -\partial \phi^T \cdot \left(\sum_{n=1}^{\infty} \frac{(-1)^n}{(2n)!} \left(\frac{2}{F} \right)^{2n-2} D_\phi^{2n-2} \right) \cdot \partial \phi. \quad (2.10)$$

¹The decay constant of the Goldstone bosons.

²In what follows we will use also more general parametrization of U .

2.2 General properties of the tree-level scattering amplitudes

Note that, the only group factors which enter the interaction vertices are the structure constants f^{abc} . In any tree Feynman diagram each f^{abc} is contracted either with another structure constant within the same vertex or via propagator factor δ^{ab} with some structure constant entering next vertex. Therefore, using the standard argumentation for a general tree graph [12], i.e. expressing any f^{abc} as a trace $f^{abc} = -\langle i[t^a, t^b]t^c \rangle / \sqrt{2}$ and then successively using the relations like $f^{cde}t^c = -i[t^d, t^e] / \sqrt{2}$ in order to replace the contracted structure constants with the commutators of the generators inside the single trace, we can prove that any tree level on-shell amplitude has a simple group structure, namely

$$\mathcal{M}^{a_1 a_2 \dots a_n}(p_1, p_2, \dots, p_n) = \sum_{\sigma \in S_n / Z_n} \langle t^{a_{\sigma(1)}} t^{a_{\sigma(2)}} \dots t^{a_{\sigma(n)}} \rangle \mathcal{M}_{\sigma}(p_1, \dots, p_n). \quad (2.11)$$

Here all the momenta treated as incoming and the sum is taken over the permutation of the n indices $1, 2, \dots, n$ modulo cyclic permutations. As a consequence of the cyclicity of the trace we get

$$\mathcal{M}_{\sigma}(p_1, p_2, \dots, p_n) = \mathcal{M}_{\sigma}(p_2, \dots, p_n, p_1) \quad (2.12)$$

Due to the Bose symmetry, the kinematical factors $\mathcal{M}_{\sigma}(p_1, \dots, p_n)$ has to satisfy

$$\mathcal{M}_{\sigma \circ \rho}(p_1, \dots, p_n) = \mathcal{M}_{\sigma}(p_{\rho(1)}, p_{\rho(2)}, \dots, p_{\rho(n)}) \quad (2.13)$$

(where $\sigma \circ \rho$ is a composition of permutations) and therefore

$$\mathcal{M}_{\sigma}(p_1, \dots, p_n) = \mathcal{M}(p_{\sigma(1)}, p_{\sigma(2)}, \dots, p_{\sigma(n)}) \quad (2.14)$$

where we have denoted $\mathcal{M} \equiv \mathcal{M}_{\text{id}}$ (here id is identical permutation). The amplitudes $\mathcal{M}(p_1, \dots, p_n)$ are called the *stripped* or *partial* amplitudes. Note that the same arguments can be used also for the Feynman rules for the interaction vertices, the general form of which can be written as

$$V_n^{a_1 a_2 \dots a_n}(p_1, p_2, \dots, p_n) = \sum_{\sigma \in S_n / Z_n} \langle t^{a_{\sigma(1)}} t^{a_{\sigma(2)}} \dots t^{a_{\sigma(n)}} \rangle V_n(p_{\sigma(1)}, p_{\sigma(2)}, \dots, p_{\sigma(n)}). \quad (2.15)$$

After some algebra we get explicitly (see appendix A for details) $V_{2n+1}(p_1, \dots, p_{2n+1}) = 0$ and

$$V_{2n}(p_1, \dots, p_{2n}) = \frac{(-1)^n}{(2n)!} \left(\frac{2}{F^2} \right)^{n-1} \sum_{k=1}^{2n-1} (-1)^{k-1} \binom{2n-2}{k-1} \sum_{i=1}^{2n} (p_i \cdot p_{i+k}). \quad (2.16)$$

Let us note that besides (2.3), (2.4) we need not to use any algebraic relations specific for the concrete group G when deriving this formula and it is therefore valid for general G . In the general case we can therefore define the stripped amplitudes and stripped vertices, however, their relation is not straightforward and may depend on the group G . In what follows we will concentrate on the case $G = \text{SU}(N)$.

2.3 Tree-level amplitudes for $G = \text{SU}(N)$

2.3.1 Flavor ordered Feynman rules

The standard way of calculation of the tree-level amplitudes $\mathcal{M}^{a_1 \dots a_n}(p_1, \dots, p_n)$ is to evaluate the contributions of all tree Feynman graphs with n external legs build from the complete vertices (2.15) and propagators $\Delta_{ab} = i\delta_{ab}/p^2$. This includes rather tedious group algebra which is specific for each group G . In the special case of $G = \text{SU}(N)$ the calculations can be further simplified. Because we have the completeness relations for the generators t^a in the form

$$\sum_{a=1}^{N^2-1} \langle X t^a \rangle \langle t^a Y \rangle = \langle XY \rangle - \frac{1}{N} \langle X \rangle \langle Y \rangle, \quad (2.17)$$

we can simply merge the traces from the vertices of any tree Feynman graphs in one single trace preserving at the same time the order of the generators t^{a_j} inside the trace. Note that the “disconnected” $1/N$ terms have to cancel in the sum in order to produce the single trace in (2.11).³ This enables us to formulate simple “flavor ordered Feynman rules” directly for the stripped amplitudes \mathcal{M} completely in terms of the stripped vertices V_n . The general recipe is exactly the same as in the more familiar case of $\text{SU}(N)$ Yang-Mills theory, i.e. the tree graphs built from the stripped vertices and propagators are decorated with cyclically ordered external momenta and the corresponding ordering of the momenta inside the stripped vertices are kept.

Let us note that such a simple way of the calculation of the stripped amplitudes might not be possible for general group G . For instance for $G = \text{SO}(N)$ we have the following completeness relations

$$\sum_{a=1}^{N(N-1)/2} \langle X t^a \rangle \langle t^a Y \rangle = \frac{1}{2} (\langle XY \rangle - \langle XY^T \rangle) \quad (2.18)$$

the second term of which reverses the order of the generators in the merged vertex and the aforementioned simple argumentation leading to the flavor ordered Feynman rules has to be modified.

The $\text{SU}(N)$ case has also another useful feature. As a consequence of the completeness relations (2.17) for the group generators of $\text{SU}(N)$ and the analogous relation

$$\sum_{a=1}^{N^2-1} \langle X t^a Y t^a \rangle = \langle X \rangle \langle Y \rangle - \frac{1}{N} \langle XY \rangle \quad (2.19)$$

it can be proved [12] that the traces $\langle t^{a_{\sigma(1)}} t^{a_{\sigma(2)}} \dots t^{a_{\sigma(n)}} \rangle$ and $\langle t^{a_{\rho(1)}} t^{a_{\rho(2)}} \dots t^{a_{\rho(n)}} \rangle$ are orthogonal in the leading order of N in the sense that

$$\sum_{a_1, a_2, \dots, a_n} \langle t^{a_{\sigma(1)}} t^{a_{\sigma(2)}} \dots t^{a_{\sigma(n)}} \rangle \langle t^{a_{\rho(1)}} t^{a_{\rho(2)}} \dots t^{a_{\rho(n)}} \rangle^* = N^{n-2} (N^2 - 1) \left(\delta_{\sigma\rho} + O\left(\frac{1}{N^2}\right) \right) \quad (2.20)$$

³As we shall see in what follows, this fact can be understood as a consequence of the decoupling of the $\text{U}(1)$ Goldstone boson in the nonlinear $\text{U}(N)$ sigma model.

where $\delta_{\sigma\rho} = 1$ for $\rho = \sigma$ modulo cyclic permutation and zero otherwise. This relation is enough to uniquely determine the coefficients \mathcal{T}_σ in the general expansion of the form

$$\mathcal{T}^{a_1 a_2 \dots a_n} = \sum_{\sigma \in S_n / Z_n} \langle t^{a_{\sigma(1)}} t^{a_{\sigma(2)}} \dots t^{a_{\sigma(n)}} \rangle \mathcal{T}_\sigma, \quad (2.21)$$

(provided the coefficients \mathcal{T}_σ are N -independent) as the leading in N terms of the “scalar product”

$$\sum_{a_1, a_2, \dots, a_n} \mathcal{T}^{a_1 a_2 \dots a_n} \langle t^{a_{\sigma(1)}} t^{a_{\sigma(2)}} \dots t^{a_{\sigma(n)}} \rangle^* = N^{n-2} (N^2 - 1) \left(\mathcal{T}_\sigma + O\left(\frac{1}{N^2}\right) \right) \quad (2.22)$$

Because the stripped amplitudes and vertices by construction do not depend on N , the coefficients at the individual traces in the representation (2.11) are unique and therefore the stripped amplitudes and vertices are unique.

2.3.2 Dependence on the parametrization

Up to now we have identified the Goldstone boson fields ϕ^a using the exponential parametrization (2.4) of the group elements $U(\phi^a)$. However, according to the equivalence theorem, the amplitudes $\mathcal{M}^{a_1 a_2 \dots a_n}(p_1, p_2, \dots, p_n)$ are the same for any other parametrization $U(\tilde{\phi}^a)$ where

$$\tilde{\phi}^a = \phi^a + F^a(\phi) \quad (2.23)$$

where $F^a(\phi) = O(\phi^2)$ is at least quadratic in the fields ϕ . Therefore, according to the aforementioned uniqueness, the stripped amplitudes for the nonlinear $SU(N)$ sigma model do not depend on the parametrization. Note, however, that this is not true for the stripped vertices which do depend on the parametrization because the complete vertices $V_n^{a_1 a_2 \dots a_n}(p_1, p_2, \dots, p_n)$ do.

As far as the on-shell tree-level amplitudes are concerned, in various calculations we are thus free to use the most suitable parametrization and consequently the most useful form of the corresponding stripped vertices for a given purpose. We shall often take advantage of this freedom in what follows.

A wide class of parameterizations for the chiral nonlinear sigma model with $G = U(N)$ and $G = SU(N)$ has been discussed in [1]. The general form of such a parameterization reads

$$U = \sum_{k=0}^{\infty} a_k \left(\sqrt{2} \frac{i}{F} \phi \right)^k \quad (2.24)$$

where $a_0 = a_1 = 1$ and the remaining real coefficients a_k are constrained by the requirement $UU^\dagger = 1$. The exponential parametrization (2.4) corresponds to the choice $a_n = 1/n!$. In fact, as was proved in [1], for $SU(N)$ nonlinear sigma model with $N > 2$, the exponential parametrization is the only admissible choice within the above class of parameterizations (2.24) compatible with the nonlinearly realized symmetry with respect to the $SU(N)$ chiral transformations (2.2). On the other hand, for $SU(2)$ and for the extended chiral group $G = U(N)$ with arbitrary N , the parameterizations of the form (2.24) represent an infinite-parametric class. The more detailed discussion can be found in appendix A.

2.3.3 Interrelation of the cases $G = U(N)$ and $G = SU(N)$

Let us note, that the $SU(N)$ and $U(N)$ chiral nonlinear sigma models are tightly related. Within the exponential parametrization we can write in the $U(N)$ case

$$U = \exp\left(\frac{i}{F}\sqrt{\frac{2}{N}}\phi^0\right)\widehat{U} \quad (2.25)$$

where $\widehat{U} \in SU(N)$ and ϕ^0 is the additional $U(1)$ Goldstone boson corresponding to the $U(1)$ generator $t^0 = \mathbf{1}/\sqrt{N}$. We get then

$$U^{-1}\partial_\mu U = \frac{i}{F}\sqrt{\frac{2}{N}}\partial_\mu\phi^0 + \widehat{U}^+\partial_\mu\widehat{U} \quad (2.26)$$

and as a consequence,

$$\mathcal{L}^{(2)} = \frac{1}{2}\partial\phi^0 \cdot \partial\phi^0 + \frac{F^2}{4}\langle\partial_\mu\widehat{U}\partial^\mu\widehat{U}^{-1}\rangle. \quad (2.27)$$

Therefore ϕ^0 completely decouples. This means that for the on-shell amplitudes in this model

$$\mathcal{M}^{a_1 a_2 \dots a_n}(p_1, p_2, \dots, p_n) = 0 \quad (2.28)$$

whenever at least one $a_j = 0$. Note that this statement does not depend on the parametrization. We can therefore reproduce the on-shell amplitudes of the $SU(N)$ chiral nonlinear sigma model from that of the $U(N)$ one simply by assigning to the indices a_i the values corresponding the $SU(N)$ Goldstone bosons. Keeping this in mind, in what follows we will freely switch between the $U(N)$ and $SU(N)$ case and use the general parameterizations (2.24) also in the context of the $SU(N)$ chiral nonlinear sigma model.

The fact that the $U(1)$ Goldstone boson decouples gives also a nice physical explanation why the “disconnected” $1/N$ term can be omitted in the relation (2.17) when summing over virtual states in the tree-level Feynman graphs for the $SU(N)$ nonlinear sigma model. This term can be interpreted as the subtraction of the extra $U(1)$ virtual state contained in the first “connected” part. However, because this state decouples, no such correction is in fact needed.

The decoupling of the $U(1)$ Goldstone boson is an effect analogous to the decoupling of the $U(1)$ component of the gauge field in the case of the $U(N)$ Yang-Mills theory. For the tree-level amplitudes (and the corresponding stripped amplitudes) we get as a consequence a set of identities constraining their form. For instance taking only one $a_j = 0$ (say a_1) in (2.28), we get the “dual Ward identity” (or the $U(1)$ decoupling identity)

$$\mathcal{M}(p_1, p_2, p_3, \dots, p_n) + \mathcal{M}(p_2, p_1, p_3, \dots, p_n) + \dots + \mathcal{M}(p_2, p_3, \dots, p_1, p_n) = 0 \quad (2.29)$$

exactly as in the Yang-Mills case (see e.g. [12] and references therein).

2.4 Explicit examples of $SU(N)$ on-shell amplitudes

Using (2.11) we can reconstruct the complete amplitude $\mathcal{M}^{a_1 \dots a_n}(p_1, \dots, p_n)$ just from a single stripped amplitude $\mathcal{M}(p_1, \dots, p_n)$ which is given by the sum of Feynman diagrams with ordered external legs $\{1, 2, \dots, n\}$. Though the aim of this paper is not to calculate scattering amplitudes using the Feynman diagram approach, in this section we provide explicit examples for diagrammatic calculation of the stripped 4pt and 6pt amplitudes of the chiral nonlinear $SU(N)$ sigma model (the 8pt and 10pt amplitudes we postpone to the appendix B) as the reference result for the recursive formula given in section 4.

We can easily see that the only poles in the stripped amplitude are of the form $1/s_{i,j}$ where

$$s_{i,j} = p_{i,j}^2 \quad \text{with} \quad p_{i,j} = \sum_{k=i}^j p_k \quad (2.30)$$

(Obviously $s_{i,j} = s_{j+1,i-1}$ due to momentum conservation). The variables $s_{i,j}$ are therefore well suited for presentation of the amplitudes.

As we have discussed above, the $SU(N)$ stripped amplitudes are essentially the same as those for the $U(N)$ case and, as we have discussed above, they are independent on the parametrization of the unitary matrix U in (2.3). The most convenient one for diagrammatic calculation of on-shell scattering amplitudes is the *minimal* parametrization [11]

$$U = \sqrt{2} \frac{i}{F} \phi + \sqrt{1 - 2 \frac{\phi^2}{F^2}} = 1 + \sqrt{2} \frac{i}{F} \phi - 2 \sum_{k=1}^{\infty} \left(\frac{1}{2F^2} \right)^k C_{n-1} \phi^{2k} \quad (2.31)$$

where C_n are the Catalan numbers (A.12). The stripped Feynman rules for vertices can be written in terms of $s_{i,j}$ as follows (see appendix A for details)

$$V_{2n+2}(s_{i,j}) = \left(\frac{1}{2F^2} \right)^n \frac{1}{2} \sum_{k=0}^{n-1} C_k C_{n-k-1} \sum_{i=1}^{2n+2} s_{i,i+2k+1} \quad (2.32)$$

Note that within this parametrization the stripped vertices do not depend on the off-shellness of the momenta entering the vertex and when expressed in terms of the variables $s_{i,j}$ they are identical taken both on-shell or off-shell. This rapidly speeds up the calculation, because there are no partial cancelations between the numerators and propagator denominators within the individual Feynman graphs and it allows us to find the final expressions for the amplitudes in very compact form.

The four-point amplitude is directly given by the Feynman rule in the simple parametrization,

$$2F^2 \mathcal{M}(1, 2, 3, 4) = s_{1,2} + s_{2,3}. \quad (2.33)$$

Note that for n -point amplitude $\sum_{k=1}^n p_k = 0$ and this can be used to systematically eliminate p_n or equivalently $s_{,n}$.

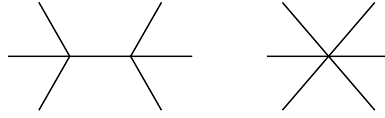


Figure 1. Graphical representation of the 6-point amplitude (2.34) with cycling tacitly assumed.

The six-point amplitude is given by diagrams in figure 1. The explicit formula reads

$$\begin{aligned}
 4F^4 \mathcal{M}(1, 2, 3, 4, 5, 6) &= \\
 &= -\frac{(s_{1,2}+s_{2,3})(s_{1,4}+s_{4,5})}{s_{1,3}} - \frac{(s_{1,4}+s_{2,5})(s_{2,3}+s_{3,4})}{s_{2,4}} - \frac{(s_{1,2}+s_{2,5})(s_{3,4}+s_{4,5})}{s_{3,5}} \\
 &\quad + (s_{1,2} + s_{1,4} + s_{2,3} + s_{2,5} + s_{3,4} + s_{4,5})
 \end{aligned} \tag{2.34}$$

This can be rewritten as

$$4F^4 \mathcal{M}(1, 2, 3, 4, 5, 6) = -\frac{1}{2} \frac{(s_{1,2} + s_{2,3})(s_{1,4} + s_{4,5})}{s_{1,3}} + s_{1,2} + \text{cycl},$$

with ‘cycl’ defined for n -point amplitude as

$$A[s_{i,j}, \dots, s_{m,n}] + \text{cycl} \equiv \sum_{k=0}^{n-1} A[s_{i+k,j+k}, \dots, s_{m+k,n+k}], \tag{2.35}$$

which will quite considerably shorten the 8- and 10-point formulae. These are postponed to appendix B.

3 Recursive methods for scattering amplitudes

Feynman diagrams are completely universal way how to calculate scattering amplitudes in any theory (that has Lagrangian description). However, it is well-known that in many cases they are also very ineffective. Despite the expansion contains many diagrams each of them being a complicated function of external data, most terms vanish in the sum and the result is spectacularly simple. The most transparent example is Parke-Taylor formula [37] for all tree-level Maximal-Helicity-Violating amplitudes.⁴ The simple structure of the result is totally invisible in the standard Feynman diagrams expansion.

Several alternative approaches and methods have been discovered in last decades, let us mention e.g. the Berends-Giele recursive relations for the currents [38] and the more recent BCFW (Britto, Cachazo, Feng and Witten) recursion relations for on-shell tree-level amplitudes that reconstruct the result from its poles using simple Cauchy theorem [18, 19].

3.1 BCFW recursion relations

For concreteness let us consider tree-level stripped on-shell amplitudes of n massless particles in $SU(N)$ Yang-Mills theory (“gluodynamics”).⁵ The partial amplitude \mathcal{M}_n is a

⁴Scattering amplitudes of gluons where two of them have negative helicity and the other ones have positive helicity.

⁵The recursion relations can be also formulated for more general cases and also for massive particles. See [39] for more details.

gauge-invariant rational function of external momenta and additional quantum numbers h (helicities in case of gluons)

$$\mathcal{M}_n \equiv \mathcal{M}_n(p_1, p_2, \dots, p_n; h_1, h_2, \dots, h_n). \quad (3.1)$$

The external momenta are generically complex but if we are interested in physical amplitudes we can set them to be real in the end. Let us pick two arbitrary indices i, j and perform following shift.

$$p_i \rightarrow p_i(z) = p_i + zq, \quad p_j \rightarrow p_j(z) = p_j - zq \quad (3.2)$$

such that the momentum q is orthogonal to both p_i and p_j , ie. $q^2 = (q \cdot p_i) = (q \cdot p_j) = 0$ and the shifted momenta remain on-shell. Let us note that such q can be found only for the case of spacetime dimensions $d \geq 4$. The amplitude becomes a meromorphic function $\mathcal{M}_n(z)$ of complex parameter z with only simple poles. The original expression corresponds to $z = 0$. If $\mathcal{M}_n(z)$ vanishes for $z \rightarrow \infty$ we can use the Cauchy theorem to reconstruct $\mathcal{M}_n = \mathcal{M}_n(0)$,

$$0 = \frac{1}{2\pi i} \int_{C(\infty)} \frac{dz}{z} \mathcal{M}_n(z) = \mathcal{M}_n(0) + \sum_k \frac{\text{Res}(\mathcal{M}_n, z_k)}{z_k} \quad (3.3)$$

where $C(\infty)$ is closed contour at infinity. \mathcal{M}_n can be then expressed as

$$\mathcal{M}_n = - \sum_k \frac{\text{Res}(\mathcal{M}_n, z_k)}{z_k} \quad (3.4)$$

where k is sum of all residues of $\mathcal{M}_n(z)$ in the complex z -plane. Residues of $\mathcal{M}_n(z)$ can be straightforwardly calculated for the following reason: the only poles of \mathcal{M}_n are $p_{a,b}^2 = 0$ where $p_{a,b} = (p_a + p_{a+1} + \dots + p_b)$. The poles of $\mathcal{M}_n(z)$ have still the same locations just shifted, namely $p_{a,b}^2(z) = 0$ where $i \in (a, a+1, \dots, b)$ or $j \in (a, a+1, \dots, b)$. If none of the indices i, j or both of them are in this range, the dependence on z in $p_{a,b}(z)$ cancels and it is not pole in z anymore. It is easy to identify all locations of the corresponding poles z_{ab} . Suppose that particle $i \in (a, a+1, \dots, b)$,

$$p_{a,b}^2(z) = (p_a + \dots + p_{i-1} + (p_i + zq) + p_{i+1} + \dots + p_b)^2 = 0 \quad \Rightarrow \quad z_{a,b} = - \frac{p_{a,b}^2}{2(q \cdot p_{a,b})}. \quad (3.5)$$

In the original amplitude \mathcal{M}_n the residue on the pole $p_{a,b}^2 = 0$ is given by unitarity: on the factorization channel with given helicity the amplitude factorizes into two sub-amplitudes, and therefore

$$\text{Res}(\mathcal{M}_n, z_{a,b}) = \sum_{h_{ab}} \mathcal{M}_L(z_{a,b})^{-h_{ab}} \frac{i}{2(q \cdot p_{a,b})} \mathcal{M}_R^{h_{ab}}(z_{a,b}) \quad (3.6)$$

where the summation over the helicities h_{ab} of the one-particle intermediate state is taken. The “left” and “right” sub-amplitudes $\mathcal{M}_{L,R}^{\pm h_{ab}}(z_{a,b})$ are

$$\mathcal{M}_L^{-s_{ab}}(z_{a,b}) = \mathcal{M}_{b-a+2}(p_a, \dots, p_i(z_{a,b}), \dots, p_b, -p_{a,b}(z_{a,b}); h_a, \dots, -h_{ab}) \quad (3.7)$$

$$\mathcal{M}_R^{s_{ab}}(z_{a,b}) = \mathcal{M}_{n-(b-a)}(p_{a,b}(z_{a,b}), p_{b+1}, \dots, p_j(z_{a,b}), \dots, p_{a-1}; h_{ab}, \dots, h_{a-1}). \quad (3.8)$$

The amplitude \mathcal{M}_n can be then written as

$$\mathcal{M}_n = \sum_{ab, h_{ab}} \mathcal{M}_L^{-h_{ab}}(z_{a,b}) \frac{i}{p_{a,b}^2} \mathcal{M}_R^{h_{ab}}(z_{a,b}). \quad (3.9)$$

It is convenient to choose i and j to be adjacent because it eliminates the number of factorization channels we have to consider.

3.2 Reconstruction formula with subtractions

The BCFW recursion relations discussed above are very generic and applicable for a large class of theories. The main restriction is the requirement of large z behavior: $\mathcal{M}_n(z) \rightarrow 0$ for $z \rightarrow \infty$. However, this behavior is not guaranteed in general and there exist examples when it is broken no matter which pair of momenta p_i and p_j is chosen to be shifted. In such a case, an additional term (dubbed *boundary term*) is present on the right hand side of eq. (3.9). The boundary term, which is hard to obtain in general case, has been studied by various methods in the series of papers [40, 41] and [42], however no general solution is still available. Sometimes this problem can be cured by means of considering more general approach when all the external momenta p_k are deformed (such an *all-line shift* has been introduced in [43], see also [44])

$$p_k \rightarrow p_k(z) = p_k + zq_k, \quad (3.10)$$

where z is a complex parameter and q_k are appropriate vectors compatible with the requirements of the momentum conservation and on-shell constraint for $p_k(z)$, ie. $p_k \cdot q_k = q_k^2 = 0$. The on-shell amplitude

$$\mathcal{M}_n(z) \equiv \mathcal{M}_n(p_1(z), p_2(z), \dots, p_n(z)) \quad (3.11)$$

become again meromorphic function of the variable z the only singularities of which are simple poles and the residue at these poles have the simple structure (3.6) dictated by unitarity. In some cases the desired behavior $\mathcal{M}_n(z) \rightarrow 0$ for $z \rightarrow \infty$ can be achieved in this way. However, in general case the behavior of $\mathcal{M}_n(z)$ for $z \rightarrow \infty$ is power-like with non-negative power of z . This fact requires some modification of the reconstruction procedure.

This can be done as follows. Let us suppose that we have made any (linear) deformation of the external momenta $p_k \rightarrow p_k(z)$ in such a way that the deformed amplitude $\mathcal{M}_n(z)$ is a meromorphic function the only singularities of which are simple poles and let us assume the following asymptotic behavior

$$\mathcal{M}_n(z) \approx z^k \quad (3.12)$$

when $z \rightarrow \infty$. Let us denote the poles of $\mathcal{M}_n(z)$ as z_i , $i = 1, 2, \dots, n$. Assume a_j , $j = 1, 2, \dots, k+1$ to be complex numbers satisfying $|a_j| < R$ different from the poles z_i . Then we can write for $z \neq a_j$ inside the disc $D(R)$ (i.e. inside the domain $|z| < R$ the boundary

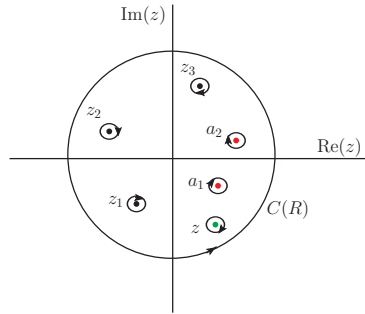


Figure 2. Illustration of the contour used for the derivation of the subtracted Cauchy formula (3.14) with $k = 1$ and $n_{C(R)} = 3$.

of which is a circle $C(R)$ of the radius R the following “ $k + 1$ times subtracted Cauchy formula” (see figure 2)

$$\begin{aligned} & \frac{1}{2\pi i} \int_{C(R)} dw \frac{\mathcal{M}_n(w)}{w - z} \prod_{j=1}^{k+1} \frac{1}{w - a_j} \\ &= \mathcal{M}_n(z) \prod_{j=1}^{k+1} \frac{1}{z - a_j} + \sum_{j=1}^{k+1} \frac{\mathcal{M}_n(a_j)}{a_j - z} \prod_{l=1, l \neq j}^{k+1} \frac{1}{a_j - a_l} + \sum_{i=1}^{n_{C(R)}} \frac{\text{Res}(\mathcal{M}_n; z_i)}{z_i - z} \prod_{j=1}^{k+1} \frac{1}{z_i - a_j}. \end{aligned} \quad (3.13)$$

Here $z_1, z_2, \dots, z_{n_{C(R)}}$ are the poles inside $D(R)$ and $\text{Res}(\mathcal{M}_n; z_i)$ are corresponding residues. In the limit $R \rightarrow \infty$ the integral vanishes due to (3.12) and $D(\infty)$ will contain all n poles. As a result we get a reconstruction formula with $k + 1$ subtractions

$$\mathcal{M}_n(z) = \sum_{i=1}^n \frac{\text{Res}(\mathcal{M}_n; z_i)}{z - z_i} \prod_{j=1}^{k+1} \frac{z - a_j}{z_i - a_j} + \sum_{j=1}^{k+1} \mathcal{M}_n(a_j) \prod_{l=1, l \neq j}^{k+1} \frac{z - a_l}{a_j - a_l}. \quad (3.14)$$

This is the desired generalization of the usual prescription. In order to reconstruct the amplitude with the asymptotic behavior (3.12) from its pole structure, we need therefore along with the residues at the poles z_i (which are fixed by unitarity) also supplementary information, namely the $k + 1$ values $\mathcal{M}_n(a_j)$ of the amplitude at the points a_j . Such additional information is the weakest point of the relations (3.14): there exists no universal recipe how to get the values $\mathcal{M}_n(a_j)$ for a general theory. This corresponds to the well known analogous situation of $k + 1$ subtracted dispersion relations, which allow to reconstruct a general amplitude from its discontinuities uniquely up to the $k + 1$ generally unknown subtraction constants. Note that, provided we choose a_j in such a way that $\mathcal{M}_n(a_j) = 0$ (i.e. a_j are the roots of the deformed amplitude $\mathcal{M}_n(z)$), we can reproduce the formula

$$\mathcal{M}_n(z) = \sum_{i=1}^n \frac{\text{Res}(\mathcal{M}_n; z_i)}{z - z_i} \prod_{j=1}^{k+1} \frac{z - a_j}{z_i - a_j} \quad (3.15)$$

first written in this context by Benincasa and Conde [45] and further discussed by Bo Feng, Yin Jia, Hui Luo and Mingxing Luo in [46].

4 BCFW-like relations for semi-on-shell amplitudes

The straightforward application of the BCFW reconstruction procedure is not possible for the $SU(N)$ nonlinear sigma model because the amplitudes $\mathcal{M}_n(z)$ do not have appropriate asymptotic behavior for $z \rightarrow \infty$. The reason is that due to the derivative coupling of the Goldstone bosons the interaction vertices are quadratic in the momenta. Therefore after the BCFW shift the vertices along the “hard” z -dependent line of the Feynman graph are in general linear in z and the linear large z behavior of the propagators cannot compensate for it. For instance, under the shift⁶ (3.2) with $i = 1, j = 2$ we get for the 6pt amplitude (2.34) for $z \rightarrow \infty$

$$\mathcal{M}_6(z) = -2z \left(\frac{(q \cdot p_{2,3})(s_{1,4} + s_{4,5} - s_{1,3})}{s_{1,3}} + \frac{(q \cdot p_{2,5})(q \cdot p_{2,3})}{(q \cdot p_{2,4})} + \frac{(q \cdot p_{2,5})(s_{3,4} + s_{4,5} - s_{3,5})}{s_{3,5}} \right) + O(z^0). \quad (4.1)$$

and analogously $\mathcal{M}_n(z) = O(z)$ for general⁷ n . As discussed in the previous section, in order to reconstruct such an amplitude from its pole structure, it would be sufficient to know the values of $\mathcal{M}_n(z)$ for two fixed values of z . However, such an information is difficult to gain solely from the Feynman graph analysis restricted only to the amplitudes \mathcal{M}_n . It is therefore useful to take into account also more flexible objects, namely the semi-on-shell amplitudes, which unlike the on-shell amplitudes depend on the parametrization of the matrix U and from which the on-shell amplitudes can be straightforwardly derived. As we would like to show in this section, appropriate choice of parametrization together with suitable way of BCFW-like deformation of the semi-on-shell amplitudes allows to substitute for the missing information on the amplitudes \mathcal{M}_n and to construct generalized BCFW-like relations for them.

4.1 Semi-on-shell amplitudes and Berends-Giele relations

The semi-on-shell amplitudes $J_n^{a_1 a_2 \dots a_n}(p_1, p_2, \dots, p_n)$ (or *currents* in the terminology of the original paper [38], where they were introduced for QCD and more generally for the $SU(N)$ Yang-Mills theory) can be defined in our case as the matrix elements of the Goldstone boson field $\phi^a(0)$ between vacuum and the n Goldstone boson states $|\pi^{a_1}(p_1) \dots \pi^{a_n}(p_n)\rangle$

$$J_n^{a_1 a_2 \dots a_n}(p_1, p_2, \dots, p_n) = \langle 0 | \phi^a(0) | \pi^{a_1}(p_1) \dots \pi^{a_n}(p_n) \rangle. \quad (4.2)$$

Here the momentum p_{n+1} attached to $\phi^a(0)$

$$p_{n+1} = - \sum_{j=1}^n p_j. \quad (4.3)$$

is off-shell. Note that $J_n^{a_1 a_2 \dots a_n}(p_1, p_2, \dots, p_n)$ has a pole for $p_{n+1}^2 = 0$.

⁶Under the all-line (anti)holomorphic BCFW shift the large z behavior is the same. Here we can use the general formulae derived in [44] which relate the number n of external particles, the sum H of their helicities and the overall dimension c of the couplings to the asymptotics of the amplitude under the all-line

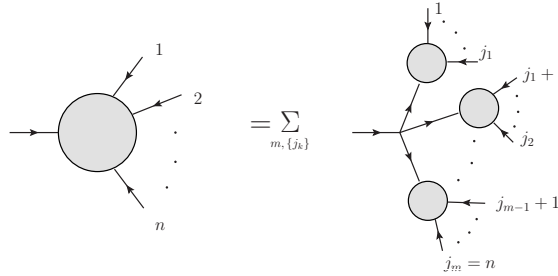


Figure 3. Graphical representation of the Berends-Giele recursive relations

In complete analogy with the on-shell amplitudes, at the tree level the right hand side of (4.2) can be expressed in terms of the flavor-stripped semi-on-shell amplitudes $J_n(p_1, p_2, \dots, p_n)$ in the form

$$\langle 0 | \phi^a(0) | \pi^{a_1}(p_1) \dots \pi^{a_n}(p_n) \rangle_{\text{tree}} = \sum_{\sigma \in S_n} \text{Tr}(t^a t^{a_{\sigma(1)}} \dots t^{a_{\sigma(n)}}) J_n(p_{\sigma(1)}, p_{\sigma(2)}, \dots, p_{\sigma(n)}). \quad (4.4)$$

Let us note that, at higher orders in the loop expansion the group structure contains also multiple trace terms. We normalize the one particle states according to

$$J_1(p) = 1. \quad (4.5)$$

In this section the above semi-on-shell flavor-stripped amplitudes $J_n(p_1, p_2, \dots, p_n)$ will be the main subject of our interest. The on-shell stripped amplitudes $\mathcal{M}(p_1, p_2, \dots, p_{n+1})$ can be extracted from them by means of the Lehmann-Symanzik-Zimmermann (LSZ) formulas

$$\mathcal{M}(p_1, p_2, \dots, p_{n+1}) = - \lim_{p_{n+1}^2 \rightarrow 0} p_{n+1}^2 J_n(p_1, p_2, \dots, p_n). \quad (4.6)$$

The main advantage of the semi-on-shell amplitudes $J_n(p_1, p_2, \dots, p_n)$ (in what follows we also use short-hand notation $J(1, 2, \dots, n)$) is that they allow to abandon the Feynman diagram approach using appropriate recursive relation. The latter has been first formulated by Berends and Giele in the context of QCD [38] and proved to be very efficient for the calculation of the tree-level multi-gluon amplitudes. For the $U(N)$ nonlinear sigma model the generalized recurrent relations of Berends-Giele type can be written in the form (see figure 3)

$$J(1, 2, \dots, n) = \frac{i}{p_{1,n}^2} \sum_{m=2}^n \sum_{\{j_k\}} i V_{m+1}(p_{1,j_1}, p_{j_1+1,j_2}, \dots, p_{j_{m-1}+1,n}, -p_{1,n}) \prod_{k=1}^m J(j_{k-1}+1, \dots, j_k) \quad (4.7)$$

holomorphic ($O(z^a)$) and anti-holomorphic ($O(z^s)$) shift. These formulae reads $2s = 4 - n - c + H$ and $2a = 4 - n - c - H$. In our case $H = 0$ and the only coupling constant is F^{-1} , therefore $c = 2 - n$, therefore in general case $a = s = 1$ independently on n .

⁷The general statement can be derived by induction from Berends-Giele recursive relations discussed in the next subsection.

n	2	3	4	5	6	7	8	9	10	11
$t(2n+1)$	4	12	33	88	232	609	1 596	4 180	10 945	28 656
$b(2n+1)$	5	17	50	138	370	979	2 575	6 755	17 700	46 356
$f(2n+1)$	4	21	126	818	5 594	39 693	289 510	2 157 150	16 348 960	125 642 146
$t_4(2n+1)$	3	6	10	15	21	28	36	45	55	66
$b_4(2n+1)$	4	10	20	35	56	84	120	165	220	286
$f_4(2n+1)$	3	12	55	273	1 428	7 752	43 263	246 675	1 430 715	8 414 640

Table 1. A comparison of the number t of the terms on the right hand side of the Berends-Giele recursive relation with the total number b of terms needed for the Berends-Giele recursive calculation of the amplitude $J(1, 2, \dots, 2n+1)$ and with the total number f of flavor ordered Feynman graphs contributing to the same amplitude. In the last three row we compare these numbers with the analogous ones for the case of “ ϕ^4 theory”.

where the sum is over all splittings of the ordered set $\{1, 2, \dots, n\}$ into m non-empty ordered subsets $\{j_{k-1} + 1, j_{k-1} + 2, \dots, j_k\}$, (here $j_0 = 0$ and $j_m = n$),⁸ V_{m+1} is the flavor-stripped Feynman rule for vertices with $m+1$ external legs and $p_{i,k} = \sum_{j=i}^k p_j$ as above.

Let us note that, because the Lagrangian of the nonlinear sigma model includes infinite number of vertices with increasing number of fields, the above Berends-Giele relation for J_n have to contain vertices up to $n+1$ legs, i.e. much more terms than in the case of power-counting renormalizable theories like QCD where the number of vertices is finite.⁹ This fact rather reduces the efficiency of these relation for the calculations of the amplitudes. We illustrate this in the table 1, where the number of terms on the right hand side of the Berends-Giele relation (4.7) written for J_{2n+1} (denoted as $t(2n+1)$) and the total number of terms necessary for the calculation of the same semi-on-shell amplitude using the Berends-Giele recursion (denoted as $b(2n+1)$) is compared with the total number $f(2n+1)$ of the flavor ordered Feynman graphs contributing to J_{2n+1} and with the same numbers valid for the theory with only quadrilinear vertices (“ ϕ^4 theory”) denoted with subscript “4”. See appendix C for more details and for derivation of the explicit formulae for these and other related cases.

On the other hand, as we will see in what follows, the Berends-Giele relations can be used as a very suitable tool for the investigation of the general properties of the semi-on-shell amplitudes. Let us mention e.g. the following simple relations valid for $J(1, 2, \dots, n)$

$$J(1, 2, \dots, 2n) = 0 \quad (4.8)$$

$$J(1, 2, \dots, n) = J(n, n-1, \dots, 2, 1). \quad (4.9)$$

These relation are valid independently on the field redefinition. However, as we shall see in what follows, some properties of the semi-on-shell amplitudes are not valid universally and are tightly related to a given parametrization.

⁸Explicitly

$$\sum_{\{j_k\}} \equiv \sum_{j_1=1}^{n-m+1} \sum_{j_2=j_1+1}^{n-m+2} \cdots \sum_{j_{m-1}=j_{m-2}+1}^{n-m+(m-1)}.$$

⁹The number of terms on the right hand side of (4.7) grows exponentially with increasing n in contrast to the polynomial growths typical for the renormalizable theories. See appendix C for details.

4.2 Cayley parametrization

Unlike the on-shell amplitudes $\mathcal{M}^{a_1 \dots a_n}(p_1, p_2, \dots, p_n)$, which are physical observables and do not depend on the choice of the field variables provided the different choices are related by means of admissible (generally nonlinear) transformations, the concrete form of $J_n^{a_1 \dots a_n}(p_1, p_2, \dots, p_n)$ as well as the flavor-stripped amplitudes $J_n(p_1, p_2, \dots, p_n)$ depends on the parametrization of the $U(N)$ nonlinear sigma model. In what follows we will almost exclusively use the so called Cayley parameterizations

$$U = \frac{1 + \frac{i}{\sqrt{2F}}\phi}{1 - \frac{i}{\sqrt{2F}}\phi} = 1 + 2 \sum_{n=1}^{\infty} \left(\frac{i}{\sqrt{2F}}\phi \right)^n, \quad (4.10)$$

where the Goldstone boson fields are arranged into the hermitian matrix $\phi = \phi^a t^a$ with t^a being the $U(N)$ generators. As described in appendix A, representation (4.10) is a special member of a wide class of parameterizations suited for the construction of the flavor-stripped Feynman rules. The interrelation between the field ϕ and analogous field $\tilde{\phi}$ of the more usual exponential parametrization $U = \exp\left(\frac{i}{F}\tilde{\phi}\right)$ is through the following admissible nonlinear field redefinition

$$\phi = 2F \tan\left(\frac{i}{2F}\tilde{\phi}\right) = \tilde{\phi} + O(\tilde{\phi}^3). \quad (4.11)$$

As is shown in appendix A, the flavor-stripped Feynman rules for vertices read in the Cayley parametrization

$$V_{2n+1} = 0 \quad (4.12)$$

$$V_{2n+2} = -\frac{(-1)^n}{2^{n+1}} \left(\frac{1}{F}\right)^{2n} \sum_{j=0}^n \sum_{i=1}^{2n+2} (p_i \cdot p_{i+2j+1}) = \frac{(-1)^n}{2^n} \left(\frac{1}{F}\right)^{2n} \left(\sum_{i=0}^n p_{2i+1}\right)^2,$$

where we have used the momentum conservation in the last row. For the first non-trivial vertex V_4 we get

$$V_4 = -\frac{1}{2F^2}(p_1 + p_3)^2 = -\frac{1}{2F^2}(p_2 + p_4)^2 \quad (4.13)$$

and the first two non-trivial semi-on-shell amplitudes read in the Cayley parametrization

$$J(1, 2, 3) = \frac{1}{2F^2 p_4^2} (p_1 + p_3)^2 \quad (4.14)$$

$$J(1, 2, 3, 4, 5) = \frac{1}{4F^4 p_6^2} \left[\frac{(p_1 + p_2 + p_3 + p_5)(p_1 + p_3)^2}{(p_1 + p_2 + p_3)^2} + \frac{(p_1 + p_3 + p_4 + p_5)^2 (p_3 + p_5)^2}{(p_3 + p_4 + p_5)^2} + \frac{(p_1 + p_5)^2 (p_2 + p_4)^2}{(p_2 + p_3 + p_4)^2} - (p_1 + p_3 + p_5)^2 \right] \quad (4.15)$$

Let us illustrate explicitly the dependence of the semi-on-shell amplitudes on the parametrization. Using the exponential one we obtain different amplitude $J(1, 2, 3)$, namely

$$J(1, 2, 3)_{\text{exp}} = -\frac{1}{6F^2} \frac{(p_1 + p_2)^2 + (p_2 + p_3)^2 - 2(p_1 + p_3)^2}{p_4^2}. \quad (4.16)$$

However, both $J(1, 2, 3)$ and $J(1, 2, 3)_{\text{exp}}$ give the same on-shell amplitude (2.33).

In the next subsection we will prove additional useful properties of the semi-on-shell amplitudes.

4.3 Scaling properties of semi-on-shell amplitudes

The Cayley parametrization is specific in the sense that the semi-on-shell amplitudes $J_n(p_1, \dots, p_n)$ in this parametrization obey simple scaling properties when some subset of the momenta p_i are scaled $p_i \rightarrow tp_i$ and the scaling parameter t is then sent to zero. Here we will study two important scaling limits, corresponding to the case when *all odd* or *all even* on-shell momenta are scaled. As we shall see in the following section, these two scaling limits are the key ingredients for the construction of the BCFW-like relations for semi-on-shell amplitudes in the Cayley parametrization.

We will prove that for $n > 1$ and $t \rightarrow 0$

$$J_{2n+1}(tp_1, p_2, tp_3, p_4, \dots, p_{2r}, tp_{2r+1}, p_{2r+2}, \dots, p_{2n}, tp_{2n+1}) = O(t^2) \quad (4.17)$$

and

$$\lim_{t \rightarrow 0} J_{2n+1}(p_1, tp_2, p_3, tp_4, \dots, tp_{2r}, p_{2r+1}, tp_{2r+2}, \dots, tp_{2n}, p_{2n+1}) = \frac{1}{(2F^2)^n}. \quad (4.18)$$

The general proof of (4.17) and (4.18) is by induction. Let us first verify the base cases. While the second statement holds already for $n = 1$

$$J_3(p_1, tp_2, p_3) = \frac{1}{F^2} \frac{(p_1 \cdot p_3)}{(p_1 + tp_2 + p_3)^2} \rightarrow \frac{1}{2F^2}, \quad (4.19)$$

the first one is not valid unless $n = 2$. Indeed

$$J_3(tp_1, p_2, tp_3) = \frac{1}{2F^2} \frac{t(p_1 \cdot p_3)}{(p_1 \cdot p_2) + (p_2 \cdot p_3) + t(p_1 \cdot p_3)} = O(t). \quad (4.20)$$

On the other hand, using the explicit form of J_5 (cf. (4.15)) we get

$$J_5(tp_1, p_2, tp_3, p_4, tp_5) = O(t^2); \quad (4.21)$$

we can therefore proceed by induction starting at $n = 2$.

Let us first prove the scaling property (4.17). Suppose, that (4.17), (4.18) holds for all \bar{n} , where $1 < \bar{n} < n$ and write for the left hand side of (4.17) the Berends-Giele relation (4.7) expressing J_{2n+1} in terms of $J_{2\bar{n}+1}$ with $\bar{n} < n$. After the scaling $p_{2k+1} \rightarrow tp_{2k+1}$, the $t \rightarrow 0$ behavior of p_{2n+2}^2 and V_{m+1} is $O(t^0)$ and $O(t^r)$ where $r \geq 0$ respectively. The scaling of the remaining semi-on-shell amplitudes on the right hand side of (4.7) can be deduced from the induction hypothesis. Note that it depends on the number of the external on-shell legs of $J(j_{i-1} + 1, \dots, j_i)$ as well as on the parity of $j_{i-1} + 1$, because the semi-on-shell amplitude with scaled even or odd momenta scales differently. Namely, according to the induction hypothesis, the scaling of these building blocks of the right hand side of (4.7) is as follows (see figure 4)

$$\begin{aligned} J(j) = 1 = O(t^0), \quad J(2j-1, 2j, 2j+1) = O(t), \quad J(2j, \dots, 2k) = O(t^0), \\ J(2j+1, \dots, 2k+1) = O(t^2) \quad \text{for } k-j > 1. \end{aligned} \quad (4.22)$$

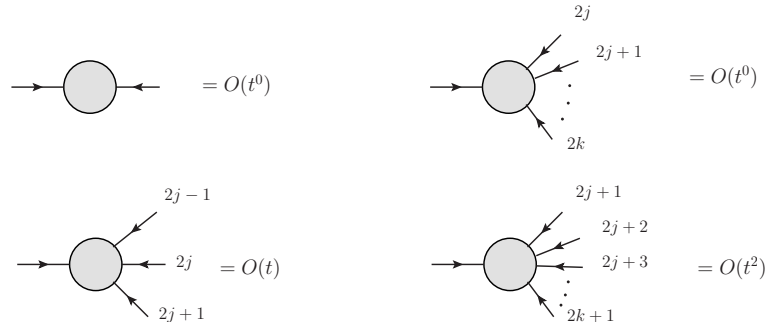


Figure 4. Scaling of the building blocks on the right hand hand of the Berends-Giele recursion relation according to the induction hypothesis when the odd momenta are scaled.

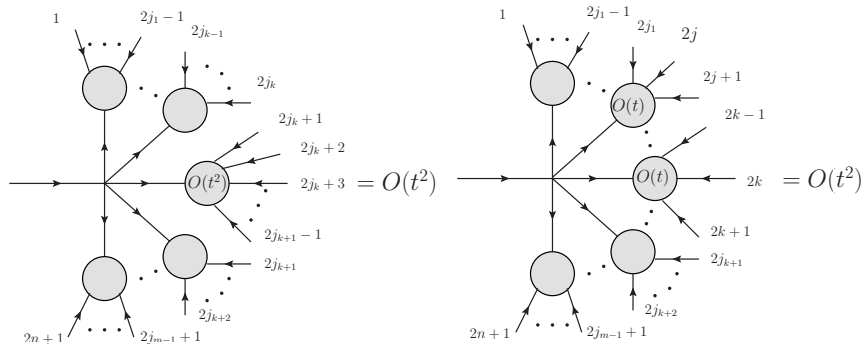


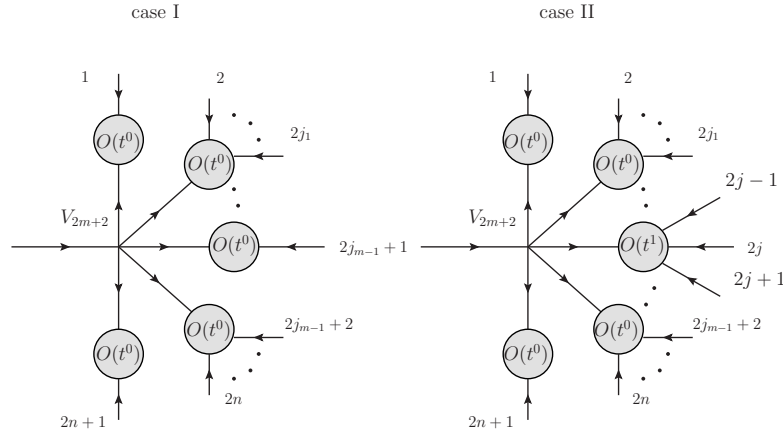
Figure 5. The terms on the right hand hand of the Berends-Giele recursion relation which are automatically $O(t^2)$ using the induction hypothesis when the odd momenta are scaled.

This implies, that those terms of Berends-Giele relations which are depicted in figure 5, i.e. those which contain at least one block $J(2j + 1, \dots, 2k + 1) = O(t^2)$ with $k - j > 1$ or at least two building blocs $J(2j - 1, 2j, 2j + 1)$ are automatically $O(t^2)$. Therefore, the only dangerous terms on the right hand side of (4.7) are those without the buildings block of the type $J(2j + 1, \dots, 2k + 1) = O(t^2)$ with $k - j > 1$ and at the same time without (case I) or with just one (case II) building block $J(2j - 1, 2j, 2j + 1) = O(t)$ (see figure 6). To these terms the induction hypothesis cannot be applied directly.

In the case I, the odd lines of the corresponding vertex V_{2m+2} are attached to $J(2j_k + 1) = 1$ and such a vertex is then proportional to the squared sum of the odd momenta tp_{2j_k+1} , (cf. (4.13))

$$V_{2m+2}(tp_1, p_{2,2j_1}, tp_{2j_1+1}, \dots, tp_{2n+1}) \sim (tp_1 + tp_{2j_1+1} + \dots + tp_{2n+1})^2 \quad (4.23)$$

which means that it scales as $O(t^2)$. This is in fact the scaling of the complete contribution of the terms in the case I, because all the remaining building blocs are of the order $O(t^0)$ for $t \rightarrow 0$.



$$V_{2m+2} \sim (tp_1 + tp_{2j_1+1} + \dots + tp_{2n+1})^2 = O(t^2), \quad V_{2m+2} \sim (tp_{2j-1} + p_{2j} + tp_{2j+1} + \sum_k tp_{2j_k+1})^2 = O(t^1)$$

Figure 6. Typical terms on the right hand hand of the Berends-Giele recursion relation to which the induction hypothesis (4.17) cannot be applied directly. In both cases, to all (case I) or to all but one (case II) odd lines of the vertex the blocks J_1 are attached. In the case II, one building block J_3 is attached to remaining odd line.

In the case II with exactly one building block $J_3(tp_{2j-1}, p_{2j}, tp_{2j+1}) = O(t)$ (note that, it has to be attached to the odd line of the vertex V_{2m+2}), all the other odd lines of V_{2m+2} are attached to $J(2j_k + 1) = 1$ and such a vertex is then proportional to the squared sum of the momenta tp_{2j_k+1} and the momentum of the line which is attached to $J_3(tp_{2j-1}, p_{2j}, tp_{2j+1})$, namely

$$V_{2m+2} \sim \left(tp_{2j-1} + p_{2j} + tp_{2j+1} + \sum_k tp_{2j_k+1} \right)^2 = O(t). \quad (4.24)$$

Therefore the complete contribution of the dangerous terms in the case II is in fact $O(t^2)$ for $t \rightarrow 0$ because both V_{2m+2} and $J_3(tp_{2j-1}, p_{2j}, tp_{2j+1})$ scale as $O(t)$ and again all the remaining building blocks are of the order $O(t^0)$ for $t \rightarrow 0$. All the other “non-dangerous” terms on the right hand side of the Berends-Giele relations scale at least as $O(t^2)$, which finishes the proof of (4.17).

Let us now prove (4.18), i.e. the case when all even momenta are scaled. Suppose validity of this relation for $\bar{n} < n$ and again write the Berends-Giele relation for the left hand side of (4.18). Thanks to the just proven statement (4.17), the terms on the right hand side of (4.7) with at least one building block $J(j_k + 1, \dots, j_{k+1})$ with odd j_k and $j_{k+1} - j_k > 1$ do not contribute in the limit $t \rightarrow 0$. Such a block can be attached only to the even line of the vertex V_{m+1} . Therefore, the only terms which can contribute in the limit $t \rightarrow 0$ have the form depicted in figure 7, i.e. those with the building blocks J_1 attached to all even lines of the vertex.

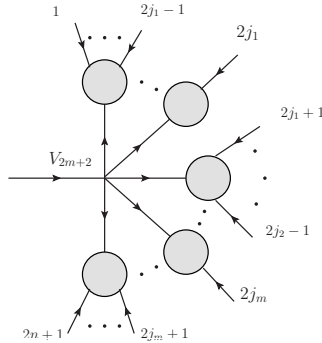


Figure 7. Typical terms on the right hand hand of the Berends-Giele recursion relation which contribute to (4.18). Here to all even lines of the vertex the blocks J_1 are attached.

According to the induction hypothesis and using the explicit form of V_{2k+2} this gives for $t \rightarrow 0$

$$-\frac{(-1)^k}{2^k F^{2k}} \prod_{l=1}^{k+1} \frac{1}{(2F^2)^{j_l - j_{l-1} - 1}} = -\frac{(-1)^k}{2^n F^{2n}} \quad (4.25)$$

where we denote $j_0 = 0$ and $j_{k+1} = n + 1$. Sum of all such contributions is

$$\sum_{k=1}^n \sum_{1 \leq j_1 < j_2 < \dots < j_k \leq n} \frac{(-1)^{k-1}}{2^n F^{2n}} = \frac{1}{2^n F^{2n}} \sum_{k=1}^n \binom{n}{k} (-1)^{k-1} = \frac{1}{2^n F^{2n}}, \quad (4.26)$$

which finishes the proof.

Another independent scaling properties of the semi-on-shell amplitudes J_{2n+1} can be proven using the same strategy. For instance, when all odd momenta and one additional even momentum (say p_{2r}) are scaled, we get

$$\lim_{t \rightarrow 0} J_{2n+1}(tp_1, p_2, tp_3, p_4, \dots, tp_{2r-1}, tp_{2r}, tp_{2r+1}, \dots, p_{2N}, tp_{2n+1}) = 0 \quad (4.27)$$

for $n > 1$. We postpone the proof to the appendix D.

Let us note that due to the homogeneity of $J(1, 2, \dots, 2n+1)$ we can rewrite the relations (4.17) and (4.18) as a statement on the asymptotic behavior of the scaled amplitudes for $t \rightarrow \infty$, namely

$$\lim_{t \rightarrow \infty} J_{2n+1}(tp_1, p_2, \dots, p_{2n}, tp_{2n+1}) = \lim_{t \rightarrow \infty} J_{2n+1}(p_1, t^{-1}p_2, \dots, t^{-1}p_{2n}, p_{2n+1}) = \frac{1}{(2F^2)^n} \quad (4.28)$$

and

$$J_{2n+1}(p_1, tp_2, \dots, tp_{2n}, p_{2n+1}) = J_{2n+1}(t^{-1}p_1, p_2, \dots, p_{2n}, t^{-1}p_{2n+1}) = O(t^{-2}). \quad (4.29)$$

4.4 BCFW reconstruction

As we have mentioned in the previous subsection, the standard BCFW-like deformation of the external momenta p_i yields deformed amplitudes which behave as a non-negative power

of z for $z \rightarrow \infty$. As a result, for the reconstruction of the amplitude from its pole structure we need to use the general reconstruction formula (3.14) for which additional information on the on-shell amplitude (its values at several points) is necessary. However, such an information is not at our disposal. We solve this problems by the following trick: we relax some demands placed on the usual BCFW-like deformation and allow more general ones for which either the reconstruction formula without subtractions can be applied or additional information on the deformed amplitudes is accessible. The momentum conservation cannot be evidently avoided, what remains is the on-shell condition of all the external momenta. It seems therefore to be natural to relax this constraint and instead of the on-shell amplitudes \mathcal{M}_{2n+2} to use the semi-on-shell amplitudes J_{2n+1} , or the cut semi-on-shell amplitudes M_{2n+1} defined as

$$M_{2n+1}(p_1, \dots, p_{2n+1}) = p_{1,2n+1}^2 J_{2n+1}(p_1, \dots, p_{2n+1}). \quad (4.30)$$

Motivated by the results of the previous section let us assume the following deformation of the semi-on-shell amplitude M_{2n+1} in the Cayley parametrization

$$M_{2n+1}(z) \equiv M_{2n+1}(p_1, zp_2, p_3, zp_4, \dots, zp_{2r}, p_{2r+1}, zp_{2r+2}, \dots, zp_{2n}, p_{2n+1}) \quad (4.31)$$

i.e. all even momenta are scaled by the complex parameter z and the odd momenta are not deformed

$$p_{2k}(z) = zp_{2k}, \quad p_{2k+1}(z) = p_{2k+1} \quad (4.32)$$

Note that in contrast to the standard BCFW shift this deformation is possible for general number of space-time dimensions d . The physical amplitude corresponds to $z = 1$. For $n = 1$ we get explicitly

$$M_3(z) = \frac{1}{F^2}(p_1 \cdot p_3) \quad (4.33)$$

For general n let us denote the sums of all odd (even) momenta as

$$p_- = \sum_{k=0}^n p_{2k+1}, \quad p_+ = \sum_{k=1}^n p_{2k}. \quad (4.34)$$

Then in general case the function $M_{2n+1}(z)$ has the following important properties:

1. With generic fixed p_i it is a meromorphic function of z with simple poles.
2. The asymptotics of $M_{2n+1}(z)$ can be deduced form the known properties of J_{2n+1} , namely for $n > 1$ we get as a consequence of (4.29)

$$M_{2n+1}(z) = (p_+ z + p_-)^2 J_{2n+1}(p_1, zp_2, \dots, zp_{2n}, p_{2n+1}) = O(z^0). \quad (4.35)$$

3. For $n \geq 1$ we have according to known scaling property (4.18) of J_{2n+1}

$$\lim_{z \rightarrow 0} M_{2n+1}(z) = \frac{1}{(2F^2)^n} p_-^2 \quad (4.36)$$

The first two properties allows us to write for $M_{2n+1}(z)$ the reconstruction formula with one subtraction, i.e. the relation (3.14) with $k = 0$. The third property is the key one for the complete reconstruction and determines both the “subtraction point” $a_1 = 0$ and the “subtraction constant” $M_{2n+1}(a_1) = p_-^2/(2F^2)^n$. The resulting formula reads¹⁰

$$M_{2n+1}(z) = \frac{1}{(2F^2)^n} p_-^2 + \sum_P \frac{\text{Res}(M_{2n+1}, z_P)}{z - z_P} \frac{z}{z_P} \quad (4.37)$$

where the sum is over the poles z_P of $M_{2n+1}(z)$. The position of the poles is known and the corresponding residues can be determined recursively as in usual BCFW relations, however, there are some subtleties.

The poles z_P of $M_{2n+1}(z)$ correspond to the vanishing denominators of the deformed propagators $p_P^2(z) = 0$, where

$$p_P^2(z) \equiv p_{i,j}(z)^2 = 0, \quad \text{for } 2 \leq j - i < 2n \quad (4.38)$$

and where $j - i$ is even; in this formula $p_{i,j}(z) = zp_{i,j}^+ + p_{i,j}^-$ with

$$p_{i,j}^+ = \sum_{i \leq 2k \leq j} p_{2k}, \quad p_{i,j}^- = \sum_{i \leq 2k+1 \leq j} p_{2k+1}, \quad (4.39)$$

i.e. $p_{i,j}^\pm$ is a sum of all even (odd) momenta from the ordered set $p_i, p_{i+1}, \dots, p_{j-1}, p_j$. Explicitly for $j - i > 2$

$$z_{i,j}^\pm = \frac{-(p_{i,j}^+ \cdot p_{i,j}^-) \pm \left(-G(p_{i,j}^+, p_{i,j}^-)\right)^{1/2}}{p_{i,j}^{+2}} \quad (4.40)$$

where $G(a, b) = a^2 b^2 - (a \cdot b)^2$ is the Gram determinant, which is nonzero for generic momenta p_i, \dots, p_j . Therefore in the generic case for $j - i > 2$ we deal with doublets of single poles.

The case of three-particle poles corresponding to $j - i = 2$ has to be treated separately. In this case either $p_{i,j}^{+2} = 0$ or $p_{i,j}^{-2} = 0$ (this sets in for $p_{i,j}^+ = p_{i+1}$ or for $p_{i,j}^- = p_{i+1}$ respectively; let us remind that p_k are on-shell). In the first case we have only one pole

$$z_{2j-1,2j+1} = -\frac{(p_{2j-1} \cdot p_{2j+1})}{p_{2j} \cdot (p_{2j-1} + p_{2j+1})} \quad (4.41)$$

while in the second case we have apparently two poles

$$z_{2j,2j+2}^+ = 0 \quad (4.42)$$

$$z_{2j,2j+2}^- \equiv z_{2j,2j+2} = -\frac{p_{2j+1} \cdot (p_{2j} + p_{2j+2})}{(p_{2j} \cdot p_{2j+2})} \quad (4.43)$$

¹⁰Let us note, that we could write analogous reconstruction formula directly for the currents J_{2n+1} as we did in [49]. In such a case we do not need any subtraction. The price to pay is that we get two more poles, the residues of which cannot be determined recursively from unitarity. Fortunately, the relation (4.29) and the residue theorem can be used in order to obtain the unknown residues in terms of the remaining ones. The resulting formula is fully equivalent to (4.37), however it is a little bit less elegant.

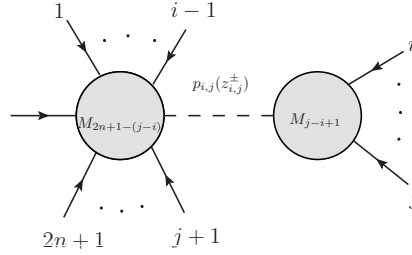


Figure 8. Graphical representation of the right hand side of the relation (4.45).

However $z_{2j,2j+2}^+ = 0$ cannot be a pole according to (4.36) and the corresponding residue has to be zero.

The residues of the function $M_{2n+1}(z)$ are dictated by unitarity and at the poles they factorize (see figure 8). Writing for $j - i > 2$

$$(zp_{i,j}^+ + p_{i,j}^-)^2 = p_{i,j}^{+2}(z - z_{i,j}^+)(z - z_{i,j}^-) \quad (4.44)$$

we get for $j - i > 2$

$$\text{Res}\left(M_{2n+1}, z_{i,j}^{\pm}\right) = \pm \frac{M_L^{(i,j)}(z_{i,j}^{\pm})M_R^{(i,j)}(z_{i,j}^{\pm})}{p_{i,j}^{+2}(z_{i,j}^+ - z_{i,j}^-)} \quad (4.45)$$

where we denoted

$$M_L^{(i,j)}(z_{i,j}^{\pm}) = M_{2n+1-(j-i)}(p_1(z_{i,j}^{\pm}), \dots, p_{i-1}(z_{i,j}^{\pm}), p_{i,j}(z_{i,j}^{\pm}), p_{j+1}(z_{i,j}^{\pm}), \dots, p_{2n+1}(z_{i,j}^{\pm})) \quad (4.46)$$

$$M_R^{(i,j)}(z_{i,j}^{\pm}) = M_{j-i+1}(p_i(z_{i,j}^{\pm}), p_{i+1}(z_{i,j}^{\pm}), \dots, p_j(z_{i,j}^{\pm})). \quad (4.47)$$

Note that, while the amplitude $M_L^{(i,j)}$ remains semi-on-shell, the amplitude $M_R^{(i,j)}$ is fully on-shell, because the deformed momentum $p_{i,j}(z)$ is on-shell for $z = z_{i,j}^{\pm}$.

The formula (4.45) is valid also for the three-particle pole $z_{2j,2j+2}$ given by (4.43). However the pole $z_{2j-1,2j+1}$ deserves a special remark because the corresponding residue is determined by the formula different from (4.45), namely

$$\text{Res}\left(M_{2n+1}, z_{2j-1,2j+1}\right) = \frac{M_L^{(2j-1,2j+1)}(z_{2j-1,2j+1})M_R^{(2j-1,2j+1)}(z_{2j-1,2j+1})}{2p_{2j-1,2j+1}^+ \cdot p_{2j-1,2j+1}^-} \quad (4.48)$$

where $M_{L,R}^{(2j-1,2j+1)}(z_{2j-1,2j+1})$ are given by (4.46) and (4.47) with $z_{i,j}^{\pm}$ replaced by $z_{2j-1,2j+1}$.

To summarize, we have found a closed system of recursive BCFW-like relations for the tree cut semi-on-shell amplitudes M_{2n+1} , which consists of the reconstruction formula (4.37), the pole positions (4.40), (4.41) and (4.43) and the residue formulae (4.45) and (4.48). Note that the initial condition for the recursion (4.33) can be understood as the

special case of (4.37) for $n = 1$ because then there is no pole $z_{i,j}$ with $2 \leq j - i < 2$ and the sum of the residue contributions is empty. The physical amplitude $M_{2n+1}(p_1, \dots, p_{2n+1})$ corresponds to $z = 1$

$$M_{2n+1}(p_1, \dots, p_{2n+1}) = \frac{1}{(2F^2)^n} p_-^2 + \sum_P \frac{\text{Res}(M_{2n+1}, z_P)}{z_P} \frac{1}{1 - z_P}. \quad (4.49)$$

As a final result we get then using (4.45), (4.48), (4.41), (4.43) and (4.44)

$$M_{2n+1}(p_1, \dots, p_{2n+1}) = \frac{1}{(2F^2)^n} p_-^2 + \sum_P M_L^{(P)}(z_P) \frac{R_P}{p_P^2} M_R^{(P)}(z_P). \quad (4.50)$$

Note that there is an extra function R_P in contrast to the standard BCFW formula (3.9), namely

$$R_P = \begin{cases} z_P^{-2} & \text{for } z_P = z_{2j,2j+2} \\ z_P^{-1} & \text{for } z_P = z_{2j-1,2j+1} \\ \frac{1}{z_{i,j}^+ - z_{i,j}^-} \frac{1 - z_{i,j}^-}{z_{i,j}^+} & \text{for } z_P = z_{i,j}^\pm \end{cases} \quad (4.51)$$

For further convenience, we rewrite (4.50) with help of (4.33) in the following more explicit form

$$\begin{aligned} M_{2n+1}(p_1, \dots, p_{2n+1}) &= \frac{1}{(2F^2)^n} p_-^2 + \\ &+ \sum_{j=1}^{n-1} M_L^{(2j,2j+2)}(z_{2j,2j+2}) \frac{1}{p_{2j,2j+2}^2} \frac{p_{2j} \cdot p_{2j+2}}{F^2} \\ &- \sum_{j=1}^n M_L^{(2j-1,2j+1)}(z_{2j-1,2j+1}) \frac{1}{p_{2j-1,2j+1}^2} \frac{p_{2j-1,2j+1}^+ \cdot p_{2j-1,2j+1}^-}{F^2} \\ &+ \sum_{2 < j-i < 2n} \frac{1}{z_{i,j}^+ - z_{i,j}^-} \left(M_L^{(i,j)}(z_{i,j}^+) \frac{1}{p_{i,j}^2} M_R^{(i,j)}(z_{i,j}^+) \frac{1 - z_{i,j}^-}{z_{i,j}^+} - M_L^{(i,j)}(z_{i,j}^-) \frac{1}{p_{i,j}^2} M_R^{(i,j)}(z_{i,j}^-) \frac{1 - z_{i,j}^+}{z_{i,j}^-} \right). \end{aligned} \quad (4.52)$$

The on-shell amplitude is then

$$\mathcal{M}_{2n}(1, 2, \dots, 2n-1; 2n) = - \lim_{p_{1,2n-1}^2 \rightarrow 0} M_{2n-1}(1). \quad (4.53)$$

4.5 Explicit example of application of BCFW relations: 6pt amplitude

As an illustration let us apply the BCFW-like recursive relations (4.37) to the amplitude $M_5(z) \equiv M_5(p_1, zp_2, p_3, zp_4, p_5)$. In this case we have three poles, all of them being three-particle, namely

$$z_{1,3} = 1 - \frac{s_{1,3}}{s_{1,2} + s_{2,3}}, \quad z_{2,4} = \left(1 - \frac{s_{2,4}}{s_{2,3} + s_{3,4}} \right)^{-1}, \quad z_{3,5} = 1 - \frac{s_{3,5}}{s_{3,4} + s_{4,5}} \quad (4.54)$$

where the variables $s_{i,j}$ are given by (2.30). The residues are given by the relations (4.45) for $z_{2,4}$ and (4.48) for $z_{1,3}$ and $z_{3,5}$. After simple algebra using the explicit form of the poles (4.54) we get

$$\begin{aligned}\frac{\text{Res}(M_5, z_{1,3})}{z_{1,3}} &= \frac{1}{4F^4}(1 - z_{1,3})(s_{2,5} - s_{2,4} + s_{3,4} - s_{3,5}) - \frac{1}{4F^4}(s_{1,5} - s_{1,4} - s_{4,5}) \\ \frac{\text{Res}(M_5, z_{3,5})}{z_{3,5}} &= \frac{1}{4F^4}(1 - z_{3,5})(s_{1,4} - s_{1,3} + s_{2,3} - s_{2,4}) - \frac{1}{4F^4}(s_{1,5} - s_{1,2} - s_{2,5}) \\ \frac{\text{Res}(M_5, z_{2,4})}{z_{2,4}} &= \frac{1}{4F^4}(s_{1,5} - s_{1,4} + s_{2,4} - s_{2,5}).\end{aligned}\quad (4.55)$$

Note that the potential unphysical poles $z_{i,j}(p_k) = 0$ have canceled completely. We have also

$$(1 - z_{1,3})^{-1} = \frac{s_{1,2} + s_{2,3}}{s_{1,3}}, \quad (1 - z_{3,5})^{-1} = \frac{s_{3,4} + s_{4,5}}{s_{3,5}}, \quad (1 - z_{2,4})^{-1} = 1 - \frac{s_{2,3} + s_{3,4}}{s_{2,4}}. \quad (4.56)$$

These factors are responsible for setting of the physical poles in the resulting amplitude. After inserting this to the formula (4.49) we get for the individual contributions to the semi-on-shell amplitude in the Cayley parametrization

$$\begin{aligned}\frac{\text{Res}(M_5, z_{1,3})}{z_{1,3}(1 - z_{1,3})} &= \frac{1}{4F^2} \left[\frac{(s_{1,4} + s_{4,5} - s_{1,5})(s_{1,2} + s_{2,3})}{s_{1,3}} + s_{2,5} - s_{2,4} + s_{3,4} - s_{3,5} \right] \\ \frac{\text{Res}(M_5, z_{3,5})}{z_{3,5}(1 - z_{3,5})} &= \frac{1}{4F^2} \left[\frac{(s_{1,2} + s_{2,5} - s_{1,5})(s_{3,4} + s_{4,5})}{s_{3,5}} + s_{1,4} - s_{1,3} + s_{2,3} - s_{2,4} \right] \\ \frac{\text{Res}(M_5, z_{2,4})}{z_{2,4}(1 - z_{2,4})} &= \frac{1}{4F^2} \left[\frac{(s_{1,4} + s_{2,5} - s_{1,5})(s_{2,3} + s_{3,4})}{s_{2,4}} + s_{1,5} - s_{1,4} + s_{2,4} - s_{2,5} - s_{2,3} - s_{3,4} \right] \\ \frac{p_-^2}{4F^2} &= \frac{1}{4F^2} [s_{1,3} - s_{1,2} - s_{2,3} + s_{1,5} - s_{1,4} + s_{2,4} - s_{2,5} + s_{3,5} - s_{3,4} - s_{4,5}].\end{aligned}\quad (4.57)$$

Finally we get

$$\begin{aligned}4F^2 M_5(1) &= \frac{(s_{1,4} + s_{4,5} - s_{1,5})(s_{1,2} + s_{2,3})}{s_{1,3}} + \frac{(s_{1,2} + s_{2,5} - s_{1,5})(s_{3,4} + s_{4,5})}{s_{3,5}} \\ &\quad + \frac{(s_{1,4} + s_{2,5} - s_{1,5})(s_{2,3} + s_{3,4})}{s_{2,4}} \\ &\quad + 2s_{1,5} - s_{1,2} - s_{1,4} - s_{2,3} - s_{2,5} - s_{3,4} - s_{4,5}.\end{aligned}\quad (4.58)$$

Taking this amplitude on-shell according to (4.53), i.e. setting $s_{1,5} \rightarrow 0$ and changing the overall sign, we reproduce the parametrization independent physical amplitude (2.34).

5 More properties of stripped semi-on-shell amplitudes

The BCFW recursive relations provides us with a Lagrangian-free formulation of the tree-level nonlinear $SU(N)$ sigma model in the Cayley parametrization. We can use them similarly as the Berends-Giele relations as a tool for the investigation of further interesting

features of the stripped semi-on-shell amplitudes M_{2n+1} and J_{2n+1} . As we have already mentioned, these features are not universal because of the parametrization dependence of M_{2n+1} and J_{2n+1} , however, their implications for the fully on-shell amplitudes hold universally.¹¹ In this section we will concentrate on the problem of single soft limits (Adler zeroes) and double soft limit of the semi-on-shell amplitudes.

The presence of Adler zeroes for the *on-shell* Goldstone boson amplitudes $\mathcal{M}^{a_1 \dots a_{2n}}(p_1, \dots, p_{2n})$, i.e. validity of the limit

$$\lim_{p_j \rightarrow 0} \mathcal{M}^{a_1 a_2 \dots a_{2n}}(p_1, p_2, \dots, p_{2n}) = 0, \quad (5.1)$$

is a well known consequence of the nonlinearly realized chiral symmetry. More generally it is an universal (non-perturbative) feature in the theories with spontaneous breakdown of a global symmetry. In such theories the amplitudes with one extra Goldstone boson π^a in the *out* (or *in*) state vanishes when the Goldstone boson becomes soft, e.g.

$$\lim_{p \rightarrow 0} \langle f + \pi^a(p), \text{out} | i, \text{in} \rangle = 0, \quad (5.2)$$

provided the π^a cannot be emitted from the external lines corresponding to the states $|i, \text{in}\rangle$ or $|f, \text{out}\rangle$. In the $SU(N)$ nonlinear sigma model the Adler zero is present also for the stripped on-shell amplitudes $\mathcal{M}_{2n}(p_1, p_2, \dots, p_{2n})$ due to the leading N orthogonality relations (2.20) and corresponding uniqueness of the decomposition (2.11). However, this property is not guaranteed automatically for the semi-on-shell amplitudes M_{2n+1} and the soft Goldstone boson behavior can depend on the parametrization. For instance using the Cayley parametrization, we find for the amplitude $M_3 = (p_1 \cdot p_3)/F^2$ the Adler zero for soft p_1 and p_3 , however there is no zero for soft p_2 in general when keeping p_4 off-shell. For the same amplitude in the exponential parametrization (cf. (4.16)) we have no Adler zero at all. As we shall show in this section, for the semi-on-shell amplitudes M_{2n+1} in the Cayley parametrization we can prove, using the BCFW-like relation, the Adler zero for half of the momenta (namely for those p_j with *odd* index j).

The double soft limit of the Goldstone boson on-shell amplitudes $\mathcal{M}^{a_1 a_2 \dots a_{2n+2}}(p_1, p_2, \dots, p_{2n+2})$ is more complicated and has been studied relatively recently in connection with the regularized action of the broken generators on the n Goldstone boson states [50]. Motivated by direct inspection of the six Goldstone boson amplitude in the nonlinear chiral $SU(2)$ sigma model it was conjectured that provided the two soft momenta are sent to zero with the same rate, the following limit holds

$$\begin{aligned} & \lim_{t \rightarrow 0} \mathcal{M}^{a_1 a_2 \dots a_{2n}}(tp, tq, p_1, p_2, \dots, p_{2n}) \\ &= -\frac{1}{2F^2} \sum_{i=1}^n f^{abc} f^{ca_i d} \frac{p_i \cdot (p-q)}{p_i \cdot (p+q)} \mathcal{M}^{a_1 \dots a_{i-1} d a_{i+1} \dots a_{2n}}(p_1, p_2, \dots, p_{2n}), \end{aligned} \quad (5.3)$$

where f^{abc} are the structure constants. Analogous statement has been then rigorously proven for the tree-level amplitudes in the $\mathcal{N} = 8$ supergravity using BCFW relations.

¹¹Let us remind that the on-shell amplitudes are parametrization independent.

In fact, for the on-shell amplitudes, the formula (5.3) can be proven non-perturbatively under some assumptions for the general enough case of the theory with global symmetry breaking (including the case of chiral nonlinear sigma model with general chiral group G) using the symmetry arguments only (cf. the PCAC soft-pions theorems [48]). We postpone the details to the appendix E.

In terms of the stripped *on-shell* amplitudes the relation (5.3) can be rewritten as

$$\begin{aligned} & \lim_{t \rightarrow 0} \mathcal{M}_{2n+2}(p_1, \dots, p_{i-1}, tp_i, \dots, tp_j, p_{j+1}, \dots, p_{2n+2}) \\ &= \frac{1}{4F^2} \delta_{j,i+1} \left(\frac{p_{i+2} \cdot (p_i - p_{i+1})}{p_{i+2} \cdot (p_i - p_{i+1})} - \frac{p_{i-1} \cdot (p_i - p_{i+1})}{p_{i-1} \cdot (p_i - p_{i+1})} \right) \mathcal{M}_{2n}(p_1, \dots, p_{i-1}, p_{i+2}, \dots, p_{2n+2}). \end{aligned} \quad (5.4)$$

In this section we will prove this relation also for the tree-level semi-on-shell amplitudes J_{2n+1} (and consequently for M_{2n+1}) of the $SU(N)$ nonlinear sigma model in the Cayley parametrization using suitable form of the generalized BCFW representation.

5.1 Adler zeroes

In this subsection we will use the BCFW-like relations (4.52) derived in the previous section and prove the presence of an Adler zero at M_{2n+1} when one of the *odd* momenta, say p_{2l-1} , is soft, i.e. we will prove that for $l = 1, 2, \dots, n + 1$

$$\lim_{t \rightarrow 0} M_{2n+1}(p_1, p_2, \dots, p_{2l-2}, tp_{2l-1}, p_{2l+1}, \dots, p_{2n+1}) = 0. \quad (5.5)$$

For the fundamental amplitude $M_3(p_1, p_2, p_3)$ we have explicitly¹²

$$M_3(tp_1, p_2, p_3) = M_3(p_1, p_2, tp_3) = \frac{1}{F^2} t(p_1 \cdot p_3) \rightarrow 0. \quad (5.6)$$

In the general case the proof of (5.5) is by induction. Let us assume validity of (5.5) for $m < n$. This assumption also means that, taking the cut semi-on-shell amplitude M_{2m+1} on shell, i.e. for $p_{1,2n+1}^2 \rightarrow 0$, the Adler zero is in fact present at $M_{2m+1}|_{\text{on-shell}} = -\mathcal{M}_{2m+2}$ for all momenta, i.e.

$$\lim_{t \rightarrow 0} M_{2m+1}(p_1, p_2, \dots, tp_j, \dots, p_{2m+1})|_{\text{on-shell}} = 0 \quad (5.7)$$

for all $j = 1, \dots, 2m + 1$ due to the cyclicity of \mathcal{M}_{2m+2} .

Let us now substitute $p_{2l-1} \rightarrow tp_{2l-1}$ to the right hand side of (4.52). Note that, under such substitution, the position of the poles $z_{2j,2j+2}$, $z_{2j-1,2j+1}$ and $z_{i,j}^\pm$ become t -dependent. The t -dependence of the right hand side of (4.52) is therefore both explicit (due to the explicit dependence on p_{2l-1}) and implicit (due to the implicit t -dependence of the poles z_P).

We will now inspect the behavior of the individual terms under the limit $t \rightarrow 0$. The first term gives finite limit

$$\frac{1}{(2F^2)^n} p_-^2 \rightarrow \frac{1}{(2F^2)^n} p_-^2|_{p_{2l-1} \rightarrow 0}. \quad (5.8)$$

¹²Note however that for $t \rightarrow 0$ according to (4.18).

$$M_3(p_1, tp_2, p_3) \rightarrow \frac{1}{2F^2} (p_1 + p_3)^2$$

and therefore the statement analogous to (5.5) for even momenta does not hold.

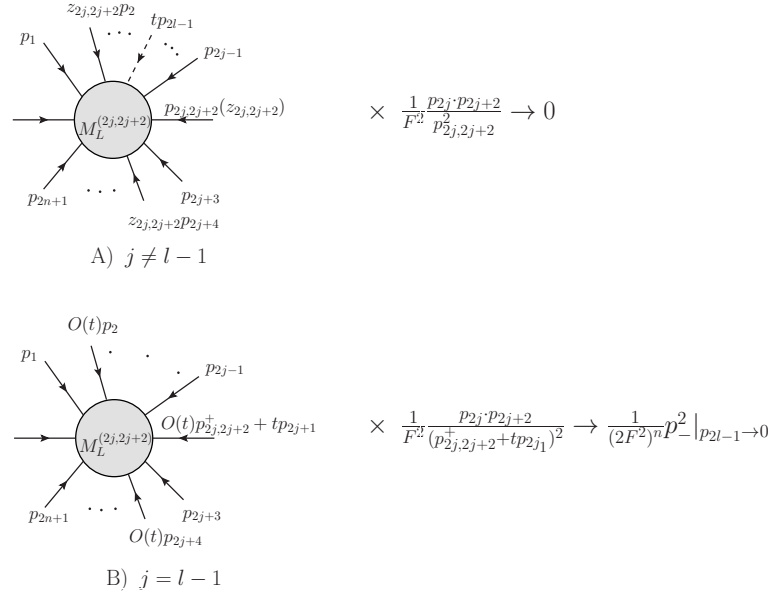


Figure 9. Graphical representation of the $t \rightarrow 0$ limit of the second term on the right hand side of (4.52). The soft momentum is denoted by dashed line in the case A. In the case B, $O(t)$ indicates the order of the t -dependent $z_{2j,2j+2}$.

As far as the second term is concerned, the individual terms of the sum over j vanish in this limit unless $j = l - 1$. The reason is as follows. For $j \neq l - 1$ (the case A in the figure 9), the kinematical factor $p_{2j} \cdot p_{2j+2}/p_{2j,2j+2}^2$ as well as the position of the pole $z_{2j,2j+2}$ are t -independent and because tp_{2l-1} is placed on the *odd* position in $M_L^{(2j,2j+2)}(z_{2j,2j+2})$, we can safely¹³ use the induction hypothesis to conclude that

$$\lim_{t \rightarrow 0} M_L^{(2j,2j+2)}(z_{2j,2j+2})|_{p_{2l-1} \rightarrow 0} = 0.$$

For $j = l - 1$ (the case B in the figure 9), the kinematical factor $p_{2j} \cdot p_{2j+2}/p_{2j,2j+2}^2$ becomes explicitly t -dependent and tends to $1/2$ for $t \rightarrow 0$, while $M_L^{(2j,2j+2)}(z_{2j,2j+2})$ has both explicit (through $p_{2j,2j+2} = z_{2j,2j+2}(p_{2j} + p_{2j+2}) + tp_{2j+1}$) and implicit t -dependence. In this case $z_{2j,2j+2} = O(t)$, as can be seen from (4.43). Therefore, all *even* momenta in $M_L^{(2j,2j+2)}(z_{2j,2j+2})$ are scaled by $O(t)$ factor, in the same way as in (4.18). We can therefore conclude with help of (4.18) that

$$\lim_{t \rightarrow 0} M_L^{(2j,2j+2)}(z_{2j,2j+2}) \frac{1}{p_{2j,2j+2}^2} \frac{p_{2j} \cdot p_{2j+2}}{F^2} = \delta_{j,l-1} \frac{1}{(2F^2)^n} P_-^2 |_{p_{2l-1} \rightarrow 0}. \quad (5.9)$$

The third term on the right hand side of (4.52) can be treated exactly in the same way as the second (see figure 10). Also here the individual terms of the sum over j do not

¹³Indeed, in general the momenta $p_k(z_{2j,2j+2})$ and $p_{2j,2j+2}(z_{2j,2j+2})$ are t -independent and nonzero.

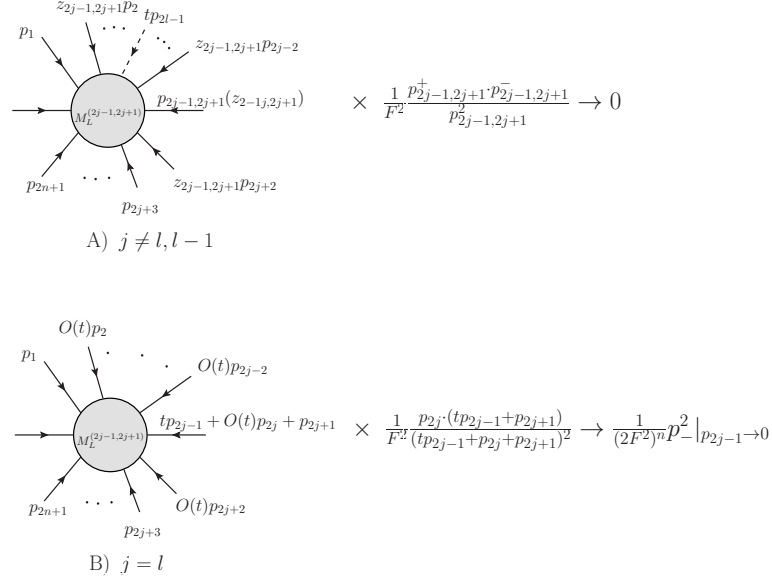


Figure 10. Graphical representation of the $t \rightarrow 0$ limit of the third term on the right hand side of (4.52). The soft momentum is denoted by dashed line in the picture A. In the picture B, we show only the $j = l$ case, the $j = l - 1$ case is treated analogously. $O(t)$ indicates the order of the t -dependent $z_{2j, 2j+2}$.

contribute with the only exception of $j = l$ and $j = l - 1$ by induction hypothesis applied to $M_L^{(2j-1, 2j+1)}(z_{2j-1, 2j+1})$ which has for $j \neq l, l - 1$ only explicit t -dependence. In the remaining two cases $j = l$ and $j = l - 1$, the explicitly t -dependent kinematical factors $p_{2j-1, 2j+1}^+ \cdot p_{2j-1, 2j+1}^- / p_{2j-1, 2j+1}^2$ tend again to $1/2$ and within $M_L^{(2j-1, 2j+1)}(z_{2j-1, 2j+1})$ the even momenta are scaled by $z_{2j-1, 2j+1} = O(t)$ (see (4.41)) and thus (4.18) can be used¹⁴ to conclude that

$$\lim_{t \rightarrow 0} M_L^{(2j-1, 2j+1)}(z_{2j-1, 2j+1}) \frac{1}{p_{2j-1, 2j+1}^2} \frac{p_{2j-1, 2j+1}^+ \cdot p_{2j-1, 2j+1}^-}{F^2} = (\delta_{j,l} + \delta_{j,l-1}) \frac{1}{(2F^2)^n} p_-^2 \Big|_{p_{2l-1} \rightarrow 0}. \quad (5.10)$$

The fourth term on the right hand side of (4.52) vanish completely in the limit $t \rightarrow 0$. This is easy to see for those terms of the sum over (i, j) for which¹⁵ $\lim_{t \rightarrow 0} z_{i,j}^\pm \neq 0$. In this case either $M_L^{(i,j)}(z_{i,j}^\pm)$ or $M_R^{(i,j)}(z_{i,j}^\pm)$ have explicit t -dependence through $t p_{2l-1}$ (which is for $M_L^{(i,j)}(z_{i,j}^\pm)$ on odd position) and thus the induction hypothesis in the form (5.5) or (5.7)

¹⁴Note that, the odd momenta are t -dependent with the only exception of $p_{2j-1, 2j+1}$ ($z_{2j-1, 2j+1}$) $|_{p_{2j \mp 1} \rightarrow t p_{2j \mp 1}}$ the limit of which is $p_{2j \pm 1}$.

¹⁵It is easy to realize that $\lim_{t \rightarrow 0} z_{i,j}^+ \neq \lim_{t \rightarrow 0} z_{i,j}^-$ for generic p_k .

can be used.¹⁶ By direct inspection of (4.40) we find that the only case for which the above argumentation does not apply is the case $j - i = 4$ with i even and $i \leq 2l - 1 \leq j$. Here $\lim_{t \rightarrow 0} z_{i,j}^- \neq 0$ and so for the “minus” part of this (i, j) term we can use the induction hypothesis as above. However, the “plus” part might be problematic because

$$z_{i,j}^+ = -\frac{(p_{2l-1} \cdot p_{2l-1 \pm 2})}{(p_{2l-1 \pm 2} \cdot p_{i,j}^+)} t + O(t^2). \quad (5.11)$$

Using this formula and (4.15) we find after some algebra

$$M_R^{(i,j)}(z_{i,j}^+) = M_5(p_i(z_{i,j}^{t+}), \dots, tp_{2l-1}, \dots, p_j(z_{i,j}^{t+})) = O(t^2). \quad (5.12)$$

which shows that also the “plus” part has vanishing $t \rightarrow 0$ limit.

Putting therefore the only nonzero contributions (5.8), (5.9) and (5.10) together we get finally

$$\begin{aligned} & \lim_{t \rightarrow 0} M_{2n+1}(p_1, p_2, \dots, p_{2l-2}, tp_{2l-1}, p_{2l+1}, \dots, p_{2n+1}) \\ &= \frac{1}{(2F^2)^n} p_{2l-1}^2 \Big|_{p_{2l-1} \rightarrow 0} \left(1 + \sum_{j=1}^{n-1} \delta_{j,l-1} - \sum_{j=1}^n (\delta_{j,l} + \delta_{j,l-1}) \right) = 0, \end{aligned}$$

which finishes the proof.

5.2 Double-soft limit

Let us now study the behavior of the semi-on-shell amplitude J_{2n+1} in the Cayley parametrization under the double soft limit, i.e. the case when two external momenta, say p_i and p_j , are scaled according to $p_{i,j} \rightarrow tp_{i,j}$ and t is sent to zero. In this section we will prove, that for $1 < i < j < 2n + 1$

$$\begin{aligned} & \lim_{t \rightarrow 0} J_{2n+1}(p_1, \dots, p_{2n+1}) \Big|_{p_i \rightarrow tp_i, p_j \rightarrow tp_j} \\ &= \delta_{j,i+1} \frac{1}{2F^2} \left(\frac{(p_i \cdot p_{i+2})}{p_{i+2} \cdot (p_{i+1} + p_i)} - \frac{(p_i \cdot p_{i-1})}{p_{i-1} \cdot (p_{i+1} + p_i)} \right) J_{2n-1}(p_1, \dots, p_{i-1}, p_{i+2}, \dots, p_{2n+1}), \end{aligned} \quad (5.13)$$

which has an identical form as (5.5).¹⁷ The key ingredient of the proof is the generalized form of the BCFW representation mentioned in section 3.2 written for a suitable two-parameter complex deformation of the amplitude J_{2n+1} . Such a representation allows us to calculate the double soft limit with help of the known behavior of the poles and corresponding residues in this limit. Useful information on this behavior can be inferred from the statement (5.5) concerning the Adler zeroes proved in the previous subsection.

¹⁶Let us remind that $M_R^{(i,j)}(z_{i,j}^\pm)$ is fully on-shell.

¹⁷Indeed,

$$\frac{(p_i \cdot p_{i+2})}{p_{i+2} \cdot (p_{i+1} + p_i)} - \frac{(p_i \cdot p_{i-1})}{p_{i-1} \cdot (p_{i+1} + p_i)} = \frac{1}{2} \left(\frac{p_{i+2} \cdot (p_i - p_{i+1})}{p_{i+2} \cdot (p_i - p_{i+1})} - \frac{p_{i-1} \cdot (p_i - p_{i+1})}{p_{i-1} \cdot (p_i - p_{i+1})} \right).$$

The above mentioned deformation of J_{2n+1} can be defined as the following function of two complex variables z and t

$$S_{i,j}^n(z, t) = J(p_1, \dots, p_{2n+1})|_{p_i \rightarrow tp_i, p_j \rightarrow zp_j}, \quad (5.14)$$

therefore

$$S_{i,j}^n(1, 1) = J_{2n+1}(p_1, \dots, p_{2n+1}) \quad (5.15)$$

Various types of the double soft limit correspond then to various ways of taking the limit $(z, t) \rightarrow (0, 0)$ in the double complex plane (z, t) ; the limit (5.14) corresponds to $\lim_{t \rightarrow 0} S_{i,j}^n(t, t) \equiv S_{i,j}^{n,0}$.

For $z \rightarrow \infty$ and $t > 0$ fixed the following asymptotic behavior holds

$$S_{i,j}^n(z, t) = O(z^0), \quad (5.16)$$

as can be easily proved e.g. by induction with help of the Berends-Giele recursive relations (4.7). We can therefore write the generalized BCFW relation with one subtraction in the form (3.14)

$$S_{i,j}^n(z, t) = S_{i,j}^n(a, t) + \sum_{k,l} \frac{\text{Res}\left(S_{i,j}^n; z_{k,l}(t)\right)}{z - z_{k,l}(t)} \frac{z - a}{z_{k,l}(t) - a}. \quad (5.17)$$

where $a \neq z_{k,l}(t)$ is a priori arbitrary, however, as we shall see in what follows, appropriate choice of a can simplify the calculation.

The poles $z_{k,l}(t)$ for $k \leq j \leq l$ correspond to the conditions $p_{k,l}^2|_{p_i \rightarrow tp_i, p_j \rightarrow zp_j} = 0$, or explicitly

$$z_{k,l}(t) = -\frac{p_{k,l}^2|_{p_i \rightarrow tp_i, p_j \rightarrow 0}}{2(p_j \cdot p_{k,l})|_{p_i \rightarrow tp_i}}. \quad (5.18)$$

The residues at the poles $z_{k,l}(t)$ factorize

$$\begin{aligned} \text{Res}\left(S_{i,j}^n; z_{k,l}(t)\right) &= \frac{1}{2(p_j \cdot p_{k,l})|_{p_i \rightarrow tp_i}} [J_{2n+1-(l-k)}(p_1, \dots, p_{k-1}, p_{k,l}, p_{l+1}, \dots, p_{2N+1}) \\ &\quad \times M_{l-k+1}(p_k, \dots, p_l)|_{p_i \rightarrow tp_i, p_j \rightarrow zp_j}]|_{z \rightarrow z_{k,l}(t)}, \end{aligned} \quad (5.19)$$

where M_{l-k+1} is the cut amplitude (4.30). Namely the latter two formulae along with (5.5) contain sufficient amount of information for the calculation of the double soft limit.

Let us first assume $i < j$ where i is odd and j arbitrary. This choice is a technical one, and as we shall see, the general case can be easily obtained using the symmetry properties of the amplitude. In what follows we set $a = 1$ in (5.17), the double soft limit then simplifies to

$$S_{i,j}^{n,0} \equiv \lim_{t \rightarrow 0} S_{i,j}^n(t, t) = \lim_{t \rightarrow 0} \sum_{k,l} \frac{\text{Res}\left(S_{i,j}^n; z_{k,l}(t)\right)}{t - z_{k,l}(t)} \frac{t - 1}{z_{k,l}(t) - 1}, \quad (5.20)$$

where we have used the existence of the Adler zero for $S_{i,j}^n(1, t) = J_{2n+1}(p_1, \dots, tp_i, \dots, p_{2n+1})$ and i odd (cf. (5.5)).

For generic p_r there exist a finite limit

$$z_{k,l}(0) = \lim_{t \rightarrow 0} z_{k,l}(t) \neq 1 \quad (5.21)$$

In fact the only nonzero contributions to the right hand side of (5.20) stem from the cases for which $z_{k,l}(0) = 0$. Indeed, for $z_{k,l}(0) \neq 0$ we get for the corresponding contribution

$$\frac{1}{z_{k,l}(0)(z_{k,l}(0) - 1)} \lim_{t \rightarrow 0} \text{Res} \left(S_{i,j}^n; z_{k,l}(t) \right), \quad (5.22)$$

and, according to (5.5), on the right hand side of (5.19) we get either

$$\lim_{t \rightarrow 0} [M_{l-k+1}(p_k, \dots, p_l) |_{p_i \rightarrow t p_i, p_j \rightarrow z p_j}]_{z \rightarrow z_{k,l}(t)} = 0 \quad (5.23)$$

for $k \leq i < j \leq l$ or

$$\lim_{t \rightarrow 0} J_{2n+1-(l-k)}(p_1, \dots, t p_i, \dots, p(k, l)(t), p_{k+1}, \dots, p_{2n+1}) = 0 \quad (5.24)$$

for $i < k < j \leq l$. In both cases the complementary factor has finite limit and therefore

$$\lim_{t \rightarrow 0} \text{Res} \left(S_{i,j}^n; z_{k,l}(t) \right) = 0. \quad (5.25)$$

Let us therefore discuss the contributions from the poles for which $z_{k,l}(0) = 0$. Note that, for generic p_r such a pole does not exist provided $j > i + 2$. We can therefore immediately conclude

$$S_{i,j}^{n,0} = 0 \quad \text{for } j > i + 2. \quad (5.26)$$

What remains are the following two alternatives for which the three-particle poles $z_{k,l}(t)$ with $l = k + 2$ can vanish in the limit $t \rightarrow 0$ (see figure 11)

1. $j = i + 1$ and either $k = i$ or $k = i - 1$. In this case either

$$p_{i-1,i+1}^2 |_{p_i \rightarrow t p_i, p_j \rightarrow 0} \rightarrow p_{i-1}^2 = 0 \quad (5.27)$$

or

$$p_{i,i+2}^2 |_{p_i \rightarrow t p_i, p_j \rightarrow 0} \rightarrow p_{i+2}^2 = 0 \quad (5.28)$$

2. $j = i + 2$ and $k = i$, in this case

$$p_{i,i+2}^2 |_{p_i \rightarrow t p_i, p_j \rightarrow 0} = p_{i+1}^2 = 0. \quad (5.29)$$

In what follows we will discuss separately the cases $j = i + 1$ and $j = i + 2$. Let us first study the double soft limit of two adjacent momenta, i.e. $j = i + 1$ where i is odd. We will investigate the contributions of individual poles $z_{k,l}(t)$ on the right hand side of (5.20) separately. In this case we get for $i > 1$ only two potentially nonzero contributions (i.e. (5.28) and (5.27)) to the right hand side of (5.20), namely

$$S_{i,i+1}^{n,0} = \lim_{t \rightarrow 0} \frac{\text{Res} \left(S_{i,i+1}^n; z_{i-1,i+1}(t) \right)}{t - z_{i-1,i+1}(t)} \frac{t-1}{z_{i-1,i+1}(t) - 1} + \lim_{t \rightarrow 0} \frac{\text{Res} \left(S_{i,i+1}^n; z_{i,i+2}(t) \right)}{t - z_{i,i+2}(t)} \frac{t-1}{z_{i,i+2}(t) - 1}. \quad (5.30)$$

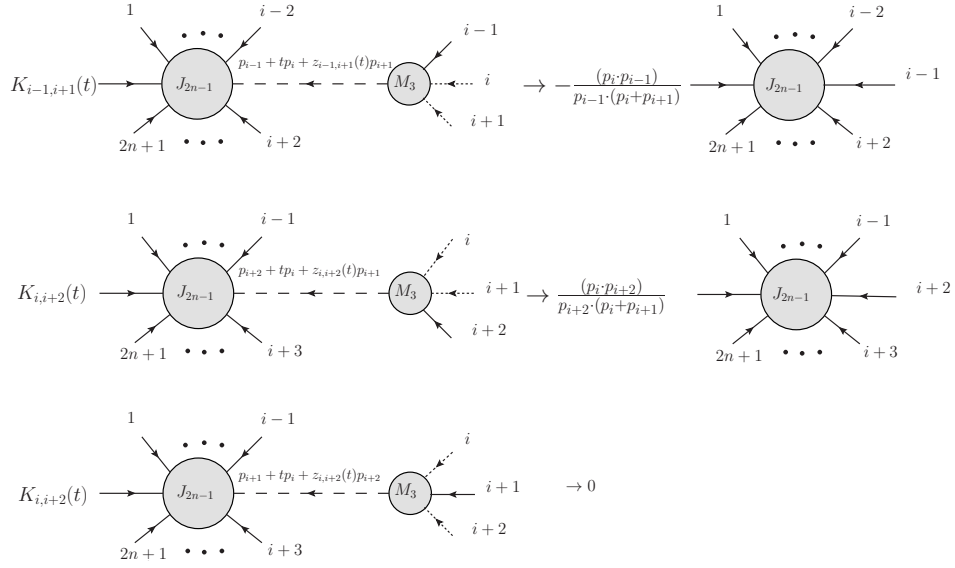


Figure 11. Graphical representation of the $t \rightarrow 0$ limit of the three cases (5.27), (5.28) and (5.29) for which $z_{k,l}(t) \rightarrow 0$. The soft momenta are denoted by dotted lines. The multiplicative factors $K_{k,l}(t)$ stays for $(t-1)/(t-z_{k,l}(t))(z_{k,l}(t)-1)$.

We get for the poles $z_{i-1,i+1}(t)$ and $z_{i,i+2}(t)$

$$z_{k,k+2}(t) = -\frac{p_{k,k+2}^2|_{p_i \rightarrow tp_i, p_j \rightarrow 0}}{2(p_j \cdot p_{k,k+2})|_{p_i \rightarrow tp_i}} = -t \frac{(p_i \cdot p_r)}{(p_j \cdot p_r)} + O(t^2), \quad (5.31)$$

where either $r = i + 2$ (for $k = i$) or $r = i - 1$ (for $k = i - 1$), and as a consequence,

$$\frac{1}{t - z_{k,k+2}(t)} \frac{t-1}{z_{k,k+2}(t) - 1} = \frac{1}{t} \frac{(p_j \cdot p_r)}{p_r \cdot (p_j + p_i)} (1 + O(t)). \quad (5.32)$$

We have further

$$p_{k,k+2}(t) = tp_i + z_{k,k+2}(t)p_j + p_r \rightarrow p_r \neq 0 \quad (5.33)$$

and therefore in both cases

$$\begin{aligned} \lim_{t \rightarrow 0} J_{2n-1}(p_1, \dots, p_{k-1}, p_{k,k+2}(t), p_{k+3}, \dots, p_{2n+1}) \\ = J_{2n-1}(p_1, \dots, p_{i-2}, p_{i-1}, p_{i+2}, \dots, p_{2n+1}). \end{aligned} \quad (5.34)$$

For the remaining ingredients of the formula (5.19) we get

$$M_3(tp_i, z_{i,i+2}(t)p_{i+1}, p_{i+2}) = \frac{1}{F^2} t (p_i \cdot p_{i+2}) \quad (5.35)$$

$$M_3(p_{i-1}, tp_i, z_{i-1,i+1}(t)p_{i+1}) = \frac{1}{F^2} z_{i-1,i+1}(t) (p_{i-1} \cdot p_{i+1}) = -t \frac{1}{F^2} (p_i \cdot p_{i-1}) (1 + O(t)). \quad (5.36)$$

Inserting this into the formulae (5.19) and (5.30) get finally for $i > 1$

$$\begin{aligned} & S_{i,i+1}^{n,0} \\ &= \frac{1}{2F^2} \left(\frac{(p_i \cdot p_{i+2})}{p_{i+2} \cdot (p_{i+1} + p_i)} - \frac{(p_i \cdot p_{i-1})}{p_{i-1} \cdot (p_{i+1} + p_i)} \right) J_{2n-1}(p_1, \dots, p_{i-2}, p_{i-1}, p_{i+2}, \dots, p_{2n+1}). \end{aligned} \quad (5.37)$$

In the same way, for $i=1$ only the first term on the right hand side of (5.37) contributes.

Let us proceed to the case 2. when $j = i + 2$ and $z_{i,i+2}(t) \rightarrow 0$ for $t \rightarrow 0$ is the only pole which can give nonzero contribution to (5.20). In this case we have

$$S_{i,i+2}^{n,0} = \lim_{t \rightarrow 0} \frac{\text{Res} \left(S_{i,i+2}^n; z_{i,i+2}(t) \right)}{t - z_{i,i+2}(t)} \frac{t - 1}{z_{i,i+2}(t) - 1}. \quad (5.38)$$

The formulae (5.31), (5.32), (5.33), (5.34) are still valid with $r = i + 1$, but now we have

$$M_3(tp_i, p_{i+1}, z_{i,i+2}(t)p_{i+2}) = \frac{1}{F^2} t z_{i,i+2}(t) (p_i \cdot p_{i+2}) = O(t^2). \quad (5.39)$$

which implies $S_{i,i+2}^{n,0} = 0$.

To summarize, we have for $k > 0$

$$\begin{aligned} & \lim_{t \rightarrow 0} J_{2n+1}(p_1, \dots, p_{2k}, tp_{2k+1}, \dots, tp_j, \dots, p_{2n+1}) = \\ &= \delta_{j,2k+2} \frac{1}{2F^2} J_{2n-1}(p_1, \dots, p_{2k}, p_{2k+3}, \dots, p_{2n+1}) \\ & \quad \left(\frac{(p_{2k+1} \cdot p_{2k+3})}{p_{2k+3} \cdot (p_{2k+2} + p_{2k+1})} - \frac{(p_{2k+1} \cdot p_{2k})}{p_{2k} \cdot (p_{2k+2} + p_{2k+1})} \right) \end{aligned} \quad (5.40)$$

and for $k = 0$

$$\lim_{t \rightarrow 0} J_{2n+1}(tp_1, \dots, tp_j, \dots, p_{2n+1}) = \delta_{j,2} \frac{1}{2F^2} \frac{(p_1 \cdot p_3)}{(p_2 \cdot p_3) + (p_1 \cdot p_3)} J_{2n-1}(p_3, \dots, p_{2n+1}).$$

As it is clear from the above discussion, the ‘‘asymmetry’’ of the latter result stems from the fact that p_{2n+2} is off-shell and therefore the three-particle pole corresponding to $(p_3 + p_4 + \dots + p_{2n+1})^2 = (p_{2n+2} - p_1 - p_2)^2 \rightarrow p_{2n+2}^2 \neq 0$ does not contribute.

Because

$$J(1, 2, \dots, 2n + 1) = J(2n + 1, 2n, \dots, 2, 1), \quad (5.41)$$

we get for $j < 2k + 1$

$$\begin{aligned} & J_{2n+1}(p_1, \dots, tp_j, \dots, p_{2k}, tp_{2k+1}, \dots, p_{2n+1}) \\ &= J_{2n+1}(p_{2n+1}, \dots, tp_{2k+1}, p_{2k}, \dots, tp_j, \dots, p_1). \end{aligned} \quad (5.42)$$

On the right hand side of this identity the momentum p_{2k+1} stays on the odd position and thus

$$\begin{aligned} & \lim_{t \rightarrow 0} J_{2n+1}(p_1, \dots, tp_j, \dots, p_{2k}, tp_{2k+1}, \dots, p_{2n+1}) \\ &= \delta_{j,2k} \frac{1}{2F^2} J_{2n-1}(p_1, \dots, p_{2k-1}, p_{2k+2}, \dots, p_{2n+1}) \\ & \quad \left(-\frac{(p_{2k} \cdot p_{2k-1})}{p_{2k-1} \cdot (p_{2k} + p_{2k+1})} + \frac{(p_{2k} \cdot p_{2k+2})}{p_{2k+2} \cdot (p_{2k} + p_{2k+1})} \right) \end{aligned} \quad (5.43)$$

Putting (5.40) and (5.43) together the final result (5.14) follows.

6 Summary and conclusion

We have studied various aspects of the $SU(N)$ chiral nonlinear sigma model which describes the low-energy dynamics of the Goldstone bosons corresponding to the spontaneous chiral symmetry breaking $SU(N) \times SU(N) \rightarrow SU(N)$. As we have shown, the tree-level scattering amplitudes of the Goldstone bosons can be constructed from the stripped amplitudes, which are identical as those of the $U(N)$ chiral nonlinear sigma model. It is therefore possible to use this correspondence and to investigate both the $SU(N)$ and $U(N)$ cases on the same footing. Especially we are allowed to choose any parametrization (field redefinition) of the chiral unitary matrix $U(x)$ entering the Lagrangian from the wide class of parametrizations admissible for the extended $U(N)$ case, because the fully on-shell stripped amplitudes do not depend on the parametrization. For the direct calculation of the flavor ordered Feynman graphs, the most convenient choice proved to be the minimal parametrization (2.31), which we have chosen in order to calculate the on-shell amplitudes up to 10 Goldstone bosons.

The proliferation of the Feynman graphs with increasing number of the Goldstone bosons call for alternative methods of calculation. The more efficient method is based on the Berends-Giele recursive relations for the semi-on-shell amplitudes, but due to the infinite number of the interaction vertices in the Lagrangian of the nonlinear sigma model, the number of terms necessary to evaluate the n -point amplitude grows much faster (exponentially) with n than for the case of the power-counting renormalizable theories (where the growth is polynomial).

The BCFW recursive relations could make the calculation of the on-shell stripped amplitude as effective as for the renormalizable theories at least as far as the number of terms (which is in both cases related to the number of factorization channels) is concerned. However, the standard way of the BCFW reconstruction is not directly applicable for the nonlinear sigma model because of the bad behavior of the BCFW deformed amplitudes at infinity. We have therefore proposed an alternative deformation of the semi-on-shell amplitudes based on the scaling of all odd or all even momenta, for which we were able to prove exact results concerning the behavior of the semi-on-shell amplitudes when the scaling parameter tended to zero. Using the Berends-Giele recursive relations we were able to prove this scaling properties for general n -point amplitude. An essential ingredient of the proof was the fact that the semi-on-shell amplitudes (unlike the on-shell ones) are parametrization dependent and we could therefore make an appropriate choice of the parametrization (the Cayley one). We have then used these exact scaling properties for a generalized BCFW reconstruction formula (with one subtraction) which determines fully all the semi-on-shell amplitudes in the Cayley parametrization including the basic four-point one. Putting then the semi-on-shell amplitudes on-shell we reconstruct simply the parametrization independent on-shell amplitudes. In contrast to the standard BCFW relations our procedure is not restricted to $d \geq 4$ space-time dimensions.

The BCFW recursive relation are also a suitable tool for investigation of the properties of the amplitudes. We have illustrated this in two cases, namely we have proved the presence of the Adler zero and established the general form of the double soft limit for the semi-on-shell amplitudes in the Cayley parametrization.

The existence of BCFW recursion relations for power-counting non-renormalizable effective theory as the $SU(N)$ chiral nonlinear sigma model gives an evidence that the on-shell methods can be used for much larger classes of theories than has been considered so far. It also indicates that the $SU(N)$ chiral nonlinear sigma model is rather special and deeper understanding of all its properties is desirable. For future directions, it would be interesting to see whether the construction can be re-formulated purely in terms of on-shell scattering amplitudes not using the semi-on-shell ones. Next possibility is to focus on loop amplitudes. As was shown in [20] the loop integrand can be also in certain cases constructed using BCFW recursion relations, it would be spectacular if the similar construction can be applied for effective field theories.

Acknowledgments

We would like to thank Nima Arkani-Hamed and David McGady for useful discussions and comments on the manuscript. JT is supported by NSF grant PHY-0756966. This work is supported in part by projects MSM0021620859 of Ministry of Education of the Czech Republic and GAUK- 514412.

A General parametrization

In this appendix we will discuss a very general class of parameterizations of the $U(N)$ sigma model originally studied in [1], which is suited for a derivation of the stripped Feynman rules. Within this class the field $U(x) \in U(N)$ is expressed in the form

$$U = \sum_{k=0}^{\infty} a_k \left(\sqrt{2} \frac{i}{F} \phi \right)^k \quad (\text{A.1})$$

where $\phi = t^a \phi^a$, ϕ^a are the Goldstone boson fields, t^a are the $U(N)$ generators normalized according to $\langle t^a t^b \rangle = \delta^{ab}$ and a_k are real coefficients. These coefficients are not completely arbitrary, because the unitarity condition $U^\dagger U = 1$ implies the following constraint

$$\sum_{k=0}^n a_k a_{n-k} (-1)^k = \delta_{n,0}. \quad (\text{A.2})$$

For $n = 0$ we get $a_0^2 = 1$ and without lose of generality we can set $a_0 = 1$. In order to preserve the correct normalization of the kinetic term and to keep the interpretation of F as the decay constant for the fields ϕ^a we have to fix also $a_1 = 1$.

For n odd the relations (A.2) are satisfied automatically while for $n = 2k$ we can solve them for a_{2k} and get a recurrent formula for the even coefficients expressed in terms of the odd ones

$$a_{2k} = -\frac{(-1)^k}{2} a_k^2 - \sum_{j=1}^{k-1} (-1)^j a_j a_{2k-j}. \quad (\text{A.3})$$

This gives up to $k = 3$

$$\begin{aligned} a_2 &= \frac{1}{2}a_1^2 = \frac{1}{2}, \\ a_4 &= -\frac{1}{2}a_2^2 + a_1a_3 = -\frac{1}{8} + a_3, \\ a_6 &= \frac{1}{2}a_3^2 + a_1a_5 - a_2a_4 = \frac{1}{16} - \frac{1}{2}a_3 + \frac{1}{2}a_3^2 + a_5. \end{aligned} \quad (\text{A.4})$$

The explicit solution of the recurrent relations (A.3) to all orders can be easily found by means of the following trick. Let us introduce the generating function $f(x)$ of the above coefficients a_k

$$f(x) = \sum_{k=0}^{\infty} a_k x^k. \quad (\text{A.5})$$

The relations of unitarity with the initial conditions $a_0 = a_1 = 1$ are then equivalent to

$$f(-x)f(x) = 1, \quad f(0) = 1, \quad f'(0) = 1 \quad (\text{A.6})$$

which represents a functional equations for the generating functions $f(x)$. Let us define $f_{\pm}(x)$ to be the even and odd part of $f(x)$, i.e. $f_{\pm}(x) = (f(x) \pm f(-x))/2$. From (A.6) we get then

$$f_+(x)^2 - f_-(x)^2 = 1 \quad (\text{A.7})$$

or finally

$$f_+(x) = \sqrt{1 + f_-(x)^2}. \quad (\text{A.8})$$

The formal series expansion of both sides of the last equation at $x = 0$ gives the solution of the recurrent relations (A.3), i.e. the explicit expressions for a_{2k} in terms of an infinite number of free parameters a_{2k+1} . The general solution of the functional equation (A.6) is then

$$f(x) = f_-(x) + \sqrt{1 + f_-(x)^2} \quad (\text{A.9})$$

where $f_-(x)$ is arbitrary odd real function analytic for $x = 0$ satisfying $f'(0) = 1$. The minimal parameter-free solution corresponds to the choice $a_{2k+1} = 0$ for $k > 0$, i.e. $f_-^{\min}(x) = x$ and

$$f_{\min}(x) = x + \sqrt{1 + x^2} \quad (\text{A.10})$$

i.e. for $k \geq 1$

$$a_{2k}^{\min} = \frac{(-1)^{k+1}}{2^{2k-1}} C_{k-1}, \quad (\text{A.11})$$

where

$$C_n = \frac{1}{n+1} \binom{2n}{n} \quad (\text{A.12})$$

are the Catalan numbers.

Another frequently used choices are the exponential and Cayley parameterizations corresponding to $f_{\text{exp}}(x)$ and $f_{\text{Cayley}}(x)$ respectively, where

$$f_{\text{exp}}(x) = e^x \quad (\text{A.13})$$

$$f_{\text{Cayley}}(x) = \frac{1 + (x/2)}{1 - (x/2)}, \quad (\text{A.14})$$

or in terms of the coefficients a_k

$$a_k^{\text{exp}} = \frac{1}{k!} \quad (\text{A.15})$$

$$a_k^{\text{Cayley}} = \frac{1}{1 + \delta_{k,0}} \frac{1}{2^{k-1}}. \quad (\text{A.16})$$

These two parameterizations can be understood as minimal parameter-free variants with respect to other two possible forms of the general solutions of the functional equation (A.6), namely

$$f(x) = \exp g(x) \quad (\text{A.17})$$

and

$$f(x) = \frac{h(x)}{h(-x)} \quad (\text{A.18})$$

where $g(x)$ and $h(x)$ are arbitrary real functions analytic for $x = 0$ for which

$$g(x) = -g(-x), \quad (\text{A.19})$$

$$g(0) = 0, \quad g'(0) = 1 \quad (\text{A.20})$$

and

$$h'(0) = \frac{1}{2}h(0) \neq 0. \quad (\text{A.21})$$

As was proved in [1], for $N > 2$ the only parametrization from the class (A.1) admissible also for $SU(N)$ sigma model is the exponential one. The reason is that, under the general axial $SU(N)$ transformation

$$U(x)' = \sum_{k=0}^{\infty} a_k \left(\sqrt{2} \frac{i}{F} \phi' \right)^k = U_A \sum_{k=0}^{\infty} a_k \left(\sqrt{2} \frac{i}{F} \phi \right)^k U_A \quad (\text{A.22})$$

which defines corresponding nonlinear transformation of the matrix of the Goldstone boson fields $\phi = \sum_{a=1}^{N^2-1} \phi^a t^a$ the $SU(N)$ condition for the trace $\langle \phi' \rangle = 0$ is not preserved unless $a_k = 1/k!$. Of course, in the case $N > 2$ we can use different admissible parameterizations of $SU(N)$ which, however, do not belong to the class (A.1) (see e.g. [47]).

Let us now find the stripped Feynman rules. Using the general parametrization (A.1) we can write the Lagrangian of the nonlinear $U(N)$ sigma model in the expanded form

$$\mathcal{L}^{(2)} = \frac{F^2}{4} \langle \partial U \cdot \partial U^+ \rangle = \sum_{n,m=0}^{\infty} v_{n,m} \langle \partial \phi \phi^n \cdot \partial \phi \phi^m \rangle. \quad (\text{A.23})$$

where we get for $v_{n,m}$ after some algebra (and using the unitarity condition (A.2))

$$v_{n,m} = (1 + (-1)^{n+m}) \frac{(-i)^{n+m}}{4F^{n+m}} \sum_{k=0}^m a_k a_{m+n+2-k} (-1)^{k+1} (k-1-m) \quad (\text{A.24})$$

Therefore only the terms with even number of fields survive, explicitly

$$\mathcal{L}^{(2)} = \sum_{n=0}^{\infty} \mathcal{L}_{2n+2}^{(2)} \quad (\text{A.25})$$

where

$$\mathcal{L}_{2n+2}^{(2)} = \sum_{k=0}^{2n} v_{k,2n-k} \langle \partial \phi \phi^k \cdot \partial \phi \phi^{2n-k} \rangle. \quad (\text{A.26})$$

The usual Feynman rules for the vertices can be easily obtained as a sum over permutations

$$\begin{aligned} V_{2n+2}^{a_1, \dots, a_{2n+2}}(p_1, p_2, \dots, p_{2n+1}; p_{2n+2}) &= -2^{n+1} \sum_{\sigma \in S_{2n+2}} \langle t^{a_{\sigma(1)}} \dots t^{a_{\sigma(2n+2)}} \rangle \\ &\times \sum_{k=0}^{2n} v_{k,2n-k} (p_{\sigma(1)} \cdot p_{\sigma(1)+k+1}) \end{aligned} \quad (\text{A.27})$$

The stripped Feynman rule then follows in the form

$$V_{2n+2}(p_1, p_2, \dots, p_{2n+1}; p_{2n+2}) = -2^{n+1} \sum_{k=0}^{2n} \sum_{i=1}^{2n+2} v_{k,2n-k} (p_i \cdot p_{i+k+1}) \quad (\text{A.28})$$

Inserting (A.15) into (A.24) we get after some algebra for the exponential parametrization

$$v_{k,2n-k}^{\text{exp}} = \frac{(-1)^n}{2F^{2n}} \frac{(-1)^k}{(2n+2)!} \binom{2n}{k}. \quad (\text{A.29})$$

while for the Cayley parametrization we have $v_{2k+1,2n-2k-1}^{\text{Cayley}} = 0$ and

$$v_{2k,2n-2k}^{\text{Cayley}} = \frac{(-1)^n}{2F^{2n}} \frac{1}{2^{2n+1}}. \quad (\text{A.30})$$

Similar calculations can be made also for the minimal parametrization, but the result is much more lengthy and we will not need it explicitly. Instead we will rewrite the Feynman rules for the vertex V_{2n+2} with $2n+2$ external legs in terms of the variables

$$s_{i,j} = p_{i,j}^2 \quad (\text{A.31})$$

where $1 \leq i < j \leq 2n+1$ and

$$p_{i,j} = \sum_{k=i}^j p_k \quad (\text{A.32})$$

Here we identify

$$s_{2n+2,2n+2+k} = s_{k+1,2n+1} \quad (\text{A.33})$$

$$s_{i,2n+2+k} = s_{k+1,i-1}. \quad (\text{A.34})$$

The scalar products $(p_i \cdot p_j)$ can be then expressed as

$$(p_i \cdot p_i) = s_{i,i} \quad (\text{A.35})$$

$$(p_i \cdot p_{i+1}) = \frac{1}{2} (s_{i,i+1} - s_{i,i} - s_{i+1,i+1}) \quad (\text{A.36})$$

and for $k \geq 2$

$$(p_i \cdot p_{i+k}) = \frac{1}{2} (s_{i,i+k} - s_{i,i+k-1} + s_{i+1,i+k-1} - s_{i+1,i+k}). \quad (\text{A.37})$$

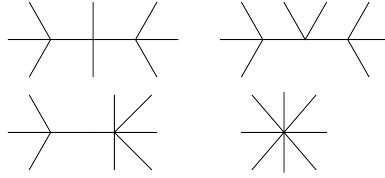


Figure 12. Graphical representation of the 8-point amplitude (B.1) with cycling tacitly assumed.

On-shell we get $s_{i,i} = 0$ and $s_{1,2n+1} = 0$. The stripped Feynman rule in these variables can be written in the form valid for $n \geq 1$

$$V_{2n+2}(s_{i,j}) = (-1)^n \left(\frac{2}{F^2} \right)^n \sum_{k=0}^n w_{k,n} \sum_{i=1}^{2n+2} s_{i,i+k} \quad (\text{A.38})$$

where

$$w_{0,n} = (-1)^n 2F^{2n} (2v_{0,2n} - v_{1,2n-1}) \quad (\text{A.39})$$

$$w_{k,n} = (-1)^n 2F^{2n} (2v_{k,2n-k} - v_{k-1,2n+1-k} - v_{k+1,2n-1-k}) \quad \text{for } k < n \quad (\text{A.40})$$

$$w_{n,n} = (-1)^n 2F^{2n} (v_{n,n} - v_{n-1,n+1}). \quad (\text{A.41})$$

Within the general parametrization we get from (A.24) and (A.2) after some algebra

$$w_{k,n} = \frac{(-1)^k}{1 + \delta_{kn}} a_{k+1} a_{2n+1-k}. \quad (\text{A.42})$$

For the above special cases this reads for $N \geq 1$

$$w_{k,n}^{\text{exp}} = \frac{(-1)^k}{1 + \delta_{kn}} \frac{1}{(2n+2)!} \binom{2n+2}{k+1} \quad (\text{A.43})$$

$$w_{k,n}^{\text{Cayley}} = \frac{(-1)^k}{1 + \delta_{kn}} \frac{1}{2^{2n}} \quad (\text{A.44})$$

$$w_{0,n}^{\text{min}} = w_{2k,n}^{\text{min}} = 0 \quad (\text{A.45})$$

$$w_{2k+1,n}^{\text{min}} = \frac{1}{1 + \delta_{2k+1,n}} \frac{(-1)^n}{2^{2n}} C_k C_{n-k-1}. \quad (\text{A.46})$$

Note that, for the minimal parametrization the coefficients $w_{0,n}^{\text{min}}$ at $s_{i,i} = p_i^2$ vanish, therefore the stripped Feynman rules for vertices do not depend on the off-shellness of the momenta in this case. This fact has been observed already in [11] without calculating the explicit Feynman rules.

B More examples of amplitudes

The eight-point amplitude is

$$\begin{aligned}
8F^6 \mathcal{M}(1, 2, 3, 4, 5, 6, 7, 8) &= \\
&= \frac{1}{2} \frac{(s_{1,2} + s_{2,3})(s_{1,4} + s_{4,7})(s_{5,6} + s_{6,7})}{s_{1,3}s_{5,7}} + \frac{(s_{1,2} + s_{2,3})(s_{1,4} + s_{4,5})(s_{6,7} + s_{7,8})}{s_{1,3}s_{6,8}} \\
&\quad - \frac{(s_{1,2} + s_{2,3})(s_{4,5} + s_{4,7} + s_{5,6} + s_{5,8} + s_{6,7} + s_{7,8})}{s_{1,3}} + 2s_{1,2} + \frac{1}{2}s_{1,4} + \text{cycl} \quad (\text{B.1})
\end{aligned}$$

and graphically in figure 12. Finally the ten-point amplitude is given by

$$\begin{aligned}
16F^8 \mathcal{M}(1, 2, 3, 4, 5, 6, 7, 8, 9, 10) &= -\frac{s_{1,2} + s_{2,3}}{s_{1,3}} \left\{ \right. \\
&\quad \frac{1}{2} \frac{(s_{1,4} + s_{4,9})(s_{5,8} + s_{6,9})(s_{6,7} + s_{7,8})}{s_{5,9}s_{6,8}} + \frac{1}{2} \frac{(s_{1,4} + s_{4,5})(s_{1,8} + s_{6,9})(s_{6,7} + s_{7,8})}{s_{1,5}s_{6,8}} \\
&\quad + \frac{1}{2} \frac{(s_{1,8} + s_{4,9})(s_{4,5} + s_{5,8})(s_{6,7} + s_{7,8})}{s_{4,8}s_{6,8}} + \frac{(s_{1,4} + s_{4,5})(s_{1,6} + s_{6,7})(s_{1,8} + s_{8,9})}{s_{1,5}s_{1,7}} \\
&\quad + \frac{(s_{1,4} + s_{4,5})(s_{1,6} + s_{6,9})(s_{7,8} + s_{8,9})}{s_{1,5}s_{7,9}} + \frac{(s_{1,8} + s_{4,9})(s_{4,7} + s_{5,8})(s_{5,6} + s_{6,7})}{s_{4,8}s_{5,7}} \\
&\quad + \frac{(s_{1,6} + s_{4,9})(s_{4,5} + s_{5,6})(s_{7,8} + s_{8,9})}{s_{4,6}s_{7,9}} - \frac{1}{2} \frac{(s_{1,4} + s_{1,8} + s_{4,5} + s_{4,9} + s_{5,8} + s_{6,9})(s_{6,7} + s_{7,8})}{s_{6,8}} \\
&\quad - \frac{(s_{1,8} + s_{4,9})(s_{4,5} + s_{4,7} + s_{5,6} + s_{5,8} + s_{6,7} + s_{7,8})}{s_{4,8}} \\
&\quad - \frac{(s_{1,4} + s_{1,6} + s_{4,5} + s_{4,7} + s_{5,6} + s_{6,7})(s_{1,8} + s_{8,9})}{s_{1,7}} \\
&\quad - \frac{(s_{1,4} + s_{1,6} + s_{4,5} + s_{4,9} + s_{5,6} + s_{6,9})(s_{7,8} + s_{8,9})}{s_{7,9}} \\
&\quad - \frac{(s_{1,4} + s_{4,5})(s_{1,6} + s_{1,8} + s_{6,7} + s_{6,9} + s_{7,8} + s_{8,9})}{s_{1,5}} \\
&\quad - \frac{(s_{1,4} + s_{4,9})(s_{5,6} + s_{5,8} + s_{6,7} + s_{6,9} + s_{7,8} + s_{8,9})}{s_{5,9}} \\
&\quad \left. + 2s_{1,4} + s_{1,6} + 2s_{1,8} + 2s_{4,5} + s_{4,7} + 2s_{4,9} + 2s_{5,6} + s_{5,8} + 2s_{6,7} + s_{6,9} + 2s_{7,8} + 2s_{8,9} \right\} \\
&\quad - \frac{1}{2} \frac{(s_{1,2} + s_{1,4} + s_{2,3} + s_{2,5} + s_{3,4} + s_{4,5})(s_{1,6} + s_{1,8} + s_{6,7} + s_{6,9} + s_{7,8} + s_{8,9})}{s_{1,5}} \\
&\quad + 5s_{1,2} + 2s_{1,4} + \text{cycl} \quad (\text{B.2})
\end{aligned}$$

with one-to-one correspondence with figure 13.

C Relative efficiency of Feynman diagrams and Berends-Giele relations

In this appendix we review the solution of several types of recursive relations which count the number of ordered Feynman graphs needed for the semi-on-shell amplitude $J(1, 2, \dots, n)$ in the nonlinear sigma model and related toy models.

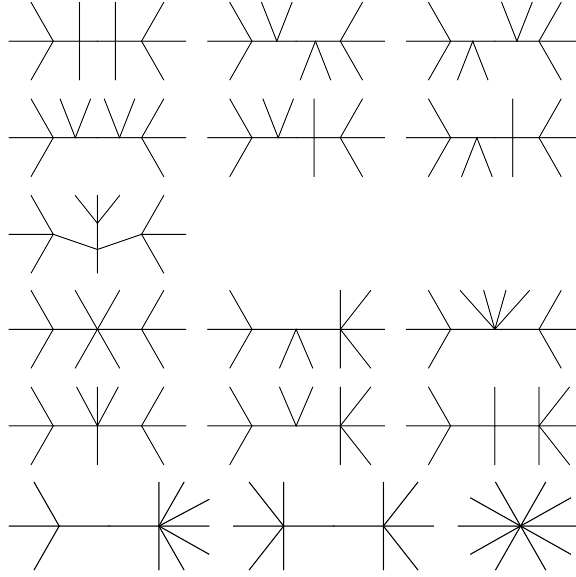


Figure 13. Graphical representation of the 10-point amplitude (B.2) with cycling tacitly assumed.

C.1 Number of the Feynman graphs

Let us start with the case of nonlinear sigma model, i.e. with the case with infinite number of vertices in the interaction Lagrangian. The above recursive relations, which determine the number $f(2n+1)$ of the (flavor ordered) Feynman graphs which contribute to $J(1, 2, \dots, 2n+1)$, are tightly related to the Berends-Giele relations (4.7). Indeed, after making the following substitution to (4.7)

$$J(1, 2, \dots, 2n+1) \rightarrow f(2n+1), \quad \frac{i}{p_{2n+2}^2} \rightarrow 1, \quad iV_{2k+1} \rightarrow 0, \quad iV_{2k+2} = 1, \quad (\text{C.1})$$

the individual terms on the right hand side just count the number of Feynman graphs generated from these terms by the iterations of the recursive procedure. As a result we get for $f(2n+1)$ the following recursive relation

$$f(2n+1) = \sum_{k=1}^n \sum_{\{n_i\}} \prod_{i=1}^{2k+1} f(2n_i+1), \quad (\text{C.2})$$

with the initial condition $f(1) = 1$. In the above formula the sum over $\{n_i\}$ is constrained by the requirement

$$\sum_{i=1}^{2k+1} (2n_i+1) = 2n+1 \Leftrightarrow \sum_{i=1}^{2k+1} n_i = n-k \quad (\text{C.3})$$

i.e. it corresponds to the sum over all possible decompositions of ordered set of $2n+1$ momenta to non-empty clusters with odd number of momenta in each cluster (cf. (4.8) and figure 3), i.e. more explicitly

$$f(2n+1) = \sum_{k=1}^n \sum_{\sum_i n_i = n-k} \prod_{i=1}^{2k+1} f(2n_i+1), \quad f(1) = 1. \quad (\text{C.4})$$

Standard method for solution of this type of recursive relation is based on the generating function defined as

$$A(x) = \sum_{n=0}^{\infty} f(2n+1)x^n. \quad (\text{C.5})$$

The recursive formula (C.4) implies the following equation for $A(x)$

$$A = 1 + \sum_{k=1}^{\infty} x^k A^{2k+1} = 1 + \frac{x A^3}{1 - x A^2} \quad (\text{C.6})$$

or

$$x = \frac{B}{(B+1)^2(2B+1)} \equiv \frac{B}{g(B)} \quad (\text{C.7})$$

where $B = A - 1$ and $g(z) = (z+1)^2(2z+1)$. In this form, the problem is prepared for the application of the Lagrange-Bürmann inversion formula

$$B(x) = \sum_{n=0}^{\infty} \frac{x^n}{n!} \frac{d^{n-1}}{dz^{n-1}} g(z)^n \Big|_{z=0} = \sum_{n=1}^{\infty} \frac{x^n}{n!} \frac{d^{n-1}}{dz^{n-1}} (z+1)^{2n} (2z+1)^n \Big|_{z=0}. \quad (\text{C.8})$$

After straightforward algebra with help of Leibnitz rule we get for $n \geq 1$

$$f(2n+1) = \frac{2^{n-1}}{n} \sum_{k=0}^{n-1} \binom{n}{k+1} \binom{2n}{k} 2^{-k} = 2^{n-1} {}_2F_1\left(1-n, -2n, 2; \frac{1}{2}\right), \quad (\text{C.9})$$

where ${}_2F_1(\alpha, \beta, \gamma; z)$ is the hypergeometric function. In the same way one can solve the recurrence relations for the number of ordered Feynman graphs for the semi-on-shell amplitudes $J(1, 2, \dots, n)$ in the cases when only quadrilinear vertices (“ ϕ^4 theory”), only trilinear vertices (“ ϕ^3 theory”) or both trilinear and quadrilinear vertices (“ $\phi^3 + \phi^4$ theory”) are present in the Lagrangian. In the first case, similarly to the nonlinear sigma model, only $J(1, 2, \dots, n)$ with n odd can be nonzero, while in the remaining two cases $J(1, 2, \dots, n)$ both parities of n are generally allowed. Let us denote the number of the Feynman graphs for $J(1, 2, \dots, n)$ as $f_4(n)$, $f_3(n)$ and $f_{3+4}(n)$ respectively. We get the following recurrence relations

$$f_4(2n+1) = \sum_{n_1+n_2+n_3=n-1, n_i \geq 0} f_4(2n_1+1) f_4(2n_2+1) f_4(2n_3+1) \quad (\text{C.10})$$

$$f_3(n) = \sum_{n_1+n_2=n, n_i \geq 1} f_3(n_1) f_3(n_2) \quad (\text{C.11})$$

$$f_{3+4}(n) = \sum_{n_1+n_2=n, n_i \geq 1} f_{3+4}(n_1) f_{3+4}(n_2) \quad (\text{C.12})$$

$$+ \sum_{n_1+n_2+n_3=n, n_i \geq 1} f_{3+4}(n_1) f_{3+4}(n_2) f_{3+4}(n_3)$$

with initial conditions $f_j(1) = 1$, $j = 3, 4, 3+4$. The corresponding generating functions

$$A_4(x) = \sum_{n=0}^{\infty} f_4(2n+1)x^n, \quad A_{3,3+4}(x) = \sum_{n=1}^{\infty} f_{3,3+4}(n)x^n \quad (\text{C.13})$$

n	2	3	4	5	6	7	8	9	10	11
$f_3(n)$	1	2	5	14	42	132	429	1 430	4 862	16 796
$f_{3+4}(n)$	1	3	10	38	154	654	2 871	12 925	59 345	276 835
$f_4(2n+1)$	3	12	55	273	1 428	7 752	43 263	246 675	1 430 715	8 414 640
$f(2n+1)$	4	21	126	818	5 594	39 693	289 510	2 157 150	16 348 960	125 642 146

Table 2. Number of flavor ordered Feynman graphs for $J(1, \dots, n)$ and $J(1, \dots, 2n+1)$ in the models of the type ϕ^3 , $\phi^3 + \phi^4$, ϕ^4 and nonlinear sigma model.

then satisfy

$$A_4 = 1 + xA_4^3, \quad A_3 = x + A_3^2, \quad A_{3+4} = x + A_{3+4}^2 + A_{3+4}^3. \quad (\text{C.14})$$

In the second case we get

$$A_3(x) = \frac{1 - \sqrt{1 - 4x}}{2} = \frac{1}{2} \left(1 - \sum_{n=0}^{\infty} \binom{1/2}{n} (-4x)^n \right) \quad (\text{C.15})$$

and therefore

$$f_3(n) = \frac{1}{n} \binom{2(n-1)}{n-1} = C_{n-1} \quad (\text{C.16})$$

where C_n are the Catalan numbers. In the first case, writing

$$x = \frac{A_4 - 1}{A_4^3} = \frac{B_4}{(B_4 + 1)^3} \quad (\text{C.17})$$

and using the Lagrange-Bürmann inversion formula we get for $n > 0$

$$f_4(2n+1) = \frac{1}{n!} \frac{d^{n-1}}{dz^{n-1}} (z+1)^{3n} \Big|_{z=0} = \frac{1}{2n+1} \binom{3n}{n}. \quad (\text{C.18})$$

In the third case, we get from

$$x = A_{3+4} (1 - A_{3+4} - A_3^2) \quad (\text{C.19})$$

and using the Lagrange-Bürmann inversion formula

$$f_{3+4}(n) = \frac{1}{n!} \frac{d^{n-1}}{dz^{n-1}} \left(\frac{1}{1-z-z^2} \right)^n \Big|_{z=0} = \frac{(-1)^n}{n!} \frac{d^{n-1}}{dz^{n-1}} \left(\frac{1}{z_1-z} \right)^n \left(\frac{1}{z_2-z} \right)^n \Big|_{z=0} \quad (\text{C.20})$$

(where $z_1 = -\phi$, $z_2 = \phi - 1$ and $\phi = (1 + \sqrt{5})/2$ is the Golden ratio) the result

$$\begin{aligned} f_{3+4}(n) &= (-1)^{n+1} \frac{\phi^{1-n}}{n} \sum_{k=0}^{n-1} \binom{n-1+k}{k} \binom{2(n-1)-k}{n-1} \left(\frac{\phi}{1-\phi} \right)^k \\ &= \left(-\frac{4}{\phi} \right)^{n-1} \Gamma \left(n - \frac{1}{2} \right) {}_2F_1 \left(1-n, n, 2-2n; \frac{\phi}{1-\phi} \right). \end{aligned} \quad (\text{C.21})$$

The first ten members of the above sequences are illustrated in the table 2.

C.2 Efficiency of the Berends-Giele relations

We can compare this with the number of terms generated by Berends-Giele recursion. For the nonlinear sigma model, the number of terms on the right hand side of (4.7) is just

$$t(2n+1) = \sum_{k=1}^n \sum_{\{n_i\}} 1 = \sum_{k=1}^n \binom{n+k}{n-k} = F_{2n+1} - 1 \quad (\text{C.22})$$

where

$$F_n = \frac{1}{\sqrt{5}} (\phi^n - (\phi-1)^n) \quad (\text{C.23})$$

are the Fibonacci numbers and $\phi = (1 + \sqrt{5})/2$ is the Golden ratio. Therefore, using the known results for $J(1, 2, \dots, 2m+1)$ with $m < n$ at each step, we need to evaluate altogether

$$b(2n+1) = \sum_{m=1}^n t(2m+1) = \frac{1}{\sqrt{5}} \left(\phi^3 \frac{\phi^{2n}-1}{\phi^2-1} - (\phi-1)^3 \frac{(\phi-1)^{2n}-1}{(\phi-1)^2-1} \right) - n \quad (\text{C.24})$$

terms in order to calculate $J(1, 2, \dots, 2n+1)$ using the Berends-Giele recursion. We show the sequences $t(2n+1)$ and $b(2n+1)$ in the first and second row of table 1 respectively.

In the same way we can calculate analogous numbers $t_j(n)$ and $b_j(n)$ for $j = 3, 4, 3+4$, i.e. for “ ϕ^3 theory”, “ ϕ^3 theory” or “ $\phi^3 + \phi^4$ theory”. For instance, for $t_4(2n+1)$ we have (see table 1 for numerical values)

$$t_4(2n+1) = \binom{n+1}{2}, \quad b_4(2n+1) = \sum_{m=1}^n t_4(2m+1) = \frac{1}{6} n(n+1)(n+2). \quad (\text{C.25})$$

Note the exponential growth of $t(2n+1)$ and $b(2n+1)$ with increasing n in contrast to the only polynomial growth of $t_4(2n+1)$ and $b_4(2n+1)$.

D Other example of scaling properties of the semi-on-shell amplitudes

In this appendix we prove the following scaling limit

$$\lim_{t \rightarrow 0} J_{2n+1}(tp_1, p_2, tp_3, p_4, \dots, tp_{2r-1}, tp_{2r}, tp_{2r+1}, \dots, p_{2N}, tp_{2n+1}) = 0 \quad (\text{D.1})$$

which is valid for $n > 1$. Let us note, however, that

$$J_3(tp_1, tp_2, tp_3) = J_3(p_1, p_2, p_3) \neq 0. \quad (\text{D.2})$$

On the other hand, for $N = 2$ we get by direct calculation

$$\lim_{t \rightarrow 0} J_5(tp_1, tp_2, tp_3, p_4, tp_5) = \lim_{t \rightarrow 0} J_5(tp_1, p_2, tp_3, tp_4, tp_5) = 0 \quad (\text{D.3})$$

and we can therefore proceed by induction based on Berends-Giele relations almost exactly as in the case of the proof of (4.17). The only modification here is that, along with the “dangerous” contributions without blocks $J(j_k + 1, \dots, j_{k+1})$ where j_k is even and

$j_{k+1} - j_k > 1$ attached to the odd line of the vertex V_{m+1} (provided at least one such a block is present, the contribution vanish either by the induction hypothesis or by (4.17)) we have to discuss separately new type of “dangerous” terms with building block $J(p_{2r-1}, p_{2r}, p_{2r+1})$ (this block does not vanish due to (D.2)). The “old” dangerous terms do not in fact contribute as was already discussed within the proof of (4.17). The “new” dangerous terms have the following general form form

$$\begin{aligned} & \frac{i}{p_{2N+2}^2} iV_{2k+2}(p_1, p_{2,2j_1}, p_{2j_1+1}, \dots, p_{2j_l+2,2r-2}, p_{2r-1,2r+1}, p_{2r+2,2j_{l+1}} \dots \\ & \dots, p_{2j_{k-1},2n}, p_{2n+1}, -p_{1,2n+1}) \\ & \times J(p_1)J(2, \dots, 2j_1)J(p_{2j_1+1}) \dots J(2j_l + 2, \dots, 2r - 2) \\ & \times J(p_{2r-1}, p_{2r}, p_{2r+1})J(2r + 2, \dots, 2j_{l+1}) \dots J(2j_{k-1}, \dots, 2n)J(p_{2n+1}). \end{aligned} \quad (\text{D.4})$$

Note that, $p_{2r-1,2r+1}$ is attached to the odd line of the vertex V_{2k+2} and scales as

$$p_{2r-1,2r+1} \rightarrow t p_{2r-1,2r+1} \quad (\text{D.5})$$

i.e. in the same way as the remaining momenta attached to the odd lines of the vertex. The vertex being proportional the squared sum of the odd line momenta scales therefore as $O(t^2)$, and the contributions of the “new” dangerous terms vanish. This finishes the proof.

E Double soft limit of Goldstone boson amplitudes

In this appendix we will discuss the properties of the on-shell scattering amplitudes of the Goldstone bosons, which are dictated by the symmetry, namely the limits of the amplitudes for soft external momenta. Some of these properties have been obtained in the special case of pions by PCAC methods in the late sixties (see e.g. [48]). Here we enlarge and reformulate them in a more general form appropriate for our purposes with stress on the proof of the double soft limit discussed recently for pions and $\mathcal{N} = 8$ supergravity in [50].

Let us assume a general theory with spontaneous symmetry breaking according to the pattern $G \rightarrow H$ where the homogeneous space G/H is a symmetric space, i.e. the vacuum little group H is the maximal subgroup invariant with respect to some involutive automorphism of G (“parity”). This implies the following structure of the Lie algebra of G

$$\begin{aligned} [T^a, T^b] &= i f_T^{abc} T^c \\ [T^a, X^b] &= i f_X^{abc} X^c \\ [X^a, X^b] &= i F^{abc} T^c. \end{aligned} \quad (\text{E.1})$$

Here T^a and X^a are the unbroken and broken generators respectively and f_T^{abc} , f_X^{abc} and F^{abc} are the structure constants. The chiral nonlinear sigma model is a special case for which $f_T^{abc} = f_X^{abc} = F^{abc} = f^{abc}$.

The invariance of the theory with respect to the group G can be expressed in terms of the Ward identities for the correlators in the general form

$$ip^\mu \langle \tilde{V}_\mu^a(p) \tilde{O}_1(p_1) \dots \tilde{O}_n(p_n) \rangle = - \sum_{i=1}^n i \langle \tilde{O}_1(p_1) \dots \delta_T^a \tilde{O}_i(p_i + p) \dots \tilde{O}_n(p_n) \rangle \quad (\text{E.2})$$

$$ip^\mu \langle \tilde{A}_\mu^a(p) \tilde{O}_1(p_1) \dots \tilde{O}_n(p_n) \rangle = - \sum_{i=1}^n i \langle \tilde{O}_1(p_1) \dots \delta_X^a \tilde{O}_i(p_i + p) \dots \tilde{O}_n(p_n) \rangle. \quad (\text{E.3})$$

Here $V_\mu^a(x)$ and $A_\mu^a(x)$ are the Noether currents corresponding to the generators T^a and X^a respectively (in analogy with the chiral theories we will call them *vector* and *axial* currents in what follows and to the Ward identities (E.2) and (E.3) we will refer to the *vector* and *axial* WI), $O_i(x)$ are (generally composite) local operators, $\delta_T^a O_i(x)$ and $\delta_X^a O_i(x)$ are their infinitesimal transforms with respect to the generators T^a and X^a . The tilde means the Fourier transform

$$\tilde{O}_i(p) = \int d^4x e^{ip \cdot x} O_i(x). \quad (\text{E.4})$$

According to the Goldstone theorem the spectrum of the theory contains as many Goldstone bosons π^a as the broken generators X^a for which the currents $A_\mu^a(x)$ play the role of the interpolating fields, i.e.

$$\langle 0 | A_\mu^a(0) | \pi^b(p) \rangle = ip_\mu F \delta^{ab}. \quad (\text{E.5})$$

where F is the Goldstone boson decay constant. Let us denote $M^{a_1 \dots a_n}(p_1, \dots, p_n)$ the on-shell scattering amplitude of the Goldstone bosons $\pi^{a_1}(p_1), \dots, \pi^{a_n}(p_n)$. In what follows we will concentrate on the properties of $M^{a_1 \dots a_n}(p_1, \dots, p_n)$ dictated by the symmetry, i.e. those which are encoded in the WI (E.2) and (E.3).

E.1 Vector WI and symmetry with respect to H

The invariance with respect to the unbroken subgroup H implies

$$\sum_{i=1}^n f_X^{aa_i b} M^{a_1 \dots a_{i-1} b a_{i+1} \dots a_n}(p_1, \dots, p_n) = 0. \quad (\text{E.6})$$

This can be understood as the consequence of the vector WI of the form

$$-ip^\mu \langle \tilde{V}_\mu^a(p) \tilde{A}_{\mu_1}^{a_1}(p_1) \dots \tilde{A}_{\mu_n}^{a_n}(p_n) \rangle = - \sum_{i=1}^n i \langle \tilde{A}_{\mu_1}^{a_1}(p_1) \dots \delta_T^a \tilde{A}_{\mu_i}^{a_i}(p_i + p) \dots \tilde{A}_{\mu_n}^{a_n}(p_n) \rangle. \quad (\text{E.7})$$

Note that the infinitesimal transformations $\delta^a V_\nu^b$ and $\delta^a A_\nu^b$ of these currents with respect to the generator T^a of the unbroken subgroup H are as follows

$$\delta_T^a A_\nu^b = -f_X^{abc} A_\nu^c \quad (\text{E.8})$$

$$\delta_T^a V_\nu^b = -f_T^{abc} V_\nu^c. \quad (\text{E.9})$$

Because there is no pole for $p \rightarrow 0$ in the correlator on the left hand side of (E.7), we get in this limit

$$\sum_{i=1}^n f_X^{aa_i b} \langle \tilde{A}_{\mu_1}^{a_1}(p_1) \dots \tilde{A}_{\mu_i}^{a_i}(p_i) \dots \tilde{A}_{\mu_n}^{a_n}(p_n) \rangle = 0. \quad (\text{E.10})$$

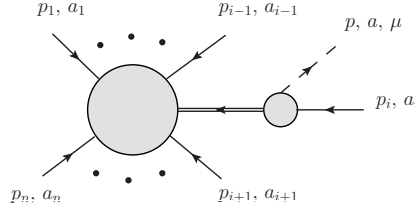


Figure 14. Graphical representation of the singular contributions to the matrix element (E.13).

Using the LSZ formula we get according to (E.5)

$$\langle \tilde{A}_{\mu_1}^{a_1}(p_1) \dots \tilde{A}_{\mu_n}^{a_n}(p_n) \rangle = \left(\prod_{i=1}^n \frac{i}{p_i^2} Z_{\mu_i} \right) M^{a_1 \dots a_n}(p_1, \dots, p_n) + R_{\mu_1 \dots}^{a_1 \dots} \quad (\text{E.11})$$

where $Z_{\mu_i} = iF p_{i\mu_i}$ and the remnant $R_{\mu_1 \dots}^{a_1 \dots}$ is regular on shell in the sense that

$$\lim_{p_i^2 \rightarrow 0} \left(\prod_{i=1}^n p_i^2 \right) R_{\mu_1 \dots}^{a_1 \dots} = 0. \quad (\text{E.12})$$

which implies (E.6) for the on-shell amplitude $M^{a_1 \dots a_n}(p_1, \dots, p_n)$.

E.2 Soft vector current singularity

Let us assume now the following matrix element

$$\langle \tilde{V}_\mu^a(p) | \pi^{a_1}(p_1) \dots \pi^{a_i}(p_i) \dots \pi^{a_n}(p_n) \rangle. \quad (\text{E.13})$$

In what follows we will discuss the behavior of this object in the limit $p \rightarrow 0$. On the level of the Feynman graphs, the only singularities in the soft limit $p \rightarrow 0$ are those which stem from the one-Goldstone-boson-reducible graphs for which the vector current $\tilde{V}_\mu^a(p)$ is attached to the external Goldstone boson line. The potential singularities are therefore of the form (see figure 14)

$$\langle \tilde{V}_\mu^a(p) \phi^{a_j}(0) | \pi^{a_i}(p_i) \rangle_{1PI} i \Delta^{a_j a_k}((p-p_i)^2) \langle \phi^{a_k}(0) | \pi^{a_1}(p_1) \dots \widehat{\pi^{a_i}(p_i)} \dots \pi^{a_n}(p_n) \rangle_{1PI} \quad (\text{E.14})$$

where the subscript *1PI* means one-Goldstone-boson-irreducible block, the hat means omitting of the corresponding particle, $\phi^a(x)$ is the Goldstone boson interpolating field normalized as

$$\langle 0 | \phi^a(0) | \pi^b(p) \rangle = \delta^{ab} \quad (\text{E.15})$$

and $\Delta^{a_j a_k}(q^2)$ is a Goldstone boson propagator. For $q^2 \rightarrow 0$ we have

$$\Delta^{a_j a_k}(q^2) = \frac{\delta^{a_j a_k}}{q^2} (1 + O(q^2)). \quad (\text{E.16})$$

As a consequence of the Lorentz invariance, invariance with respect to H and LSZ formulae we have

$$\langle \tilde{V}_\mu^a(p) \phi^{a_j}(0) | \pi^{a_i}(p_i) \rangle_{1PI} = i f_X^{a a_i a_j} F_V(p^2) (2p_i - p)_\mu + O((p-p_i)^2) \quad (\text{E.17})$$

where $F_V(p^2)$ is the on-shell vector form-factor defined as¹⁸

$$\langle \pi^{a_j}(p-p_i) | \tilde{V}_\mu^a(p) | \pi^{a_i}(p_i) \rangle = i f_X^{a_i a_j} F_V(p^2) (2p_i - p)_\mu. \quad (\text{E.18})$$

We can fix the normalization of the vector currents V_μ^a in such a way that

$$F_V(p^2) = 1 + O(p^2). \quad (\text{E.19})$$

Analogously we have

$$\langle \phi^{a_k}(0) | \pi^{a_1}(p_1) \dots \widehat{\pi^{a_i}(p_i)} \dots \pi^{a_n}(p_n) \rangle_{1PI} = M^{a_1 \dots a_{i-1} a_{i+1} \dots a_n}(p_1, \dots, p_n) + O((p-p_i)^2). \quad (\text{E.20})$$

Using $(p-p_i)^2 = -2(p \cdot p_i) + p^2$ and putting all the ingredients together we get for $p \rightarrow 0$

$$\begin{aligned} & \langle \tilde{V}_\mu^a(p) | \pi^{a_1}(p_1) \dots \pi^{a_i}(p_i) \dots \pi^{a_n}(p_n) \rangle \\ &= \sum_{i=1}^n f_X^{a_i d} \frac{(2p_i - p)_\mu}{2(p \cdot p_i)} M^{a_1 \dots a_{i-1} d a_{i+1} \dots a_n}(p_1, \dots, p_n) + O(1). \end{aligned} \quad (\text{E.21})$$

E.3 Axial WI and Adler zero

To illustrate the method which we will use in the next subsection, let us briefly recapitulate the textbook example of the derivation of the Adler zero for the amplitude $M^{a_1 \dots a_n}(p_1, \dots, p_n)$ (see e.g. [51]). Let us start with the axial WI in the form

$$-i p^\mu \langle \tilde{A}_\mu^a(p) \tilde{A}_{\mu_1}^{a_1}(p_1) \dots \tilde{A}_{\mu_n}^{a_n}(p_n) \rangle = - \sum_{i=1}^n i \langle \tilde{A}_{\mu_1}^{a_1}(p_1) \dots \delta_X^a \tilde{A}_{\mu_i}^{a_i}(p+p_i) \dots \tilde{A}_{\mu_n}^{a_n}(p_n) \rangle \quad (\text{E.22})$$

where now

$$\begin{aligned} \delta_X^a A_\nu^b &= -F^{abc} V_\nu^c \\ \delta_X^a V_\nu^b &= -f_X^{abc} A_\nu^c. \end{aligned} \quad (\text{E.23})$$

Applying on both sides of (E.22) the LSZ reduction to all but one axial currents, we get the conservation of the axial current in terms of the transversality of the matrix element of A_μ^a between the initial and final states $|i\rangle$ and $\langle f|$

$$-i p^\mu \langle f | \tilde{A}_\mu^a(p) | i \rangle = 0. \quad (\text{E.24})$$

On the other hand from (E.11) we get the Goldstone boson pole dominance for $p^2 \rightarrow 0$

$$-i p^\mu \langle f | \tilde{A}_\mu^a(p) | i \rangle = \frac{1}{p^2} p^\mu Z_\mu \langle f + \pi^a(p) | i \rangle - i p^\mu R_{\mu,fi}^a \quad (\text{E.25})$$

where $Z_\mu = iF p_\mu$ and the remnant $R_{\mu,fi}^a$ is regular in this limit

$$\lim_{p^2 \rightarrow 0} p^2 R_{\mu,fi}^a = 0. \quad (\text{E.26})$$

¹⁸The form of the right hand side is dictated by H -invariance, Bose and crossing symmetry.

Putting (E.24) and (E.25) together we get for the amplitude with emission of the Goldstone boson $\pi^a(p)$ in the final state

$$\langle f + \pi^a(p) | i \rangle = \frac{1}{F} p^\mu R_{\mu,fi}^a. \quad (\text{E.27})$$

Provided the following stronger regularity condition holds

$$\lim_{p \rightarrow 0} p^\mu R_{\mu,fi}^a = 0, \quad (\text{E.28})$$

we get

$$\langle f + \pi^a(0) | i \rangle = 0, \quad (\text{E.29})$$

i.e. the Adler zero for $p \rightarrow 0$.

An useful off-shell generalization of the formula (E.25) reads

$$-ip^\mu \langle \tilde{A}_\mu^a(p) \tilde{A}_{\mu_1}^{a_1}(p_1) \dots \tilde{A}_{\mu_n}^{a_n}(p_n) \rangle = iF \langle \pi^a(p) | \tilde{A}_{\mu_1}^{a_1}(p_1) \dots \tilde{A}_{\mu_n}^{a_n}(p_n) \rangle - ip^\mu R_{\mu,\mu_1\dots}^{a,a_1\dots} \quad (\text{E.30})$$

where

$$\lim_{p^2 \rightarrow 0} p^2 R_{\mu,\mu_1\dots}^{a,a_1\dots} = 0. \quad (\text{E.31})$$

and using the Ward identity (E.22) and (E.23) we get

$$\begin{aligned} & F \langle \pi^a(p) | \tilde{A}_{\mu_1}^{a_1}(p_1) \dots \tilde{A}_{\mu_n}^{a_n}(p_n) \rangle \\ &= p^\mu R_{\mu,\mu_1\dots}^{a,a_1\dots} + \sum_{i=1}^n F^{aa_i c} \langle \tilde{A}_{\mu_1}^{a_1}(p_1) \dots \tilde{V}_{\mu_i}^c(p + p_i) \dots \tilde{A}_{\mu_n}^{a_n}(p_n) \rangle. \end{aligned} \quad (\text{E.32})$$

E.4 Double soft limit

Our starting point is the axial WI (E.22) rewritten in the form

$$\begin{aligned} & -ip^\mu \langle \tilde{A}_\mu^a(p) \tilde{A}_\nu^b(q) \tilde{A}_{\mu_1}^{a_1}(p_1) \dots \tilde{A}_{\mu_n}^{a_n}(p_n) \rangle \\ &= -i \langle \delta_X^a \tilde{A}_\nu^b(p + q) \tilde{A}_{\mu_1}^{a_1}(p_1) \dots \tilde{A}_{\mu_n}^{a_n}(p_n) \rangle \\ & \quad - \sum_{i=1}^n i \langle \tilde{A}_\nu^b(q) \tilde{A}_{\mu_1}^{a_1}(p_1) \dots \delta_X^a \tilde{A}_{\mu_i}^{a_i}(p + p_i) \dots \tilde{A}_{\mu_n}^{a_n}(p_n) \rangle. \end{aligned} \quad (\text{E.33})$$

Multiplying then both sides by $-iq^\nu$ and using the axial WI (E.22) once again we get

$$\begin{aligned} & -p^\mu q^\nu \langle \tilde{A}_\mu^a(p) \tilde{A}_\nu^b(q) \tilde{A}_{\mu_1}^{a_1}(p_1) \dots \tilde{A}_{\mu_n}^{a_n}(p_n) \rangle \\ &= q^\nu F^{abc} \langle \tilde{V}_\nu^c(p + q) \tilde{A}_{\mu_1}^{a_1}(p_1) \dots \tilde{A}_{\mu_n}^{a_n}(p_n) \rangle \\ & \quad + \sum_{i \neq j; i,j=1}^n F^{aa_j c} F^{ba_i d} \langle \tilde{A}_{\mu_1}^{a_1}(p_1) \dots \tilde{V}_{\mu_i}^d(p_i + q) \dots \tilde{V}_{\mu_j}^c(p + p_j) \dots \tilde{A}_{\mu_n}^{a_n}(p_n) \rangle \\ & \quad + \sum_{i=1}^n F^{aa_i c} f_X^{bcd} \langle \tilde{A}_{\mu_1}^{a_1}(p_1) \dots \tilde{A}_{\mu_i}^d(p + q + p_i) \dots \tilde{A}_{\mu_n}^{a_n}(p_n) \rangle. \end{aligned} \quad (\text{E.34})$$

The left hand side of (E.34) is symmetric with respect to the interchange of $(p, a) \leftrightarrow (q, b)$; its right hand side can be therefore rewritten in the manifestly symmetric form

$$\begin{aligned}
& -p^\mu q^\nu \langle \tilde{A}_\mu^a(p) \tilde{A}_\nu^b(q) \tilde{A}_{\mu_1}^{a_1}(p_1) \dots \tilde{A}_{\mu_n}^{a_n}(p_n) \rangle \\
&= -\frac{1}{2} (p-q)^\nu F^{abc} \langle \tilde{V}_\nu^c(p+q) \tilde{A}_{\mu_1}^{a_1}(p_1) \dots \tilde{A}_{\mu_n}^{a_n}(p_n) \rangle \\
&+ \sum_{i \neq j; i, j=1}^n F^{aa_jc} F^{ba_i d} \langle \tilde{A}_{\mu_1}^{a_1}(p_1) \dots \tilde{V}_{\mu_i}^d(p_i+q) \dots \tilde{V}_{\mu_j}^c(p+p_j) \dots \tilde{A}_{\mu_n}^{a_n}(p_n) \rangle \\
&+ \frac{1}{2} \sum_{i=1}^n \left(F^{aa_i c} f_X^{bcd} + F^{ba_i c} f_X^{acd} \right) \langle \tilde{A}_{\mu_1}^{a_1}(p_1) \dots \tilde{A}_{\mu_i}^d(p+q+p_i) \dots \tilde{A}_{\mu_n}^{a_n}(p_n) \rangle. \quad (\text{E.35})
\end{aligned}$$

On the other hand, the LSZ formula gives for $p^2, q^2 \rightarrow 0$

$$\begin{aligned}
\langle \tilde{A}_\mu^a(p) \tilde{A}_\nu^b(q) \tilde{A}_{\mu_1}^{a_1}(p_1) \dots \tilde{A}_{\mu_n}^{a_n}(p_n) \rangle &= \sum_{c,d} \frac{i}{p^2} \langle 0 | A_\mu^a | \pi^c(p) \rangle \frac{i}{q^2} \langle 0 | A_\nu^b | \pi^d(q) \rangle \\
&\times \langle \pi^c(p) \pi^d(q) | \tilde{A}_{\mu_1}^{a_1}(p_1) \dots \tilde{A}_{\mu_n}^{a_n}(p_n) \rangle + R_{\mu\nu}^{ab, \dots} \quad (\text{E.36})
\end{aligned}$$

where the regular remnant satisfies

$$\lim_{p^2, q^2 \rightarrow 0} p^2 q^2 R_{\mu\nu}^{ab, \dots} = 0. \quad (\text{E.37})$$

Therefore, using (E.5) we get

$$\begin{aligned}
& -p^\mu q^\nu \langle \tilde{A}_\mu^a(p) \tilde{A}_\nu^b(q) \tilde{A}_{\mu_1}^{a_1}(p_1) \dots \tilde{A}_{\mu_n}^{a_n}(p_n) \rangle \\
&= F^2 \langle \pi^a(p) \pi^b(q) | \tilde{A}_{\mu_1}^{a_1}(p_1) \dots \tilde{A}_{\mu_n}^{a_n}(p_n) \rangle - p^\mu q^\nu R_{\mu\nu}^{ab, \dots}. \quad (\text{E.38})
\end{aligned}$$

On the other hand applying the LSZ reduction to (E.34), (E.35) (let us note that only the first terms on the right hand side has the appropriate poles at $p^2, q^2 \rightarrow 0$) we get

$$\begin{aligned}
& p^\mu q^\nu \langle \tilde{A}_\mu^a(p) \tilde{A}_\nu^b(q) | \pi^{a_1}(p_1) \dots \pi^d(p_i) \dots \pi^{a_n}(p_n) \rangle \\
&= q^\nu F^{abc} \langle \tilde{V}_\nu^c(p+q) | \pi^{a_1}(p_1) \dots \pi^d(p_i) \dots \pi^{a_n}(p_n) \rangle \\
&= p^\mu F^{bac} \langle \tilde{V}_\mu^c(p+q) | \pi^{a_1}(p_1) \dots \pi^d(p_i) \dots \pi^{a_n}(p_n) \rangle \\
&= -\frac{1}{2} F^{abc} (p-q)^\mu \langle \tilde{V}_\mu^c(p+q) | \pi^{a_1}(p_1) \dots \pi^d(p_i) \dots \pi^{a_n}(p_n) \rangle \quad (\text{E.39})
\end{aligned}$$

and as a consequence of LSZ reduction of (E.38)

$$\begin{aligned}
& F^2 \langle \pi^a(p) \pi^b(q) | \pi^{a_1}(p_1) \dots \pi^{a_i}(p_i) \dots \pi^{a_n}(p_n) \rangle \\
&= -\frac{1}{2} F^{abc} (p-q)^\mu \langle \tilde{V}_\mu^c(p+q) | \pi^{a_1}(p_1) \dots \pi^d(p_i) \dots \pi^{a_n}(p_n) \rangle + p^\mu q^\nu R_{\mu\nu}^{ab, \dots} |_{\text{LSZ}}. \quad (\text{E.40})
\end{aligned}$$

According to (E.21) we have for $p, q \rightarrow 0$

$$\begin{aligned}
& -\frac{1}{2}F^{abc}(p-q)^\mu \langle \tilde{V}_\mu^c(p+q) | \pi^{a_1}(p_1) \dots \pi^d(p_i) \dots \pi^{a_n}(p_n) \rangle \\
&= -\frac{1}{2} \sum_{i=1}^n F^{abc} f_X^{ca_i d} \frac{(2p_i - p - q) \cdot (p - q)}{2((p+q) \cdot p_i)} \langle \pi^{a_1}(p_1) \dots \pi^d(p_i) \dots \pi^{a_n}(p_n) \rangle + O(p-q) \\
&= -\frac{1}{2} \sum_{i=1}^n F^{abc} f_X^{ca_i d} \frac{p_i \cdot (p - q)}{p_i \cdot (p + q)} \langle \pi^{a_1}(p_1) \dots \pi^d(p_i) \dots \pi^{a_n}(p_n) \rangle \\
&\quad + O\left(p - q, \frac{p^2 - q^2}{p_i \cdot (p + q)}\right) \tag{E.41}
\end{aligned}$$

For $p^2 = q^2 = 0$ we finally get

$$\begin{aligned}
& F_0^2 \langle \pi^a(p) \pi^b(q) | \pi^{a_1}(p_1) \dots \pi^{a_i}(p_i) \dots \pi^{a_n}(p_n) \rangle \\
&= -\frac{1}{2} \sum_{i=1}^n F^{abc} f_X^{ca_i d} \frac{p_i \cdot (p - q)}{p_i \cdot (p + q)} \langle \pi^{a_1}(p_1) \dots \pi^d(p_i) \dots \pi^{a_n}(p_n) \rangle \\
&\quad + p^\mu q^\nu R_{\mu\nu}^{ab, \dots} |_{\text{LSZ}} + O(p - q). \tag{E.42}
\end{aligned}$$

Provided condition stronger than (E.37) holds, namely $\lim_{p, q \rightarrow 0} p^\mu q^\nu R_{\mu\nu}^{ab, \dots} |_{\text{LSZ}} = 0$ (cf. (E.28)), we get as a result

$$\begin{aligned}
& \lim_{t \rightarrow 0} F_0^2 \langle \pi^a(tp) \pi^b(tq) | \pi^{a_1}(p_1) \dots \pi^{a_i}(p_i) \dots \pi^{a_n}(p_n) \rangle \\
&= -\frac{1}{2} \sum_{i=1}^n F^{abc} f_X^{ca_i d} \frac{p_i \cdot (p - q)}{p_i \cdot (p + q)} \langle \pi^{a_1}(p_1) \dots \pi^d(p_i) \dots \pi^{a_n}(p_n) \rangle. \tag{E.43}
\end{aligned}$$

For the chiral nonlinear sigma model corresponding to the symmetry breaking $G \times G \rightarrow G$, we have $F^{abc} = f_X^{abc} = f_T^{abc}$ and we get the formula (5.3) as a special case.

References

- [1] J.A. Cronin, *Phenomenological model of strong and weak interactions in chiral $U(3) \times U(3)$* , *Phys. Rev.* **161** (1967) 1483 [INSPIRE].
- [2] S. Weinberg, *Dynamical approach to current algebra*, *Phys. Rev. Lett.* **18** (1967) 188 [INSPIRE].
- [3] S. Weinberg, *Nonlinear realizations of chiral symmetry*, *Phys. Rev.* **166** (1968) 1568 [INSPIRE].
- [4] L.S. Brown, *Field theory of chiral symmetry*, *Phys. Rev.* **163** (1967) 1802 [INSPIRE].
- [5] P. Chang and F. Gursey, *Unified formulation of effective nonlinear pion-nucleon Lagrangians*, *Phys. Rev.* **164** (1967) 1752 [INSPIRE].
- [6] S. Weinberg, *Phenomenological Lagrangians*, *Physica A* **96** (1979) 327 [INSPIRE].
- [7] J. Gasser and H. Leutwyler, *Chiral perturbation theory to one loop*, *Annals Phys.* **158** (1984) 142 [INSPIRE].

- [8] J. Gasser and H. Leutwyler, *Chiral perturbation theory: expansions in the mass of the strange quark*, *Nucl. Phys. B* **250** (1985) 465 [INSPIRE].
- [9] L. Susskind and G. Frye, *Algebraic aspects of pionic duality diagrams*, *Phys. Rev. D* **1** (1970) 1682 [INSPIRE].
- [10] H. Osborn, *Implications of adler zeros for multipion processes*, *Lett. Nuovo Cim.* **2S1** (1969) 717 [INSPIRE].
- [11] J.R. Ellis and B. Renner, *On the relationship between chiral and dual models*, *Nucl. Phys. B* **21** (1970) 205 [INSPIRE].
- [12] M.L. Mangano and S.J. Parke, *Multiparton amplitudes in gauge theories*, *Phys. Rept.* **200** (1991) 301 [hep-th/0509223] [INSPIRE].
- [13] L.J. Dixon, *Calculating scattering amplitudes efficiently*, [hep-ph/9601359](#) [INSPIRE].
- [14] B. Feng and M. Luo, *An introduction to on-shell recursion relations*, [arXiv:1111.5759](#) [INSPIRE].
- [15] J. Drummond, *Hidden simplicity of gauge theory amplitudes*, *Class. Quant. Grav.* **27** (2010) 214001 [[arXiv:1010.2418](#)] [INSPIRE].
- [16] Z. Bern, L.J. Dixon, D.C. Dunbar and D.A. Kosower, *One loop N point gauge theory amplitudes, unitarity and collinear limits*, *Nucl. Phys. B* **425** (1994) 217 [hep-ph/9403226] [INSPIRE].
- [17] Z. Bern, L.J. Dixon, D.C. Dunbar and D.A. Kosower, *Fusing gauge theory tree amplitudes into loop amplitudes*, *Nucl. Phys. B* **435** (1995) 59 [hep-ph/9409265] [INSPIRE].
- [18] R. Britto, F. Cachazo and B. Feng, *New recursion relations for tree amplitudes of gluons*, *Nucl. Phys. B* **715** (2005) 499 [hep-th/0412308] [INSPIRE].
- [19] R. Britto, F. Cachazo, B. Feng and E. Witten, *Direct proof of tree-level recursion relation in Yang-Mills theory*, *Phys. Rev. Lett.* **94** (2005) 181602 [hep-th/0501052] [INSPIRE].
- [20] N. Arkani-Hamed, J.L. Bourjaily, F. Cachazo, S. Caron-Huot and J. Trnka, *The all-loop integrand for scattering amplitudes in planar $N = 4$ SYM*, *JHEP* **01** (2011) 041 [[arXiv:1008.2958](#)] [INSPIRE].
- [21] C. Berger, Z. Bern, L.J. Dixon, F. Febres Cordero, D. Forde et al., *Precise predictions for $W + 4$ jet production at the large hadron collider*, *Phys. Rev. Lett.* **106** (2011) 092001 [[arXiv:1009.2338](#)] [INSPIRE].
- [22] E. Witten, *Perturbative gauge theory as a string theory in twistor space*, *Commun. Math. Phys.* **252** (2004) 189 [hep-th/0312171] [INSPIRE].
- [23] Z. Bern, L.J. Dixon and V.A. Smirnov, *Iteration of planar amplitudes in maximally supersymmetric Yang-Mills theory at three loops and beyond*, *Phys. Rev. D* **72** (2005) 085001 [hep-th/0505205] [INSPIRE].
- [24] L.F. Alday and J.M. Maldacena, *Gluon scattering amplitudes at strong coupling*, *JHEP* **06** (2007) 064 [[arXiv:0705.0303](#)] [INSPIRE].
- [25] L.F. Alday, J. Maldacena, A. Sever and P. Vieira, *Y -system for scattering amplitudes*, *J. Phys. A* **43** (2010) 485401 [[arXiv:1002.2459](#)] [INSPIRE].
- [26] J. Drummond, J. Henn, G. Korchemsky and E. Sokatchev, *Dual superconformal symmetry of scattering amplitudes in $N = 4$ super-Yang-Mills theory*, *Nucl. Phys. B* **828** (2010) 317 [[arXiv:0807.1095](#)] [INSPIRE].

- [27] J. Drummond, J. Henn, G. Korchemsky and E. Sokatchev, *On planar gluon amplitudes/Wilson loops duality*, *Nucl. Phys. B* **795** (2008) 52 [[arXiv:0709.2368](#)] [[INSPIRE](#)].
- [28] J.M. Drummond, J.M. Henn and J. Plefka, *Yangian symmetry of scattering amplitudes in $N = 4$ super Yang-Mills theory*, *JHEP* **05** (2009) 046 [[arXiv:0902.2987](#)] [[INSPIRE](#)].
- [29] Z. Bern, J. Carrasco and H. Johansson, *New relations for gauge-theory amplitudes*, *Phys. Rev. D* **78** (2008) 085011 [[arXiv:0805.3993](#)] [[INSPIRE](#)].
- [30] N. Arkani-Hamed, J.L. Bourjaily, F. Cachazo, A.B. Goncharov, A. Postnikov et al., *Scattering amplitudes and the positive grassmannian*, [arXiv:1212.5605](#) [[INSPIRE](#)].
- [31] N. Arkani-Hamed, F. Cachazo, C. Cheung and J. Kaplan, *A duality for the S matrix*, *JHEP* **03** (2010) 020 [[arXiv:0907.5418](#)] [[INSPIRE](#)].
- [32] L. Mason and D. Skinner, *Dual superconformal invariance, momentum twistors and grassmannians*, *JHEP* **11** (2009) 045 [[arXiv:0909.0250](#)] [[INSPIRE](#)].
- [33] L. Mason and D. Skinner, *The complete planar S -matrix of $N = 4$ SYM as a Wilson loop in twistor space*, *JHEP* **12** (2010) 018 [[arXiv:1009.2225](#)] [[INSPIRE](#)].
- [34] J. Bedford, A. Brandhuber, B.J. Spence and G. Travaglini, *A recursion relation for gravity amplitudes*, *Nucl. Phys. B* **721** (2005) 98 [[hep-th/0502146](#)] [[INSPIRE](#)].
- [35] F. Cachazo and P. Svrček, *Tree level recursion relations in general relativity*, [hep-th/0502160](#) [[INSPIRE](#)].
- [36] C. Cheung, *On-shell recursion relations for generic theories*, *JHEP* **03** (2010) 098 [[arXiv:0808.0504](#)] [[INSPIRE](#)].
- [37] S.J. Parke and T. Taylor, *An amplitude for n gluon scattering*, *Phys. Rev. Lett.* **56** (1986) 2459 [[INSPIRE](#)].
- [38] F.A. Berends and W. Giele, *Recursive calculations for processes with N gluons*, *Nucl. Phys. B* **306** (1988) 759 [[INSPIRE](#)].
- [39] S. Badger, E.N. Glover, V. Khoze and P. Svrček, *Recursion relations for gauge theory amplitudes with massive particles*, *JHEP* **07** (2005) 025 [[hep-th/0504159](#)] [[INSPIRE](#)].
- [40] B. Feng, J. Wang, Y. Wang and Z. Zhang, *BCFW recursion relation with nonzero boundary contribution*, *JHEP* **01** (2010) 019 [[arXiv:0911.0301](#)] [[INSPIRE](#)].
- [41] B. Feng and C.-Y. Liu, *A note on the boundary contribution with bad deformation in gauge theory*, *JHEP* **07** (2010) 093 [[arXiv:1004.1282](#)] [[INSPIRE](#)].
- [42] B. Feng and Z. Zhang, *Boundary contributions using fermion pair deformation*, *JHEP* **12** (2011) 057 [[arXiv:1109.1887](#)] [[INSPIRE](#)].
- [43] K. Risager, *A direct proof of the CSW rules*, *JHEP* **12** (2005) 003 [[hep-th/0508206](#)] [[INSPIRE](#)].
- [44] T. Cohen, H. Elvang and M. Kiermaier, *On-shell constructibility of tree amplitudes in general field theories*, *JHEP* **04** (2011) 053 [[arXiv:1010.0257](#)] [[INSPIRE](#)].
- [45] P. Benincasa and E. Conde, *On the tree-level structure of scattering amplitudes of massless particles*, *JHEP* **11** (2011) 074 [[arXiv:1106.0166](#)] [[INSPIRE](#)].
- [46] B. Feng, Y. Jia, H. Lüo and M. Luo, *Roots of amplitudes*, [arXiv:1111.1547](#) [[INSPIRE](#)].
- [47] J. Bijnens, K. Kampf and S. Lanz, *Leading logarithms in N -flavour mesonic chiral perturbation theory*, *Nucl. Phys. B* **873** (2013) 137 [[arXiv:1303.3125](#)] [[INSPIRE](#)].

- [48] R.F. Dashen and M. WEinstein, *Soft pions, chiral symmetry and phenomenological Lagrangians*, *Phys. Rev.* **183** (1969) 1261 [INSPIRE].
- [49] K. Kampf, J. Novotny and J. Trnka, *Recursion relations for tree-level amplitudes in the SU(N) non-linear σ -model*, [arXiv:1212.5224](#) [INSPIRE].
- [50] N. Arkani-Hamed, F. Cachazo and J. Kaplan, *What is the simplest quantum field theory?*, *JHEP* **09** (2010) 016 [[arXiv:0808.1446](#)] [INSPIRE].
- [51] S. Weinberg, *The quantum theory of fields. Vol. 2: modern applications*, Cambridge University Press, Cambridge U.K. (1996).